DOCTOR OF PHILOSOPHY

Early-stage drug discovery of HIV-1 frameshifting modulators

Fernandes, Abigail Brenda

Award date:
2015

Awarding institution:
University of Dundee

Early-stage drug discovery of HIV-1 frameshifting modulators

Abigail Brenda Fernandes

A dissertation submitted in fulfilment of the requirements
for the degree of Doctor of Philosophy

University of Dundee
August 2015

Declaration

I hereby declare that I, Abigail Brenda Fernandes, am the sole author of this thesis. All the work outlined within this thesis was carried out by me. Any work other than my own is clearly stated and acknowledged. All references cited within have been consulted by me. None of the work within this thesis has been previously awarded for a higher degree.

Signed:  Date: August 6, 2015

Supervisor Statement

I certify that Abigail Brenda Fernandes has fulfilled the conditions of ordinance 39 and relevant regulations, thereby qualifying her to submit this thesis in application for the degree of Doctor of Philosophy.

Signed:  Date: August 7, 2015

Acknowledgements

First and foremost, I would like to thank my supervisor Dr. David Gray, for his reliable support, expertise and guidance during my entire PhD. I am also extremely grateful to Dr. Sam Wilson for accepting me in his lab and providing invaluable support, supervision and reagents during the last year of my PhD. Without you both, this thesis would not have been possible.

I would like to extend my gratitude to everyone who has positively contributed to the completion of my studies. Many thanks to Dr. Tony Hope for your indispensable advice during the drug discovery process of this PhD. Your positive attitude and enthusiasm was greatly appreciated. Thank you to members of the Gray and Wilson labs for experimental support and advice. To Dr. Colin Henderson, thank you for encouraging me and believing in me throughput this PhD.

To the wonderful friends I was fortunate to make both in Dundee and Glasgow, thank you for your constant encouragement and unequivocal support. I am especially grateful to Lauren, Moneeza, Susan, Arun, Polly and Fiona, for the great memories and for making my nomadic experience so much easier, both literally and emotionally.

Anthony, thank you for always listening and motivating me to do better; you have made the darkest of days so much brighter. To my parents, Baltazar and Angela, and my sister, Amber, I cannot thank you enough for your unwavering support, love and patience. The qualities you have instilled in me and the opportunities you selflessly provided have brought me to where I am today.

Table of Contents

List of Figures

List of Tables

List of Abbreviations

ADMET	Absorption, distribution, metabolism, excretion and toxicity
AIDS	Acquired immunodeficiency syndrome
APC	Adenomatous polyposis coli
AZT	azidothymidine or zidovudine
CA	Capsid
CV	Coefficient of variation
DDU	Drug Discovery Unit (Dundee, UK)
DMEM	Dulbecco's minimal essential medium
DMSO	Dimethyl sulfoxide
DNA	Deoxyribonucleic acid
dNTP	Deoxyribonucleotide
DRC	Dose- response curves
eGFP	Enhanced green fluorescent protein
ELISA	Enzyme-linked immunosorbent assay
Env	Envelope
eRF1	Eukaryotic release factor
ESCRT	Endosomal sorting complex required for transport complex
FACS	Flow cytometry-activated cell sorting
FBS	Fetal bovine serum
FCS	Fetal calf serum
FLuc	Firefly luciferase
FRET	Fluorescence resonance energy transfer
G418	Geneticin
Gag	group-specific antigen
gRNA	Genomic RNA
HAART	Highly active antiretroviral therapy
HCV	Hepatitis C virus
HIV-1	Human immunodeficiency virus type 1
IN	Integrase
IRES	Internal ribosome entry site
ISTI	Integrase strand transfer inhibitor
LAV	Lymphoadenopathy- associated virus
LB	Luria broth

LC-MS	Liquid chromatography –Mass spectrometry
LTR	Long terminal repeats
MA	Matrix
MHC	Major histocompatibility complex
MOI	Multiplicity of infection
mRNA	Messenger RNA
NaAc	Sodium Acetate
NC	Nucleocapsid
Nef	Negative factor
NMD	Nonsense-mediated decay
NNRTI	non-nucleoside reverse transcriptase inhibitor
NRTI	nucleoside reverse transcriptase inhibitors
ORF	Open reading frame
PBMC	Peripheral blood mononuclear cell
PBS	Phosphate buffered saline
PFA	Paraformaldehyde
PIC	Pre-integration complex
PEG10	Paternally expressed gene
Pol	Polymerase
PR	Protease
PTC	Premature termination codon
RFU	Red fluorescent units
RFP	Red fluorescent protein
RLuc	Renilla luciferase
RNA	Ribonucleic acid
RPMI	Roswell Park Memorial Institute
RRE	Rev response element
RT	Reverse transcriptase
SAR	Structure-activity relationship
SARS-CoV	Severe acute respiratory syndrome coronavirus
SBDD	Structure-based drug design
SD	Standard deviation
SDS-PAGE	Sodium dodecyl sulphate- polyacrylamide gel electrophoresis
SOC	Super Optimal Broth
SOP	Standard Operating Procedure

SP	Spacer peptide
SU	Surface unit
Tat	Trans-activator of transcription
TM	Transmembrane
TPSA	Topological polar surface area
tRNA	Transfer RNA
UV-Vis	Ultraviolet-visible
Vif	Virion infectivity factor
VLP	Virus-like particle
Vpr	Viral protein R
Vpu	Viral protein U

Abstract

Human immunodeficiency virus type I (HIV-1) is a global health issue affecting approximately 35 million people worldwide. Despite the success of highly active antiretroviral therapy (HAART), drug resistant viruses and adverse drug reactions raise the need for new classes of antiretroviral drugs. During HIV-1 replication, the viral frameshifting element orchestrates expression of a specific ratio of the essential Gag and Gag-Pol polyproteins from overlapping reading frames. This process is vital for viral assembly and maturation, since altering the ratio of Gag and Gag-Pol polyproteins through HIV-1 frameshifting, perturbs HIV-1 replication.

To identify modulators of HIV-1 frameshifting, a bi-cistronic fluorescent construct was designed to establish a clonally-derived cell culture model of HIV-1 Gag:Gag-Pol frameshifting. Following assay development and validation of screening parameters, a primary diversity screen with 92,071 small molecules was conducted. The initial screening triage of hit compounds led to the selection of several false positives due to auto-fluorescent compound properties. I subsequently re-designed the screening cascade to incorporate a counter-screen that was effective at eliminating false positives. Ultimately, no hit compounds were identified capable of activating or inhibiting HIV-1 frameshifting.

However, compound DDD00049811 was fortuitously discovered to inhibit the spread of HIV-1 infection, but not through the desired target of HIV-1 frameshifting. The high concentration required to elicit an antiviral response, the minimal effect in a single-cycle of HIV-1 replication and the slight cellular viability defect suggest that DDD00049811 is not a good anti-HIV-1 candidate drug. My work indicates that HIV-1 frameshifting is a challenging drug target; however, addressing limitations in the strategy used in this study could allow this critical function to be drugged successfully.

Chapter 1
Introduction

1.1 HIV-1 & AIDS

Human immunodeficiency virus type 1 (HIV-1), is a lentivirus that belongs to the *Retroviridae* family and causes acquired immunodeficiency syndrome (AIDS), a disease that compromises the immune system. Initially termed lymphoadenopathy-associated virus (LAV), it was first isolated in 1983 by Robert Gallo (Gallo et al., 1983) and Luc Montagnier (Barre-Sinoussi et al., 1983). Currently, there are approximately 35 million people living with HIV-1 worldwide, and around 1.5 million people die annually as a result (World Health Organization, 2014). Due to the high genetic heterogeneity, HIV-1 is classified into four different groups, each with corresponding subtypes. Of the four HIV-1 groups, the 'major' M group is the most prevalent cause of infections in the global epidemic.

HIV-1 infection advances through three main stages. During acute infection, viral load is very high and is followed by an immune response that increases $CD4^+$ T cells (Gupta, 1993). This is followed by chronic infection or clinical latency; an asymptomatic phase characterized by reduced $CD4^+$ T cells and increased viremia. The final stage of HIV-1 infection is AIDS, which is characterized by the loss of $CD4^+$ T cells (<200 cells/mm^3) thereby giving rise to opportunistic infections (Fanales-Belasio et al., 2010; Morgan et al., 2002; Swanstrom & Coffin, 2012). The progression through these stages depends on various factors including the host immune response and viral pathogenesis.

To date, there is no available vaccine or cure for this disease. However, several drugs have been developed to control the level of HIV-1 infection, prevent the progression to AIDS-related opportunistic infections and limit virus transmission (Arts & Hazuda, 2012). Drugs are administered as a combination known as highly active retroviral treatment (HAART). HAART often consists of a mixture of three of more drugs targeting various steps in

the HIV-1 replication cycle including entry, reverse transcription, integration and viral particle maturation (described in section 1.4). However, drug resistance and deleterious side effects raise the need for new classes of antiretroviral drugs.

1.2 HIV-1 genomic organization

An HIV virion contains two identical copies of positive-sense, single stranded RNA along with polymerase-encoding proteins that are enveloped by a conical core structure made of capsid protein (Briggs et al. 2006; Luciw, 1996) (Figure 1). This 9.8 kb 5' capped and 3'-polyadenylated RNA is unspliced, contains several ORFs and encodes nine genes with structural, regulatory and accessory functions (Figure 2).

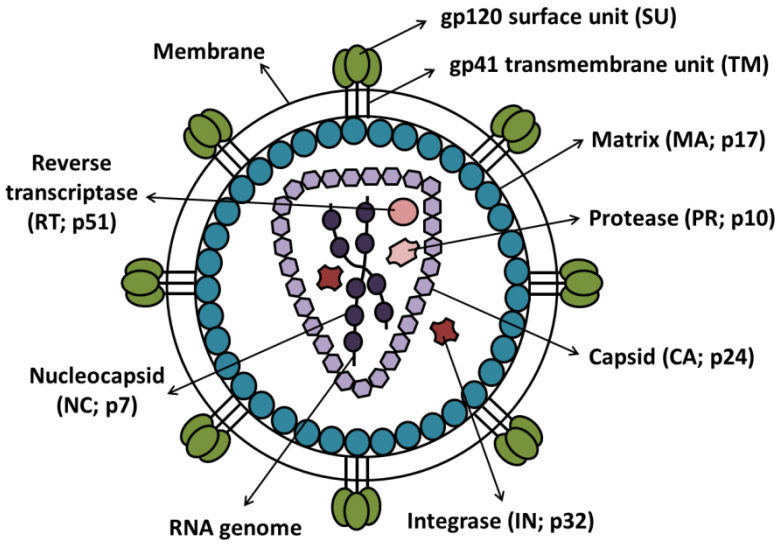

Figure 1 Schematic of mature HIV-1 virus particle
The mature HIV-1 viral particle contains two copies of positive-sense, single stranded RNA along with polymerase-encoding proteins surrounded by a conical structural core made of capsid (CA; p24) protein. This is encapsidated by a layer of matrix (MA; p17) protein which underlies the viral envelope containing glycoproteins (gp120 and gp41).

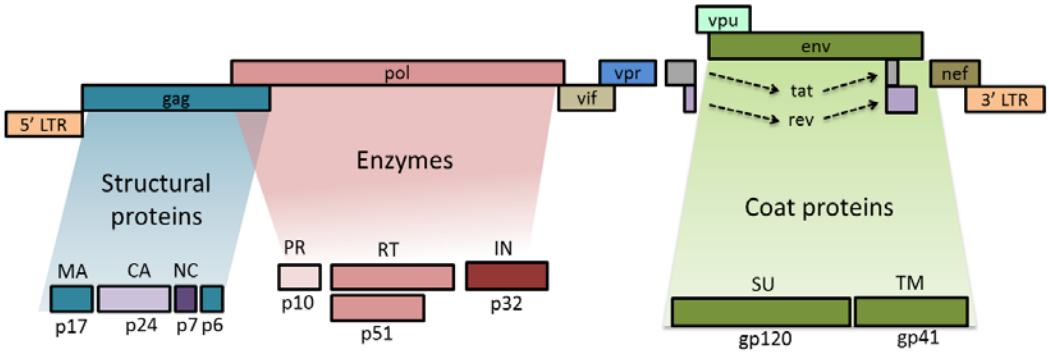

Figure 2 Genomic organization of HIV-1

The open reading frames (ORFs) of HIV-1 genes depicted above encode proteins with structural, regulatory and accessory functions. The group-specific antigen (Gag) polyprotein precursor is proteolytically cleaved into matrix (MA; p17), capsid (CA; p24), nucleocapsid (NC; p7) and p6 proteins involved in structural integrity. The Gag-Pol polyprotein produces structural proteins in addition to enzymatic proteins: protease (p10; PR), reverse transcriptase (p66/p51; RT) and integrase (p32; IN). The gp160 Env polyprotein is cleaved into surface (SU) gp120 and transmembrane (TM) gp41 envelope proteins required for viral entry. Trans-activator of transcription (Tat) and regulator of expression of viral gene expression (Rev) are regulatory proteins and accessory factors are encoded by viral-infectivity factor (vif), viral protein r (vpr), viral protein u (vpu), and negative effector (nef).

1.2.1 Genes encoding structural and enzymatic proteins

The main structural proteins of HIV-1 are encoded by the *gag*, *pol* and *env* genes. The group-specific antigen (*gag*) gene encodes a 55kDa Gag polyprotein that is produced during and plays a major role during virus assembly and release (detailed in section 1.5.4). Briefly, the Gag precursor contains the matrix (MA; p17), capsid (CA; p24), spacer peptide 1 (SP1), nucleocapsid (NC; p7), spacer peptide 1 (SP2) and p6 domains (Figure 2). The MA domain plays a vital role during virion assembly by targeting and facilitating the binding of the Gag precursor to the plasma membrane, and incorporating viral Env proteins into assembling virions (Freed & Martin, 1995; Johnson, 2011). The CA domain aids in viral assembly and is responsible for the formation of the core structure of immature and mature virions through Gag dimerization and multimerization (Franke et al., 1994; Gitti et al., 1996; Briggs & Kräusslich, 2011). Following the C-terminus of CA, SP1 also has regulatory roles in Gag processing and Gag-Gag interactions during viral assembly (Datta et al., 2011). It has also been suggested that CA regulates nuclear import of the pre-integration complex (PIC) during the early stages of HIV-1 replication (Matreyek & Engelman, 2013). The NC domain is responsible for chaperoning viral genomic RNA during replication and binds to the RNA packaging signal to facilitate packaging of viral genomic RNA into viral particles (Levin et al., 2005; Rein, et al., 1998). Furthermore, NC enhances the efficiency of reverse transcription and also supports viral assembly (Swanson & Malim, 2008). The p6 domain, also known as the late domains (Göttlinger et al., 1991; Huang et al., 1995), is required for recruiting the endosomal sorting complex required for transport complex (ESCRT) to facilitate virion budding (Ehrlich & Carter, 2012; Katzmann, Babst, & Emr, 2001; Votteler & Sundquist, 2013) and incorporating accessory viral protein R (Vpr) during viral assembly (Paxton et al., 1993).

During translation of the Gag precursor, a 160kDa Gag-Pol precursor polyprotein is produced approximately 5% of the time as a result of programmed -1 ribosomal frameshifting (described in section 1.5.3). The Gag-Pol precursor encodes the viral enzymes PR, RT and IN. PR facilitates

the maturation of virions from an immature Gag lattice into a conical core structure through proteolytic cleavage of the Gag and Gag-Pol polyproteins into mature MA, CA, NC, p6, PR, RT and IN proteins (Jacks, et al., 1988; Sundquist & Kräusslich, 2012). Reverse transcriptase is a heterodimer with active sites for RNA-dependent DNA polymerase, a DNA-dependent DNA polymerase and an RNaseH domain that ultimately synthesizes viral cDNA from viral genomic RNA (Jacobo-Molina et al., 1993; Kohlstaedt et al., 1992; Rodgers et al., 1995). Integrase which consists of the N-terminal, core and C-terminal domain (Chiu & Davies, 2004) catalyses the integration of HIV-1 cDNA into cellular chromosomal DNA through 3' processing and strand transfer of viral cDNA (Bushman et al., 1990).

The envelope (*env*) gene encodes a 160kDa Env surface glycoprotein which is synthesized in the endoplasmic reticulum and transported to the Golgi apparatus. It is then cleaved into surface gp120 and transmembrane gp41 envelope proteins, a non-covalently linked heterodimer complex on the lipoprotein-rich membrane (Allan et al., 1985; Veronese et al., 1985). The Env glycoprotein complex consists of trimers of three gp120 molecules and three gp41 molecules that mediates binding and entry into host cells through the interaction of gp120 with the CD4 receptor (Klatzmann et al., 1989; McDougal et al., 1986) and CCR5 or CXCR5 co-receptors on helper T cells (G Alkhatib et al., 1996). Following binding, conformational changes lead to gp41-mediated fusion of the viral and host cell membranes (S. A. Gallo et al., 2003). These glycoprotein complexes are either incorporated in budding virions or released as separate subunits after disassembly.

1.2.2 Genes encoding regulatory and accessory proteins

The viral *tat* and *rev* genes regulate HIV-1 gene expression. Tat (trans-activator of transcription) is a multifunctional, early regulatory protein that is required for HIV-1 gene expression and replication (Dayton et al., 1986). It plays a role in HIV-1 RNA splicing and transactivates cellular and viral genes through binding of the trans-acting response (TAR) element (Jablonski et al., 2009). Rev (regulator of expression of viral gene expression), a late

regulatory protein, is generated from multiply spliced mRNA, binds to the Rev response element (RRE) on incomplete or unspliced mRNAs to facilitate their nuclear export (Swanson & Malim, 2008). This primarily regulates the expression of structural mRNAs late in the replication cycle.

HIV-1 accessory proteins are multifunctional and encoded by the *nef*, *vpr*, *vpu* and *vif* genes. *Nef* (negative factor) is a myristoylated 27kDa accessory protein that downregulates cell surface expression of CD4 and major histocompatibility complex 1 (MHC1) expression (Doms & Trono, 2000; Montal, 2003). It is an important factor that is not required for HIV-1 replication in cell culture, but progresses AIDS pathogenesis (Laguette et al., 2010) in infected hosts by amplifying viral titres (Kestler et al., 1991). Viral protein R (Vpr) is a highly conserved HIV-1 accessory protein with various functions that are not fully understood. Two of the most well-studied functions include Vpr-induced cell cycle arrest of the G2/M phase in host cells (Di Marzio et al., 1995; He et al., 1995; Rogel et al., 1995) and enhanced infection of non-dividing cells such as monocyte-derived macrophages (Agostini et al., 2002; Jacquot et al., 2007). Vpu (viral protein U), helps release of virions through displacing tetherin/BST2 from the sites of virion assembly and uses ubiquitin-mediated degradation to downregulated CD4 expression (Margottin et al., 1998; Montal, 2003; Neil et al., 2008). Vif (virion infectivity factor), promotes the degradation of the host restriction factor APOBEC3G, and is required for HIV replication in macrophages, lymphocytes and PBMCs (Malim & Emerman, 2008; Sheehy et al., 2002; Strebel, 2003).

1.3 Overview of the HIV-1 replication cycle

The early stages of the HIV-1 replication cycle include viral entry, reverse transcription, nuclear import and DNA integration, while the late stages include viral RNA (vRNA) transcription, translation, viral assembly, budding and maturation (Figure 3).

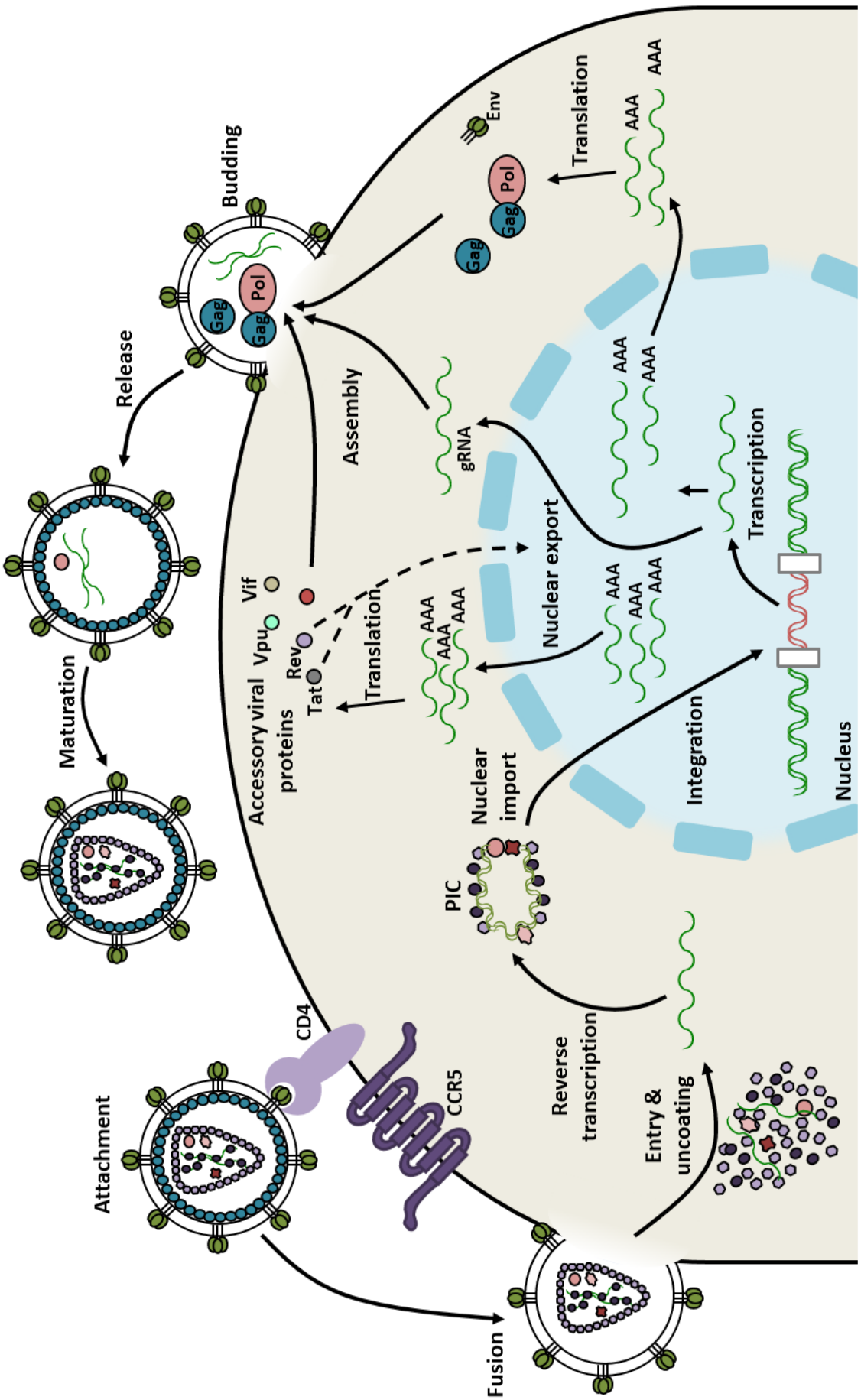
Budding
Release
Maturation
Assembly
Translation
Env
Gag
Pol
AAA
gRNA
Nuclear export
Transcription
Vif
Vpu
Rev
Tat
Accessory viral proteins
Nuclear import
PIC
Integration
Nucleus
CD4
CCR5
Attachment
Reverse transcription
Entry & uncoating
Fusion

Figure 3 Schematic of HIV-1 replication cycle

Major stages of the HIV-1 replication cycle are depicted above and described in the sections 1.3. Briefly, HIV-1 attaches to receptors on the host cell and fuses with the cell membrane resulting in entry of the single-stranded viral RNA (ssRNA) genome into the host cell cytoplasm. The ssRNA is reverse transcribed into dsDNA by virally-encoded reverse transcriptase (RT). dsDNA is imported into the nucleus within the pre-integration complex (PIC) and integrated into the host genome by virally-encoded integrase (IN). Cellular RNA polymerase II transcribes the proviral DNA into viral RNA which is used to generate unspliced, partially spliced and fully spliced RNAs that are exported to the cytoplasm. Translation of several mRNA species produce regulatory proteins, Tat and Rev, which enter the nucleus to enhance transcription; accessory proteins; structural and enzymatic polyproteins (Gag and Gag-Pol); and envelope proteins. Following assembly of viral RNA and viral proteins, immature virions are released and mature into infectious virions following protease-mediated cleavage of the Gag and Gag-Pol polyproteins into mature structural and enzymatic proteins.

1.3.1 Early stages of HIV-1 replication

To infect a host target cell, the HIV-1 viral particle uses the gp120 envelope protein to bind to the CD4 receptor on host cells such as T-cell precursors, monocytes, macrophages, T-lymphocytes and dendritic cells (Fanales-Belasio et al., 2010). This induces a conformational change in the trimeric envelope structure, allowing gp120 to further bind to a chemokine receptor, usually CCR5 or CXCR4 (Ghalib Alkhatib & Berger, 2007). Preferential binding to chemokine receptors influences HIV tropism. While almost all HIV-1 strains use the CCR5 co-receptor found on macrophages and CCR5-expressing $CD4^+$ T cells (known as M-tropic or R5 viruses) (Coakley et al., 2005), some viruses prefer primary CXCR4-expressing $CD4^+$ T cells (known as T-tropic or X4 viruses) and other HIV-1 isolates bind to both chemokine receptors (known as dual tropic or X4R5 viruses). Following the binding of CD4 and a chemokine receptor, the gp41 hydrophobic fusogenic peptide is inserted into the cell membrane. This subsequently induces a conformational change that promotes fusion of the viral and cell membranes (Weiss, 1993). The viral capsid then enters the cell, uncoats and releases the RNA genome in the host cell cytoplasm.

RT acts as an RNA-dependent DNA polymerase to reverse transcribe positive-sense viral RNA using a $tRNA_{lys3}$ primer. This cellular primer binds to the primer binding site at the 5' end of HIV RNA and initiates synthesis of a minus strand DNA, thereby resulting in a RNA/DNA hybrid. This acts as a substrate for viral RNAseH which degrades the RNA strand template. A positive DNA strand is polymerized from the minus DNA strand by the DNA-dependent DNA polymerase domain of RT, resulting in linear proviral double-stranded DNA flanked by similar sequences known as long terminal repeats (LTR). These play a vital role in integration and transcription (J.-C. Paillart et al. 2004; Vogt, 1997).

Proviral DNA with viral proteins (RT, NC, MA, Vpr) and cellular proteins are associated within a pre-integration complex (PIC) and imported in the nucleus, potentially using a host cell-dependent mechanism (Fassati, 2006).

This nuclear import process is still unclear, but postulated to depend on viral components such as CA, IN, MA, Vpr, triple-stranded proviral DNA within the polypurine tract of HIV-1 and some host factors (Bouyac-Bertoia et al., 2001; Bukrinsky et al., 1993; Gallay et al., 1997; Gallay, Swingler et al., 1995; Haffar et al., 2000; Heinzinger et al., 1994; Hilditch & Towers, 2014; Yamashita & Emerman, 2004). Integrase-mediated processing of the 3' end of viral double stranded DNA generates sticky ends by creating nucleophilic hydroxyl groups (Katzman et al., 1989). Through a transesterification reaction, strand transfer takes place as the viral 3'-hydroxyl ends are ligated to the cellular DNA 5'-phosphate group (Vink et al., 1990). This is followed by cellular-mediated DNA repair to process the 5'-overhangs of proviral DNA to 'complete integration' (Daniel et al., 2004; Fujiwara & Mizuuchi, 1988; Yoder & Bushman, 2000), preferably integrates within transcribing genes (Schröder et al., 2002).

1.3.2 Late stages of HIV-1 replication

Transcription conducted by cellular DNA-dependent RNA polymerase II, is initiated at the U3 promoter located within the LTR of HIV-1 RNA. This generates a full length HIV-1 mRNA that contains cellular mRNA components such as 5' cap and a 3' poly-A tail (Rabson and Graves, 1997). Early transcription promotes the production of early regulatory proteins, Tat and Rev, which enhance transcriptional elongation (Bieniasz et al., 1998; Fujinaga et al., 1998). HIV-1 is a complex retrovirus that generates multiple mRNA species by cellular-mediated splicing of the viral RNA. This includes unspliced RNA which not only serves as genomic RNA, but also encodes Gag and Gag-Pol, and spliced mRNAs expressing Env, regulatory and accessory genes. Unlike cellular proteins which need to be spliced for nuclear export, unspliced and partially spliced HIV-1 RNA is transported to the cytoplasm by viral Rev and cellular proteins (Muesing et al., 1987; Rosen et al., 1988).

Translation of all viral unspliced and spliced mRNAs is conducted by cellular host machinery. Upon export to the cytoplasm, a proportion of unspliced genomic RNA is packaged into assembling virions, some genomic RNAs are

translated into Gag and Gag-Pol polyproteins (Swanstrom and Willis, 1997). Programmed -1 ribosomal frameshifting (described in section 1.5) produces a specific ratio of Gag and Gag-Pol polyproteins which are required for structure and enzymatic activity. Spliced mRNAs that encode the regulatory *tat* and *rev* genes are transported to the nucleus to undergo translation so that Tat and Rev proteins can enhance viral mRNA transcription and help transport unspliced RNAs from the nucleus to the cytoplasm, respectively (Cochrane et al., 1990; Cullen, 2003; Dillon et al., 1990; Hadzopoulou-Cladaras et al., 1989; Muesing et al., 1987; Rosen et al., 1988; Zapp & Green, 1989). Multiple spliced mRNA species are transported to the cytoplasm where they undergo translation to synthesize various structural, regulatory and accessory proteins (Cullen, 2003).

1.3.2.1 Assembly, release and maturation

Following synthesis, Gag is trafficked to the plasma membrane, where it interacts with vRNA and Env to facilitate assembly of viral particles. Within the Gag precursor, the basic MA region plays an important role in targeting Gag to lipid rafts at the site of assembly by binding to negatively charged groups on the phosphatidylinositol-4,5-bisphosphate ($PI(4,5)P_2$) phospholipid at the inner leaflet of the plasma membrane (Ono et al., 2004; Saad et al., 2006; Shkriabai et al., 2006). This binding exposes the myristic acid moiety at the N-terminus of Gag which inserts into the inner leaflet to anchor Gag to the plasma membrane (Saad et al., 2006).

To package dimerized viral RNA into assembly virions, the NC domain of Gag uses the packaging signal at the 5'- terminus of genomic viral RNA (Jalalirad & Laughrea, 2010; J.-C. Paillart et al., 2004). Following binding of the basic zinc-finger motif of NC to sites within the 5-UTR (including the packaging signal) and the RRE of vRNA in the cytosol (Kutluay & Bieniasz, 2010), vRNA is chaperoned to the plasma membrane where further interactions are established throughout the HIV-1 genome (Kutluay et al., 2014). These interactions promote Gag multimerization during assembly. The HIV-1 Gag-Pol precursor polyprotein produced by -1 ribosomal frameshifting also

assembles with viral gRNA, Gag and envelope proteins into nascent immature viral particles. Envelope glycoproteins (gp120 and gp41) are non-covalently incorporated, independent of Gag, following translation and cleavage at the endoplasmic reticulum and Golgi apparatus, respectively (Checkley et al., 2011). While the mechanism underlying Env incorporation is unclear, it has been postulated that the long intracellular tail may interact with MA and project into the underlying Gag lattice to promote Env incorporation (Checkley et al., 2011). Small cellular RNAs such as $tRNA^{Lys}$ are also packaged into assembling virions to initiate reverse transcription by binding to the primer binding site within the 5'-LTR of vRNA (Kleiman et al., 2010). While the N-terminus of Gag (containing MA) is bound to the inner leaflet of the plasma membrane during assembly, the C-terminus is oriented towards the centre of the virus particle forming an immature Gag lattice (J A G Briggs et al., 2009; Fuller , Wilk et al., 1997; Wright et al., 2007). Lateral protein-protein interactions with the CA and SP1 domains primarily mediate Gag multimerization to encapsidate and assemble viral components in an immature Gag lattice (Muriaux & Darlix, 2010).

Following assembly, the p6 protein of Gag recruits cellular endosomal sorting complex required for transport complex (ESCRT) complexes which consists of four ESCRT protein complexes (0, I, II and III) to facilitate budding and membrane scission (Ehrlich & Carter, 2012; Van Engelenburg et al., 2014; Votteler & Sundquist, 2013). This occurs through the late domains located on the N-terminus of p6: PR-Thr/Ser-Ala-PR (P(T/S)AP) and Tyr-PR-X_n-Leu (YPX_nL), whereby X_n denotes 1-4 amino acids (n) of any residue (X). To facilitate budding, PTAP interacts with tumour susceptibility gene 101 (TSG101), a cellular component of ESCRT-I, while YPXnL interacts with ALIX (apoptosis-linked gene 2-interacting protein X), an ESCRT-associated factor (Demirov et al., 2002; Garrus et al., 2001; Martin-Serrano et al., 2001; VerPlank et al., 2001). While the PTAP-TSG101 interaction is essential for budding, the YPX_nL-ALIX interaction is required in certain cell types and is required for optimal viral replication (Fujii et al., 2009). While the mechanism through which the ESCRT machinery leads to membrane scission

remains unclear, ESCRT machinery localizes at the budding head and assembles in spirals to construct the neck of the bud and drive membrane scission from within (Hanson et al., 2008; Shen et al., 2014; Van Engelenburg et al., 2014). This is potentially assisted by the energy provided by ATPase vacuolar protein sorting 4 (VPS4), which is recruited by ESCRT-III (Baumgärtel et al., 2011; Elia et al., 2011; Jouvenet et al., 2011).

Concomitant with virion release, the virally-encoded aspartyl protease expressed as part of the Gag-Pol precursor, cleaves 10 sites within the Gag and Gag-Pol precursors in a step-wise manner to initiate virion maturation (Wlodawer & Erickson, 1993). Protease mediated-cleavage of Gag results in mature MA, CA, NC and p6 proteins and spacer peptides, SP1 and SP2, while Gag-Pol polyprotein cleavage results in PR, RT and IN enzymes (Pettit et al., 1994). While MA associates with the inner plasma membrane to form a shell, CA plays a major role in forming outer hexameric rings in a lattice to generate the conical core capsid structure (S. Li et al., 2000). This morphological rearrangement from a donut-shaped immature virion to a conical-shaped mature virion is a hallmark of maturation. The resulting mature viral particle contains the HIV-1 viral genome with NC, RT and IN within a conical capsid core structure that is capable of infecting other host cells.

1.4 HIV-1 therapeutics

Over the past 28 years, significant progress has been made to transform HIV-1/AIDS from a fatal condition to a chronic, but manageable disease. Approximately 32 drugs have been approved for treating HIV-positive patients. These target various steps in the HIV-1 replication cycle such as entry, reverse transcription, integration and protease-mediated viral maturation. Drugs targeting these various stages are administered in combination, known as HAART (highly active retroviral treatment), and commonly consists of a mixture of three of more drugs, such as a protease inhibitor or non-nucleoside reverse transcriptase inhibitor (NNRTI) with two nucleoside reverse transcriptase inhibitors (NRTIs).

The first HIV-1 therapeutic, AZT (azidothymidine or zidovudine), is a NRTI that targets reverse transcription by inhibiting viral DNA polymerization (Mitsuya et al., 1985). NRTIs are mono-phosporylated nucleotide analogs that resemble cellular dNTPs and are incorporated into nascent HIV-1 DNA by viral RT. However, these analogs lack a 3`-hydroxyl group which is required for further dNTP addition, and therefore terminate chain formation. NNRTIs, another class of reverse transcriptase inhibitors, bind to the hydrophobic binding site of RT and inhibit polymerase activity, and therefore viral transcriptional elongation (Goldman et al., 1991). NRTIs such as AZT have a higher affinity for viral RT compared to cellular DNA polymerases, however toxicity is an issue due to AZT incorporation in germ-line DNA and vertical transmission of modified DNA (Mitsuya et al., 1985; Yarchoan & Broder, 1987).

The development of HIV-1 protease inhibitors (PIs) has been extremely successful as there are currently 10 clinically available potent inhibitors (Llibre et al., 2013). These bind to the protease active site and prevent protease-mediated cleavage of the Gag and Gag-Pol polyproteins into mature viral proteins, subsequently compromising infectious viral particle formation. Due to chemical structural similarities between PIs, they are often administered in combination with other HIV-1 therapeutics to avoid cross-resistance at the HIV-1 protease active site (Nijhuis et al., 2001).

Another class of HIV-1 inhibitors target viral entry by potentially targeting either the attachment of HIV-1 gp120 to host CD4 receptors, binding of HIV-1 to co-receptors, or fusion of viral and host membranes. Maraviroc and enfuvirtide are two currently available clinical inhibitors. Maraviroc is a CCR5 receptor antagonist that reduces plasma HIV-1 RNA levels by >1.6 $\log_{10}$ in patients with R5 virus and elevated CD4 levels (Fätkenheuer et al., 2008; Gulick et al., 2008). While patients with CXCR4-virus did not virologically or immunologically benefit, their CD4 levels increased (Goodrich et al. 2007).

Integrase inhibitors are the most recent class of antiretroviral drugs targeting either the 3' processing step or strand transfer, in order to inhibit HIV-1 replication. Integrase strand transfer inhibitors (ISTIs) include a class of compounds known as diketo aryl (DKA) and DKA-like inhibitors (Hazuda et al., 2004; Zhuang et al., 2003) which subsequently reduce HIV-1 infection (Hazuda et al., 2000; Hazuda et al., 2004). At higher concentrations, DKAs can also suppress 3' processing (D J Hazuda et al., 2000; Marchand et al., 2003). Currently approved integrase inhibitors from this class include raltegravir (RAL, Isentress, formerly MK-0518), elvitegravir (EVG, formerly GS-9137) and dolutegravir (DTG).

1.4.1 Concerns with current anti-HIV-1 therapeutics

HAART therapy has been successful at controlling HIV-1 infection with a sustained response (J. A. Johnson & Sax, 2014). Life-long HAART has proven beneficial in places like South Africa, where the life expectancy has significantly increased (by 11 years) over the span of 8 years (Bor et al., 2013). Furthermore, HAART has effectively prevented transmission of HIV from mother-to-child (Connor et al., 1995). However, while the incidence rate of HIV-1 infections has decreased, the AIDS epidemic continues to thrive. HAART effectively controls viral load and reduces mortality and morbidity (Hammer et al., 1997; Ho et al., 1995; Palella et al., 1998), but there is no effective cure as the viruses is never eradicated, drug- resistant viruses continually emerge and current therapeutics cause considerable side effects. This raises the need to develop drugs with novel targets, especially considering the increased knowledge about the mechanisms underlying HIV-1 replication.

The drugs currently administered as HAART therapy have several disadvantages including serious side effects. This includes diarrhea, nausea, myocardial infarction, stroke (Friis-Møller et al., 2007), hepatitis, pancreatitis, muscle weakness (Boubaker et al., 2001; Coghlan et al., 2001), myopathy (Arnaudo et al., 1991), hypertriglyceridemia, glucose intolerance (Caron et al., 2001; Carr et al., 1998), lipodystrophy and accelerated

atherosclerotic disease (Bozzette et al., 2003; Carr et al., 1998; Dressman et al., 2003; Lenhard et al., 2000). Moreover, some drugs lead to toxicity through mitochondrial DNA depletion by inhibiting mitochondrial DNA dependent DNA polymerase (Arenas-Pinto et al., 2003; Feng et al., 2001). Ritonavir, a widely used protease inhibitor, is capable of increasing cholesterol and triglycerides (Friis-Møller et al., 2007) which are associated with risk of morbidity.

More importantly, prolonged exposure to currently approved drugs leads to acquired antiviral resistance, particularly cross-resistance within existing mechanistic classes (Cohen, 2002). During the 1900s, drug resistance occurred in response to NRTI treatment.Resistance to RT inhibitors developed quickly as a result of mutations that prevent the incorporation of nucleotide analogs over cellular dNTPs (Huang et al., 1998; Sarafianos et al., 1999) or those that permit RT to excise incorporated NRTIs in an ATP-dependent manner (Arion et al., 1998; Meyer et al., 1999). In response, novel RT inhibitors, such as tenofovir and etravirine, were developed and successful in decreasing the replication fitness of K65R and K103N mutation-bearing resistant viruses, respectively. This was followed by the development of protease inhibitors which acquired mutations at the protease inhibitor binding site (Nijhuis et al., 2001; Quiñones-Mateu & Arts, 2002; Quiñones-Mateu et al., 2008) and those within the protease gene, especially at cleavage sites (Clavel et al., 2000; Doyon et al., 1998; Miller, 2001; Nijhuis et al., 2001; Zhang et al., 1997), subsequently interfering with drug-binding affinity. Some problems with HIV-1 entry inhibitors such as enfuvirtide include painful injection long-term and fast emerging resistance when combined with drugs that do not completely inhibit HIV-1 replication. While many mutations are required to generate resistance against integrase inhibitors, the newest developed class of inhibitors, resistance has also emerged following treatment with raltegravir and elvitegravir (Blanco et al., 2011), due to mutations in residues involved in drug-integrase interaction. There is however, minimal cross-resistance with raltegravir and dolutegravir, the newest IN inhibitor (Hertogs et al., 2000; Richman, 2000; Tang & Shafer, 2012; Wensing et al., 2014). It is generally believe that HIV-1 eventually

generates resistance to all drugs. Since HIV-1 infected individuals have an average of about $1x10^{10}$ infected cells, potentially susceptible to three mutations per virion per replication cycle (Coffin, 1995), it is highly likely that HIV-1 will continue to generate resistance to all drugs, particularly within existing mechanistic classes.

Moreover, drug-drug interactions also pose a problem since HIV-1 patients are treated with a combination of antiretrovirals and often involve treatment of other opportunistic infections. Since drugs such as protease inhibitors are metabolized by cytochrome P450 3A (CYP3A) enzymes, combined regimens should be considered. Ritonavir, a protease inhibitor, is also capable of inhibiting CYP3A thereby reducing the metabolism of other PIs such as saquinavir (Concentrations & Kim, 2003; Fellay et al., 2002). Due to the lack of an effective cure and the disadvantages associated with currently available drugs, there still is a dire need to identify a new mechanistic class of anti-HIV drugs with better tolerability and improved resistance. One such target that has yet to be explored is programmed ribosomal frameshifting of the HIV-1 *gag* and *pol* genes.

1.5 Programmed ribosomal HIV-1 frameshifting

1.5.1 Frameshifting in viruses

-1 ribosomal frameshifting is a programmed translational recoding event that occurs during translational elongation in response to specific frameshift element within the mRNA. It primarily occurs in retroviruses and was initially observed in Rous sarcoma alpharetrovirus (Jacks et al., 1988; Jacks & Varmus, 1985). Since then, -1 frameshifting elements have been found in several other viruses, as well as retrotransposons and insertional elements (I Brierley & Pennell, 2001; Chandler & Fayet, 1993; Plant & Dinman, 2008). It is widely believed that frameshifting occurs to allow the expression of multiple genes from a small genome size, such as those of viruses and mitochondria. This is supported by the correlation between genome size and frameshifting frequency (Seligmann, 2012).

-1 programmed frameshifting leads to protein production of two genes from separate open reading frames (ORFs). This dual coding capability allows many viruses to produce enzymatic viral components such as viral reverse transcriptase in retroviruses and RNA-dependent RNA polymerases in other RNA viruses (I. Brierley, 1995; Dreher & Miller, 2006), in addition to structural viral components. In HIV-1, programmed -1 frameshifting produces a 55kDa Gag structural protein (from 0 frame) and a 160kDa Gag-Pol polyprotein (-1 frame), which is the precursor of viral enzymes such as PR, RT and IN (Jacks et al., 1988).

1.5.2 Structure of the HIV-1 frameshift element

In HIV-1, the *pol* gene is out-of-frame to an upstream *gag* gene and the expression of resulting Gag and Pol proteins is regulated by -1 ribosomal frameshifting, which occurs at a frequency of 5%. (Fanales-Belasio et al., 2010; Jacks et al., 1988). The overlapping sequence at the 3' end of *gag* and the 5' end of *pol* comprises an mRNA frameshift region that is responsible for programmed -1 frameshifting. This region consists of two cis-acting elements: a slippery site where frameshifting occurs, and a frameshift stimulatory signal which stimulates frameshifting (Somogyi et al., 1993) (Figure 4).

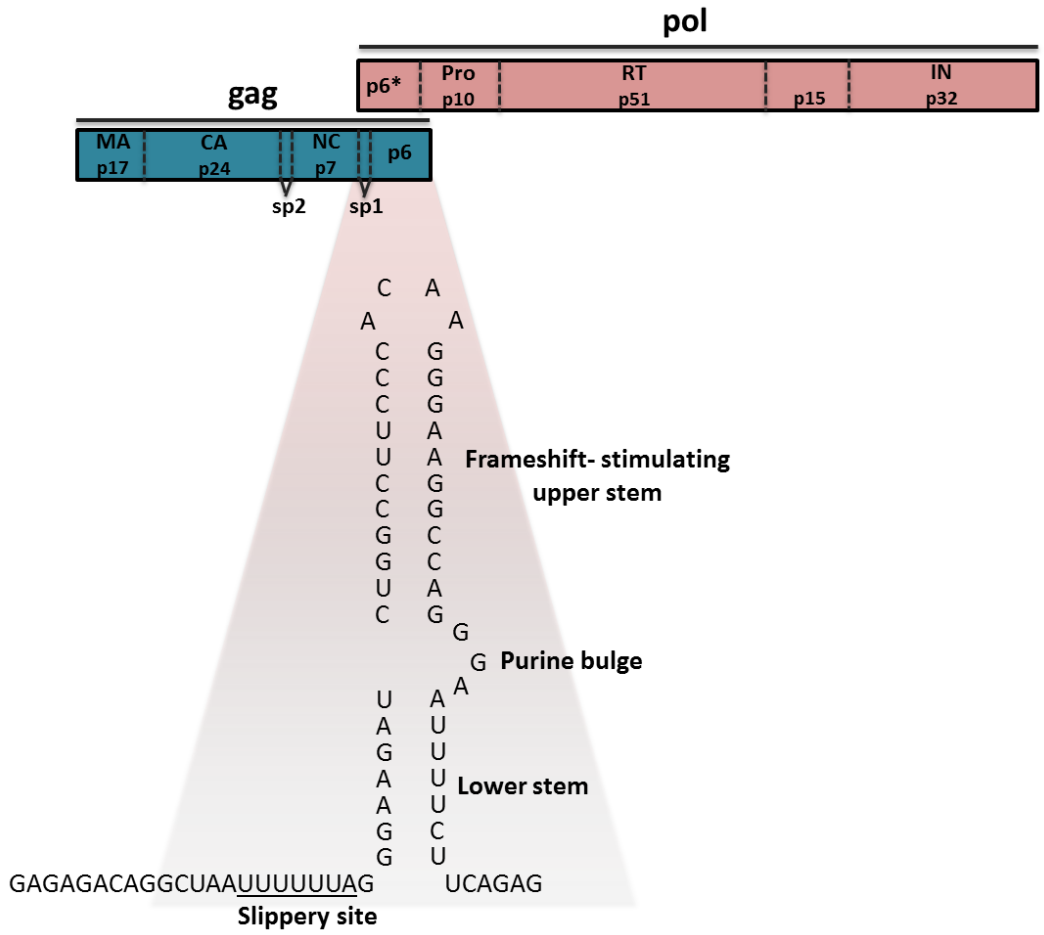

Figure 4 HIV-1 frameshift element

The depicted HIV-1 frameshift RNA element consists of a slippery site (underlined) followed by a frameshift stimulatory signal. The HIV-1 frameshift stimulatory signal has a stable upper stem and a less stable lower stem separated by a purine bulge. The stability of the upper stem plays a significant role in frameshifting.

The frameshift stimulatory signal is an RNA motif comprising an irregular two-stem helical structure whereby a stable upper stem and an unstable lower stem (Gaudin et al., 2005; Staple & Butcher, 2005) is separated by a 3-nucleotide purine bulge (GGA) (Baril et al., 2003; Dulude et al., 2002). Using HIV-1 group M subtype B, the structure of the HIV-1 frameshifting element was initially proposed by site-directed mutagenesis (Dulude et al., 2002), and confirmed using nuclear magnetic resonance (NMR) (Gaudin et al., 2005; Staple & Butcher, 2005) and structural probing experiments with an RNA transcript of the frameshift region (Kang, 1998). The structure of this RNA motif and the stability of the upper stem cause the ribosome to pause and was found necessary to stimulate frameshifting at the slippery site (Dulude et al., 2002; Fu et al., 2011; Gaudin et al., 2005; Somogyi et al., 1993; Staple & Butcher, 2005).

In eukaryotes, the slippery site is a heptanucleotide sequence comprising two homopolymeric triplets with X-XXY-YYZ consensus sequence (-indicate 0 frame) (U-UUU-UUA in HIV-1). This sequence is important in the regulation of frameshifting efficiency. Previous studies demonstrated that while only a triple A or triple U can denote YYY within the consensus slippery sequence, XXX can be a A, C, G or U homopolymeric triple sequence (Brierley et al., 1992; Dinman et al., 1991; Jacks, Power, et al., 1988). Furthermore, only 5 different sequence combinations within the last three nucleotides of the slippery site (X XXY YYZ) have been found in eukaryotes. The HIV-1 slippery site is highly conserved between subtypes; replacing it with other slippery sequences decreased frameshift efficiency and compromised HIV-1 replication (Biswas et al., 2004). Following the slippery site, is a spacer region which is 8 nucleotides long in HIV-1 and required for frameshifting efficiency (Brierley et al., 1989; Kollmus et al., 1994; Mouzakis et al., 2013).

1.5.3 Mechanism of HIV-1 frameshifting

During HIV-1 mRNA translation, most ribosomes translate the gag mRNA until encountering the Gag stop codon. However, a small proportion of ribosomes encounter the frameshifting stimulatory structure which leads

them to pause at slippery site and continue translation of Pol in the -1 reading frame (Jacks et al. 1988; Kontos et al., 2001; Lopinski et al., 2000; Somogyi et al. 1993; Tsuchihashi 1991; Tu, Tzeng, and Bruenn 1992; Coffin 1990; Weiss et al. 1985) (Figure 5). Several theories have been postulated to describe the mechanics underlying programmed -1 ribosomal frameshifting.

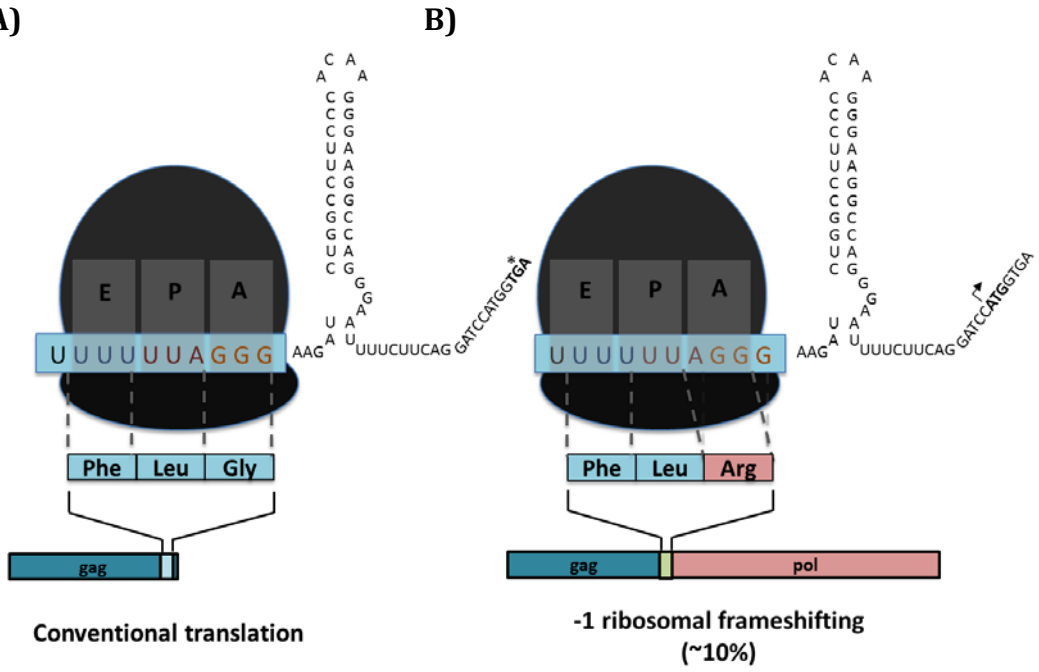

Figure 5 Translation of Gag-Pol mRNA by conventional translation and ribosomal frameshifting

A) Majority of ribosomes follow conventional rules of translation (0 frame) and therefore produce the Gag polyprotein by translating mRNA until the stop codon (*) in the 0 frame. E, P and A indicate the exit, peptidyl and acceptor sites, respectively.

B) Approximately 5% of ribosomes undergo programmed -1 frameshifting whereby the ribosome slips by one nucleotide in the 5' direction leading to the mRNA translation in the -1 frame. This results in the production of Gag-Pol polyprotein (arrow: initiation codon of Pol).

The ribosomal pause at the slippery site is likely due to the stability of the upper stem of the stimulatory signal which resists mRNA unwinding by the ribosome (Takyar, et al. 2005; Wills et al., 1991). Inducing mutations within the stem loop structure revealed a correlation between the stability of the frameshift stem loop and frameshifting efficiency. This led to the theory that the stability and strength of the stem-loop frameshift structure greatly impacted frameshifting efficiency (Hansen et al., 2007). While it is possible that the introduction of mutations within the RNA stem loop structure could affect interactions involving dimerization of genomic RNA (Hibbert & Rein, 2005; Paillart et al., 2002; Paillart et al., 2004), it is more likely that ribosomal kinetics play a role in frameshifting efficiency.

The lower stem, on the other hand, is unstable (Gaudin et al., 2005; Staple & Butcher, 2005) and does not resist ribosomal unwinding. Unwinding of the stem loop structure has been deemed necessary for translation to permit the mRNA to pass through the narrow entrance channel of translational machinery (Yusupova et al., 2001). It is however still unclear whether the ribosomal pause occurs due to initially encountering the stem loop structure or upon unwinding of the stem loop structure following frameshifting.

It was further hypothesized that the unwinding resistance and resulting ribosomal pause gives time for the tRNAs to slip from the 0 frame to the -1 frame position (Farabaugh, 2000). During conventional translation, mRNA moves by 3 nucleotides as anticodon-associated peptidyl-and aminoacyl-tRNAs shift from the ribosome P (peptidyl-) and A (aminoacyl-) sites to the E (exit-) and P sites, respectively. Frameshifting is thought to cause the mRNA to translocate by 2 nucleotides instead (Farabaugh, 1996; Léger et al., 2007), resulting in the tRNAs occupying intermediate sites. The incoming tRNA results in the unpairing of the three tRNAs from the 0-frame to the -1 frame (Léger et al. 2007; Brakier-Gingras and Dulude 2010), thereby translating the Gag-Pol polyprotein. Some propose that the affinity of codon-anticodon tRNA pairing play a role in frameshifting efficiency (Brierley et al., 1997; Tsuchihashi, 1991).

Several theories also aim to explain why only a small percentage of ribosomes (5%) conduct frameshifting in human cultured cells (Dulude et al., 2006). Since ribosomes are assumed to exist in varied energetic states as a result of "stochastic thermal fluctuations", it is possible that the small proportion of frameshifting ribosomes overcome an energetic barrier and are within a favourable and stable energetic state (Frank & Gonzalez, 2010). Furthermore, translational kinetics involving the distance between elongating ribosomes may also play a role in frameshift efficiency. Since the ribosome unwinds the stimulatory signal to frameshift, and this structure is necessary for frameshifting, the proximity of the following ribosome and the re-folding of the stimulatory signal may influence frameshifting efficiency (Liao et al. 2011; Charbonneau et al. 2012)

Alternatively, ribosomes could be specialized to frameshift by either undergoing ribosomal modifications (such as posttranscriptional and posttranslational modifications) (Plant & Dinman, 2006) or by excluding ribosomal proteins or cellular factors that are usually associated with canonical translating ribosomes (Gilbert, 2011). One potential regulatory cellular factor is the release factor eRF1. Through an unknown mechanism, reduction of eRF1 led to two-fold increase in HIV-1 frameshifting (Kobayashi et al., 2010). Furthermore, a cellular protein kinase R (PKR) which decreased translational initiation at low concentrations of the transactivation response element, led to increased HIV-1 frameshifting indicating a potential role in mediating frameshifting efficiency (Gendron et al., 2008).

1.5.4 Relevance of Gag and Gag-Pol production to HIV-1 replication kinetics

In retroviruses, -1 ribosomal frameshifting is a very regulated process and found vital for replication and infection (Ian Brierley & Dos Ramos, 2006; Dulude et al., 2006; Maia et al., 1996). The first study to demonstrate this was conducted with the L-A double-stranded RNA (dsRNA) virus in *Saccharomyces cerevisiae*, which produces a 76kDa Gag protein and a 170kDa Gag-Pol polyprotein upon -1 frameshifting (Dinman et al., 1991). By

controlling the ratio of Gag to Gag-Pol proteins using a L-A cDNA expression plasmid, the authors found that a frameshifting efficiency of 1.9% was vital for the M1 satellite viral propagation. Altering this ratio of Gag to Gag-Pol polyproteins by more than twofold had a negative impact on viral propagation (Dinman & Wickner, 1992). -1 programmed frameshifting in HIV-1 produces a specific ratio (20:1) of Gag and Gag-Pol polyproteins which are precursors for important structural and enzymatic viral proteins. During virion maturation, the Gag precursor produces MA, CA, NC and p6 proteins while Gag-Pol polyprotein produces PR, RT and IN enzymes. Moreover, the Gag and Gag-Pol precursor polyproteins produced by -1 frameshifting play vital roles in HIV-1 assembly, budding and maturation (Dulude et al., 2006; Hung, Patel, Davis, & Green, 1998; Karacostas et al., 1993; Park & Morrow, 1991; Shehu-Xhilaga et al., 2001; Telenti et al., 2002). As detailed below, compromising levels of Gag and Gag-Pol has detrimental effects on HIV-1 replication and therefore serves as an attractive drug target.

Decreasing the frameshifting efficiency of the HIV-1 gag and pol genes can lead to increased production of Gag precursor and reduced Gag-Pol levels, which in turn, abrogates the maturation of viral particles. An initial study found that infection of insect cells with recombinant Gag infectious baculovirus led to the production of immature viral particles with uncleaved Gag polyprotein (Gheysen et al., 1989). Electron microscopy confirmed that the observed budding structures resembled immature HIV-1 viral particles (Gheysen et al., 1989). In another system using a simian virus 40 late replacement vector, Gag transfection in CMT3-COS cells also led to the formation of immature virus-like particles and did not depend on proteolytic processing to express Gag in the viral supernatant (Smith et al., 1993). Uncleaved Gag polyprotein expression was observed in released virus-like particles (VLPs) following protease-deficient Gag transfection in both COS-1 cells and $CD4^+$ T cells (Kaye & Lever, 1996). Moreover, RNAse protection assays used to determine cytoplasmic and particle-associated RNA revealed that the Gag polyprotein alone was capable of packaging and encapsidating full-length viral RNA into released VLPs (Kaye & Lever, 1996). The Gag-Pol

precursor encodes viral enzymes including PR which is required for viral maturation through proteolytic cleavage of the Gag and Gag-Pol polyproteins in released immature VLPs. Therefore, abolished Gag-Pol polyprotein levels which perturb infectious HIV-1 virion production and subsequent infection, can be achieved through decreased HIV-1 frameshifting efficiency. Several studies have found that decreased HIV-1 frameshifting efficiency does indeed compromise HIV-1 replication. Natural or laboratory strains of HIV-1 frameshift stem loop structures corresponding to greater than 60% reduction in frameshifting efficiency, compromised HIV-1 replication (Telenti et al., 2002). However, while a 16-42% reduction in frameshifting efficiency led to defective Gag and Pol processing and maturation, viral replication was untarnished. In contrast, Dulude et al. (2006) demonstrated that any reduction in HIV-1 replication strongly correlated with mutation-induced defects in HIV-1 frameshifting efficiency. While these conflicting results are likely due to differences in experimental systems employed, there is sufficient evidence outlining the importance of decreased HIV-1 frameshifting efficiency and subsequent reduction of Gag-Pol polyprotein levels in HIV-1 replication.

Alternatively, increased Gag-Pol polyprotein production and decreased Gag levels potentially regulated by increased HIV-1 frameshifting, was also found detrimental to viral replication, particularly, to viral assembly and budding. Several studies found that the production of Gag-Pol alone abolished the production of virus-like particles. To study the effect of varying levels of Gag-Pol, mutations were introduced in the frameshift region of HIV-1 proviral genomes to place the *gag* and *pol* genes in the same translational reading frame. Transfection of this mutated genome in COS-1 cells led to the expression of Gag-Pol polyproteins along with the respective gene products, with RT being expressed at much higher levels in the supernatant compared to wild-type HIV-1 (Park & Morrow, 1991). Interestingly, while p24 and RT were detected in the cell supernatant, analysis of viral proteins following sucrose density gradient centrifugation revealed no evidence of viral assembly or infectious viral particle production. This was also apparent by

the lack of infection from co-culture of these transfected COS-1 cells with uninfected Supt1 T-cells, where no assembly or virion formation was detected (Park & Morrow, 1991). Similarly, the deficiency in viral particle formation and release was also observed in CMT3-COS cells transfected with the Gag-Pol polyprotein within a simian virus 40 late replacement vector. However, intracellular proteolytic processing was unperturbed (Park & Morrow, 1991; Smith et al., 1993). The effects of Gag-Pol were further characterized by inactivating the protease domain through mutagenesis and independently adding the Gag precursor (Kaye & Lever, 1996; Park & Morrow, 1992). In contrast to Gag-Pol polyprotein alone, the addition of Gag led to the production of virions containing both the Gag and Gag-Pol polyproteins with reverse transcriptase activity (Park & Morrow, 1992). This rescued effect of Gag in Gag-Pol transfected cells was also recapitulated in $CD4^+$ T cells (Kaye & Lever, 1996). These defects were also corroborated by electron microscopy analysis of $CD4^+$ T cells and rabbit epithelia RK-13 cells infected with recombinant vaccinia virus expressing artificially in-frame Gag-Pol polyprotein; this led to undetectable budding structures and HIV-1 particles (Hoshikawa et al., 1991).This indicated that Gag is not only required for virus assembly, but also for the incorporation of Gag-Pol into released virions.

Promoting Gag-Pol polyprotein through increased HIV-1 frameshifting can thus have inhibitory effects on HIV-1 replication through compromised assembly and release of viral particles. Studies show that increased HIV-1 frameshifting, to a certain degree, can inhibit HIV-1 replication. Using luciferase constructs and the detection of Gag-Pol polyproteins in HIV-1, sparsomycin (400nM) increased frameshifting efficiency by 1.3-fold, but also increased HIV-1 replication (Miyauchi et al., 2006). In contrast, Shuhu-Xhilaga et al. (2001) used Gag-Pol expression vectors to artificially introduce increased ratios of Gag:Gag-Pol in HIV-1 transfected cells and found that virion RNA packaging was unaffected. However, dimer stability of HIV-1 RNA copies and infectivity was reduced (Shehu-Xhilaga et al., 2001).

It is therefore evident that altering the ratio of HIV-1 Gag:Gag-Pol polyproteins compromises HIV-1 replication. Decreased ribosomal frameshifting, which reduces the production of Gag-Pol, produces non-infectious immature viral particles that are unable to infect host cells. Conversely, increased ribosomal frameshifting stimulates Gag-Pol synthesis and subsequently attenuates Gag production, causing a defect in viral assembly; this prevents infectious particle production. Therefore, the frameshifting efficiency that regulates this ratio of Gag and Gag-Pol polyproteins, play a vital role in HIV-1 replication, and is thus an attractive drug target.

1.5.5 Frameshifting in human genes

While frameshifting primarily takes place within retroviruses, there are two candidate human genes that undergo -1 ribosomal frameshifting and a tumour suppressor APC gene that potentially does as well. Hence, efforts to develop HIV-1 frameshift-targeted drugs should avoid adverse cellular effects by ensuring that human frameshifting genes are unaffected. The human cellular paternally expressed gene (PEG10) and human paraneoplastic antigen Ma3 gene both have retroviral origin and undergo programmed -1 ribosomal frameshifting.

PEG10 is the human ortholog of mouse *Edr* (embryonal carcinoma differentiation regulated) gene (Manktelow et al., 2005; Shigemoto et al., 2001) and is highly expressed during development (Lux et al., 2010). *PEG10* contains two overlapping reading frames and a frameshift element which undergoes -1 frameshifting at an efficiency of 15-30% *in vitro* and in cell culture to produce two proteins (Clark et al., 2007). The second ORF produced as a result of -1 frameshifting was found to encode a protease that may be essential for the developmental function of PEG10 (Clark et al., 2007). It has also been postulated that PEG10 has an oncogenic function, especially in hepatocellular carcinoma (Chunsong et al., 2006; C. M. Li et al., 2006; Okabe et al., 2003).

While the function of the mammalian Ma3 gene is unknown, it is primarily expressed in the brain and testis; and ectopically expressed in tumours associated with neurological phenotypes (Baranov et al. 2011). Bioinformatics approaches led to the discovery that the first open reading frame bears homology to retroviral Gag protein and contains a frameshifting element that leads to approximately 20% frameshifting efficiency *in vitro* and *in vivo* (Wills et al., 2006). It is uncertain whether frameshifting of the Ma3 gene has any biological or physiological relevance, but is important to consider due to the neurological effects associated with ectopic expression.

Another human gene that undergoes frameshifting is the adenomatous polyposis coli (APC) gene which plays a role in the mammalian Wnt/*Wingless* signalling pathway (Cadigan & Nusse, 1997) and has an impact on development (Cadigan & Nusse, 1997). In yeast, APC undergoes non-programmed -1 frameshifting to stabilize mRNA and control abundance, however, while it has a potential to do so in eukaryotes, it has not yet been observed (Belew et al., 2011; Carlson et al., 2010). Nevertheless, the association of truncated mammalian APC with colon cancer outlines potential relevance of frameshifting (Nekrutenko et al., 2002). Consequently, approaches used to target ribosomal frameshifting of HIV-1 Gag and Gag-Pol polyproteins should monitor the effect on frameshifting of human PEG10, Ma3 and APC genes, as this can potentially lead to detrimental cellular effects.

1.6 Approaches used to target ribosomal frameshifting

Due to the importance of -1 frameshifting in viral replication, several approaches have been used to identify antiviral therapeutics that target ribosomal frameshifting in viruses such as HIV-1. These studies were conducted in yeast, mammalian cells and bacteria.

The first study to demonstrate the antiviral effect of drugs that alter viral frameshifting, was done in yeast which have a similar underlying mechanism of frameshifting compared to mammalian cells (Dinman et al., 1991; Dinman & Wickner, 1992; Stahl et al., 1995; Wilson et al., 1988). Peptidyl-transferase

inhibitors, sparsomycin and anisomycin, altered the level of -1 frameshifting by increasing and decreasing frameshifting efficiency, respectively. This subsequently inhibited satellite viral propagation in a L-A dsRNA and M1 satellite virus system (described in section 1.5.4) (Dinman et al., 1997).

The first study to identify drugs that inhibit HIV-1 replication by altering the ratio of HIV-1 Gag and Gag:Pol was conducted using a luciferase reporter assay. The HIV-1 frameshift element was inserted within the *Firefly luciferase* gene so that luciferase production was solely dependent on -1 frameshifting. This HIV-1 frameshifting model was used to screen 56,000 chemical agents and ultimately identified a benzene derivative, RG501 (1,4-bis-[N-(3-N,N-dimethylpropyl) amidino] benzene tetrahydrochloride), which increased HIV-1 frameshift efficiency by two-fold and subsequently inhibited HIV-1 replication (Hung et al., 1998). However, RG501 had off-target effects since the frameshifting inhibitory dose was higher than the dose required to inhibit HIV-1 replication (Ian Brierley & Dos Ramos, 2006). This was also re-enforced by the ability of RG501 to alter the frameshifting efficiency of other viruses (Hung et al., 1998), and to interact with structures similar to the HIV-1 frameshift stimulatory signal including RNA helices with more than 9 base pairs, which are also found in the ribosome (Marcheschi et al., 2011).

To simultaneously monitor global translational effects, dual luciferase constructs were utilized such that the HIV-1 frameshift element was embedded between an upstream *Renilla luciferase* gene, representative of global or cap-dependent translation, and a downstream *Firefly luciferase* gene which is produced upon -1 frameshifting. These successfully mimicked -1 HIV-1 frameshifting in both yeast (Harger & Dinman, 2003) and mammalian cells (Grentzmann et al., 1998). Fluorescent bi-cistronic constructs were then designed to recapitulate HIV-1 frameshifting in yeast (Rakauskait et al., 2011), bacteria (Dulude et al., 2008) and mammalian cells (Cardno et al., 2009).

Screening efforts were also made to identify HIV-1 frameshift RNA-binders that target the stability of the frameshift structure to alter frameshifting. Dulude *et al.* (2008) used a bi-cistronic reporter assay and thioredoxin scaffold in bacteria to screen a library of arginine-rich peptides that could perturb HIV-1 frameshifting by RNA binding. By examining the fluorescence intensity of GFP (Green fluorescent protein) and RFP (Red fluorescent protein) which depend on HIV-1 frameshifting and normal translation, respectively, they identified peptides that reduced frameshifting efficiency more that 50%, without affecting normal translation (Dulude et al., 2008). They verified that observed effects were scaffold-independent and HIV-1 frameshift-specific. However, these peptides modulated frameshifting of other viruses and were not yet determined to inhibit HIV-1 replication (Dulude et al., 2008). This was followed by more efforts to identify drugs that bound to the frameshift RNA region (Marcheschi et al., 2011; Staple & Butcher, 2005). Using a fluorescent nucleotide analogue within the HIV-1 frameshift element, Marcheschi *et al.* (2008) screened 34,500 small molecules and identified a compound, doxorubicin that bound the HIV-1 RNA frameshift region and decreased frameshifting efficiency by 28%, but also inhibited global translation.

Another approach screened a resin-bound dynamic combinatorial library and identified a high-affinity ligand for the HIV-1 frameshift stem-loop region where disulfide-containing peptides bound to HIV-1 frameshift RNA (McNaughton et al., 2007). While further medicinal chemistry was performed to increase selectivity, affinity and biostability of this compound for the HIV-1 frameshift region, the effect on HIV-1 replication was not determined et al., 2010).

Antisense oligonucleotides were also used to study and screen modulators of HIV-1 frameshifting. A morpholino antisense oligonucleotide, 2'-O-methyl, phosphorothioate, targeted mRNA downstream of the slippery site and stimulated frameshifting efficiency by 40% (Howard et al., 2004). Frameshifting frequency was also enhanced when the frameshift region was

targeted by antisense RNA oligonucleotides (Olsthoorn et al., 2004), the efficiency of which was dependent on the length of the RNA (Yu et al., 2010). While the use of oligonucleotides has not been successful in inhibiting HIV-1 replication, an antisense peptide nucleic acid has been successful in compromising severe acute respiratory syndrome coronavirus (SARS-CoV) replication by binding to the frameshift region and decreasing -1 frameshifting efficiency (Ahn et al., 2011). This summarizes the approaches used thus far to study HIV-1 frameshifting and identify molecules and peptides that module the efficiency of frameshifting. While these approaches did not yield a potent HIV-1 frameshift-specific drug, the advantages and disadvantages of various approaches should be considered during future efforts to developing therapeutics targeting HIV-1 frameshifting of *gag* and *pol* genes.

1.7 Drug discovery pipeline

The drug discovery process is comprehensive and uses various disciplines (such as biology, chemistry and bioinformatics) towards the discovery and development of therapeutics against diseases. The pipeline generally involves the identification and validation of a drug target, followed by compound screening in a high-throughput manner to identify hit compounds which are optimized and enter pre-clinical and clinical trials if successful.

1.7.1 Target identification and validation

The first step in drug screening is to identify a 'druggable' biological target that has a vital mechanism or function in a specific disease. Due to the significant investment of finances, time and resources required to develop a drug, validation of a drug target is crucial to confirm and understand the effect of this target in disease. Target validation consists of developing an assay to test a compound's biological effect and therefore identify those with desired activity. These targets are usually proteins or nucleic acids, including enzymes, receptors, ion channels and transporters that lead to a beneficial therapeutic response in response to a suitable drug.

1.7.2 Assay and screening development

Following drug target validation, the assay is miniaturized for use in a high-throughput manner and at a reasonable cost by the optimization of biological and statistical parameters. The biological factors depend on the type of assay (ex. biochemical or cell-based) but often include cell density, amount of substrate or reagent and incubation period. Statistical parameters include the signal-to-noise ratio, variability, window of signal output and Z-factor (Goktug et al 2013), which uses positive and negative controls to measure the range of signal within a plate.

Screening conditions are optimized to maintain assay quality, reliability and stability without hindering throughput and costs. Fluorescence, luminescence and absorbance are some of the methods used as assay readouts in the screening process. Hence, the screening development process should ensure that the parameters underlying the mode of detection are optimized to avoid false positive or false negative results. One such example is to avoid short excitation wavelengths (especially those below 400nm) in fluorescent-based assays with small molecules to prevent compound-induced interference (Macarrón et al. 2009).

1.7.3 Screening for hit identification

1.7.3.1 Screening strategies

There are various screening strategies that usually depend on the collection of compounds used. These include random screening, hit-directed nearest neighbour screening and focused (or targeted) screening (Silverman & Holladay, 2014).

Random screening consists of using a large library of compounds to rapidly identify those that elicit a desired activity (activation, inhibition etc.). This methodology does not require any prior target structural data and rapidly processes several compounds in a high-throughput manner, regardless of compound properties (Valler & Green, 2000). This was commonly used when no known drugs affect the target of interest. Similarly, diversity screening

tests a large number of diverse molecules with varied structure that could serve as a drug candidate. This potentially generates lead molecules that help delineates structure-activity relationship.

Another method of screening, hit-directed nearest neighbour screening, was derived in an effort to improve random screening. This methodology groups compounds together based on structure, a computational approach known as clustering, in order to screen representative subsets of compounds. This is usually followed by the screening of compounds structurally similar to the initial hits obtained in an attempt to identify additional hits (Ryan et al., 2003). This is also considered a form of focused screening which is usually conducted with the knowledge of either the target structure or known ligands. Focused screening uses structural information such as three-dimensional information and target crystal structures, to computationally analyze and identify structures that will likely bind the target. This not only requires the availability of all compound structures, but a means to analyze them and knowledge of structural attributes that are needed for biological effect or activity. Furthermore, any established ligand can be used to design pharmacophores to the active site or binding site to search for similar compounds and improve hit rates (Ashton et al., 1996; Marriott et al., 1999).

1.7.3.2 Primary screen

In order to conduct primary screens, it is vital to ensure sensitivity and specificity of hits. Primary screens are usually performed in a high-throughput manner by testing compounds at a single concentration. Compounds with an active biological response are referred to as *hits*. The activity distribution of hits not only depend on the diversity of the compound libraries, but also the target and involved pathway(s) (Entzeroth et al., 2009; Gillet, 2008; Kümmel & Parker, 2011). To eliminate hits associated with assay errors, screens are run in replicates (Wu et al., 2008) or at different concentrations of compound (Inglese et al., 2006). Alternatively, activity cut-offs are arbitrarily set (for example, to 6 times the standard deviation of the mean) to reduce false positives and false negative hits.

1.7.3.3 Data handling and hit identification

Due to the large amount of data that is generated from the primary screen (and future confirmatory screens), data handling is a critical process that includes data management, storage and analysis. A main database which serves as a repository for incoming screening data has the capacity to store all pertinent screening information such as plate content, compound identity, drug concentration, plate barcodes and signal readout. Furthermore, a robust data analysis engine is necessary to computationally derive results, both statistically and visually, to identify hits.

During the selection process, hits are selected statistically, biologically and chemically. Statistically, one has to determine the optimal threshold to select true positives and eliminate true negatives. Logistically, a manageable amount of hits can be carried through into secondary assays. Secondary assays that evaluate potency, selectivity and specificity, thereby select hits, biologically. Further chemical analysis can cluster hits into groups based on similar chemical structures and chemotypes.

1.7.3.4 Confirmatory screens

Secondary screens aim to confirm specificity of hit compounds derived from a primary screen. This usually entails dose-response screens to test the activity of a hit at a range of different concentrations. This allows a quantitative assessment of the activity of a hit compound and is defined by four parameters including minimum response, maximum response, Hill slope (or Hill coefficient) and the XC_{50} value (Figure 6). The Hill slope refers to the steepness of the dose-response curve. The XC_{50} value is the inflection point of the curve corresponding to 50% response and is indicative of compound potency. These four parameters are applied to dose-response effects from hits to confirm activity.

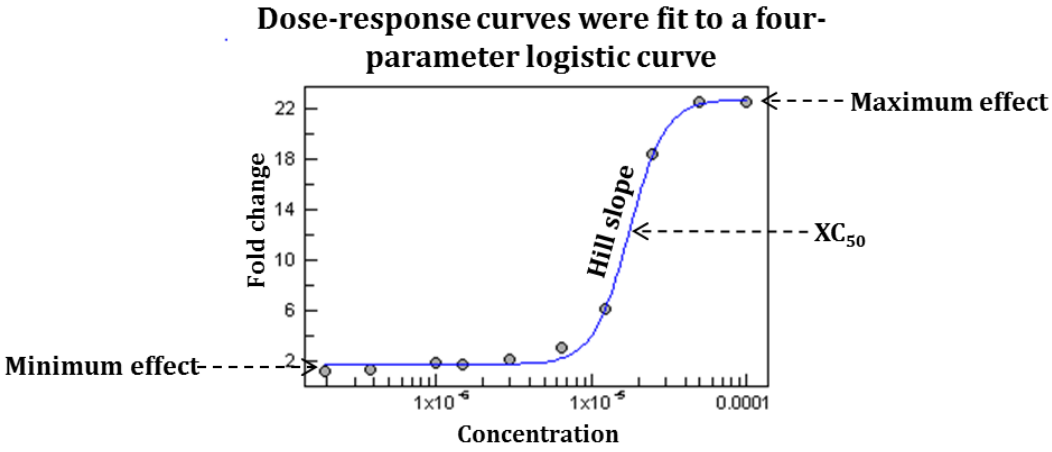

Figure 6 Four-parameter logistic curve that dose-dependent effects are fitted to.
During confirmatory screening, dose-dependent effects of compounds are fitted to a four-parameter logistic curve to indicate the minimum response, maximum response, the Hill slope and XC_{50} value indicative of potency. Curve depicted was visualized using ActivityBase XE software.

1.7.4 Lead identification and optimization

Active hits following secondary confirmatory screens are referred to as *leads* or *lead compounds*. Leads that possess undesirable chemical characteristics undergo modifications to optimize features. Such features include low toxicity, high selectivity, high affinity, high potency, high solubility, good absorption, metabolism and bioavailability.

Highly potent drugs exert a strong biological effect and are active at low concentrations. This is ideal as it minimizes cost and dosage requirements, but also the risk of unspecific off-target effects, therefore resulting in strong selectivity. Off-targets include any related target family members that may lead to different physiological or biological effects, hERG (human ether à go-go related gene) channel which is vital for cardiac function and fatal when inhibited, along with the cytochrome P450 enzyme family which is involved in drug metabolism.

Drug metabolism is often examined to confirm the dose and dosing frequency required to maintain therapeutic levels. Furthermore, the effects of enzymatically-generated drug metabolites and mode of drug excretion are

also analyzed to prevent unfavourable side effects. Absorption of the drug into the bloodstream from the point of administration, and subsequent distribution within targeting parts of the body is imperative to ensure that the solubility or affinity of the drug for an organic or aqueous environment (partition coefficient) is not affected. Moreover, a drug's effect on transporters is also monitored since they could play a role in absorption by affecting the amount of drugs in and out of cells.

Furthermore, *The Rule of 5*, proposed by Lipinski (Lipinski et al., 2012) along with analysis of compounds by Gleeson (Gleeson, 2008) found a correlation between low molecular weight compounds (MW<400), low measure of lipophilicity (log*P*<4) and state of ionization as important factors affecting ADME (absorption, distribution, metabolism, excretion). Moreover, the number of hydrogen bond-donors and -acceptors also impact the ability of a drug to "cross the blood-brain barrier" (van de Waterbeemd et al., 1998). Low topological polar surface area (TPSA), which is a three-dimensional measure of the total surface area of polar atoms in a molecule, also has favourable effects on oral bioavailability, likely due to increased membrane permeability (Ertl et al., 2000). In addition to modification for favourable lead compounds, lead analogues are also synthesized and evaluated in relevant assays. Further analysis of structure-activity relationship (SAR) of lead small molecules can help predict the outcome of some of these features and may therefore be helpful in the early stages of drug discovery.

1.7.5 Pre-clinical trials

In order for a lead compound to be designated as a *candidate drug*, it has to undergo several biological and pharmalogical tests. They are tested in animal models for parameters such as 'ADMET (absorption, distribution, metabolism, excretion and toxicity)' (described in 1.7.4) along with other pharmacokinetic tests. Drug development at the pre-clinical levels involves optimizing synthesis and manufacture of the candidate drug on a large scale. Additionally, drugs development involves the formation of different forms

(solution, pill etc.) for administration in animals for testing, and upon approval, in humans for clinical trials.

1.7.6 Clinical trials

Drugs, then termed *clinical drugs*, are subjected to clinical trials which consist of three main phases to evaluate drug dosage, side effects, toxicity and efficacy in humans.

Phase I clinical trials are conducted in approximately 20-100 healthy human volunteers to test pharmacological effects such as tolerance, safety and pharmacokinetic effects, in comparison to the outcome in pre-clinical animal studies. Phase II clinical trials are carried out with hundreds of diseased human patients to assess the effectiveness of a candidate drug along with adverse side effects, and dosage requirements. Lastly, phase III trials completed in thousands of diseased human patients and control patients strive to determine the candidate drug efficacy, side effects and long-term effects in comparison to currently approved drugs.

1.8 Objectives and rationale

As described in section 1.5.4, -1 ribosomal frameshifting is vital in producing a specific ratio of Gag and Gag-Pol polyproteins in HIV-1. This ratio and therefore the efficiency of frameshifting, is imperative for the production of mature HIV-1 particles. While approved drugs efficiently target HIV-1 entry, reverse transcription, integration and protease-mediated viral maturation, the lack of a cure, emerging resistance and undesirable side effects still raise the need for novel, effective therapeutics in novel mechanistic drug classes. HIV-1 Gag:Gag-Pol frameshifting is an attractive drug target and is the focus of this thesis. The primary objective is to discover effective small molecules that target HIV-1 frameshifting and subsequently inhibit HIV-1 infection. This was done by employing a drug discovery platform to screen diverse molecules for modulators of HIV-1 Gag:Gag-Pol frameshifting using a bicistronic fluorescence cell-based assay that recapitulates HIV-1 frameshifting *in vitro*.

Chapter 2
Materials and Methods

2.1 Cells

Human embryonic kidney 293T (HEK293T), human cervical carcinoma (HeLa) cells and African Green monkey kidney epithelial (Vero) cells were maintained in Dulbecco's minimal essential medium (DMEM) with high glucose supplemented with 10% heat-inactivated fetal bovine serum (FBS). Human T-cell lines (kindly provided by Sam Wilson), MT-4 and MT-4R5 cells (MT-4 cells expressing CCR5 co-receptor) suspension cells, were maintained in Roswell Park Memorial Institute (RPMI) media with L-glutamine and supplemented with 10% fetal calf serum (FCS) and gentamicin. All cells were maintained at 37°C and 5% CO_2 conditions and checked for mycoplasma. Stably-transfected and clonally-derived HeLa cells (described in section 2.3) were selected and maintained with 0.4mg/ml geneticin (Roche).

2.2 Plasmids

2.2.1 HIV-1 plasmids

All the following DNA plasmids were kindly provided by Dr. Sam Wilson (University of Glasgow) and used to study the replication kinetics of HIV-1. Three plasmids were used to generate pseudotyped viral particles: pHRSIN-cSGW, pCRV1-NLGP and pCMV-VSV-G. pHRSIN-cSGW is a self-inactivating GFP-expressing HIV-1 based vector (Demaison et al., 2002); pCRV1-NLGP encodes HIV-1 *gag, pol* and *rev* and pCMV-VSV-G encodes a VSV-G envelope. To generate replication-competent HIV-1 particles, pNHG (Accession: JQ585717) and pNL4-3 (Accession: M19921) plasmids were used. NHG is an HIV-1 proviral plasmid containing a portion of HIV-1_{NL4-3} and HIV-1_{HXB2} strains with GFP in place of the *nef* accessory gene. pNL4-3 encodes a complete HIV-1 proviral genome. To generate protease-deficient HIV-1 particles, a pNL4-3 Pr- (protease-deficient) plasmid was used. pNL4-3 Pr- was derived from pNHGCapNM and pNL4-3 (NIH AIDS Research and Reference Reagent Program, Catalog No. 114), harbouring a point mutation in the protease active site.

2.2.2 Dual luciferase DNA plasmids

To initially study HIV-1 frameshifting, I obtained a dual luciferase DNA plasmid which contained a mutated HIV-1 frameshift region between an upstream *Renilla luciferase* gene (RLuc) and a downstream *Firefly luciferase* (FLuc) gene in a pcDNA3.1 vector backbone (provided by DWB). This DNA plasmid, referred to as RLuc-M1-FLuc, contained a mutation and deletion in the HIV-1 frameshift region. The first round of site-directed mutagenesis (described in section 2.2.1.1) was used to create RLuc-M2-Luc, by inserting a guanine in the structural purine-rich bulge separating the upper and lower stem of the stem loop structure comprising the frameshift stimulatory signal. This was followed by the creation of a full-length frameshift dual luciferase DNA plasmid designated RLuc-HIV FS-FLuc by completing the 3' end of the stem loop structure. With RLuc-HIV FS-FLuc, Firefly luciferase was only produced upon frameshifting. A translational control DNA plasmid for each mutant was also created by adding an adenine immediately after the slippery site of the frameshift region. This ensured that FLuc was in-frame with RLuc and therefore synthesized only by ribosomes that followed conventional rules of translation. All DNA constructs are shown in Figure 7.

Following stable transfection of these DNA plasmids in HeLa cells, dual luciferase assays (Promega) were performed to examine frameshifting efficiency. Consistent with previous studies, the frameshifting efficiency of the full-length HIV-1 frameshift construct was 22% and decreased in the presence of deletions within the frameshift region, likely due to compromised structural integrity Figure 8.

Due to emerging false positive interactions between luciferase and compounds (Berry et al., 2011), these dual luciferase constructs were discontinued and bi-cistronic fluorescent constructs were employed instead.

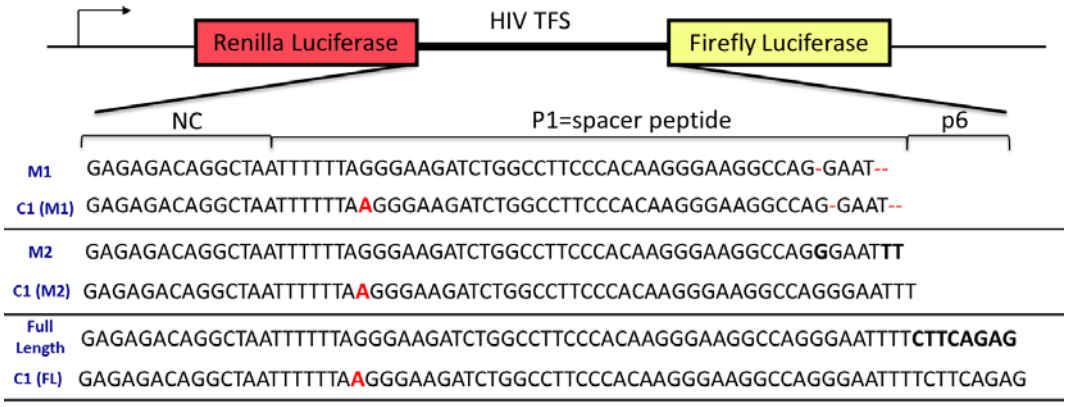

Figure 7 Dual luciferase DNA constructs initially synthesized to study HIV Gag:Gag-Pol frameshifting

M1, M2 and full length sequences are inserts embedded between dual luciferase genes that produce Firefly luciferase upon ribosomal frameshifting. M2 was synthesized by site-directed mutagenesis using M1 as a template and full length was created using M2 as a template. C1 are translational controls created for each frameshifting construct (M1, M2 and full length) to place Firefly luciferase in the same open reading frame as Renilla luciferase, thereby representing global translation.

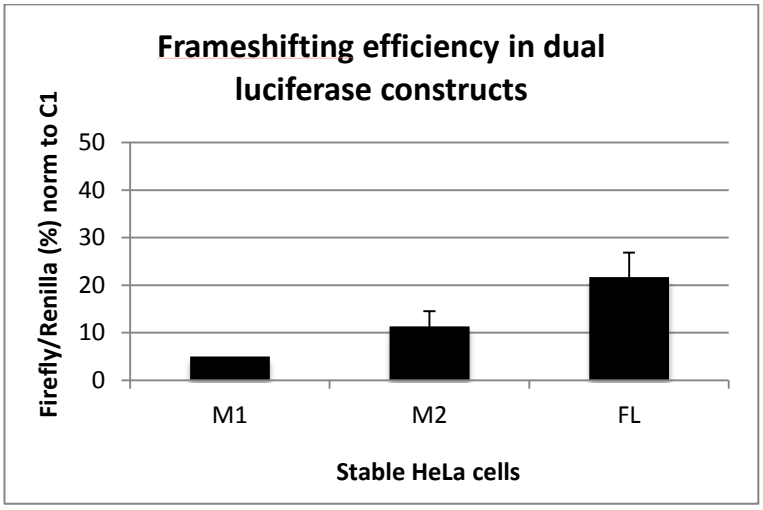

Figure 8 HIV-1 frameshifting efficiency of dual luciferase constructs

Bars represent mean frameshifting efficiency calculated by the percentage of Firefly luciferase (FLuc) to Renilla luciferase (RLuc) of each HIV FS construct (M1, M2, FL) normalized to the FLuc:RLuc ratio of the respective translational control (C1M1 C1M2, C1FL). Error bars are standard deviation from two biological replicates (n=2).

2.2.2.1 Site-directed mutagenesis

The QuikChange II Site-directed mutagenesis kit (Agilent Technologies) was used to correct the mutated HIV-1 frameshift region within the dual luciferase plasmid and to create translational control plasmids. Mutagenic oligonucleotides used to perform mutant strand synthesis reaction are listed in Table 1.

The total 50µl reaction contained 5µl of 10x buffer, 10 ng of template DNA, 125ng of each primer, 1µl of dNTP mix and 1µl of *PfuUltra* high fidelity DNA polymerase and RNase/DNase-free water. The thermal cycling conditions were as follows:

1. 95°C for 30 seconds
2. 16-18 cycles of:
   95°C for 30 seconds
   55°C for 1 minute
   68°C for 1 minute

To synthesize RLuc-HIV TFS-FLuc, 1.5µl of DMSO was also added to the reaction. Immediately following mutant strain synthesis reaction, the reaction was placed on ice for 2 minutes, followed by the addition of 1µl of DpnI restriction enzyme and incubation for 1 hour at 37°C. 1µl of the DpnI-digested reaction was added to 50µl thawed XL1-Blue super-competent cells and incubated on ice for 30 minutes. The transformation reaction was then heat pulsed at 42°C for 45 seconds and placed on ice for 2 minutes. 0.5mls of pre-heated Super Optimal Broth (SOC) media was added to the reaction and shaken at 250rpm for 1 hour at 37°C. The reaction was then spread on Luria broth (LB) agar plates with ampicillin (100µg/ml) and incubated at 37°C for 16-18 hours. 5mls of LB liquid cultures with ampicillin (100µg/ml) were inoculated with individual bacterial colonies and shaken for 16-18 hours at 37°C. Following centrifugation of inoculated cultures, plasmid DNA was purified (described in section 2.2.1.2).

To verify the DNA clones of interest, purified plasmid DNA was diagnostically digested using restriction enzymes flanking RLuc, HIV-1 frameshift region

and FLuc. Once confirmed by sequencing, plasmid DNA was prepared by maxipreps (described in section 2.2.1.3).

Table 1 Mutagenic primers used in site-directed mutagenesis of dual luciferase constructs of HIV-1 Gag:Gag-Pol frameshifting

Target	Primer sequences
RLuc-M2-FLuc	Fwd 5'-ggaaggccagGgaatTTggatccATGGAAGA-3'
	Rev 5'-TCTTCCATggatccAAattcCctggccttcc-3'
RLuc-HIV FS-FLuc	Fwd 5'-gggaaggccagggaatttTCTTCAGAGggatccATGGAAGACGCC-3'
	Rev 5'-GGCGTCTTCCATggatccCTCTGAAGAaaattccctggccttccc-3'
Control	Fwd 5'-AGACAGGCTAATTTTTTAAGGGAAGATCTGGCCTTCC-3'
	Rev 5'-GGAAGGCCAGATCTTCCCTTAAAAAATTAGCCTGTCT-3'

2.2.2.2 DNA purification by miniprep

Following DNA plasmid transformation, 5ml bacterial cultures grown overnight were pelleted at 14,000rpm for 2 minutes and resuspended in 200µl of resuspension solution I. Following this, 200µl of cell lysis solution was added, the mixture was inverted 5-6 times and incubated at room temperature for 4 minutes. Following addition of neutralization solution, mixture inversion 5-6 times and centrifugation at 14,000rpm for 15 minutes, supernatant was transferred to another tube and underwent phenol/chloroform cleanup. This entailed adding an equal amount of phenol to the supernatant which was vortexed and centrifuged at 14,000rpm for 2 minutes. An equal volume of 24:1 chloroform:isoamyl was added to the aqueous (upper layer) of phenol-treated supernatant. This was vortexed and centrifuged at 14,000rpm for 2 minutes. The aqueous layer was transferred to a new tube for ethanol precipitation whereby 0.1X the volume of 3M NaAc (ph5.5) was added and mixed. 2X the volume of ice cold ethanol (100%) was added, mixed and centrifuged at 14,000rpm for 10mins. The supernatant was discarded and the remaining pellet is washed in 500µl of ice cold ethanol (75%). Following centrifugation at 14,000rpm for 10 minutes, the supernatant was discarded and the pellet was resuspended in DNAse-and RNase-free water.

2.2.2.3 DNA purification by maxiprep protocol

Luria broth (LB) (400mls with 100µg/ml ampicillin) liquid cultures inoculated with DNA-transformed bacterial colonies were centrifuged at 5000rpm for 15 minutes following overnight agitation at 37°C. Pellets were resuspended in 10mls of resuspension solution. Following addition of 10mls of cell lysis solution, mixture was inverted 4-6 times and incubated at room temperature for 4 minutes. Neutralization solution (10mls) was added and the mixture was inverted 3-6 times and centrifuged at 10,000rpm for 30 minutes at 4°C. Supernatant was isolated using a miracloth and equal volume of isopropanol was added. Following centrifugation at 10,000rpm for 10 minutes at 4°C, the resulting pellet was dried and resuspended in 4.5mls TE. Caesium chloride (4.8g) was added, mixed to dissolve and followed by the

addition of 300µl of ethidium bromide. Following overnight centrifugation at 45,000rpm at 20°C, a syringe was used to extract the lower visible band representing DNA. This was treated with an equal volume of CsCl-saturate isopropanol, mixed, and top pink band was discarded. This was repeated 6 times until a clear bottom band remained. This was topped to 4.5mls with water, with 500µl of 3M Sodium Acetate (NaAc) and 5mls of isopropanol, and centrifuged at 10,000rpm for 10 minutes at 4°C. The pellet was resuspended in 400µl TE and precipitated with ethanol by adding 40µl of NaAc and 1ml of ice-cold 100% EtOH, inverted to mix and centrifuged at 14,000rpm for 10 minutes. The pellet was washed with 500µl of ice-cold 70% EtOH and centrifuged again. The resulting DNA pellet was dried and resuspended in 200µl of TE.

2.2.3 Bi-cistronic fluorescent DNA plasmids

Using the full-length frameshift dual luciferase DNA plasmid, a dual fluorescent full-length frameshift DNA plasmid was created by GenScript Inc. to generate the full-length HIV-1 frameshift region in between an upstream eGFP and downstream mCherry cistron. This construct is referred to as HIV-1 frameshifting or eGFP-HIV FS-mCherry. Site-directed mutagenesis (described in section 2.2.1.1) was performed to create an in-frame translational control plasmid by adding an adenine immediately after the slippery site. mCherry was in the same open reading frame as eGFP and expression was consequently indicative of global translation. This construct is referred to as translational control or eGFP-Con-mCherry

2.3 Generation of cell lines

2.3.1 Transiently- and stably-transfected cells

To assess the effect of transiently-transfected cells on eGFP and mCherry expression, $4x10^6$ HeLa cells were seeded 24 hours prior to transfection with 40µg of plasmid DNA and 80µl of lipofectamine2000 (LifeTechnologies) in T-25 flasks. Cells were replaced with fresh media 5 hours after transfection. 48 hours after transfection, cells were assessed for eGFP and mCherry

expression using flow cytometry and remainder was frozen in DMEM with 20% FBS and 7% DMSO.

To generate stably-transfected cells, 0.5 x 10^6 HeLa cells were seeded in a 6-well plate 24 hours prior to DNA transfection with 4 μg DNA using lipofectamine. Transfected cells were incubated at 37°C for 48 hours and expanded for three weeks under the selection of 0.4mg/ml geneticin.

2.3.2 Clonal cell lines

Prior to generating a clonal population of the bi-cistronic HIV-1 frameshifting and translational control cells, flow cytometry was used to determine eGFP and mCherry fluorescence of stably-transfected cells (as described in 2.4.2). Flow cytometry-activated cell sorting (described in section 2.4.1) was used to isolate 960 eGFP-positive clones from each stable cell line. One clone or cell was placed in each well of multiple 96-well plates and incubated at 37°C until cell growth was clearly visible. 50 clones that were expanded were trypsinized and transferred into 6-well plates to promote cell expansion. From the 50 clones, 10 were randomly chosen, trypsinized and subjected to flow cytometry to determine eGFP and mCherry expression. One clonal population each from eGFP-HIV control-mCherry (translational control) and eGFP-HIV TFS-mCherry (HIV-1 frameshifting) HeLa cells were then expanded and used for further experiments.

2.4 Flow cytometry

Flow cytometry was used for cell sorting and for assaying eGFP and mCherry expression in clonally-derived HeLa cells, and GFP expression in MT-4 infected cells.

2.4.1 Flow cytometry activated cell sorting (FACS)

Single cells were sorted by Rosemary Clarke (University of Dundee) using an Influx (Becton Dickinson) cytometer with a 100 micron nozzle at 20psi. This cell sorter was not equipped with a 561nm laser, so sorting was solely based on eGFP fluorescence. The pink rectangles in Figure 9 indicate the approximate sort gates used in the cloning experiment and the red rectangles

indicate the likely inclusion of cells containing eGFP alone during sorting (Figure 9). Live single cells were identified on the basis of forward scatter (FSC) and side scatter (SSC) characteristics and the gates on the GFP histograms indicate the cells collected (Figure 10).

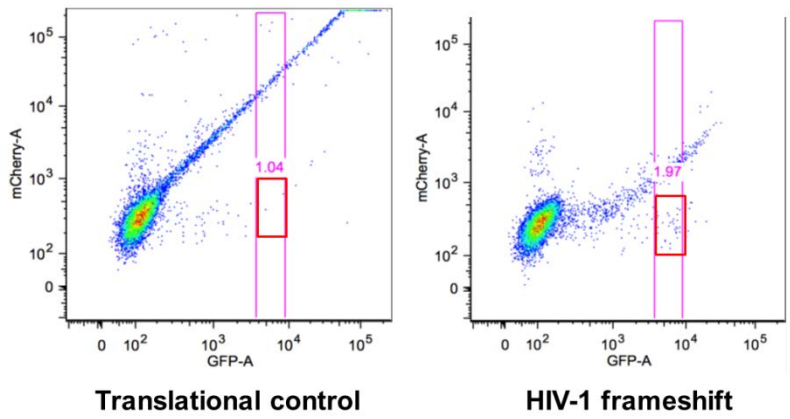

Figure 9 Flow cytometry-associated analysis of stably-transfected translational control and HIV-1 frameshift HeLa cells
Using an LSR Fortessa flow cytometer (Becton Dickinson), eGFP and mCherry fluorescence was determined in stably-transfected translational control and HIV-1 frameshifting HeLa cells. Pink gates indicate cells collected during cell sorting with the Influx cytometer (Becton Dickinson) and red rectangles indicate potential contamination with cells expressing just eGFP.

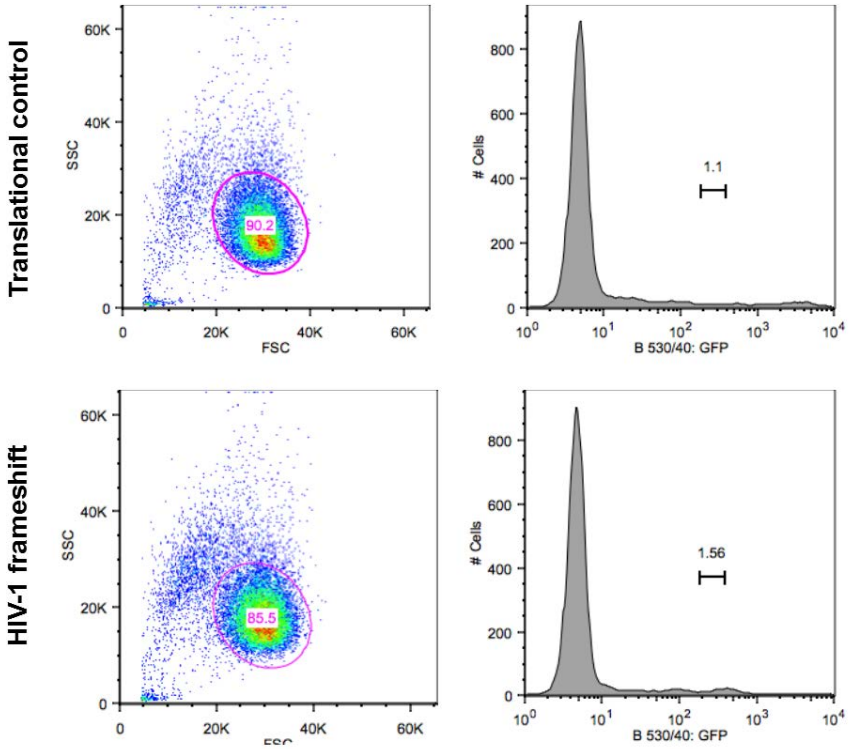

Figure 10 Gating strategy for single cell cloning by FACS
Live single cells were identified on the basis of forward scatter (FSC) and side scatter (SSC) characteristics and the gates on the GFP histograms indicate the cells collected.

2.4.2 GFP and mCherry expression

To examine eGFP and mCherry expression in clonally-derived HeLa cells, cells were trypsinized and centrifuged at 750rpm for 3 minutes at room temperature and resuspended in 0.5ml of PBS with 1% FCS. Using an LSR Fortessa flow cytometer (Becton Dickinson), 488nm laser was used to excite GFP, and emitted light was detected at 530±30nm. A 561nm laser was used to excite mCherry, and emitted light was detected at 610±20nm. To examine GFP expression in MT-4 infected cells, 100µl of cells were fixed with 100µl 4% paraformaldehyde (PFA, final concentration 2%) and analysed using the Guava Easy-Cyte 5HT instrument (Millipore).

2.5 Fluorescence microscopy

2.5.1 Confocal microscopy

To visualize eGFP and mCherry expression in stably-transfected translational control and HIV-1 frameshifting HeLa cells, 0.5 x 10^6 cells were seeded on coverslips in 6-well plates and grown overnight at 37°C. Slides were treated with 10% paraformaldehyde 24 hours later, washed with PBS and washed in water. Coverslips were then mounted on slides and a drop of 50% glycerol was placed on coverslips to visualize GFP and mCherry expression on the confocal laser-scanning microscope (Leica, Milton Keynes, UK; TCS SP5 II).

2.5.2 High-content imaging

To visualize eGFP and mCherry expression, 3,500 HeLa cells were seeded in each well of a 384-well plate (Greiner). After 48 hours, plates were run on the Operetta high-content imaging system (PerkinElmer) to visualize GFP and mCherry fluorescence.

2.6 Diversity screening

2.6.1 Primary screen

A diversity screen was conducted at the Drug Discovery Unit at the University of Dundee using the diversity screening library of 92,071 compounds. This library was assembled based on compounds with lead-like properties,

limited complexity and desirable functional groups (Brenk et al., 2008). Using a LabCyte Echo 550 acoustic dispenser, 150nl of 10mM compounds were acoustically transferred from Echo plates (LabCyte) to columns 1-10 and 13-22 in black, clear bottom 384-well assay plates (Greiner) for a final concentration of 30μM (done by James Roberts & Alex Cookson, University of Dundee). In a similar manner, 150nl of DMSO was transferred to columns 11, 12, 23 and 24 in the same 384-well assay plates and were barcoded. Following trypsinization, clonal HIV-1 frameshifting HeLa cells were resuspended in DMEM at 7 x 10^4 cells/ml. Using a Matrix Wellmate microplate dispenser (ThermoScientific), 50μl/well of this 7 x 10^4 cells/ml stock was added to the compound-and DMSO-containing 384-well assay plates and were subsequently incubated at 37°C and 5% CO_2 for 48 hours. On the day of assay, clonal HIV-1 frameshifting HeLa cells incubated with compounds were washed twice with 50μL of PBS using the Matrix Wellmate microplate dispenser and then incubated with 50μL of PBS for fluorescence assay. Using the Pherastar FS (BMG LabTech), mCherry expression was determined upon excitation and emission at 580nm and 610nm, respectively.

2.6.2 Dose-response screens

In order to conduct dose-response curves (DRCs), 30μl of compound (10mM stock) was transferred into 384-well holding plates. Using a Janus liquid handling robot (Perkin Elmer), 10-point two-fold dilutions were generated in DMSO for each compound. Following the transfer of these serial dilution curves into LabCyte Echo plates, the LabCyte Echo was used to dispense 500nl of each concentration into rows of black, clear bottom 384-well assay plates (done by James Roberts, University of Dundee). Columns 1-10 and 13-22 contained compounds for testing, which columns 11, 12, 23 and 24 contained DMSO at a final concentration of 0.3% (v/v). Replicate assay plates were created.

Similar to the primary screen, clonal HIV-1 frameshifting HeLa cells and translational control cells were trypsinized and resuspended in DMEM at 7 x 10^4 cells/ml. Using a Matrix Wellmate microplate dispenser

(ThermoScientific), 50µl/well of this 7 x 10^4 cells/ml stock was added to 384-well assay plates and were subsequently incubated at 37°C and 5% CO_2 for 48 hours. On the day of assay, cells were washed twice with 50µL of PBS using the Matrix Wellmate microplate dispenser and then incubated with 50µL of PBS for fluorescence assay. Using the Pherastar FS (BMG LabTech), mCherry expression was determined upon excitation and emission at 580nm and 610nm, respectively. Furthermore, eGFP fluorescence was also determined at excitation/emission of 485nm/520nm.

2.7 Cell viability assay

To quantify cell viability, following 48 hour incubation of compound-treated cells, resazurin was added at a final concentration of 45uM for four hours at 37°C. Using the Pherastar FS plate reader (BMGTech), fluorescence was measured at excitation of 550nm and emission of 590nm. The relative fluorescent units (RFUs) of compound-treated cells, indicative of cell viability, were quantified as a percentage relative to DMSO-treated cells.

2.8 Liquid Chromatography-Mass Spectrometry (LC-MS) and NMR

To confirm compound integrity and assess purity, hit compounds were subjected to LC-MS and NMR by Dr. Gavin Wood (University of Dundee). NMR spectra were recorded on a Bruker Avance DPX 500 spectrometer.

LC-MS analysis was performed on either an Agilent HPLC 1100 series connected to a Bruker Daltonics MicrOTOF or an Agilent Technologies 6130 quadrupole LC-MS, where both instruments were connected to an Agilent diode array detector. LC-MS chromatographic separations were conducted with a Waters Xbridge C18 column, 50mm x 2.1mm, 3.5µm particle size; mobile phase water/acetonitrile + 0.1% formic acid (gradient 95:5 to 20:80 over 6.5min), or water/acetonitrile + 0.1% ammonia (gradient 95:5 to 5:95 over 6.0min).

2.9 HIV-1 replication assay

2.9.1 Virus production

To generate pseudotyped viral particles from a single-cycle of replication, polyethylenimine (Polysciences) was used to transfect HEK293T cells with 25ng of pHRSIN-cSGW, 25ng of pCRV1-NLGP and 5ng of pCMV-VSV-G (per well) in 96-well plates. To produce HIV-1 replication competent virions, 110ng of pNHG or pNL4-3 (per well) was used with polyethylenimine (PEI) to transfect HEK293T cells in 96-well plates.

Four hours post-transfection, hit compounds were added at 10-points in 2-fold dilutions. 16 hours after drug treatment, media was replaced with fresh DMEM. 48 hours post-transfection, supernatant containing pseudotyped viral particles or replication competent HIV-1 viral particles was harvested in 100µl aliquots and stored at -80°C until further use.

2.9.2 Viral infectivity

To examine infectivity, pseudotyped viral particles or replication competent HIV-1 viral particles harvested from 96-well plates were serially diluted by three-fold. Serial dilutions of VLPs from cSGW and NHG transfections were added to MT-4 cells, while NL4-3 virus was added to MT-4 R5 cells, which express the CCR5 co-receptor and have Tat-dependent GFP expression. 6 hours post-infection, 100µl of dextran sulfate was added to infected MT-4 cells to ensure a single-cycle of replication. 48 hours post-infection, 100µl of infected cells per well were fixed with 4% PFA and used to determine GFP expression (indicative of HIV-1 infection) using flow cytometry.

In order to confirm minimal variation within a 96-well plate, VLPs from 12 wells were randomly chosen, serially titrated and used to infect MT-4 cells (Figure 11). 110ng of pNHG and pNL4-3 was also found optimal for efficient HIV-1 infection (Figure 12).

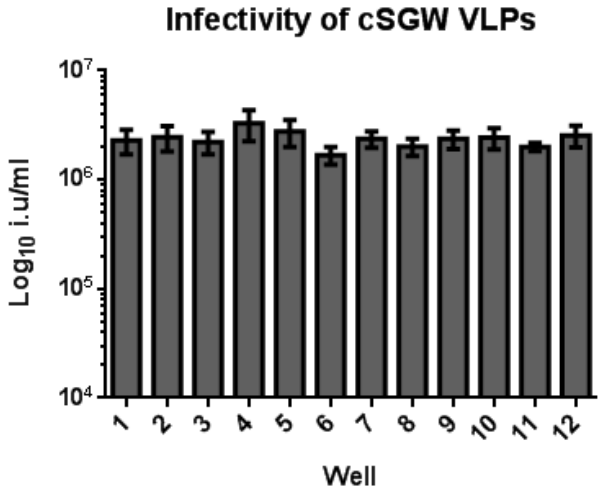

Figure 11 Well-to-well variation of cSGW VLP (virus-like particle) infectivity in 96-well plate

Viral supernatant from 12 randomly chosen wells within 96-well plates were titrated to infect MT-4 cells. Flow cytometry analysis of GFP-positive (infected) MT-4 cells confirmed minimal well-to-well variation. Bars represent mean level of infection (log_{10} infectious units/ml) ± standard deviation (n=3).

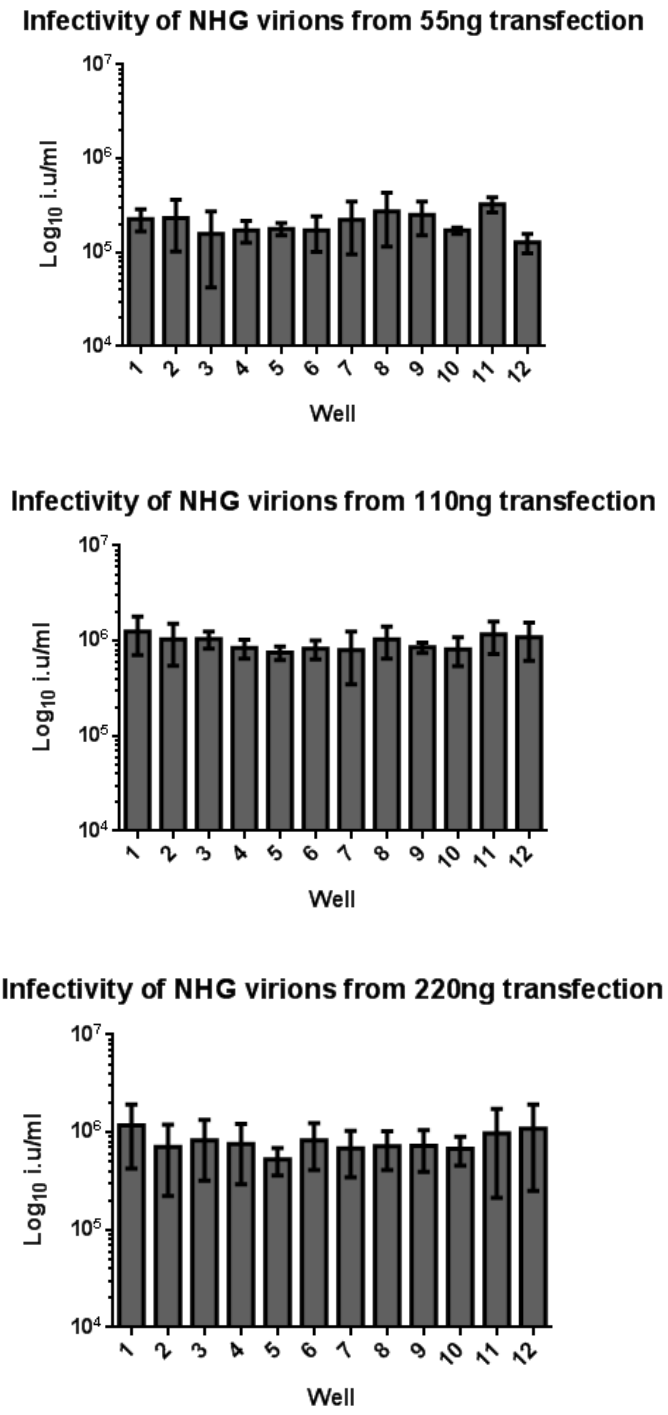

Figure 12 Effect of varying NHG (HIV-1 proviral) DNA on infectivity in 96-well plates

MT-4 cells were infected with titrated virions from HEK293T cells transfected with 55ng (A), 110ng (B) and 220 ng (C) of HIV-1 proviral plasmid, pNHG. Due to even infectivity of 110ng pNHG, this amount of DNA was used for future experiments.

Bars represent mean level of infection (log_{10} infectious units/ml) ± standard deviation (n=3).

2.10 Bunyavirus replication

To test the effect of drugs on bunyavirus replication, $3x10^5$ Vero cells per well were added to 12-well plates. The next day, cells were pre-treated with DMSO (0.5%), ritonavir (5μM), AZT (3μM) and DDD00049811 (50μM) for four hours. Media was removed and cells were infected at 6-points with 1:5 serial dilutions of 100μl titrated bunyamwera virus (generated by Junjie Feng, University of Glasgow) for 1 hour at 37°C with gentle mixing every 15mins. Virus inoculum was then removed and cells were treated with 1ml of overlay media consisting of 1.2% Avicel (w/v) and 2x DMEM with 4% FCS for 72 hours at 37°C. Cells were then fixed with 10% formaldehyde and 0.1% crystal blue for 30mins and washed with water to observe clear plaques.

Reagents, Vero cells and bunyamwera virus were kindly provided by Junjie Feng (University of Glasgow).

2.11 HIV-1 viral particle purification

To purify replication-competent HIV-1 virions, $2x10^5$ HEK293T cells were transfected with 500ng of either NHG or NL4-3 in 24-well plates using PEI. Compounds were added four hours post-transfection followed by replacement of media 24 hours post-transfection (without additional drug). 48 hours post-transfection, virus was harvested by filtering supernatant through a 0.22μM filter. 500μl of filtered viral supernatant was then applied to 900μl of ice-cold 20% sucrose in PBS. After centrifugation at 14,000rpm for 2.5 hours at 4°C, media and sucrose were carefully aspirated and the remaining viral pellet was resuspended in protein sample buffer and stored at -20°C until further use. 500μl of protein sample buffer was also added to the cell monolayer to generate whole cell lysates.

2.12 Western blotting

Western blots were used to examine protein expression of eGFP and mCherry in cell lines used in screening cascade along with HIV-1 viral proteins in secondary assays.

To analyse protein expression of GFP, mCherry and β-actin in HeLa, stable translational control HeLa and stable HIV-1 frameshifting HeLa cells (Figure

2A in Chapter 3), cells were lysed in protein sample buffer and sonicated prior to use. Approximately 30µl of cell lysate was run on 10% sodium dodecyl sulphate-polyacrylamide gel electrophoresis (SDS-PAGE) gel at 110V for 100 minutes. Proteins were then transferred on a nitrocellulose membrane for 90 minutes at 60mA which were blocked in 5% skim milk in Phosphate Buffered Saline with 0.25% Triton-X 100 (PBST) at room temperature for one hour. Blots were then incubated with the 1:2500 of mouse anti-β-actin monoclonal antibody and 1:2000 of mouse anti-mCherry [1C51] monoclonal antibody (Abcam) in blocking solution overnight at 4°C. Blots were incubated with 1:1000 rabbit anti-GFP (D5.1) monoclonal antibody (Cell Signaling Technology) in 5% w/v BSA, 1X Tris-buffered saline (TBS) and 0.1% Tween-20 at 4°C overnight. Following washes with PBST, blots were incubated with 1:7000 of either goat anti-rabbit IgG HRP (horseradish peroxidase) conjugate or rabbit anti-mouse HRP for 1 hour at room temperature. Protein signal were detected using chemiluminescent HRP detection reagent followed by exposure to hyperfilm (Kodak).

To examine the effect of hit compounds on HIV-1 Gag and Pol proteins and clonally-derived cell lines, protein lysates from infected cells and released virions were harvested 48 hours post-infection. Approximately 5-7µl of virion lysate and 10-15µl of cell lysate were run on a NuPage 4-12% Bis-Tris gels (Novex) for 2 hours at 100V. Proteins were transferred on to nitrocellulose membranes overnight at 13V and blocked for one hour in 1:3 of FCS:PBS with 1% sodium azide. Blots were then probed for the following primary antibodies for 1.5 hours at room temperature: 1:50 of anti-HIV p24 capsid antibody (183-H12-5C) and 1:300 of anti-HIV INT-4 antibody (a gift from Michael Malim). Following washes with PBS, membranes were probed with fluorescently labelled goat anti-mouse secondary antibody (ThermoScientific) for 1.5 hours. Following more washes with PBS, protein expression was visualized using a LI-COR Odyssey scanner.

2.13 HIV-1 spreading

To test the effect of drugs on HIV-1 replication kinetics, an HIV-1 spreading assay was conducted. MT-4 cells were seeded at a density of 2x 10^5 cells/well in a 24-well plate and infected with NHG virus at MOI of 0.001. Each well was treated with either no drug, DMSO (0.5%), ritonavir (5μM) or hit compounds (50μM). 50-75μl of cells were fixed with 4% PFA every 24 hours and HIV-1 infection was determined by the percentage of GFP-positive MT-4 cells using flow cytometry.

2.14 HIV-1 evolution of drug resistance

To determine optimal parameters to test the effect of drugs on HIV-1 resistance, experiment was run using different parameters:

1. 4x10^5 cells/well in 12-well plates (2x10^5 cells/ml)
2. 2x10^5 cells/well in 12-well plates (1x10^5 cells/ml)
3. 6x10^5 cells/well in 6-well plates (2x10^5 cells/ml)
4. 3x10^5 cells/well in 6-well plates (1x10^5 cells/ml)

For each of the parameters outlined above, MT-4 cells were infected with NHG virus at MOI of 0.003 and treated with either DMSO or AZT (1.87μM). Based on more effective HIV-1 spreading in 6-well plates (Figure 13), evolution of drug resistance to HIV-1 was investigated using 3x10^5 cells/well in 6-well plates.

To examine the evolution of drug resistance to HIV-1 replication, 6 x 10^5 MT-4 cells/ml were seeded in a 6-well plate. NHG virus was added at an MOI of 0.003 and cells were also treated with one of the following: 50μM DMSO, 50μM of DD49811 or 1.87μM of AZT. GFP-positive MT-4 cells, indicative of HIV-1 replication, were monitored every 24 hours by fixing 50-100μl of cells with 4% PFA (remaining cultures were replenished with media and drug). On day of maximum HIV-1 infection, virions were harvested, filtered with a 0.20 μm filter and stored at -80°C. For each passage of cells, DMSO-, DD49811-and AZT-treated cells were repeatedly infected with 12-16μl of virus harvested from DD49811-treated infected MT-4 cells from the previous passage to determine potential HIV-1 resistance of DD49811. Similarly, DMSO-and AZT-

treated MT-4 cells were continually infected with virions from AZT-treated infected MT-4 cells from the previous package to identify AZT-resistant virions.

A)

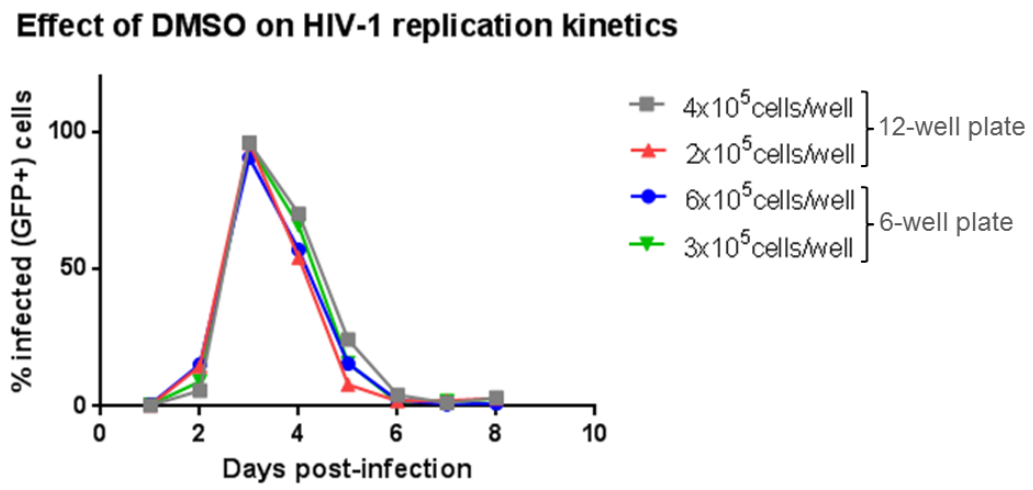

B)

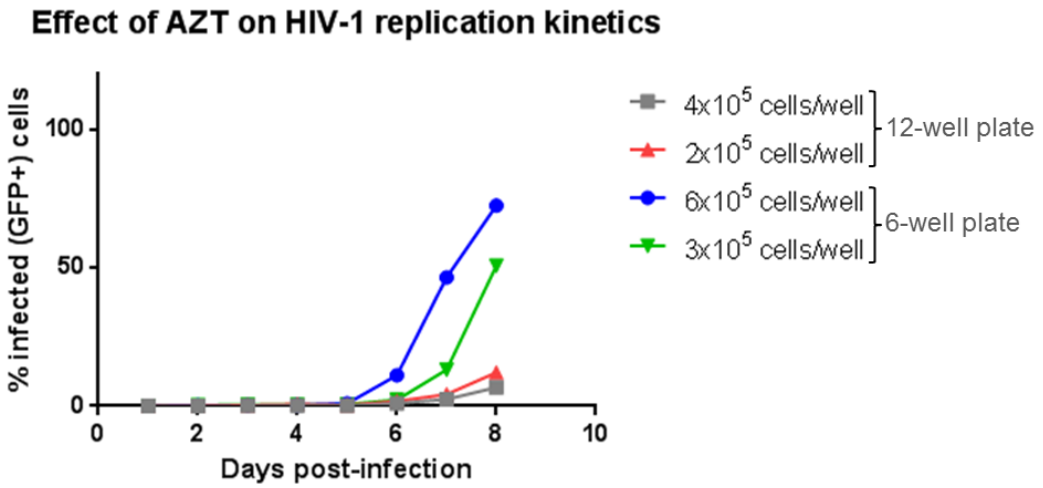

Figure 13 Effect of cell density and well area on DMSO-and AZT-induced HIV-1 replication kinetics

A) DMSO-treated MT-4 cells (0.5% (v/v)) at cell density of $1x10^5$ cells/ml and $2x10^5$ cells/ml were infected with NHG virions at MOI of 0.003 in 12-well plate and 6-well plate. GFP-positive cells were monitored every 24 hours post-infection by FACS as a measure of infectivity over 8 days.

B) AZT-treated MT-4 cells (1.87µM) at cell density of $1x10^5$ cells/ml and $2x10^5$ cells/ml were infected with NHG virions at MOI of 0.003 in 12-well plate and 6-well plate. GFP-positive cells were monitored every 24 hours post-infection by FACS as a measure of infectivity over 8 days.

2.15 Data analysis and Statistics

All raw screening data were processed using ActivityBase (IDBS, Guilford, Surrey, UK) and quality control criteria for each plate was based <10% coefficient of variation (%CV) of DMSO-treated cells (negative control). Raw data was converted to fold change relative to DMSO-treated cells (negative control). Hit identification in the first primary screen was based on a threshold of three times the standard deviation of the median fold change. Screening data were analysed and accessed using Dotmatics and Vortex software.

To assess compound potency, dose-response curves were fit using the following four-parameter equation:

$$y = A + \frac{B - A}{1 + (C/x)^D},$$

where A is the minimum fold change, B is the maximum fold change, C is the Log XC_{50} value and D is the slope factor, x is the drug concentration and Y is the fold change (described in section 1.7.3.4). The data were fitted using the Levenburg Marquardt algorithm. Poor curve fitting was manually adjusted by either eliminating obvious outliers or manually setting B to expected maximum fold change. Dose-response curves of eGFP and mCherry were generated using GraphPad Prism by plotting the mean of Log2 fold change. Error bars represented the standard deviation of 2-4 replicates.

To determine viral infectivity, flow cytometry was used to quantify the percentage of GFP expression (level of infection) in target cells infected with titrated virus. Infectious units/ml was calculated as follows:

$$\frac{(\%GFP/100)(\#\ of\ cells)}{Virus\ (ml)}$$

Infectivity data as Log_{10} infectious units/ml was representative of the mean of three viral titers within a linear range and corresponding error bars represented the standard deviation of three replicates.

2.16 Appendix

2.16.1 Quality control of wellmate microplate dispenser

Prior to using the Matrix wellmate microplate dispenser to plate cells, quality control was conducted to ensure even distribution while dispensing. Using the wellmate dispenser, 25µl of orange G dye (0.25mM stock) was added to all wells in three black, clear bottom 384-well plates (Greiner). The weight of each plate was recorded before and after orange G dye addition. The average well volume for each plate was used to calculate the percent of coefficient of variation (%CV). Using the Envision microplate reader (PerkinElmer) the absorbance in all three plates were also measured at 490 nm and was also used to %CV. The wellmate dispenser passed quality control if plates had gravimetric and fluorometric % CV of less than 10.

Chapter 3
Results: Assay and Screening Development

This chapter outlines the development of an *in vitro* cell-based assay to recapitulate HIV-1 frameshifting (-1 ribosomal frameshifting at the HIV-1 frameshift element) of *gag* and *pol* genes. This includes the design of a bi-cistronic fluorescent HIV-1 frameshift DNA construct and the establishment of a cell culture model of HIV-1 frameshifting. Furthermore, this chapter delineates the parameters examined to optimize this HIV-1 frameshifting model for high-throughput screening purposes.

3.1 Target validation and assay development

To recapitulate HIV-1 frameshifting in a cell-based assay, HIV-1 frameshift-expressing DNA constructs were used to generate a representative cell culture model. Ultimately, clonally-derived HIV-1 frameshifting HeLa cells were created using a bi-cistronic fluorescent construct harbouring the HIV-1 frameshift element.

3.1.1 Development of bi-cistronic HIV-1 frameshift DNA construct

To initially mimic HIV-1 frameshifting *in vitro*, the HIV-1 frameshift region was inserted between an upstream *Renilla* luciferase and downstream *Firefly* luciferase gene, indicative of cap-dependent translation and HIV-1 frameshifting, respectively (described in section 2.2.1). However, the use of this dual luciferase reporter was discontinued due to high affinity between small molecules and the luciferase active site which often leads to false positive hits in drug screening (Berry et al., 2011).

To avoid enzymatic assay interference, a bi-cistronic fluorescent DNA construct was created by embedding the HIV-1 frameshift region between eGFP and mCherry coding sequences so that eGFP production depended on cellular cap-dependent translation, while mCherry expression required -1 ribosomal frameshifting (Figure 14A). This bi-cistronic eGFP-HIV FS-mCherry construct represented the HIV-1 Gag-HIV FS-Pol segment in the

HIV-1 genome which is regulated by -1 ribosomal frameshifting. To mimic global translation, a control construct recapitulating conventional translation was also created using site-directed mutagenesis. This produced eGFP and mCherry by conventional ribosomal translation (Figure 14B).

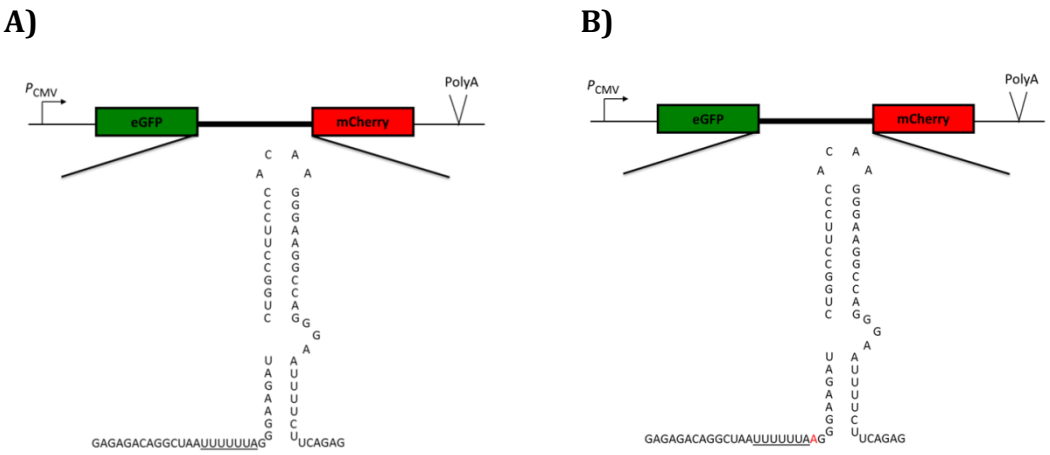

Figure 14 Bicistronic fluorescent DNA constructs designed to recapitulate HIV-1 Gag:Gag-Pol frameshifting

A) HIV-1 frameshift sequence inserted in a bicistronic fluorescent construct whereby mCherry production is solely dependent on ribosomal frameshifting at the slippery site (underlined). This construct is referred to as HIV-1 frameshifting or eGFP-HIV FS-mCherry.

B) Adenine ('A') inserted after the slippery site makes mCherry in-frame with eGFP and therefore dependent on conventional translation. This construct is referred to as the translational control or eGFP-Con-mCherry.

3.1.2 Development of cell culture model of HIV-1 frameshifting

3.1.2.1 Transiently-transfected cells do not recapitulate HIV-1 frameshifting

To determine the most suitable cell culture model of HIV-1 frameshifting, I examined the effect of transiently-transfected HeLa cells. HeLa cells transiently-transfected with bi-cistronic fluorescent HIV-1 frameshifting and translational control DNA exhibited varying eGFP and mCherry expression levels between replicates and following freeze/thaw cycles (Figure 15). This variation in eGFP and mCherry expression levels was likely an artefact of transient transfection (Figure 16). Moreover, cell viability of transiently-transfected translational control and HIV-1 frameshifting cells was very low (Table 2). As a consequence of inconsistent expression levels and low cell viability, transiently-transfected HeLa cells were also not appropriate cell culture models of global translation and HIV-1 frameshifting for high-throughput screening.

A)

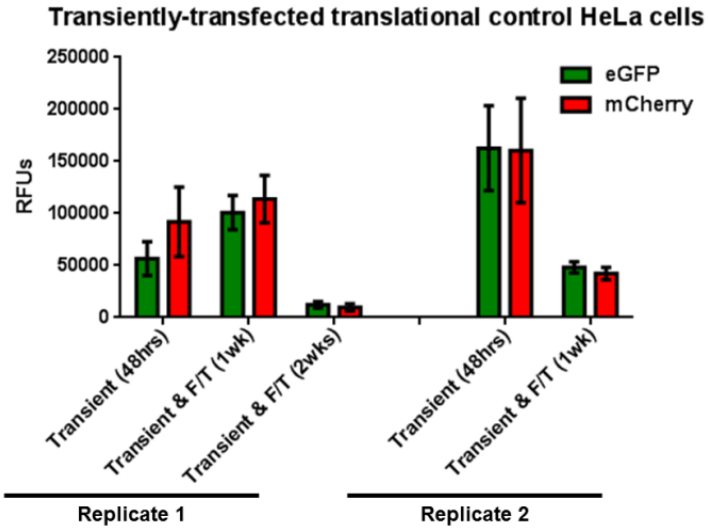

B)

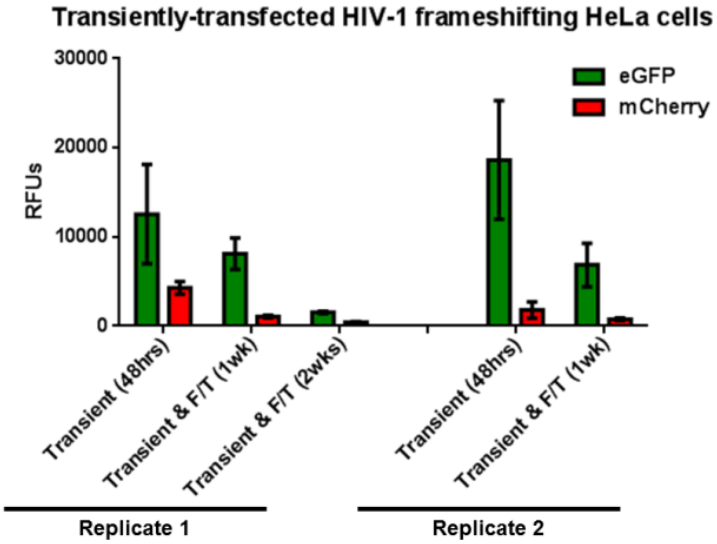

Figure 15 Transiently-transfected HeLa cells are unsuitable culture models of global translation and HIV-1 frameshifting

HeLa cells were transiently-transfected with eGFP-Con-mCherry **(A)** or eGFP-HIV FS-mCherry **(B)** and assayed for GFP and mCherry expression 48 hours post-transfection (48hrs), 1 week post-transfection following a freeze and thaw cycle (F/T (1wk)) and 2 weeks post-transfection following a freeze and thaw cycle (F/T (2wks)). eGFP and mCherry expression dramatically varied between replicates and as a result of freeze-thawing, therefore rendering transiently-transfected cells an inappropriate model for screening.

Green and red bars represent eGFP and mCherry RFUs (relative fluorescent units), respectively, as determined by the PherastarFS reader. Replicates 1 and 2 are biological replicates while data represents the mean ± SD from 8 technical replicates.

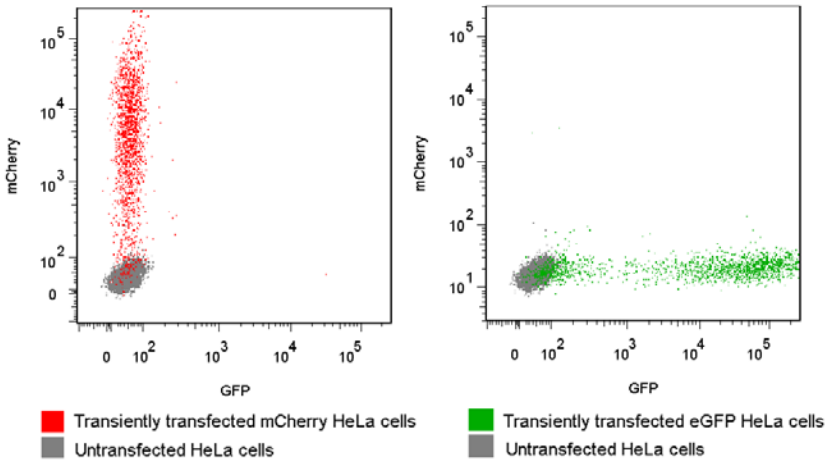

Figure 16 Transient transfection of eGFP-and mCherry-encoding DNA plasmids lead to varying levels of eGFP and mCherry expression
HeLa cells were transiently-transfected with mCherry-encoded (left) and GFP-encoded (right) DNA plasmids. 48 hours post later, FACS analysis of mCherry expression (red) and GFP expression (green) showed a wide range of expression levels in transfected cells.

Table 2 Cell viability of transiently-transfected and clonally-derived HeLa cells

Cell	Cell viability (%)
Transient translational control (Replicate 1)	77.5
Transient HIV-1 frameshifting (Replicate 1)	58
Transient translational control (Replicate 2)	69.6
Transient HIV-1 frameshifting (Replicate 2)	37.1
Clonal translational control	92.8
Clonal HIV-1 frameshifting	90

3.1.2.2 *Stably-transfected cells do not recapitulate HIV-1 frameshifting*

To develop a cell-based assay, the bi-cistronic fluorescent HIV-1 frameshifting and translational control DNA were transfected in HeLa cells to generate stable cell lines representing cell culture models of HIV-1 frameshifting and global translation, respectively. Western blot analysis and fluorescence microscopy revealed that stable translational control HeLa cells produced eGFP-Con-mCherry polyprotein and expressed equivalent eGFP and mCherry levels as a result of global translation (Figure 17A). However, stable HIV-1 frameshifting HeLa cells not only expressed very low eGFP and mCherry levels, but had undetectable levels of the eGFP-HIV FS-mCherry polyprotein expected upon frameshifting (Figure 17A). Flow cytometry analysis of eGFP and mCherry expression revealed that a large proportion of stably-transfected cells were not expressing the DNA construct of interest (Figure 17B). Since stably-transfected HIV-1 frameshifting HeLa cells were a flawed representation of HIV-1 frameshifting, I next tested the effects of clonally-derived HeLa cells.

A)

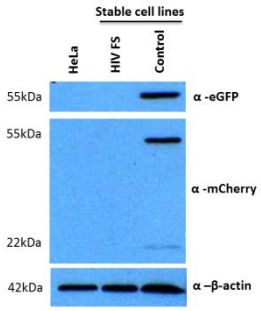

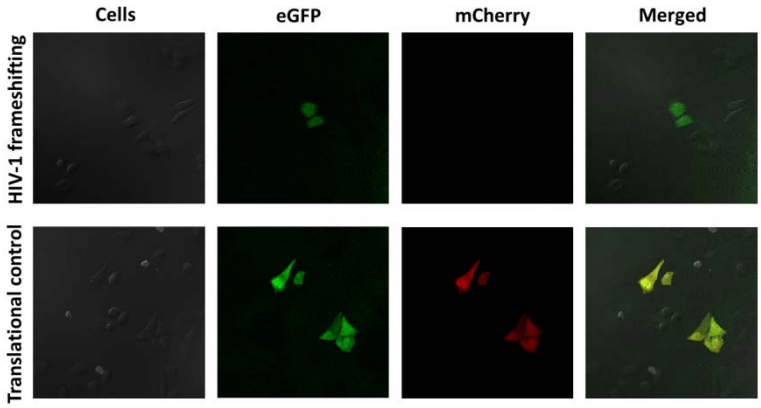

B)

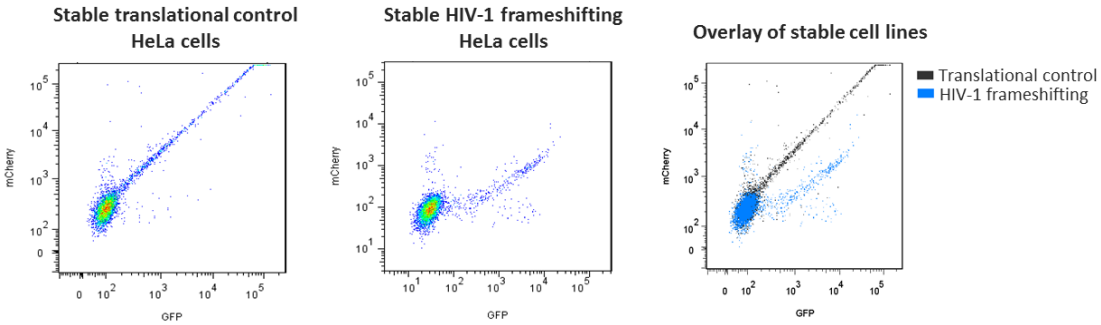

Figure 17 Stable cell lines generated using bi-cistronic fluorescent DNA constructs are not representative of global translation and HIV-1 frameshifting

A) Western blot analysis of eGFP, mCherry and β-actin expression in parental HeLa cells (Lane 1), stably-transfected translational control HeLa cells (Lane 2) and stable-transfected HIV-1 frameshifting HeLa cells. Fluorescence microscopy of stable translational control and HIV-1 frameshifting HeLa cells revealed low eGFP and mCherry expression, especially in stable HIV-1 frameshifting HeLa cells.

B) Flow cytometry analysis of stable translational control and HIV-1 frameshifting HeLa cells confirmed that majority of cells were not expressing eGFP and mCherry.

3.1.2.3 Clonally-derived HeLa cells recapitulate HIV-1 frameshifting

To generate a clonally-derived population of HIV-1 frameshifting and translational control HeLa cells, flow cytometry-activated cell sorting (FACS) was used to isolate GFP-positive cells from both stable cell lines (described in section 2.3.2). This ultimately led to 10 clones of each cell line (Figure 28 in Appendix 3.3). From these, clone 5 of translational control cells and clone 2 of HIV-1 frameshifting cells were selected for expansion since they expressed eGFP and mCherry levels corresponding to global translation and HIV-1 frameshifting, respectively. Clone 2 of HIV-1 frameshifting HeLa cells was further sorted to eliminate the population of cells not expressing either GFP or mCherry (Figure 29 in Appendix 3.3).

Since HIV-1 frameshifting produces Gag:Gag-Pol at a ratio of 20:1 (and therefore at a frequency of 5%) (Dulude et al., 2006; Hung et al., 1998; Karacostas et al., 1993; Park & Morrow, 1991; Shehu-Xhilaga et al., 2001; Telenti et al., 2002), a cell culture model of HIV-1 frameshifting should mimic this frameshifting frequency. To determine the level of frameshifting in clonally-derived HIV-1 frameshifting cells, western blot was used to detect eGFP- and mCherry-expressing polyproteins. As expected, clonally-derived translational control cells express the eGFP-mCherry polyprotein (55kDa) (Figure 18). Densitometry analysis revealed that the proportion of eGFP-mCherry polyprotein in clonally-derived HIV-1 frameshifting cells relative to translational control cells is around 7% (Figure 18). This level of frameshifting in clonally-derived HIV-1 frameshifting cells mimics the level of HIV-1 frameshifting. While a negative population of cells (not expressing eGFP and mCherry) re-emerged in clonal HIV-1 frameshifting cells (Figure 18B), they were maintained at similar levels. These clonally-derived cell lines also maintained expected levels of eGFP and mCherry expression over time after freeze/thaw cycles (Figure 19) and were therefore appropriate *in vitro* cell culture models of HIV-1 frameshifting and cellular translation.

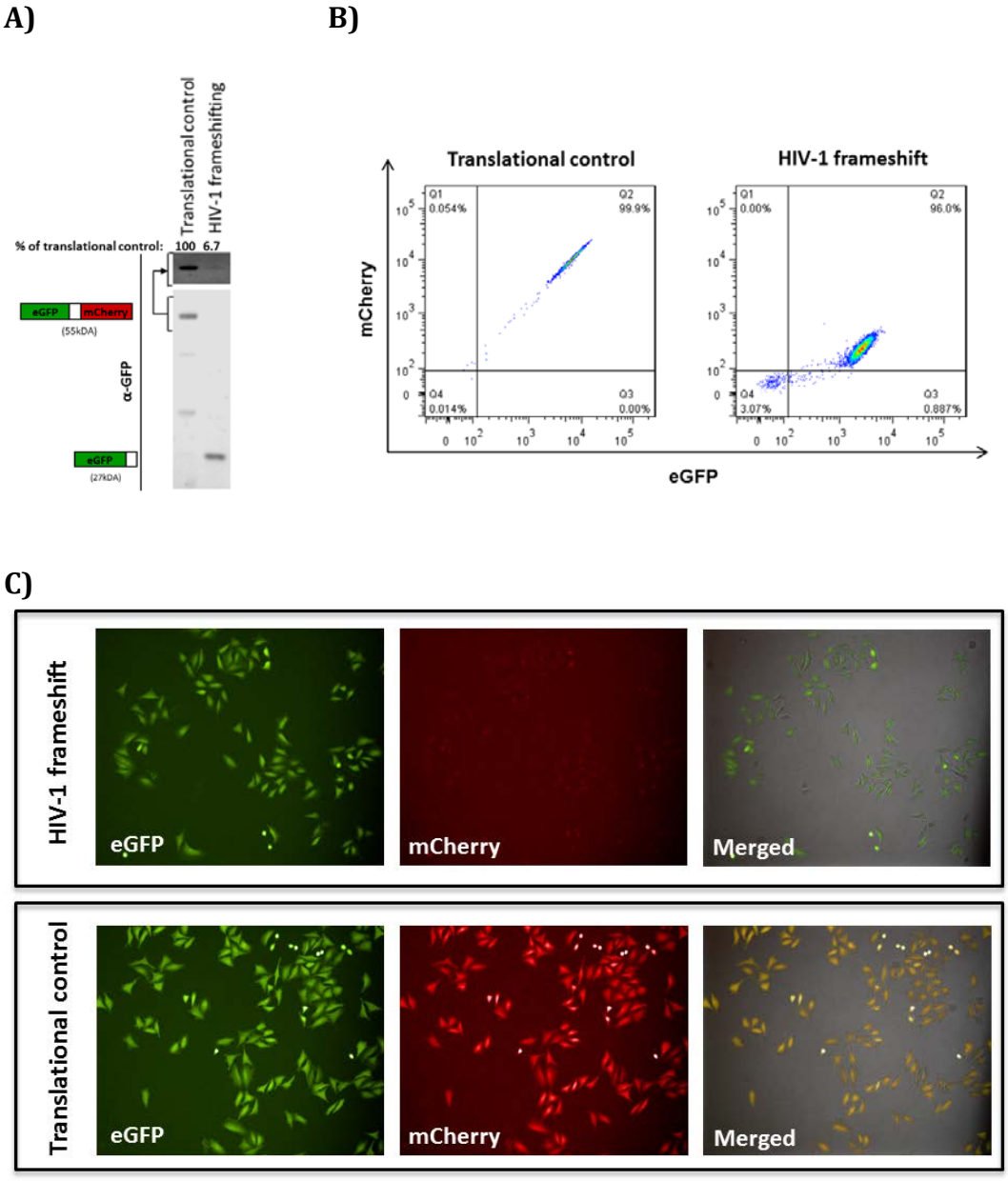

Figure 18 Clonally-derived HeLa cells generated cell culture models of HIV-1 frameshifting and cellular translation (translational control).

A) Frequency of HIV-1 frameshifting (6.7%) was determined based on western blot and densitometry analysis of the abundance of eGFP-mCherry fusion protein in clonally-derived HIV-1 frameshifting cells.

B) Flow cytometry analysis of eGFP and mCherry expression in clonally-derived translational control HeLa cells and HIV-1 frameshifting HeLa cells confirmed that they are suitable cell culture models of cellular translation and HIV-1 frameshifting, respectively.

C) Using the Operetta high-content imaging, GFP and mCherry fluorescence was examined in clonally-derived HIV-1 frameshifting and translational control HeLa cells.

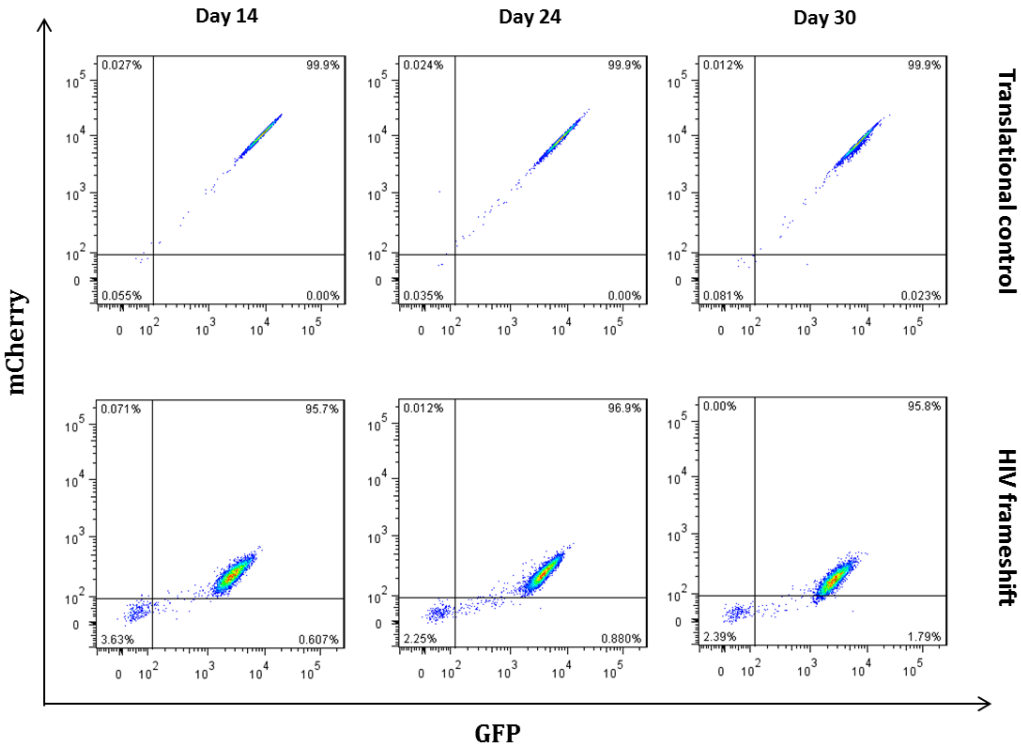

Figure 19 Clonally-derived translational control and HIV-1 frameshifting HeLa cells maintained eGFP and mCherry expression following a freeze and thaw cycle.

Clonally-derived translational control and HIV-1 frameshifting HeLa cells maintained GFP and mCherry expression up to 30 days after a freeze and thaw cycle and were therefore considered appropriate for high-throughput screening.

3.2 Screen development

Following the establishment of a HIV-1 frameshifting cell culture model, I aimed to optimize parameters for screening compounds in a high-throughput cell-based assay. These parameters include the mode of detection, quantification of signal (fluorescence), cell density, DMSO tolerance and antibiotic selection.

3.2.1 Mode of detection and quantification of signal output

In the HIV-1 frameshifting cell culture model, mCherry expression depended on the HIV-1 frameshift element and was indicative of HIV-1 frameshifting efficiency. Therefore, it was important to accurately and quantitatively measure changes in eGFP and mCherry expression to determine the effects on conventional translation and HIV-1 frameshifting, respectively.

mCherry and eGFP expression were quantified using two modes of detection: fluorescence resonance energy transfer (FRET) of the fluorescent protein pair, compared to fluorescence intensity of eGFP and mCherry, individually. In the FRET-based assay, eGFP and mCherry intensity were detected at emission wavelengths of 520nm and 610nm, respectively, following excitation of cells at 485nm. To detect each fluorophore separately, eGFP was excited at 485nm and emission was detected at 520nm while excitation of mCherry at 580nm was detected at an emission wavelength of 610nm. While individual detection of eGFP and mCherry fluorescence led to levels consistent with those observed by flow cytometry and fluorescence microscopy, FRET-based detection revealed increased mCherry levels (Figure 20). This was potentially due to crosstalk between the eGFP and mCherry spectra or eGFP signal bleed-through during quantification of mCherry fluorescence.

Individual detection that quantified appropriate levels of eGFP and mCherry in the HIV-1 frameshift cells and translational control cells confirmed that they are representative cell culture models of HIV-1 frameshifting and global translation, respectively. Furthermore, while the frameshifting frequency in

clonal HIV-1 frameshift cells (15%) was higher than levels observed *in vivo*, this frequency was maintained over time (Figure 21) and still correlated with those seen in other cell culture models of frameshifting (Baril et al., 2003; Cardno et al., 2009; Dulude et al., 2002; Hung et al., 1998).

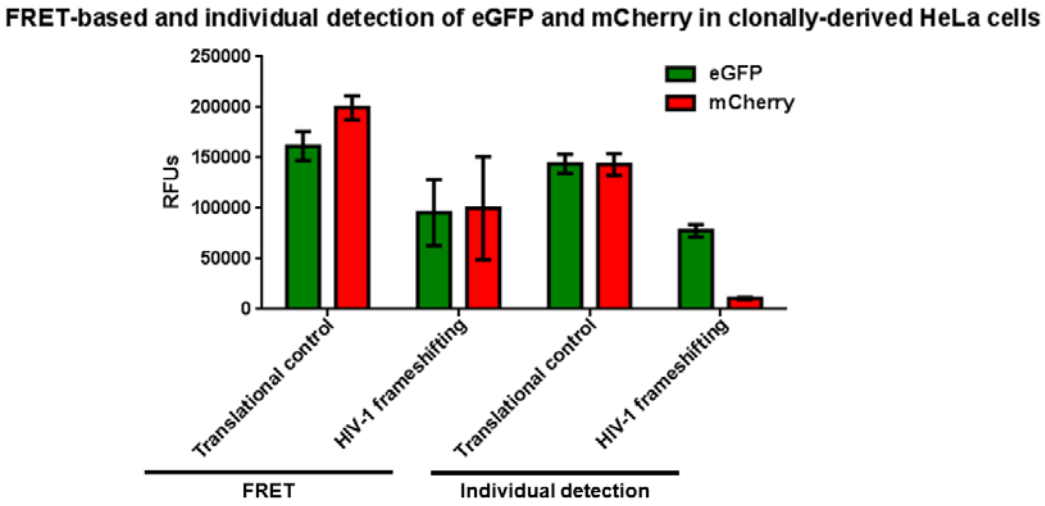

Figure 20 Fluorescence resonance energy transfer (FRET) and individual fluorophore detection in clonal translational control and HIV-1 frameshifting cells

eGFP and mCherry fluorescence in clonal translational control and HIV-1 frameshifting HeLa cells was detected individually, and by FRET using the PherastarFS reader. Unlike FRET-based detection, individual detection of fluorophores led to mCherry expression levels that correlated with FACS analysis and fluorescence microscopy.

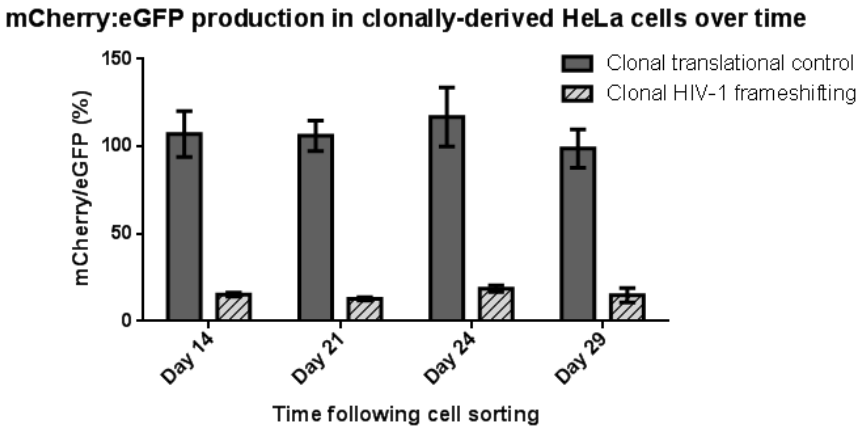

Figure 21 Clonal translational control and HIV-1 frameshifting cells maintained eGFP and mCherry expression over time

eGFP and mCherry fluorescence intensity in both clonally-derived HeLa cells were comparable for 29 days post-cell sorting.

3.2.2 Effect of cell density

To effectively miniaturize cell-based assays for screening in 384-well plates, optimal cell density was determined over the assay period. While cell viability linearly increased with higher cell densities, the increase plateaued with more than 4000 cells per well in parental HeLa cells, HIV-1 frameshift cells and translational control translational cells (Figure 22). This was potentially due to increased cell death or reduced cell proliferation rates at densities greater than 4000 cells per well. Furthermore, at densities lower than 4000 cells per well, the proportion of mCherry to eGFP in HIV frameshifting cells, increased (Figure 23). Since mCherry expression was relatively low due to frameshifting, their levels were not drastically affected in response to decreased cell densities. However, the corresponding decrease in eGFP expression led to drastic changes in the proportion of mCherry to eGFP. Therefore 4000 cells per well were considered an appropriate cell density in 384-well plates.

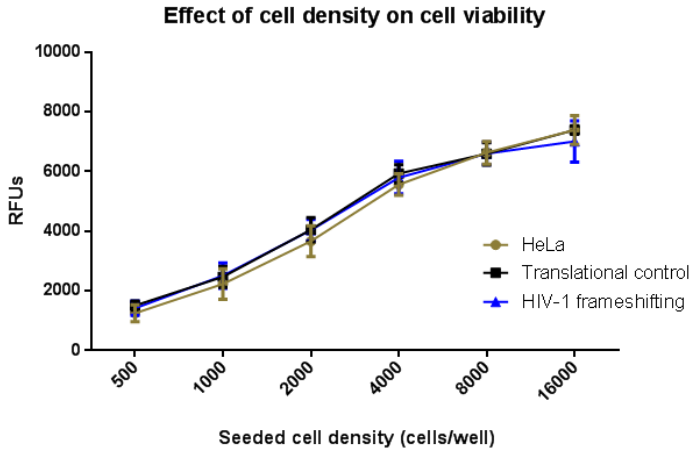

Figure 22 Effect of cell density on cell viability in clonally-derived HeLa cells

Varying number of HeLa cells, clonally-derived translational control HeLa cells and clonally-derived HIV-1 frameshifting HeLa cells were treated with resazurin (45µM) for four hours. Cell viability was quantified by measuring the relative fluorescent units (RFUs) (at excitation 550nm/emission 590nm) using a PheraStar FS plate reader. Error bars represent the standard deviation of the mean of three independent experiments (n=3).

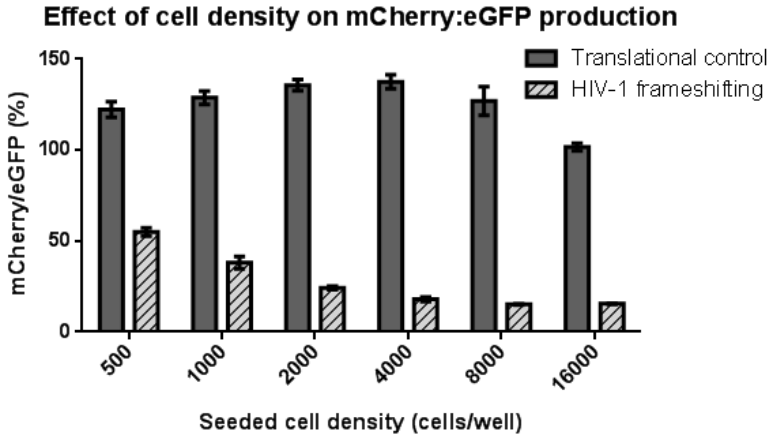

Figure 23 Effect of cell density on global translation and HIV-1 frameshifting

The proportion of mCherry to GFP expression was examined in clonally-derived HeLa cells seeded at various densities within 384-well plates. At densities less than 4000 cells per well, undetectable mCherry levels and decreasing GFP levels led to a dramatic increase in the proportion of mCherry to GFP in clonal HIV-1 frameshifting cells. Bars represent the mean percentage of mCherry relative to GFP expression ± SD of three replicates.

3.2.3 Measure of DMSO tolerance in cell-based assay

Since compounds were dissolved in dimethyl sulfoxide (DMSO), I investigated the effect of varying DMSO concentrations (0-10%) on cell viability and expression of eGFP and mCherry in parental HeLa cells, HIV-1 frameshifting and translational control cells. Cell viability dramatically decreased at DMSO concentrations greater than 1% in all three cell lines (Figure 24). Moreover, the proportion of mCherry to eGFP levels in HIV-1 frameshifting cells also dramatically increased at DMSO concentrations above 1% (Figure 25), most likely due to reduced cell viability and thus reduced eGFP levels. Therefore, due to DMSO tolerance at levels below 1%, screening was conducted using 0.3% DMSO.

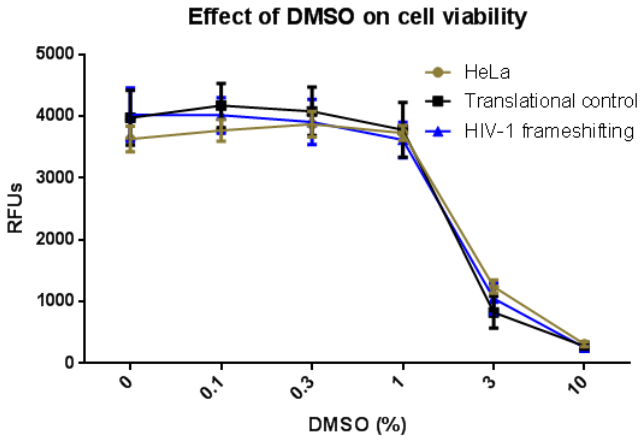

Figure 24 Effect of DMSO on cell viability in cell culture models of global translation and HIV-1 frameshifting
Using a resazurin assay, increased DMSO concentrations (>1%) led to decreased cell viability in HeLa, clonal translational control and clonal HIV-1 frameshifting HeLa cells. Values are representative of mean RFUs ± SD of three replicates.

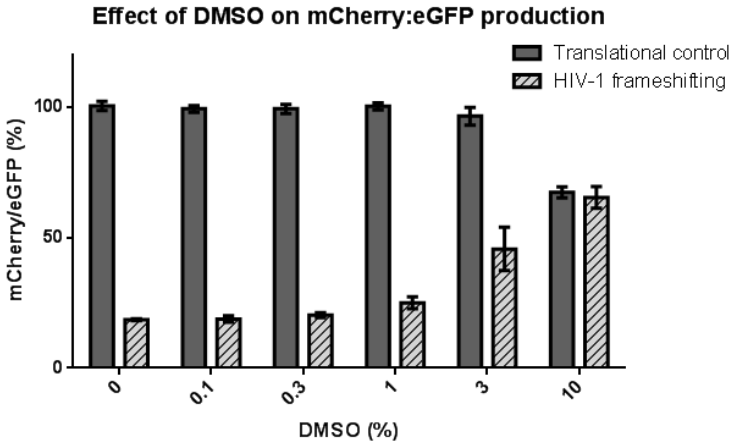

Figure 25 Effect of DMSO on global translation and HIV-1 frameshifting
The proportion of mCherry to eGFP expression was examined in clonally-derived HeLa cells treated with varying concentrations of DMSO (v/v) within 384-well plates. DMSO levels greater than 1% led to increased proportion of mCherry to eGFP in clonal HIV-1 frameshifting cells due to undetectable mCherry levels and decreasing eGFP levels. Bars represent the mean percentage of mCherry relative to eGFP expression ± SD of three replicates.

3.2.4 Effect of geneticin

Clonal HIV-1 frameshift and translational control cells were maintained in 0.4mg/ml G418 (geneticin), an aminoglycosidic antibiotic. It was hence important to investigate potential translational effects on the cell culture models of global translation and HIV-1 frameshifting since aminoglycosides inhibit protein synthesis. HIV-1 frameshifting and translational control cells treated with varying doses of G418 had no significant effects on eGFP and mCherry expression (Figure 26). G418 therefore has no translational effects in this assay, and any potential changes in eGFP and mCherry expression in response to drugs, were not G418-specific. Furthermore, removing G418 from both clonal cell lines over 7 days did not significantly impact expression levels (Figure 27). These cells could therefore be used in screening without the need of replenishing with G418 for selection within a 7 day period.

A)

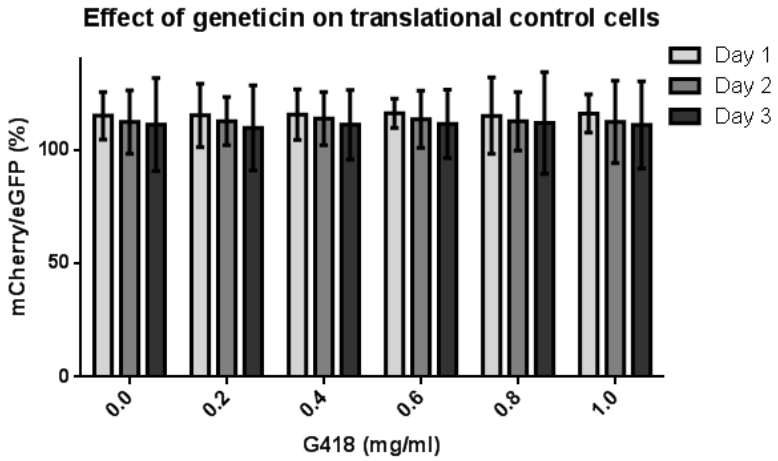

B)

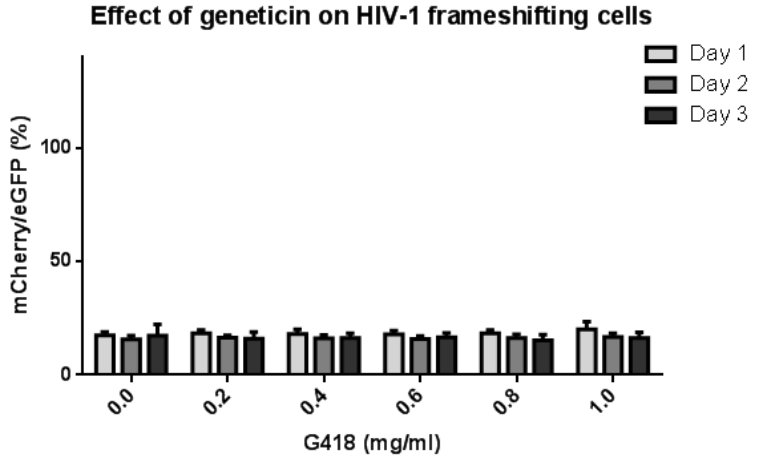

Figure 26 Effect of geneticin (G418) on global translation and HIV-1 frameshifting over 3 days

The proportion of mCherry to eGFP expression was examined in clonally-derived HeLa cells treated with varying concentrations of geneticin over three days. Up to 1mg/ml of geneticin had no significant effect on the proportion of mCherry relative to GFP in clonal translational control HeLa cells (A) and clonal HIV-1 frameshifting HeLa cells (B). Bars represent the mean percentage of mCherry relative to GFP expression ± SD of three replicates.

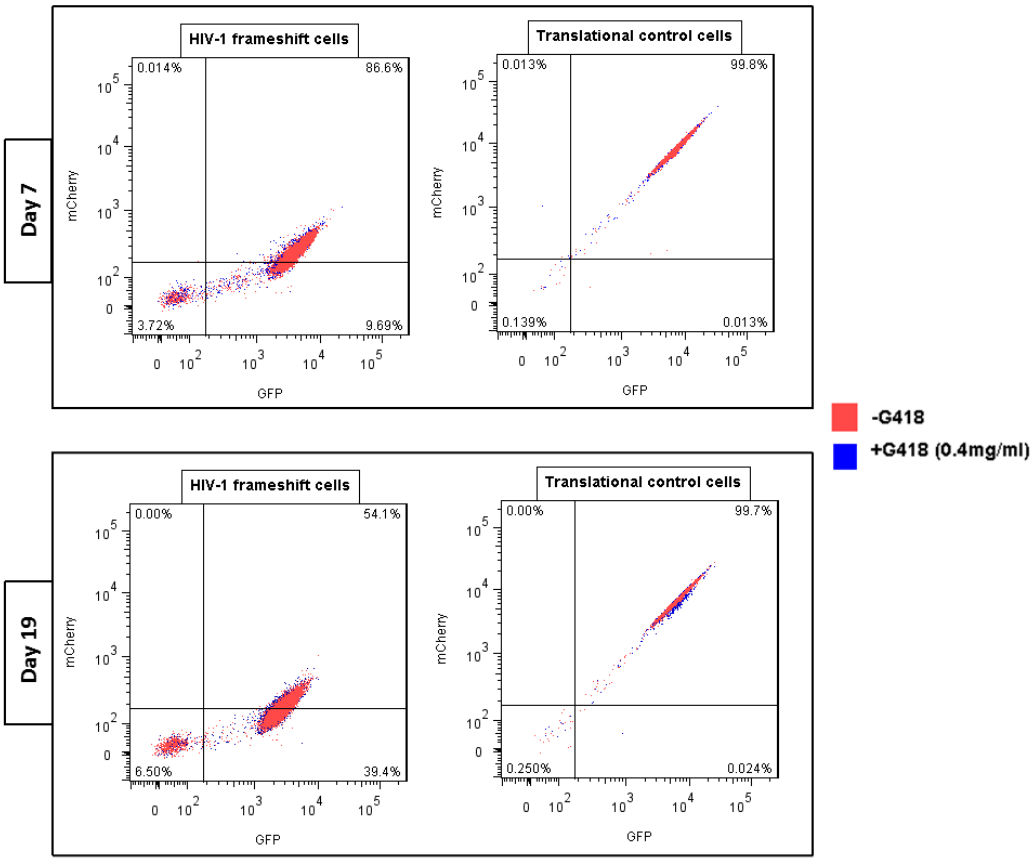

Figure 27 Removing geneticin (G418) leads to the slight accumulation of negative population in clonal translational control and HIV-1 frameshifting HeLa cells

Clonal translational control and HIV-1 frameshifting cells that were maintained in 0.4mg/ml G418 were grown for 19 days either in the presence of 0.4mg/ml G418 (blue) or in the absence of G418 (pink). FACS analysis of GFP expression and mCherry expression revealed a slight accumulation of negative population of cells, however, no significant effects as a result of G418 depletion.

3.2.5 Summary

Previous screening efforts to identify HIV-1 frameshift modulators in mammalian cells were conducted using luciferase reporter assays. Unfortunately, unspecific interactions between small molecules and luciferase led to several false positive hits (Berry et al., 2011). Consequently, I aimed to create and validate a more suitable assay that simulated the target HIV-1 frameshifting mechanism in a cell culture model.

To do this, I developed a fluorescent cell-based assay of HIV-1 frameshifting with clonally-derived HeLa cells. As outlined in this chapter, this was done using a bi-cistronic fluorescent DNA construct containing the HIV-1 frameshift element flanked by an upstream eGFP and downstream mCherry cistron. Individual fluorescence of eGFP and mCherry was accurately detected and used as a readout of cellular translation and HIV-1 frameshifting, respectively. mCherry was chosen as the fluorescent determinant of HIV-1 frameshifting due to beneficial attributes. As a monomeric fluorescent protein, mCherry does not need to oligomerize to emit fluorescence (Shaner et al., 2004). This eliminates any potential delay in fluorescence (signal output) which can result from complex protein folding. Additionally, the far-red shift required for mCherry excitation and emission, and non-existent emission spectral overlap between mCherry and eGFP further reduce the likelihood of eGFP interference.

Moreover, parameters such as cell density, DMSO tolerance, antibiotic selection and signal quantification, were optimized for high-throughput screening in a 384-well plate format (Standard operating procedure in Appendix 3.3.3). The amenability of this fluorescent cell-based assay for high-throughput screening poses several advantages over other approaches. This is a highly cost-effective and simple fluorescent cell-based assay that does not require several and complex processing steps, expensive reagents or substrates. The feasibility of conducting this assay in a 384-well plate format, combined with rapid fluorescent readout and automated fluorescence plate readers (PherastarFS, BMG LabTech) make this a robust way of screening a

large library of compounds in a timely manner. Furthermore, high reproducibility of signal output over a month and over freeze/thaw cycles makes this assay ideal for high-throughput screening.

3.3 Appendix

3.3.1 Clones isolated during cell sorting of clonally-derived translational control and HIV-1 frameshifting HeLa cells

A)

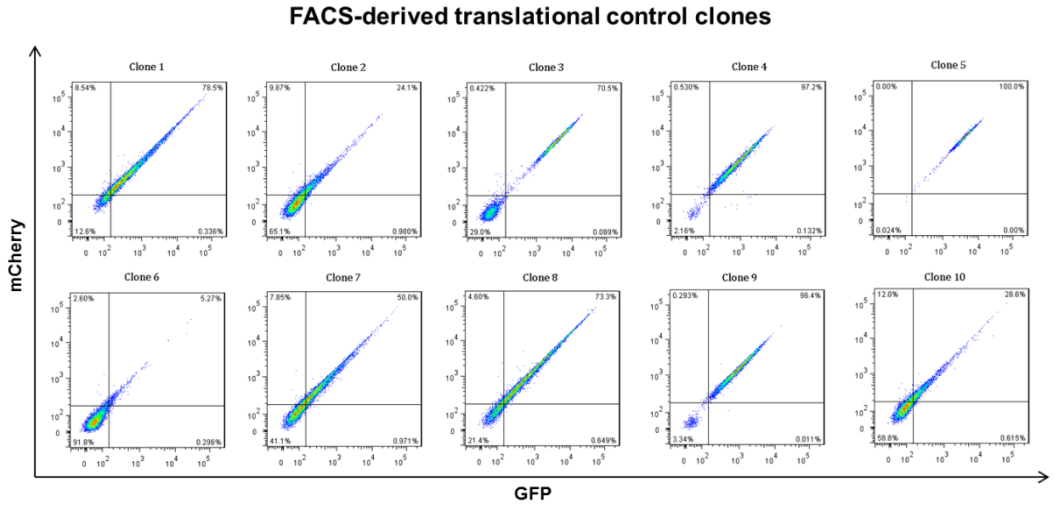

B)

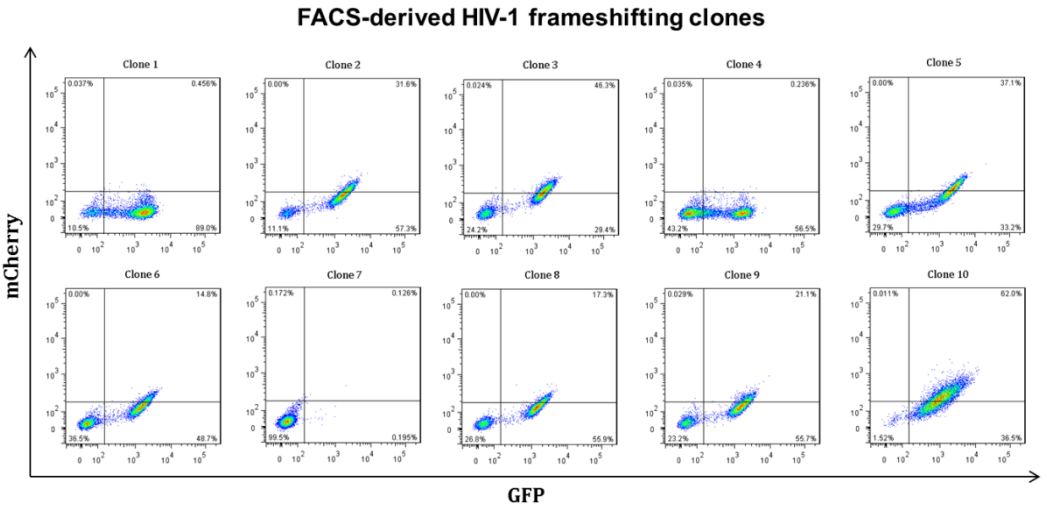

Figure 28 Clones identified from stable translational control and HIV-1 frameshifting cell lines

A) To create a clonally-derived cell culture model of cellular translation, 10 clones were isolated from stable translational control HeLa cells and subjected to flow cytometry. Clone 5 was selected for expansion into clonal translational control HeLa cells.

B) To create a clonally-derived cell culture model of HIV-1 frameshifting, 10 clones were isolated from stable HIV-1 frameshifting HeLa cells and subjected to flow cytometry. Clone 2 was selected for expansion into clonal HIV-1 frameshifting HeLa cells.

3.3.2 Re-sorting of clone isolated from clonally-derived HIV-1 frameshifting HeLa cells

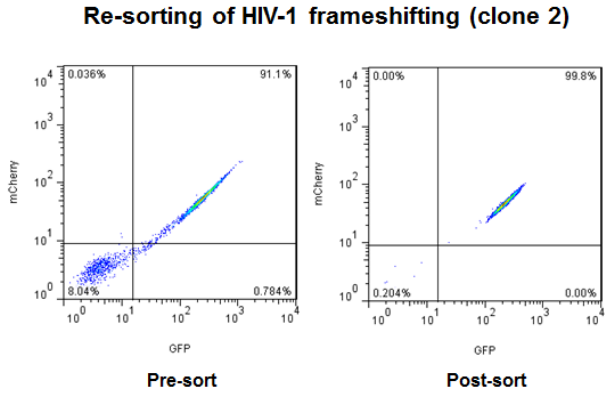

Figure 29 FACS re-sorting of clonal HIV-1 frameshifting HeLa cells
To eliminate negative population of cells from cell culture model of HIV-1 frameshifting, clonally-derived HIV-1 frameshifting HeLa cells (clone 2) underwent another round of flow-cytometry activated cell sorting.

3.3.3 Standard Operating Procedure (SOP) generated for optimization of assay and screening parameters in Chapter 3

HIV-TFS eGFP and mCherry Assay
Screen to identify HIV-1 frameshifting modulators

Table 1: Reagents

Reagent Number	Reagent Name	Reagent Concentration	Reagent Source	Catalogue Number
1	0.05% Trypsin EDTA	0.05%	Life technologies	25300
2	Phosphate Buffered Saline (PBS)	1x	Life technologies	14190
3	DMEM cell culture media		Life technologies	41966
4	Fetal bovine serum (FBS)		Life technologies	10082
5	Cell freezing medium-DMSO 1X		Sigma	C6164
6	Geneticin (G-418)	50mg/ml	Roche	04727878001

Table 2: Equipment and consumables

	Tool Name	Tool Source	Catalogue Number
1	Echo 550	Labcyte	
2	Pherastar FS	BMG Labtech	
3	Matrix Wellmate microplate dispenser Xrd-384	Fluid X	
4	384- well black plate	Greiner	781091
5	Matrix WellMate disposable tubing assembly	ThermoScientific	

Table 3: Preparation of cell culture media

Stock cell culture media	
DMEM	500mls
FBS	50mls

Supplements added to cell culture media immediately prior to use	
Supplement concentration	**Dilution factor and final concentration**
Geneticin (50mg/ml)	Dilute 125x Final concentration 0.4mg/ml

Table 4: Procedure

Step	*Step Description*
1	48 hours prior to reading mCherry expression, compounds are acoustically transferred to 384- well assay plates by Echo 550 (plate map 1).
2	Clonally-derived HIV-1 frameshift HeLa cells are washed in PBS, trypsinised, counted and re-suspended in cell culture media at $8x10^4$ cells/ml. Using the wellmate, 50µL of this suspension is added to each well of a 384- well assay plate resulting in 4000 cells being seeded per well, such that the final concentration of test compound is 30µM. Cells are incubated at 37°C in 5% CO_2 for 48hours.
3	On day of assay, HIV- TFS cells incubated with compounds are washed twice with 50µL of PBS using the wellmate and then incubated with 50µL of PBS for assay.
4	Using the Pherastar FS, plates are read at 580nm/610nm for mCherry expression

Plate Maps

Plate map 1

	1	2	3	4	5	6	7	8	9	10	11	12	13	14	15	16	17	18	19	20	21	22	23	24
A	Compounds from diversity set at final concentration of 30µM (Single- point)										DMSO	DMSO	Compounds from diversity set at final concentration of 30µM (Single- point)										DMSO	DMSO
B											DMSO	DMSO											DMSO	DMSO
C											DMSO	DMSO											DMSO	DMSO
D											DMSO	DMSO											DMSO	DMSO
E											DMSO	DMSO											DMSO	DMSO
F											DMSO	DMSO											DMSO	DMSO
G											DMSO	DMSO											DMSO	DMSO
H											DMSO	DMSO											DMSO	DMSO
I											DMSO	DMSO											DMSO	DMSO
J											DMSO	DMSO											DMSO	DMSO
K											DMSO	DMSO											DMSO	DMSO
L											DMSO	DMSO											DMSO	DMSO
M											DMSO	DMSO											DMSO	DMSO
N											DMSO	DMSO											DMSO	DMSO
O											DMSO	DMSO											DMSO	DMSO
P											DMSO	DMSO											DMSO	DMSO

Table 6: Summary of screening conditions

Component	[Final assay]
HIV –TFS cells	4000cells / 50µl
Test Compound	30µM

Chapter 4

Results: Diversity screen for HIV-1 frameshifting modulators

This chapter outlines the drug discovery process towards identifying novel and effective compounds targeting the frameshifting mechanism of HIV-1 *gag* and *pol* genes. This was done by using cell culture models of HIV-1 frameshifting and cellular translation (illustrated in Figure 30), which were developed and optimized for screening in a high-throughput manner (Chapter 3). In the HIV-1 frameshifting model, eGFP and mCherry expression are indicative of cellular translational initiation and HIV-1 frameshifting efficiency, respectively. To recapitulate conventional translation (also referred to as global or cellular translation), eGFP and mCherry were placed in frame to represent cellular translational initiation and elongation, respectively. This chapter will describe key results from the diversity screen, hit identification, confirmatory screens and the rationale underlying hit selection throughout the screening cascade.

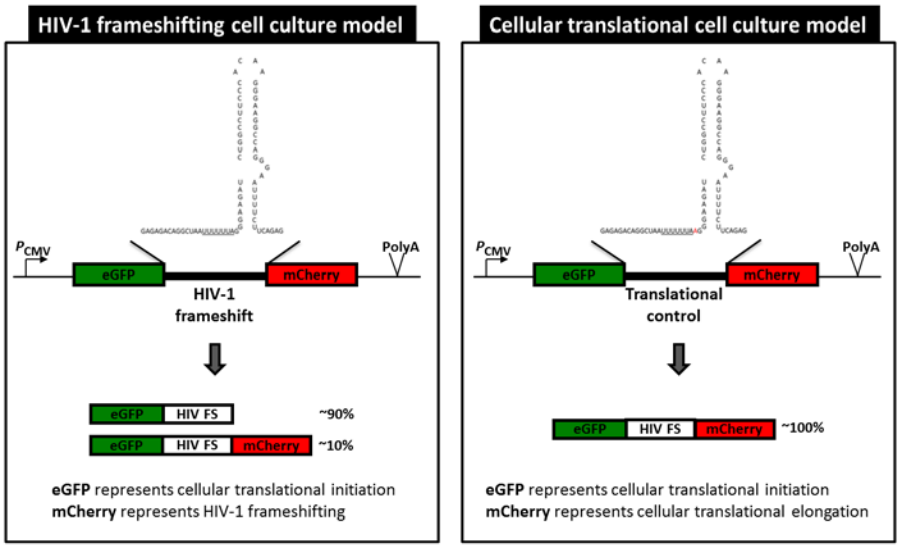

Figure 30 Cell culture models of HIV-1 frameshifting and cellular translation used in screening cascade for HIV-1 frameshift-specific modulators

In the HIV-1 frameshifting cell culture model (left), mCherry is only produced upon -1 ribosomal frameshifting at the upstream HIV-1 frameshift region at a frequency of ~5% and is therefore used as a signal output to study the effects of compounds on HIV-1 frameshifting efficiency. In the cell culture model of cellular translation (right), mCherry and eGFP are produced in the same reading frame as a result of conventional translation, and therefore represent the effect of compounds on cellular translational initiation and elongation, respectively.

4.1 Pilot screen and hit identification

To assess the potential screening quality for HIV-1 frameshifting modulators, a pilot screen was conducted to observe the rate and distribution of 'hits', which refers to compounds conferring activity. This was done by treating clonally-derived HIV-1 frameshifting HeLa cells with 1,167 compounds. These compounds belonged to three libraries within the Dundee Drug Discovery Unit's (DDU) diverse compound collection: Chemogenomics, NIH and Selleck. These small molecules within these libraries were chosen based on their diversity and known activity. A final compound concentration of 30μM was used to avoid toxic effects at higher concentrations and false negatives with low potency at lower concentrations. 48 hours after drug treatment, mCherry expression was quantified using the PherastarFS plate reader (BMG LabTech). Data analysis software, Activitybase XE (IDBS, Guilford, Surrey, UK), was used to determine mCherry fold change in compound-treated clonal HIV-1 frameshifting cells relative to DMSO-treated clonal HIV-1 frameshifting cells. This measure was used to identify active compounds ('hits') characterized by an activation or inhibition of mCherry fold change, thus indicative of an increase or decrease in HIV-1 frameshifting efficiency, respectively.

The median mCherry fold change of the pilot screen was 1.05 and the robust standard deviation was 0.13. Compounds with an effect either greater than or less than three times the standard deviation of the median were considered hits. With a 2.8% hit rate, the 33 identified hits varied in mCherry expression from 0.5-to 5-fold change, 10 of which were mCherry activators and 23 of which were mCherry inhibitors (Figure 31). The majority of these hits belong to the general subset, followed by the Selleck and the chemogenomics set. Since this pilot screen indicated potentially active compounds targeting HIV-1 frameshifting in the context of this cell-based assay, a large-scale diversity screen was conducted.

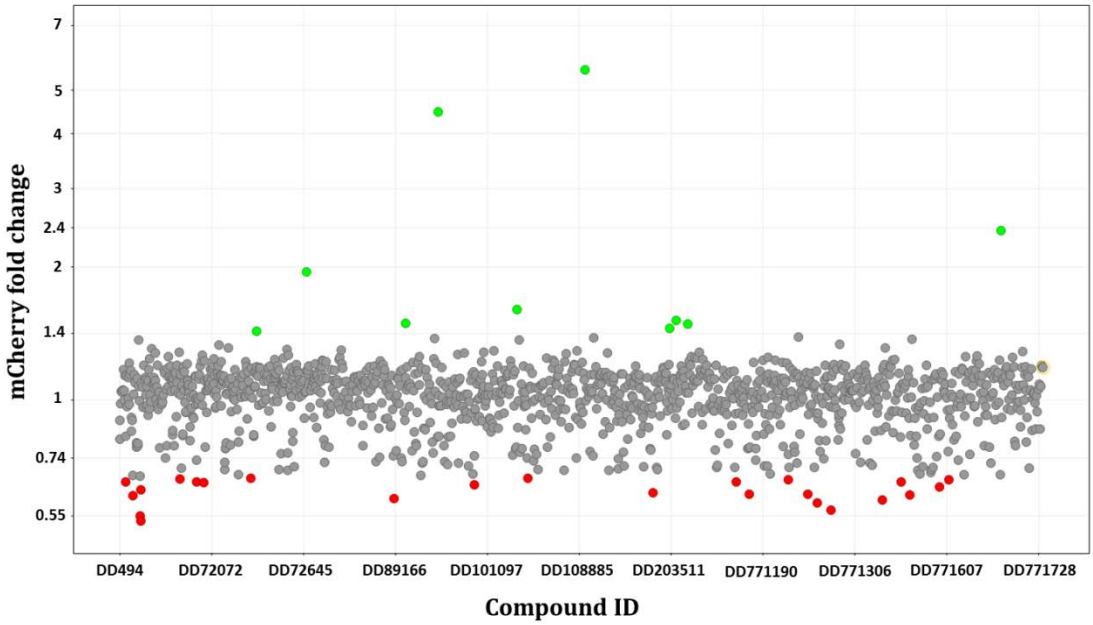

Figure 31 Scatter plot of the results from the pilot screen.
During the pilot screen, clonally-derived HIV-1 frameshifting HeLa cells (HIV FS cells) were treated with 1,167 compounds at 30μM in 384-well plates. After 48 hours, mCherry fluorescence was measured and fold change was determined relative to 0.3% DMSO-treated HIV FS cells. Points in scatter plot reveal fold change results from the pilot screen. 10 compounds with > 1.43 fold-change (green) and 23 compounds with <0.66 fold-change (red) were identified as hits using three times the median standard deviation as a cut-off.

4.2 Diversity screen and primary hit identification

To identify modulators of HIV-1 frameshifting, a diversity screen was carried out by incubating clonally-derived HIV-1 frameshifting HeLa cells with 92,071 diverse compounds at a final concentration of 30μM for 48 hours. These compounds were diverse, covered a broad chemical space and belonged to various libraries including the diverse collection, bioactive sets, chemogenomics, EasySet and focused libraries against epigenetic modifiers, protease, phosphatase, ion channel, kinase and nuclear hormone receptors. Standard screening statistics were applied to each plate run in the primary screen (described in section 2.15).

To examine the effect of compounds on HIV-1 frameshifting, mCherry fold change was quantified by measuring mCherry fluorescence of compound-treated cells relative to DMSO-treated cells. Using three times the standard deviation of the median as a threshold to identify hits, mCherry activators were identified based on greater than 1.27 mCherry fold change while mCherry inhibitors were identified by less than 0.7 fold change. Approximately 2926 hits were ultimately identified, 1455 of which activated mCherry expression and 1471 compounds that inhibited mCherry expression (Figure 32). These are referred to as 'activator hits' and 'inhibitor hits', respectively. Compared to the pilot screen, the primary diversity screen resulted in a similar distribution of hits (Figure 56 in Appendix 4.8.2) with activity of activator hits spanning a wide range, and inhibitor activity were maintained close to baseline levels. This however, was not unexpected since potential inhibitor hits aim to reduce the already naturally low level of frameshifting (~15%). The library composition of mCherry activator hits and mCherry inhibitor hits is depicted in Figure 33 and Figure 34, respectively. Within the primary hit activators and inhibitors identified, majority of hits belonged to the General set (Figure 33). This is not unexpected as most compounds run in the primary screen belonged to the General set. However, when hits were normalized to the total number of compounds within each set, the focused nuclear hormone receptor (NHR) set of compounds were highly represented as both activators and inhibitors (Figure 33 and Figure

34). Compounds in the NHR set are more lipophilic than other sets and may therefore account for the greater proportion of compounds exhibiting activity. Furthermore, a large proportion of compounds in the kinase and phosphatase sets were identified as inhibitors (Figure 34). Kinases and phosphatases play a central role in protein phosphorylation to regulate signal transduction in various cellular processes such as apoptosis, development, transcription and the immune response. Thus, the high proportion of kinase and phosphatase-targeted compounds as potential active frameshifting inhibitors suggest potential off-target inhibitory effects. Alternatively, these compounds could possess characteristics sufficient to target the HIV-1 frameshift model used in this study.

A)

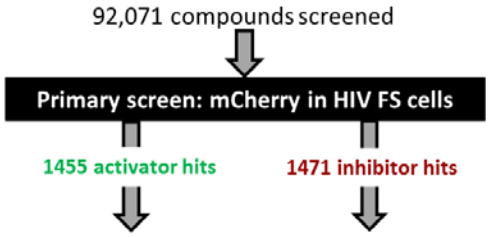

B)

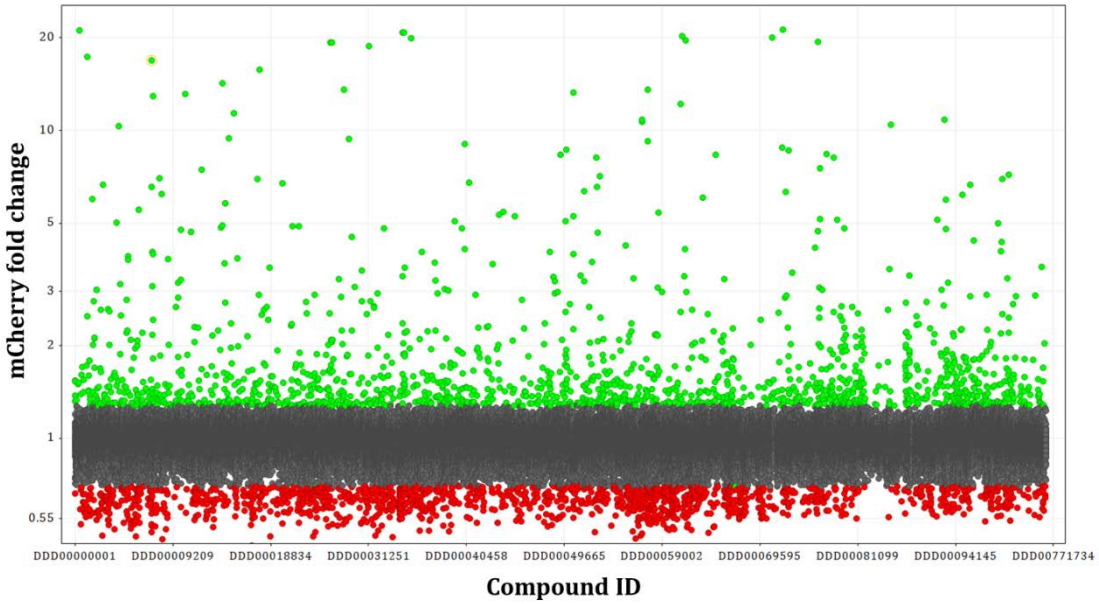

Figure 32 Hits obtained from primary diversity screen for HIV-1 frameshift modulators

The primary diversity screen was conducted by treating clonally-derived HIV-1 frameshifting with 92,071 compounds at a final concentration of 30μM. After 48 hours, mCherry fluorescence was measured and fold change was determined relative to 0.3% DMSO-treated HIV FS cells.

A) 1455 mCherry activator and 1471 mCherry inhibitor hits were obtained from primary diversity screen

B) Points in scatter plot reveal mCherry fold change results from the diversity screen. Using three times the median standard deviation as a threshold, 1455 hit compounds activated mCherry (green) and 1471 hit compounds inhibited mCherry fold change (red).

A)

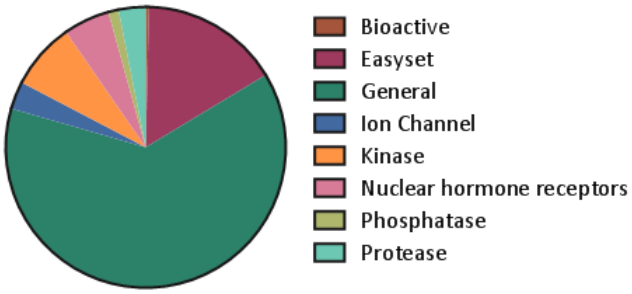

B)

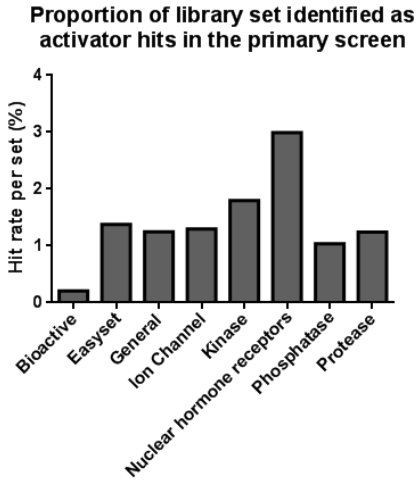

Figure 33 Library composition and hit rate of mCherry activator hits from primary screen for HIV-1 frameshift modulators

A) Library composition of mCherry activator hits

B) Proportion of library sets identified as activator hits in the primary screen

A)

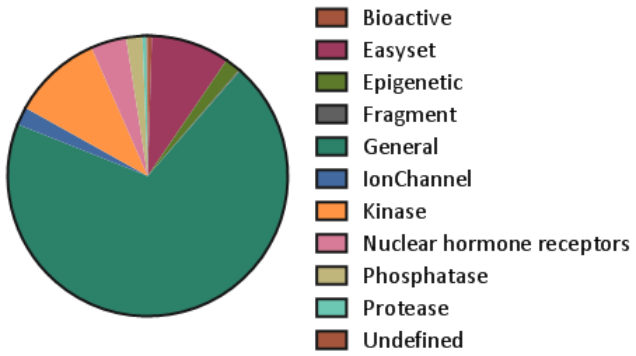

B)

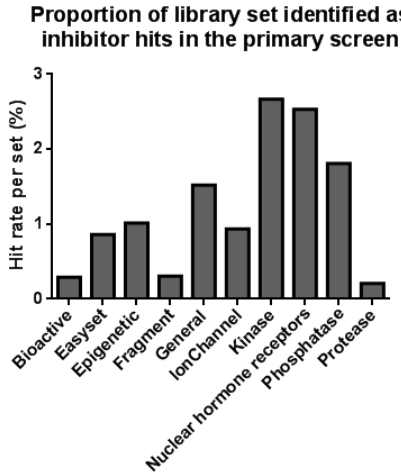

Figure 34 Library composition and hit rate of mCherry inhibitor hits from primary screen for HIV-1 frameshift modulators

A) Library composition of mCherry inhibitor hits
B) Proportion of library sets identified as inhibitor hits in the primary screen

4.2.1 Hit selection

This section outlines the rationale and hit analysis carried out to narrow down the large number of primary screen hits and eliminate those with potential for assay interference (illustrated in Figure 35).

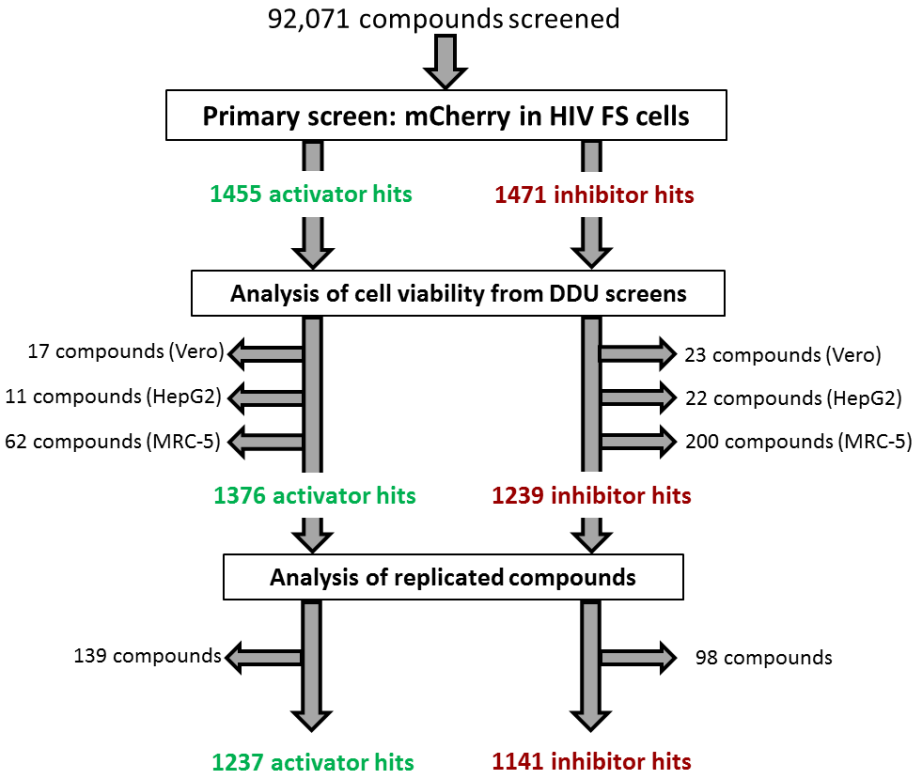

Figure 35 Workflow of hit identification and selection following primary diversity screen (Section 4.2.1).
The mCherry activator hits (green) and inhibitor hits (red) identified from the primary diversity screen were narrowed down by analysing previous Drug Discovery Unit (DDU) screening data associated with these compounds. Compounds that inhibited cell viability (pXC_{50}>4.2) and replicated compounds with inconsistent activity were eliminated.

The 3.2% hit rate of the primary diversity screen was slightly higher than other screens which range from 0.1%-1%. However, hit rate is influenced by many factors, including arbitrary thresholds and the concentration of compound used in screening. To narrow down the large number of hits generated from the diversity screen (described in 4.2), previous screening data associated with these 2,926 hits were analyzed.

Dotmatics and Vortex software were used to access and visualize cell viability data previously conducted at the DDU with MRC-5, HepG2 and Vero cells. Cell viability assays were performed in these cell lines by observing the reduction of resazurin to highly fluorescent resorufin in live cells treated with varying doses of a compound. This in turn generated a pXC_{50} value which is the -log of the drug concentration required to exhibit an effect by 50% (XC_{50}), by either activation or inhibition. Therefore, a threshold at pXC_{50} of 4.2 was set to identify compounds with inhibitory effects on cell viability in MRC-5, HepG2 or Vero cells. The eliminated hit compounds with pXC_{50} value greater than 4.2 corresponded to at least 50% inhibition of cell viability at concentrations lower than 60μM. As a result, this eliminated 90 mCherry activator hits and 245 mCherry inhibitor hits generated from the diversity screen (Figure 35).

Within the compound libraries used in the primary screen, 7.3% of small molecules were present in replicates. These replicates were represented by more than one batch originating from different sources. I eliminated compounds with inconsistent activity between batches and selected compounds that were active in all replicates. Using the statistical cut-off for hit identification in the primary screen, this corresponded to compounds exhibiting greater than 1.28 or less than 0.7 mCherry fold change. For example, two different batches of compound DDD00057099 from the 'KEY' supplier and the 'BIO' supplier led to mCherry fold change of 10.82 and 10.68, respectively. Therefore, compounds like DDD00057099 were selected as activator hits. Similarly, compound DDD00000988 which exhibited 0.55 and 0.57 mCherry fold change in two different batches was an example of inhibitor hits selected through for secondary screening.

Consequently, 139 mCherry activators and 98 mCherry inhibitors were eliminated as primary hits. As illustrated in Figure 35, this ultimately narrowed down the initial 1455 mCherry activators and 1471 inhibitors to 1237 activator hits and 1141 inhibitor hits, respectively.

4.3 Confirmatory screening using dose-response curves (DRCs)

Following the primary diversity screen, this section outlines the secondary screening conducted to confirm activity and specificity of hit compounds. This was done using dose-response curves (DRCs) which are useful in determining the amount of drug required to elicit a response, and will therefore ascertain a compound's potency and efficacy.

To determine the effect of hit compounds on HIV-1 frameshifting, the dose-dependent effect of compounds was examined on eGFP and mCherry fluorescence in clonally-derived HIV-1 frameshifting HeLa cells. Similar dose-dependent effects were examined in clonally-derived translational control HeLa cells to identify and eliminate compounds that impact cellular translation. Furthermore, cell viability assays in parental HeLa cells were used to eliminate toxic compounds.

The ultimate goal of these confirmatory screens was to identify non-toxic hit compounds that specifically affect HIV-1 frameshifting without perturbing cellular translation.

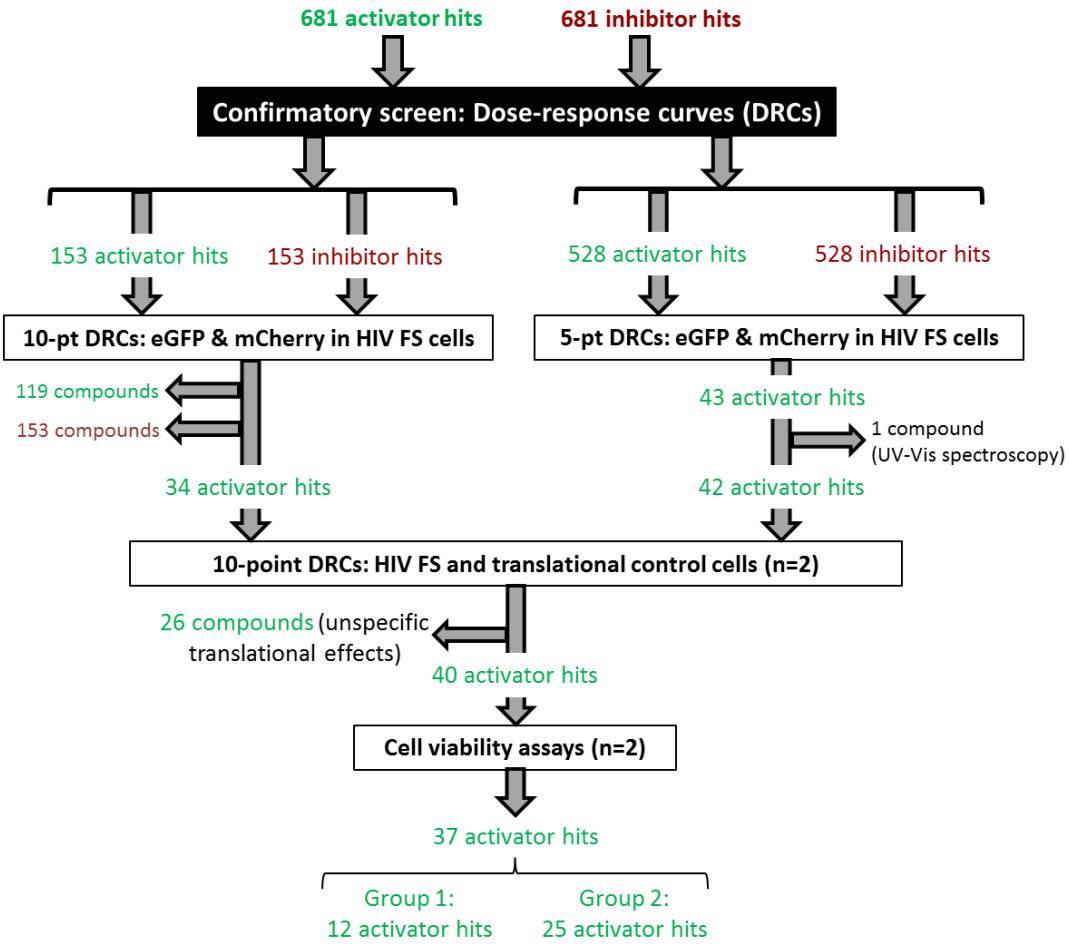

Figure 36 Workflow of confirmatory screens and subsequent hit selection (detailed in section 4.3)

4.3.1 Identification of active compounds in HIV-1 frameshifting cell culture model

4.3.1.1 Preliminary 10-point DRCs

Due to the large amount of hits generated from the primary screen, preliminary dose-response curves were conducted with a small subset of hits. 153 mCherry activators and 153 mCherry inhibitors were selected to examine their dose-dependent effect on eGFP and mCherry expression in the HIV-1 frameshifting cell culture model.

Compounds for confirmatory DRCs were chosen based on their consistency within replicates and their effects in other DDU screens. Within the 153 mCherry activator hits chosen (from 1237 hits), 22 compounds were chosen based on consistent mCherry activation within replicates and 3 compounds were selected based on their effects in a previously conducted commercial screen using a red fluorescence-based assay, referred to as screen X. The signal output of screen X was measured by quantifying fluorescence emitted at 590nm, which is comparable to the signal output in the HIV-1 frameshifting cell-based assay where mCherry fluorescence is emitted at 610nm. Therefore, based on the assumption that unspecific red fluorescent compounds are potentially activated in both screen X and HIV-1 frameshifting assay, 3 mCherry activator hits were selected for preliminary DRCs (Table 3). While DDD00010469, DDD00056808 and DDD000622545 activated mCherry in the HIV-1 frameshifting assay, they significantly inhibited fluorescence in screen X, thereby implying that mCherry activation is potentially frameshifting-specific and not due to unspecific fluorescence. The remaining 128 mCherry activator hits were randomly chosen to exhibit a wide range of mCherry fold change (Figure 37). Instead of choosing compounds with the highest activity (mCherry fold change), I chose compounds with a wide range of activity to avoid bias and the possibility of selecting unspecific auto-fluorescent compounds.

Similarly, 3 mCherry inhibitor hits that led to significant percent activation in screen X indicated that mCherry inhibition in primary diversity screen was

potentially specific to HIV-1 frameshifting and not due to quenching of the mCherry fluorophore (Table 3). These 3 compounds, DDD00017060, DDD00005747 and DDD00018807 were therefore selected for 10-point dose-response curves along with 47 compounds that consistently inhibited mCherry within replicates of the primary screen. The remaining 53 compounds were randomly chosen to exhibit a wide range of mCherry fold change in inhibition (Figure 37).

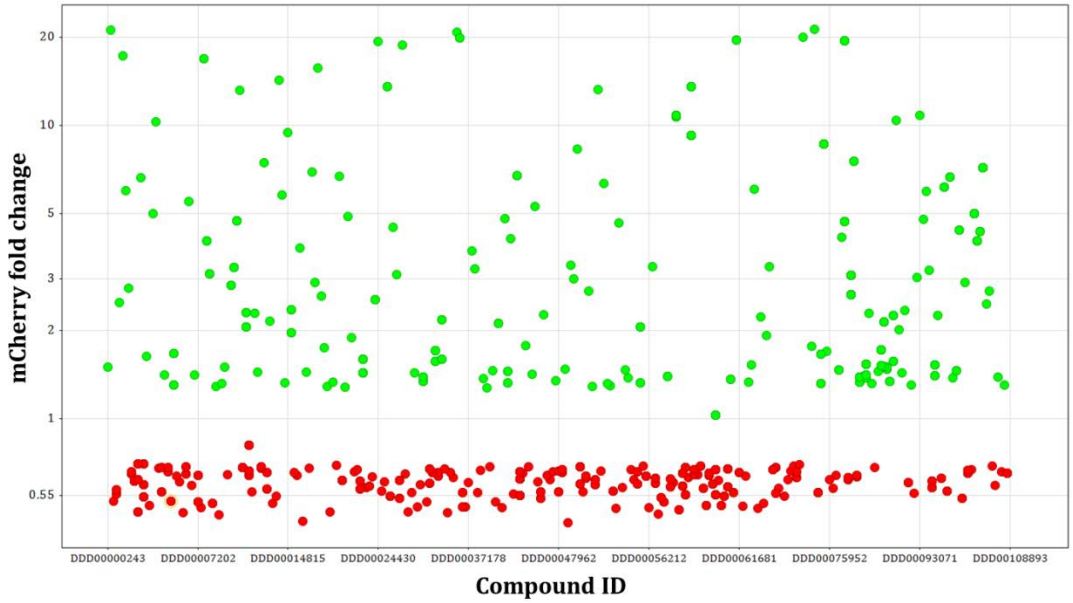

Figure 37 Scatter plot of mCherry fold change from 153 activator hits (green) and 153 inhibitor hits (red) chosen for preliminary 10-point dose-response curves.

153 activator hits (green) and 153 inhibitor hits (red) generated from the primary diversity screen was selected to conduct preliminary 10-point dose-response curves. These were randomly selected to represent compounds with a wide range of mCherry fold change.

Table 3 Compounds selected for preliminary 10-point DRCs based on effect in previously conducted fluorescent screen X

Compound	HIV FS screen (mCherry fold change)	Screen X (red fluorescence)
DDD00010469	13.16	53 % inhibition
DDD00056808	1.39	101% inhibition
DDD00062545	1.53	100% inhibition
DDD00017060	0.48	88% activation
DDD00005747	0.48	91% activation
DDD00018807	0.48	87% activation

Two biological replicates of these dose-response curves were conducted for each of the 153 mCherry activator and 153 mCherry inhibitor hits selected from the primary screen hits. Four parameter dose-response curves (described in section 1.7.3.4) were generated from the dose-dependent effect of these hits on HIV-1 frameshifting and cellular translation, characterized by mCherry and eGFP fluorescence, respectively. Since there is no confirmed modulator of HIV-1 frameshifting (positive control), a potency-based statistical cut-off was arbitrarily set to identify DRC hits. Compounds with a pXC_{50} value greater than 4.2 in mCherry activity (<60μM potency) and less than 4 in eGFP activity (>100μM potency), were selected as hits. In the context of the cell culture model of HIV-1 frameshifting, these factors correspond to compounds that inhibit or activate HIV-1 frameshifting while maintaining cellular translational initiation.

While Activitybase XE software was successful in identifying and fitting true active compounds to four-parameter curves, some fitted dose-response curves had to be manually invalidated from active to inactive (Example shown in Figure 57 in Appendix 4.8.3). In the primary screen, the difference between the median and resulting cut-off threshold value to identify activator and inhibitor hits was 0.29. Thus, compounds with ≤ 0.29 fold change difference between the minimal and maximum responses of either mCherry or GFP in DRCs, were eliminated.

From the 153 activator hits tested in the HIV-1 frameshifting cell culture model, 34 compounds were identified as mCherry activators and did not exhibit eGFP-specific effects (Figure 38). These compounds potentially stimulate HIV-1 frameshifting efficiency and are therefore selected through to the next stage of the screening cascade. From the 153 mCherry inhibitor hits tested, all active compounds also inhibited eGFP in a dose-dependent manner (Figure 39). This indicated that these false positive hits were potentially cellular translational inhibitors.

A)

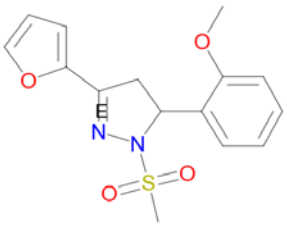

B)

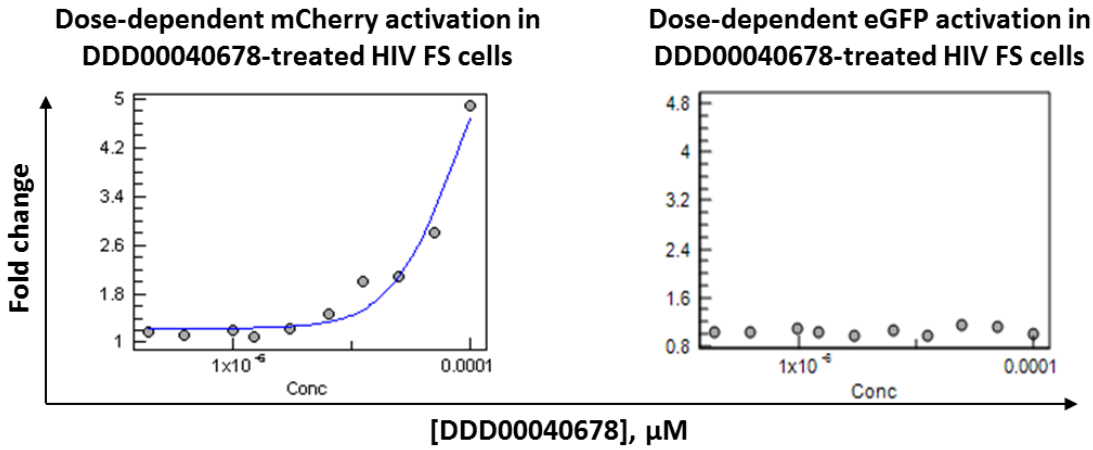

Figure 38 Representative 10-point dose-response curve (DRC) of hit compound selected as activator of HIV-1 frameshifting.

A) Structure of DDD00040678

B) Clonally-derived HIV-1 frameshifting HeLa cells were treated with 153 hits (mCherry activators from primary screen) at 10 different concentrations in order to determine their dose-dependent effect on mCherry and eGFP, which represent HIV-1 frameshifting efficiency (left) and cellular translational initiation (right), respectively. Compounds (such as DDD00040678) solely exhibiting mCherry-specific effects were identified as hits. From 153 compounds screened, 34 compounds (all mCherry activators) were selected as active hits.

A)

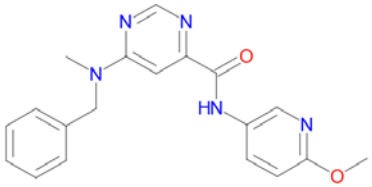

B)

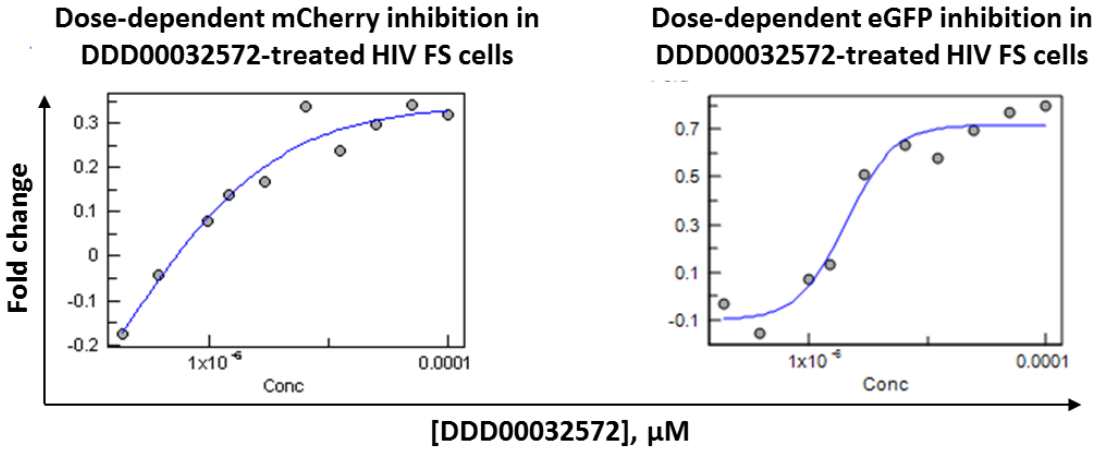

Figure 39 Representative 10-point dose-response curve (DRC) of compounds eliminated as hits active for HIV-1 frameshifting.

A) Structure of DDD00032572

B) Clonally-derived HIV-1 frameshifting HeLa cells were treated with 153 hits (mCherry inhibitors from primary screen) at 10 different concentrations in order to determine their dose-dependent effect on mCherry and eGFP, which represent HIV-1 frameshifting efficiency (left) and cellular translational initiation (right), respectively. Compounds (such as DDD00032572) exhibiting mCherry-and eGFP-specific inhibitory effects were rejected. From 153 compounds screened, all 153 compounds were eliminated from the screening cascade.

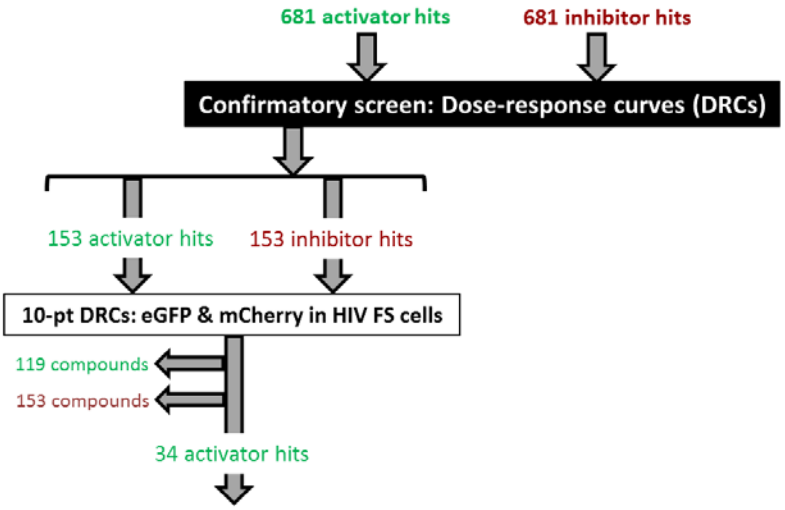

Figure 40 Hit identification results from 10-pt DRC confirmatory screening (detailed in Section 4.3.1.1)

4.3.1.2 Results from 5-point DRCs

Preliminary 10-point dose-response curves indicated that some compounds potentially increased HIV-1 frameshifting efficiency. I therefore screened a larger subset of compounds at 5 drug concentrations (5-point DRCs). These 5 concentrations corresponded to a range that elicited a response in active compounds screened with 10-point DRCs. Confirmatory screening in clonally-derived HIV-1 frameshifting HeLa cells was done with 528 activator and 528 inhibitor hits exhibiting a wide range of activity in the primary screen (Figure 58 in Appendix 4.8.4). Data was visualized using Vortex software to manually assess dose-dependent effect of compounds. Following the rationale underlying hit identification in 10-pt DRCs (section 4.3.1.1), hits were identified based on an active mCherry-specific response. As a result, 43 mCherry-specific hit compounds with unaffected eGFP levels were carried through the next stage of the screening cascade (representative examples depicted in Figure 41).

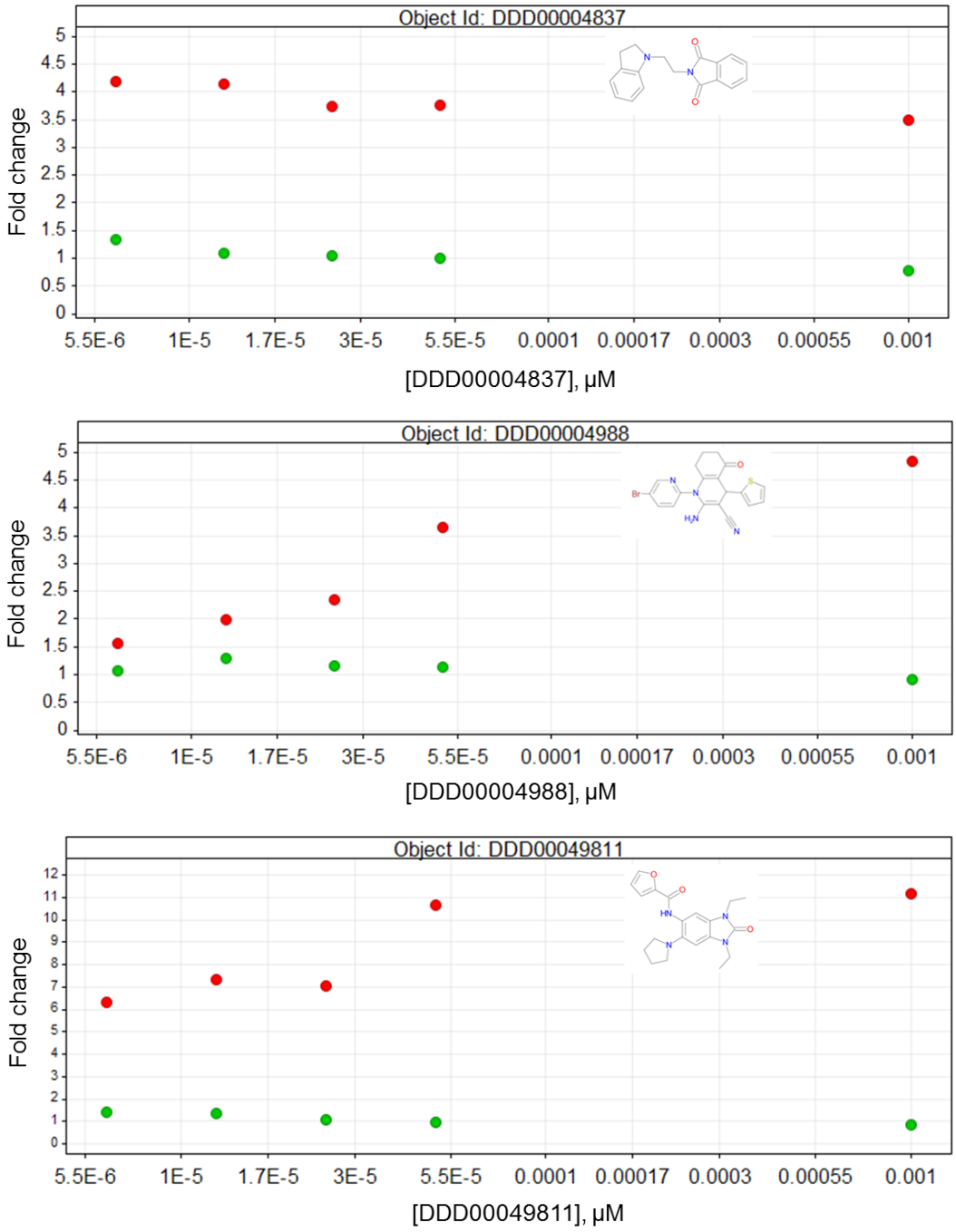

Figure 41 Representative compounds selected as activator 'hits' from 5-point dose-response curves

Clonally-derived HIV-1 frameshifting HeLa cells were treated with 528 hit compounds (mCherry activators from primary screen) at 5 different concentrations in order to determine their dose-dependent effect on mCherry (red) and eGFP (green) expression, which represent HIV-1 frameshifting efficiency and cellular translational initiation, respectively. Compounds (such as DDD00004837, DDD00004988 & DDD00049811) solely activating mCherry fold change were selected as hits. From 528 compounds screened, 43 compounds were selected for the next stage of screening.

In contrast, mCherry inhibitor hits were not identified due to off-target inhibitory activity on eGFP fluorescence. This correlated with effects observed in 10-point DRCs whereby dose-dependent reduction in mCherry expression was often associated with reduced eGFP expression. Compounds that fit this profile were eliminated from the screening cascade (representative examples depicted in Figure 42) and signified that compounds potentially capable of inhibiting HIV-1 frameshifting, also unfavourably inhibited cellular translation.

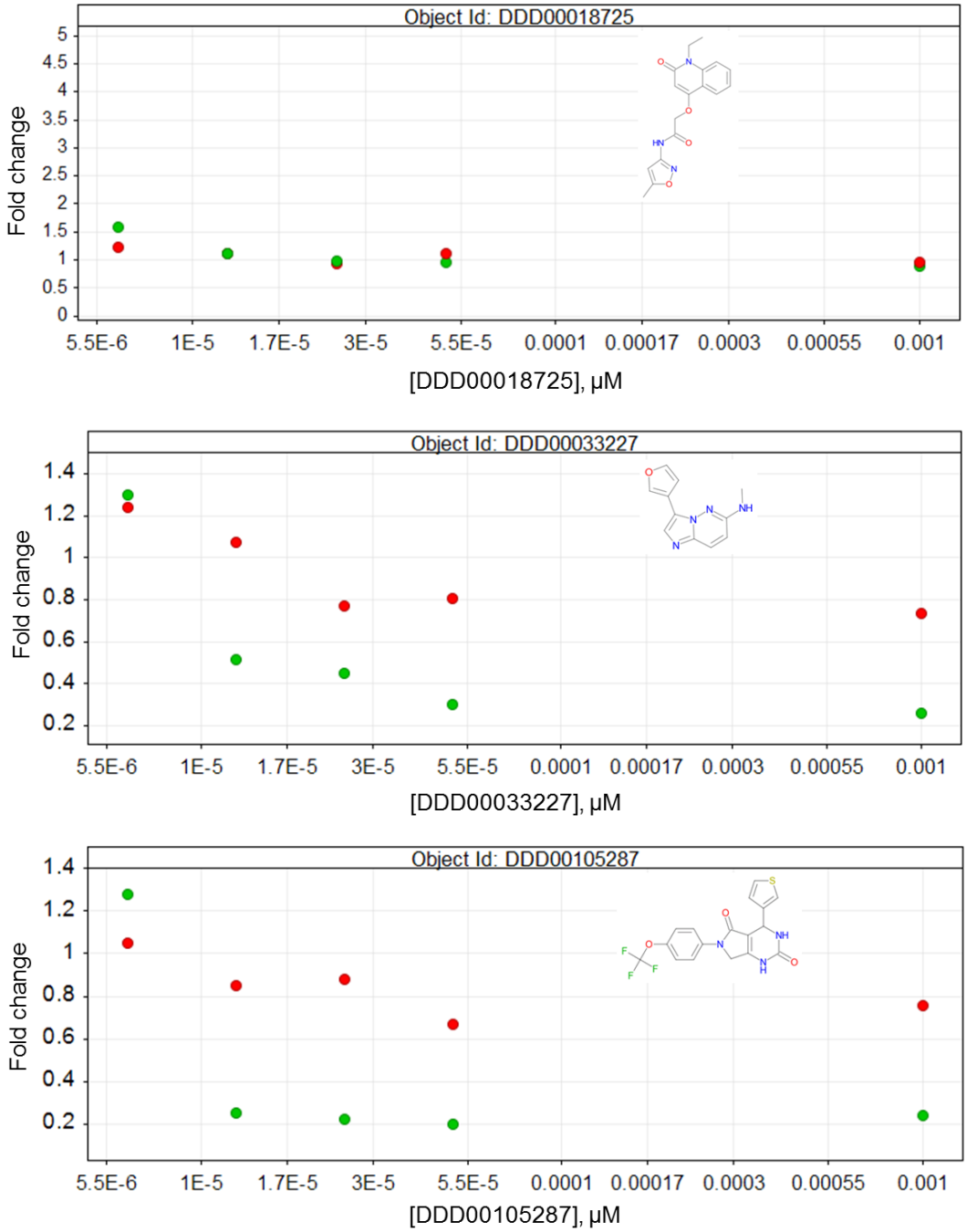

Figure 42 Representative compounds rejected as inhibitor 'hits' from 5-point dose-response curves

Clonally-derived HIV-1 frameshifting HeLa cells were treated with 528 hit compounds (mCherry inhibitors from primary screen) at 5 different concentrations in order to determine their dose-dependent effect on mCherry (red) and eGFP (green) expression, which represent HIV-1 frameshifting efficiency and cellular translational initiation, respectively. Compounds (such as DDD00018725, DDD00033227 & DDD00105287) which exhibit mCherry-and eGFP-specific inhibitory effects were eliminated from the screening cascade. From 528 compounds screened, none of the compounds were found active inhibitors of HIV-1 frameshifting.

4.3.1.2.1 Elimination of fluorescent compounds

Screening small molecules with a fluorescence cell-based assay raised the possibility of false positive hits as a result of intrinsic fluorescent properties. Due to a significant waste of resources associated with false positives, it is important to eliminate these during a screening cascade for specific and selective hits. False positive hits can depend on the assay or aggregates, and can thus interfere with the assay or readout, potentially through unspecific binding with proteins (Thorne, Auld, & Inglese, 2010). It has also been reported that 2% of screening libraries can contain fluorescent compounds (Zhang et al, 2009). This raised concerns that active hit compounds identified by increased mCherry expression in HIV-1 frameshifting cells could be attributed to auto-fluorescent properties.

To address this and eliminate compounds that could potentially interfere with this fluorescent-based assay, Ultraviolet-visible (UV-Vis) spectroscopy was conducted to determine compound absorbance over wavelengths corresponding to UV and visible light. The 528 mCherry activators and 528 mCherry inhibitors run in the 5-point DRCs (in section 4.3.1.2) were scanned at wavelengths ranging from 350nm-650nm. Absorbance spectrum, to a certain extent, is equivalent to the excitation spectrum. eGFP and mCherry fluorophores used in the cell-based HIV-1 frameshifting assay were excited at 485nm and 580nm, respectively. Compounds that were absorbed at either 485nm or 580nm were eliminated as hits since the signal output in this fluorescent assay could be affected by the compound's absorbance properties, rather than its effect on HIV-1 frameshifting. Table 4 outlines the five compounds with absorbance peaks corresponding to excitation wavelengths of eGFP. Four of the five compounds were mCherry activator hits generated from primary screen, but were found inactive using 5-point DRCs and were therefore already eliminated from the screening cascade. However, DDD00034840 which was found active in both the primary screen and 5-point DRCs, was eliminated from the screening cascade, therefore resulting in 42 hit activator hits thus far.

Absorbance can be influenced by compound characteristics such as structure, conjugated systems, colour and functional groups. Longer wavelengths corresponding to visible light are potentially indicative of molecular structure (larger conjugations due to functional groups) or colourful compounds. Therefore, compounds exhibiting absorbance at long wavelengths should also be eliminated. While these eliminated compounds may not necessarily be fluorescent or possess characteristics that would interfere with this cell-based assay, they have the potential to do so, and the elimination of false positives is an important part of the screening process.

Table 4 Compounds eliminated from UV-Vis spectroscopy

Compound	Peak absorbance (nm)	Spectral graph
DDD00090618 (mCherry activator) 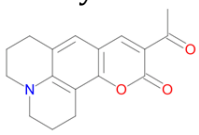	460nm	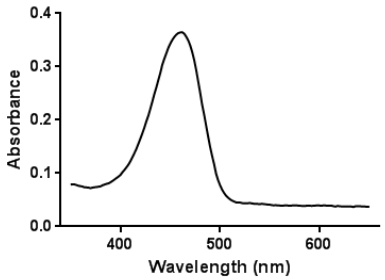
DDD00095491 (mCherry activator) 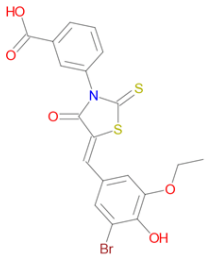	490nm	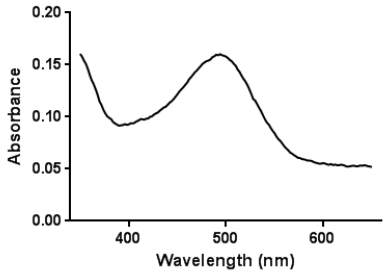
DDD00097146 (mCherry activator) 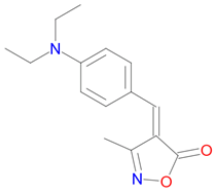	490nm	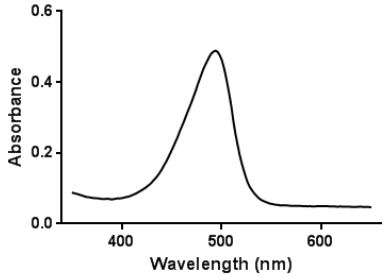
DDD00093255 (mCherry activator) 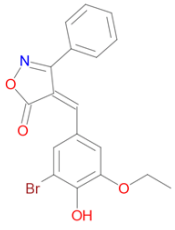	490nm	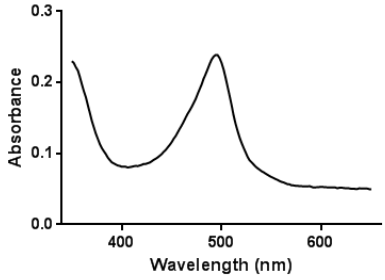
DDD00034840 (mCherry activator) 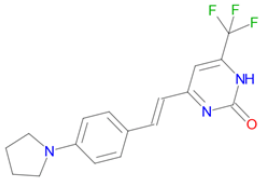	450nm	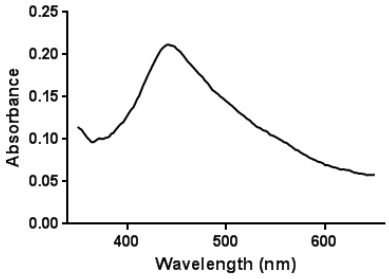

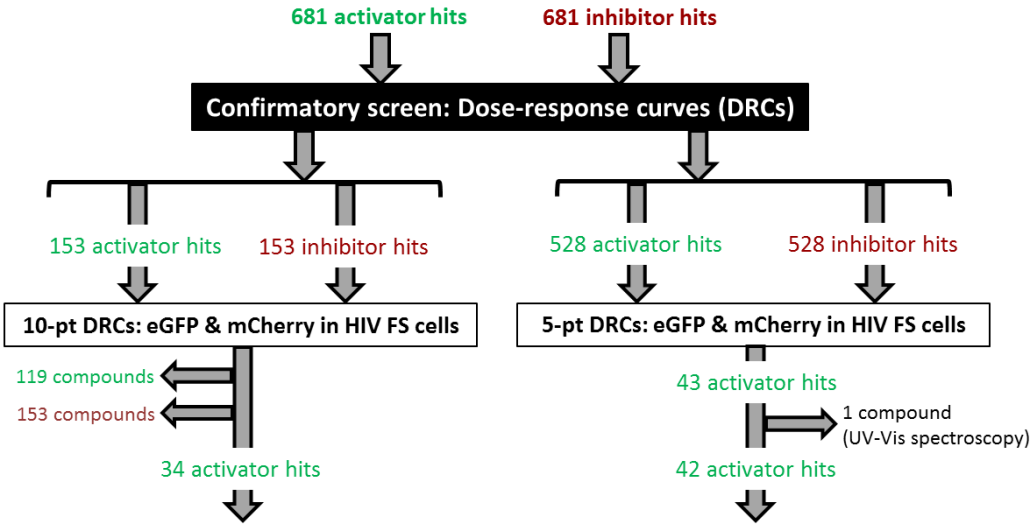

Figure 43 Hit identification from 10-pt and 5-pt DRC confirmatory screening so far (detailed in sections 4.3.1.1 and 4.3.1.2)

4.3.2 Hit selection of HIV-1 frameshifting-specific compounds

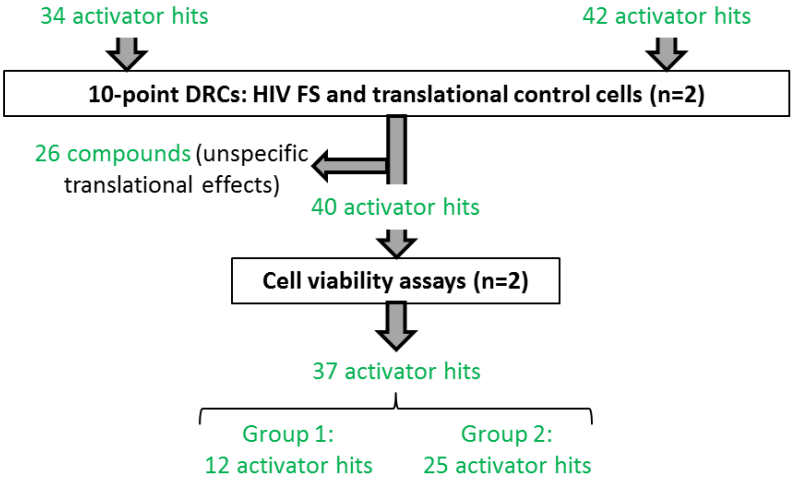

Figure 44 Workflow of confirmatory screening conducted to confirm the specificity and activity of hit compounds (detailed in this section 4.3.2)

To confirm the specificity and activity of 76 hit compounds identified so far (Figure 60 in Appendix 4.8.6), I also examined the effect of these compounds in a cellular translational cell culture model and on cell viability (Figure 44). Using both clonally-derived HIV-1 frameshifting and translational control HeLa cells, 10-point DRCs of these 76 compounds were conducted in two biological replicates.

Clonally-derived translational control cells were used as a controlled measure to eliminate compounds that impact general translation or fluorescence. In clonally-derived translational control HeLa cells, eGFP expression was indicative of cellular translational initiation while mCherry levels were indicative of cellular translational elongation (Figure 30). Therefore, compounds exhibiting dose-dependent effects on either eGFP or mCherry were eliminated as hits due to unspecific target activity (pXC_{50}>4.2). Compounds that only led to dose-dependent mCherry activation in clonally-derived HIV-1 frameshifting cells in all biological replicates, were selected as hits in the screening cascade (pXC_{50}>4.2) (representative examples shown in Figure 45).

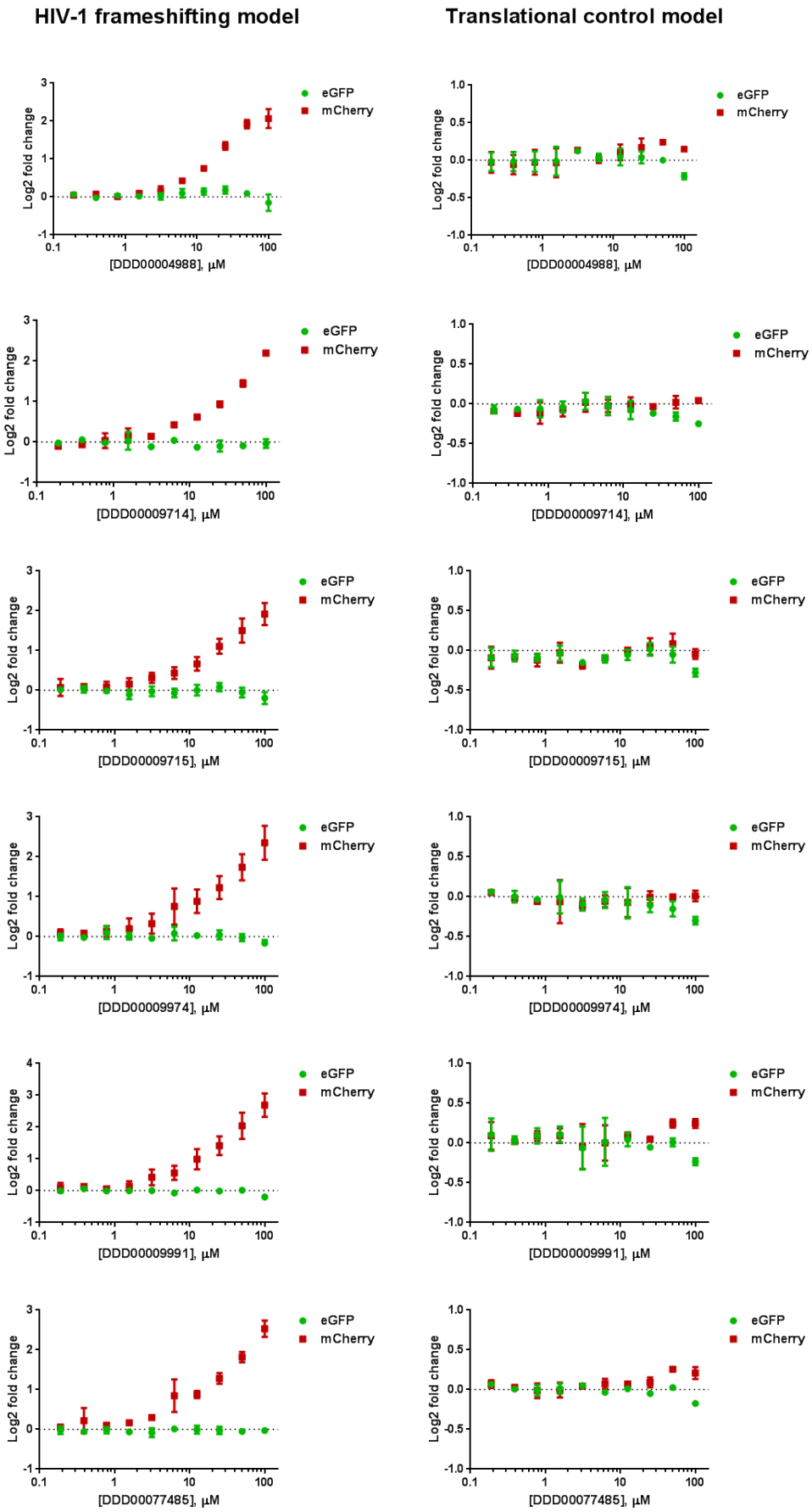
HIV-1 frameshifting model
Translational control model
eGFP
mCherry
Log2 fold change
[DDD00004988], µM
[DDD00009714], µM
[DDD00009715], µM
[DDD00009974], µM
[DDD00009991], µM
[DDD00077485], µM

Figure 45 Representative compounds selected as hits from screening cascade based on HIV-1 frameshifting-specific activity

Clonally-derived HIV-1 frameshifting HeLa cells (left) and translational control HeLa cells (right) were treated with compounds (mCherry activators from primary and confirmatory screen) at 10 different concentrations. This was used to determine the dose-dependent effect on HIV-1 frameshifting (mCherry fold change; red) and cellular translational initiation (eGFP fold change; green) in the HIV-1 frameshifting cell culture model (left) along with the dose-dependent effect on cellular translational initiation (eGFP fold change; green) and cellular translational elongation (mCherry fold change; red) in the translational control cell culture model (right). Compounds such as these, solely with mCherry-specific activity in the HIV-1 frameshifting model were selected as hits. Graphs were generated using GraphPad Prism and error bars represent the standard deviation of the mean (n=2-4).

Few exceptions were made during the hit selection process to prevent potential true active compounds from being eliminated. This took into account the nature of unspecific effects and the magnitude of translational effects. Some compounds such as DDD00007217 led to pronounced effects in the HIV-1 frameshifting model compared to the cellular translational model (Figure 46) and were therefore selected as hits due to the higher degree of activity on frameshifting. These compounds may be worth testing in secondary assays since ribosomal frameshifting is a translational process and hence, may impact cellular translation to a small degree in order to truly compromise frameshifting efficiency.

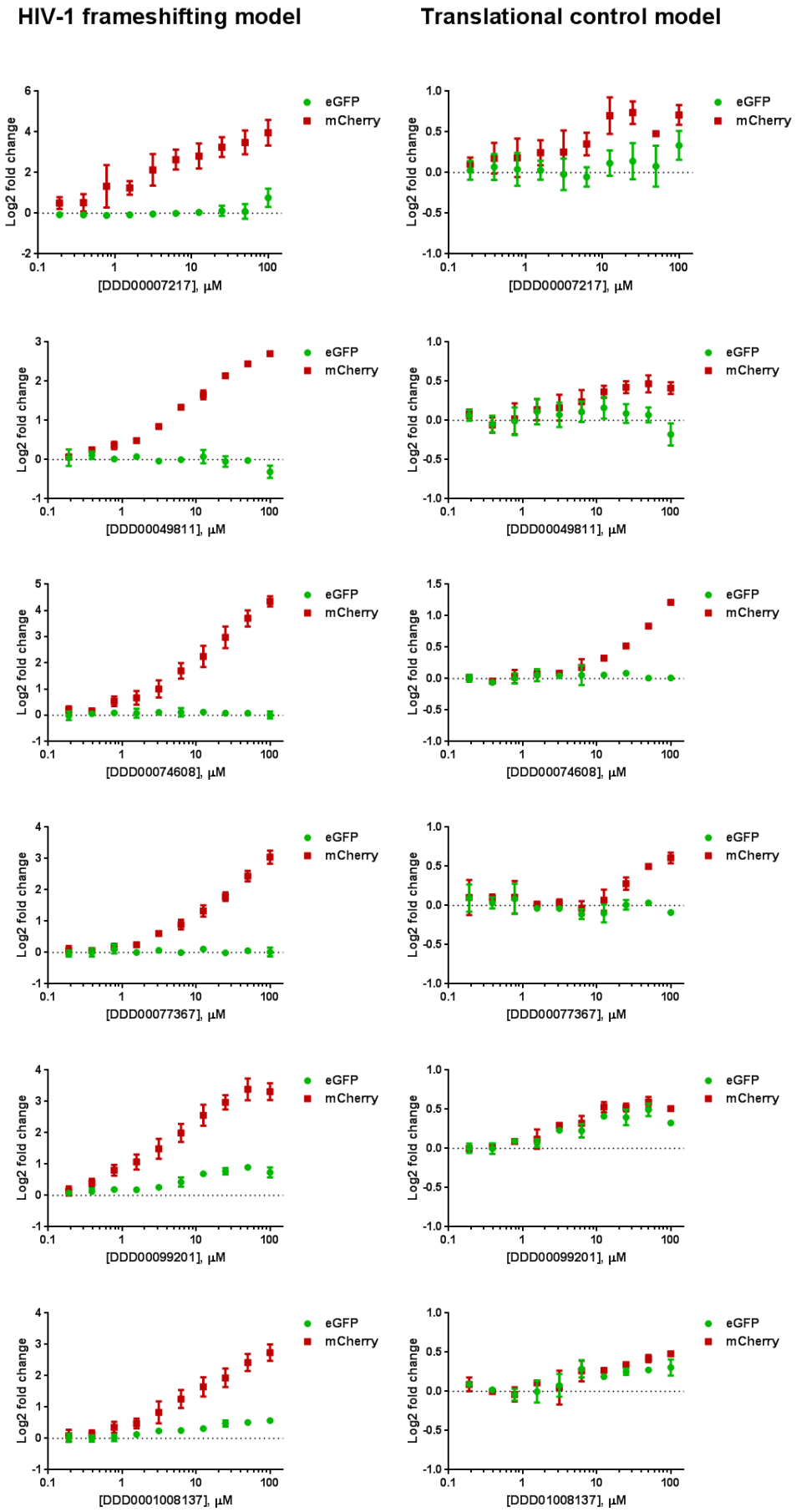
HIV-1 frameshifting model
Translational control model
Log2 fold change
eGFP
mCherry
[DDD00007217], µM
[DDD00049811], µM
[DDD00074608], µM
[DDD00077367], µM
[DDD00099201], µM
[DDD0001008137], µM
[DDD01008137], µM

Figure 46 Representative compounds with minimal unspecific effects were selected as hits based on pronounced effects on HIV-1 frameshifting

Clonally-derived HIV-1 frameshifting HeLa cells (left) and translational control HeLa cells (right) were treated with compounds (mCherry activators from primary and confirmatory screen) at 10 different concentrations. This was used to determine the dose-dependent effect on HIV-1 frameshifting (mCherry fold change; red) and cellular translational initiation (eGFP fold change; green) in the HIV-1 frameshifting cell culture model (left) along with the dose-dependent effect on cellular translational initiation (eGFP fold change; green) and cellular translational elongation (mCherry fold change; red) in the translational control cell culture model (right). Compounds such as these, with a much higher mCherry-specific effect in the HIV-1 frameshifting model, were selected as hits. Graphs were generated using GraphPad Prism and error bars represent the standard deviation of the mean (n=2-4).

Consequently, from the 76 hits tested, 26 compounds were eliminated due to unspecific effects on translation and minimal impact on HIV-1 frameshifting, determined by mCherry expression in HIV-1 frameshifting cells. To eliminate toxic compounds, I tested the dose-dependent effect of the remaining 40 hit compounds on cell viability of parental HeLa cells. 3 compounds were subsequently eliminated from the screening cascade based on compromised cell viability (Figure 47).

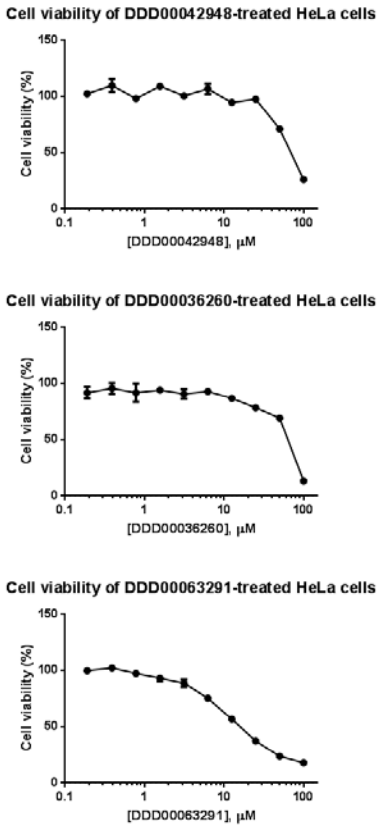

Figure 47 Compounds eliminated due to dose-dependent inhibition of cell viability

HeLa cells were treated with 10 different doses of compounds. After 48 hours, compound-treated HeLa cells were treated with resazurin (45µM) for four hours. Cell viability was quantified by measuring the fluorescence (excitation 550nm/emission 590nm) using a PheraStar FS plate reader. Points indicate the percentage of cell viability determined by the RFUs (relative fluorescent units) of compound-treated HeLa cells relative to DMSO-treated HeLa cells. Error bars represent the standard deviation of the mean (n=2).

The remaining 37 hit compounds were categorized into two groups. The first group, Group 1, consists of 12 hit compounds that only activated mCherry expression in HIV-1 frameshifting cells and did not exhibit any unspecific effects on cellular translation (Figure 45). Group 2 on the other hands, consists of 25 compounds which exhibit minimal unspecific effects on conventional translation, but were not eliminated due to their significant impact on mCherry activation in HIV-1 frameshifting cells, implying a potential role in HIV-1 frameshifting (Figure 46). The hit selection process detailed in this section is illustrated in Figure 44.

4.4 Confirmation of effects in new batch of hit compounds

To confirm the activity of the final 37 hit compounds (includes two groups) on HIV-1 frameshifting, additional follow-up confirmatory screening was conducted following re-purchasing of a new batch of compounds. From the 37 hits, 17 hit compounds were purchased from various vendors. The effect of these purchased compounds was examined on HIV-1 frameshifting, global translation and cell viability in a dose-dependent manner as detailed below.

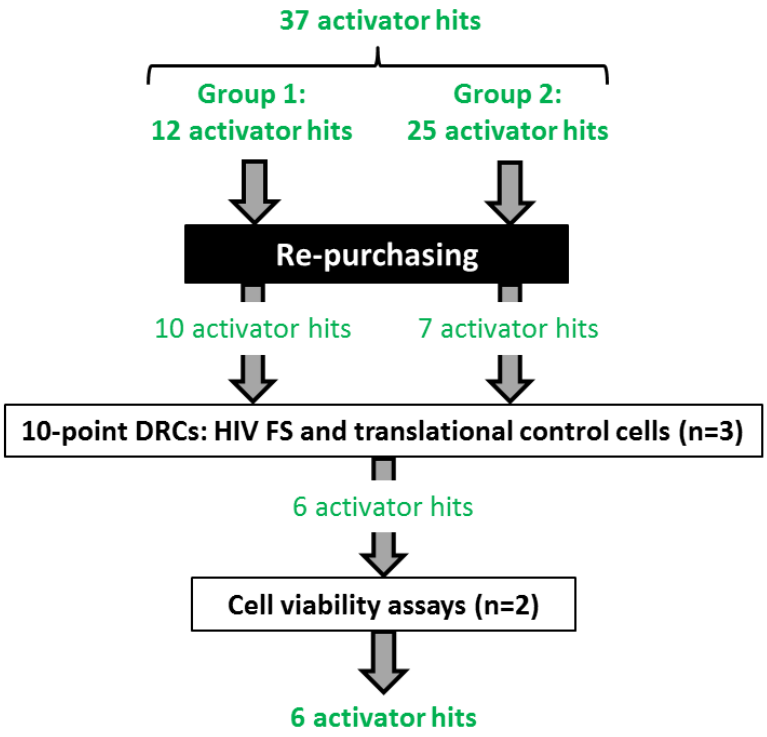

Figure 48 Workflow of hit selection from re-testing of new purchased batch of hit compounds (detailed in section 4.4)

4.4.1 Re-purchasing and Liquid Chromatography-Mass Spectrometry (LC-MS) analysis of hit compounds

Approximately 17 hit compounds were purchased from commercial vendors to confirm activity in new batches of compound. This is a vital step in drug discovery since the presence of inorganic impurities, such as heavy metals often used during compound synthesis, could confer supposed activity and lead to the selection of false positive hits (Hermann et al., 2013). Based on commercial availability and included 10 of 12 ideal hits (from group 1) and 7 of 23 hits from group 2. The new batch of compounds was registered using Activitybase software (IDBS, Guildford, UK) upon arrival (by Gavin Wood, University of Dundee). This involved recording the compound source, structure, new batch number, salt content, weight, location and form (solid or liquid) of storage to facilitate compound tracking. While only 17 of the 35 hit compounds were commercially available, time constraints prevented the in-house synthesis of the remaining 18 compounds. Due to the hygroscopic nature of DMSO (solvent for compounds), the integrity and purity of compounds was assessed using LC-MS. The identity of all 17 compounds was confirmed and these compounds were therefore used to re-test activity on HIV-1 frameshifting prior to secondary *in vitro* assays.

4.4.2 Re-test activity of re-purchased hit compounds

To confirm the effect of hit compounds on HIV-1 frameshifting, 10-pt DRCs were conducted in clonally-derived HIV-1 frameshifting and translational control HeLa cells (as described in section 4.3.2). As shown in Figure 49, 6 out of the 17 re-purchased compounds were active. These active compounds, DDD00004988, DDD00009714, DDD00009715, DDD00009974, DDD00009991 and DDD00077485, specifically activated mCherry in the HIV-1 frameshifting cells, while leaving eGFP expression unaffected. Furthermore, these 6 compounds had no adverse effects on either eGFP or mCherry expression in translational control HeLa cells, implying specific and selective target activity. As a result, these hit compounds were selected from the screening cascade conducted thus far and will be validated in secondary *in vitro* assays.

A)

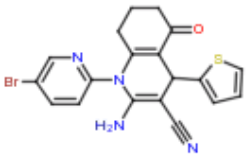

DDD00004988

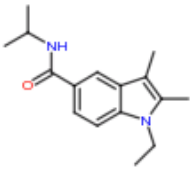

DDD00009714

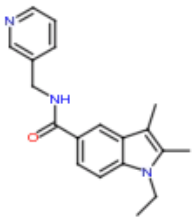

DDD00009715

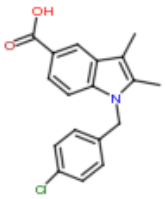

DDD00009974

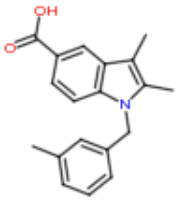

DDD00009991

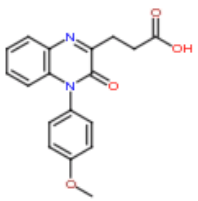

DDD00077485

B)

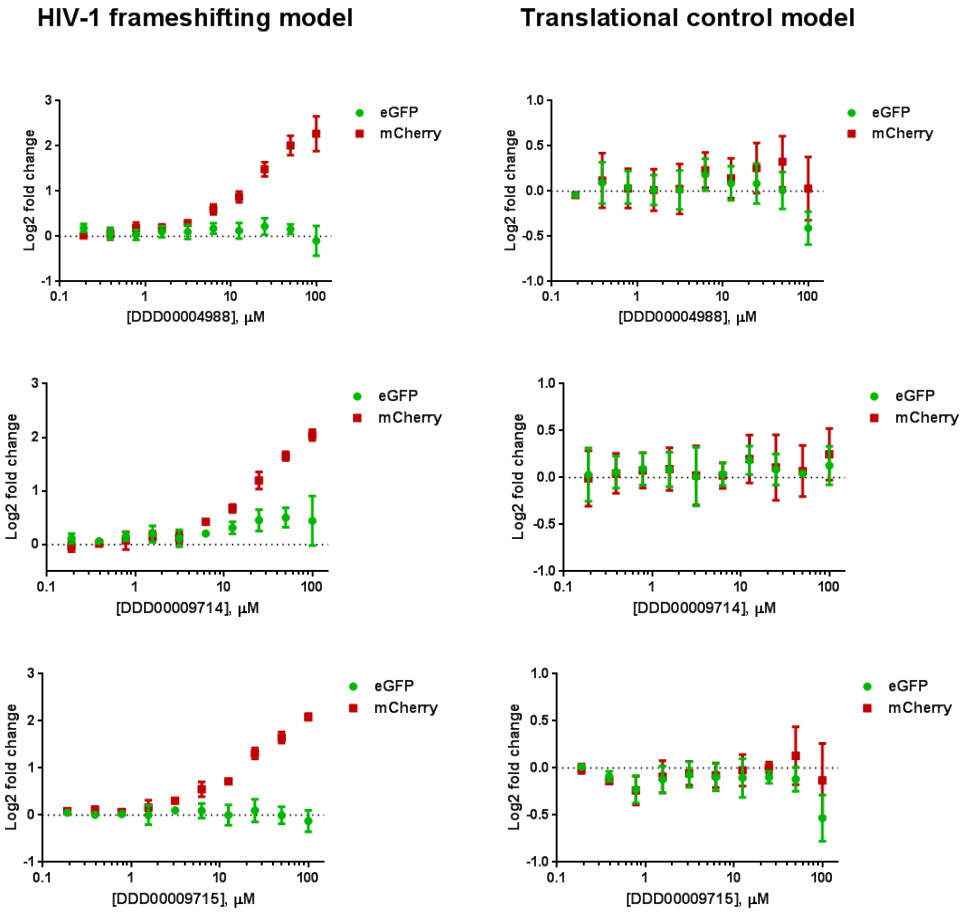

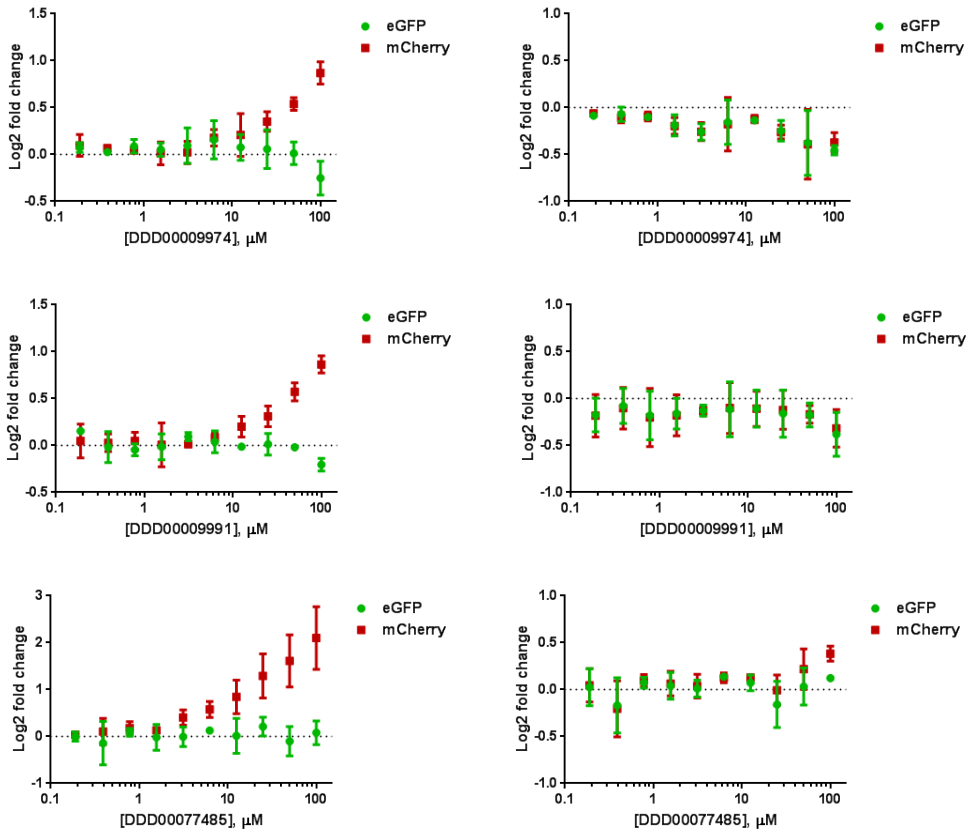

Figure 49 Compounds that activate HIV-1 frameshifting efficiency in the purchased batch

A) Compound structures of 6 final hit compounds that tested active in re-re-purchased batch.

B) Clonally-derived HIV-1 frameshifting HeLa cells (left) and translational control HeLa cells (right) were used to determine the dose-dependent effect of the new purchased batch of hit compounds on HIV-1 frameshifting efficiency and cellular translation, respectively. From 17 tested compounds, 6 compounds outlined above were active against HIV-1 frameshifting without affecting cellular translation. Graphs were generated using GraphPad Prism and error bars represent the standard deviation of the mean fold (n=3).

The remaining 11 compounds were eliminated as hits due to inactivity (Figure 61 in Appendix 4.8.7) and adverse effects on cellular translation (Figure 62 in Appendix 4.8.8) and fluorescence (Figure 50). The re-purchased batch of DDD00049811 was inactive, evident by maintained reporter fluorescence in cell culture models of both HIV-1 frameshifting and cellular translation (Figure 61 in Appendix 4.8.7).

While DDD00098509 activated mCherry in HIV-1 frameshifting cells, it also seems to stimulate cellular translational initiation, as evident by increased eGFP expression in both HIV-1 frameshifting and global translational cells. Similarly, while DDD00098130 and DDD00057691 activated mCherry in HIV-1 frameshifting cells, it had an inhibitory dose-dependent effect on cellular translation (Figure 62 in Appendix 4.8.8).

DDD00007217, DDD00040678 and DDD00074608 stimulated mCherry to a higher degree in HIV-1 frameshifting cells, but also did so by at least 2-fold in translational control cells, implying unspecific effects on translational elongation. Similarly, DDD00099201 and DDD01008137 activated mCherry in HIV-1 frameshifting cells, however, also activated GFP expression which was indicative of stimulated cellular translational initiation. While DDD00007217, DDD00040678, DDD00074608, DDD00099201 and DDD01008137 were active, they were eliminated as hits due to off-target effects on cellular translation (Figure 62 in Appendix 4.8.8).

Interestingly, while DDD00098394 and DDD00077367 activated mCherry in the HIV-1 frameshifting model, they exhibited unspecific fluorescent properties (Figure 50). This was evident by elevated eGFP fluorescence at all doses of DDD00098394, which was more likely due to fluorescence rather than an indication of translational initiation. Similarly, mCherry expression in DDD00077367-treated cells reached maximal fold change at concentrations ≥12.5uM in both HIV-1 frameshifting and translational control cells. Therefore, this was likely due to mCherry auto-fluorescence.

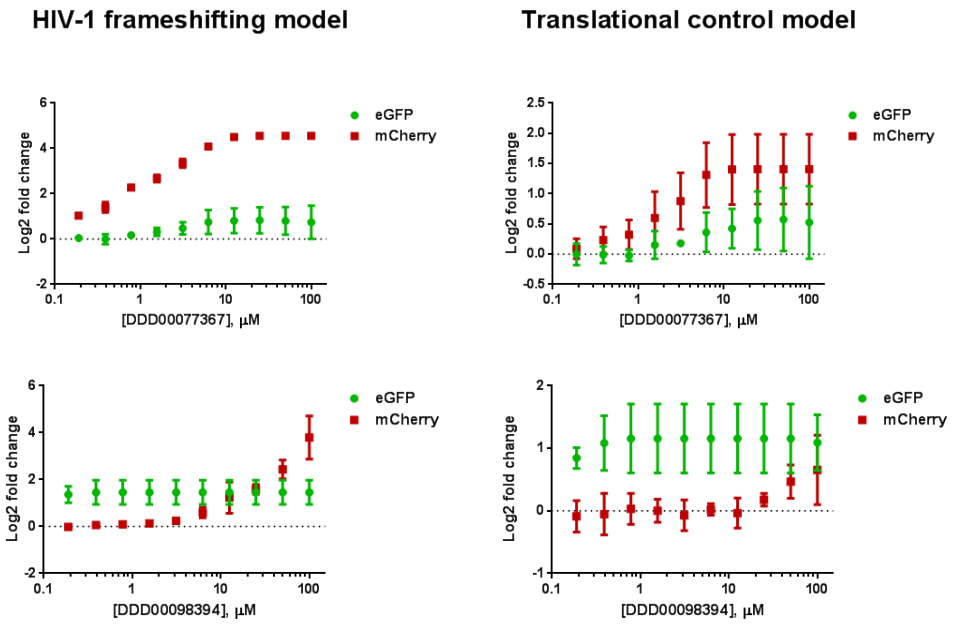

Figure 50 Potentially fluorescent properties exhibited in dose-dependent examination of HIV-1 frameshifting and cellular translation in re-purchased batch of hit compounds

Clonally-derived HIV-1 frameshifting HeLa cells (left) and translational control HeLa cells (right) were used to determine the dose-dependent effect of the new purchased batch of DDD00077367 and DDD00098394 on HIV-1 frameshifting efficiency and cellular translation, respectively. DDD00098304 is represented by two re-purchased batches (02 and 03). Graphs were generated using GraphPad Prism and error bars represent the standard deviation of the mean fold (n=3).

In addition to observing the effect of these drugs on HIV-1 frameshifting and conventional translation, cell viability was also monitored in a dose-dependent manner. Of the six hit compounds, DDD00004988, DDD00009714, DDD00009715, DDD00009974, DDD00009991 and DDD00077485, only DDD00009715 slightly decreased cell viability at high doses (100μM) (Figure 51).

Cell viability was also assessed in the inactive compounds (Figure 63 in Appendix 4.8.9). While DDD00057691 was an active modulator of HIV-1 frameshifting, as evident by a dose-dependent activation of mCherry in the HIV-1 frameshifting model (Figure 62C), it led to a dose-dependent decrease in cell viability. This also correlated with the inhibitory effect on cellular translation (Figure 62C).

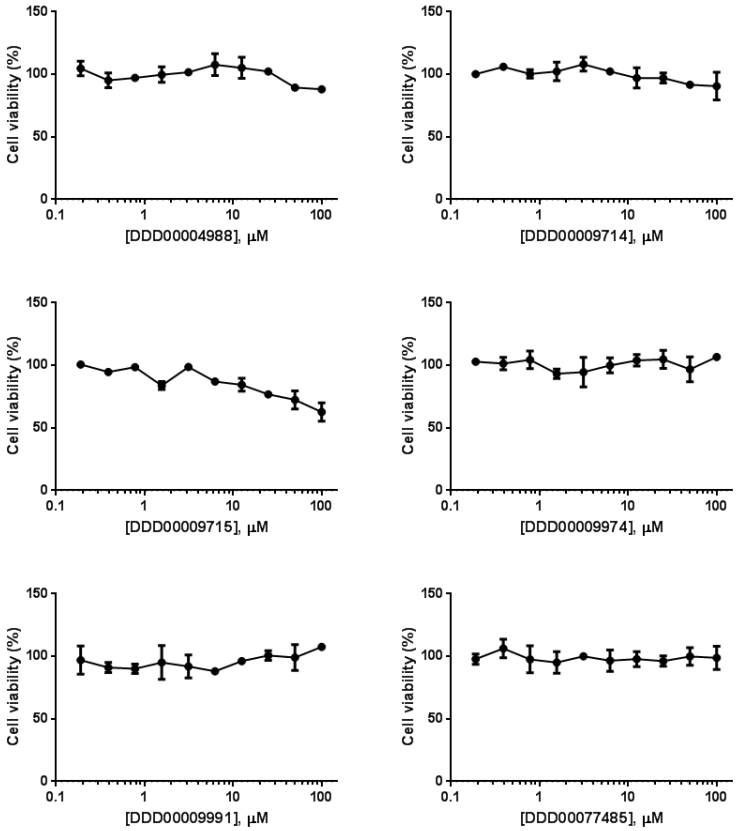

Figure 51 Effect of re-purchased batch of hit compounds on cell viability
HeLa cells were treated with 10 different doses of compounds. After 48 hours, compound-treated HeLa cells were treated with resazurin (45µM) for four hours. Cell viability was quantified by measuring the fluorescence (excitation 550nm/emission 590nm) using a PheraStar FS plate reader. Points indicate the percentage of cell viability determined by the RFUs (relative fluorescent units) of compound-treated HeLa cells relative to DMSO-treated HeLa cells. Error bars represent the standard deviation of the mean (n=3).

Therefore, based on the effect of the re-purchased batch of 17 hit compounds on HIV-1 frameshifting, cellular translation and cell viability, DDD00004988, DDD00009714, DDD00009715, DDD00009974, DDD00009991 and DDD00077485 were determined to be active target-specific hits. These 6 compounds activated mCherry in a dose-dependent manner in the HIV-1 frameshifting cell culture model, which represents efficiency of HIV-1 frameshifting. Furthermore, these 6 compounds did not have any significant adverse effects on cellular translational initiation, elongation and cell viability thereby confirming their frameshifting-specific activity in the context of these cell culture models.

4.4.3 Elucidating the failure re-testing rate of new purchased batch of compounds

To further understand why 11 of 17 re-purchased compounds were inactive against HIV-1 frameshifting, the original batch of compounds used in the primary and confirmatory screen was analysed by LC-MS (by Gavin Wood, University of Dundee).

LC-MS analysis revealed information pertaining to the molecular weight and structure, indicative of compound identity. Furthermore, data acquired by a diode-array detector (DAD) examined absorbance in the UV-Visible spectra, to identify impurities or the absence of compounds. With a failure rate of 47%, no compounds were detected in the original batch of DDD00004988, DDD00057691, DDD00074608, DDD00077367, DDD00098130, DDD00098509, DDD00099201 and DDD00097045 (Table 5).

It was surprising that the initial screening batches of DDD00004988, DDD00074608, DDD00098509 and DDD01008137 failed LC-MS analysis since the effect of these compounds on HIV-1 frameshifting, cellular translation and cell viability were very comparable in both batches. Similarly, while DDD00057691 was slightly more toxic at high concentrations and DDD00099201 exhibited slightly higher unspecific effects on conventional

translation in the re-purchased batch, the initial screening batches of both these compounds exhibited similar activity otherwise.

Inspite of the lack of compound in the original batches of compounds, the proposed activity observed in the primary and confirmatory screens was likely attributed to impurities in the sample, denoted by multiple peaks in the UV spectra. This could also explain the failed re-test in re-purchased batches of DDD00098130 and DDD00077367. Alternatively, the saturated levels of mCherry fluorescence in the re-purchased batch of DDD00077367 was suggestive of auto-fluorescent properties that was likely overlooked in the initial screening back due to degraded compound sample. On the other hand, DDD00049811 failed the first round of LC-MS, but passed the second. An extra peak could have accounted for the activity observed in the initial batch, that was absent in the re-purchased sample.

In conclusion, compound degradation and impurities in the initial batch of compounds likely played a role in the inconsistent activity observed between batches.

Table 5 LC-MS analysis of initial screening batch of hit compounds

Compound	LC-MS analysis	Conclusion
DDD00004988	Weak sample -multiple peaks in UV, no ionization.	No compound detected
DDD00049811	Main peak has MI, but significant additional peak with m/z 271.1.	Weak peak with the desired MI -probably ok
DDD00057691	Weak sample -multiple peaks in UV, no ionization.	No compound detected
DDD00074608	Weak sample -multiple peaks in UV, no ionization.	No compound detected
DDD00077367	Weak sample -multiple peaks in UV, no ionization.	No compound detected
DDD00098130	Weak sample -multiple peaks in UV, no ionization.	No compound detected
DDD00098509	Weak sample -multiple peaks in UV, no ionization.	No compound detected
DDD00099201	Weak sample -multiple peaks in UV, no ionization.	No compound detected
DDD01008137	Weak sample -multiple peaks in UV, no ionization.	No compound detected

4.5 Effect of hit compounds on HIV-1 Gag:Gag-Pol ratios in fluorescent cell-based assay

Six of the 17 re-purchased hit compounds re-tested as active frameshifting stimulators using increased mCherry fluorescence-based detection (Figure 49). To verify whether these hit compounds had any impact on frameshifting, I examined eGFP-mCherry polyprotein abundance that would be enhanced as a result of activated frameshifting in clonally-derived HIV-1 frameshifting cells. To examine polyprotein abundance, western blot was used to detect eGFP- and mCherry-expressing proteins (Figure 52).

As expected, clonally-derived translational control cells primarily expressed the eGFP-mCherry fusion protein (55kDa) as a result of conventional translation with possible degradation products (44kDa and 39kDa). Alternatively, HIV-1 frameshifting cells primarily expressed eGFP, while traces of the eGFP-mCherry fusion protein were detectable only at a higher exposure. This was likely due to the naturally-occurring low frequency of HIV-1 frameshifting (~5%) (Figure 52). Clonally-derived HIV-1 frameshifting HeLa cells treated with the 17 hit compounds (50μM) did not increase eGFP-mCherry fusion protein expression as a result of activated HIV-1 frameshifting. (Figure 52). This raised the possibility that the six hit compounds (DDD00004988, DDD00009714, DDD00009715, DDD00009974, DDD00009991 and DDD00077485) which re-tested as active HIV-1 frameshifting stimulators using a fluorometer (PherastarFS), potentially did not actually activate frameshifting. However, this was not conclusive since the eGFP-mCherry fusion protein band produced upon frameshifting was barely detectable in our hands, therefore rendering densitometry analysis susceptible to background interference. This was also evident by the varying level of eGFP-mCherry to eGFP protein expression between DMSO-treated and ritonavir-treated HIV FS cells (Figure 52-right panel).

DDD00004988, DDD00007217, DDD00009715, DDD00049811, DDD00074608, DDD00098130, DDD00098509 and DDD01008137 treatment in HIV-1 frameshifting cells reduced eGFP protein levels compared to DMSO-

treated HIV FS cells to varying degrees (Figure 52). This decrease in eGFP production could be due to reduced global translation or potentially increased eGFP-mCherry fusion protein production as a result of activated frameshifting. Since 50μM of compounds DDD00009715 and DDD00098509 slightly decreased the viability of HeLa cells (section 4.4.2), the decreased eGFP protein levels observed in Figure 52 most likely corresponds to translational or cellular defects. Due to the nearly undetectable levels of eGFP-mCherry fusion protein, it was challenging to detect any increase as a result of activated frameshifting. I thus examined the limit of detection of eGFP-and mCherry-probed proteins on western blots using Li-Cor technology to determine the detectable level of activated HIV-1 frameshifting.

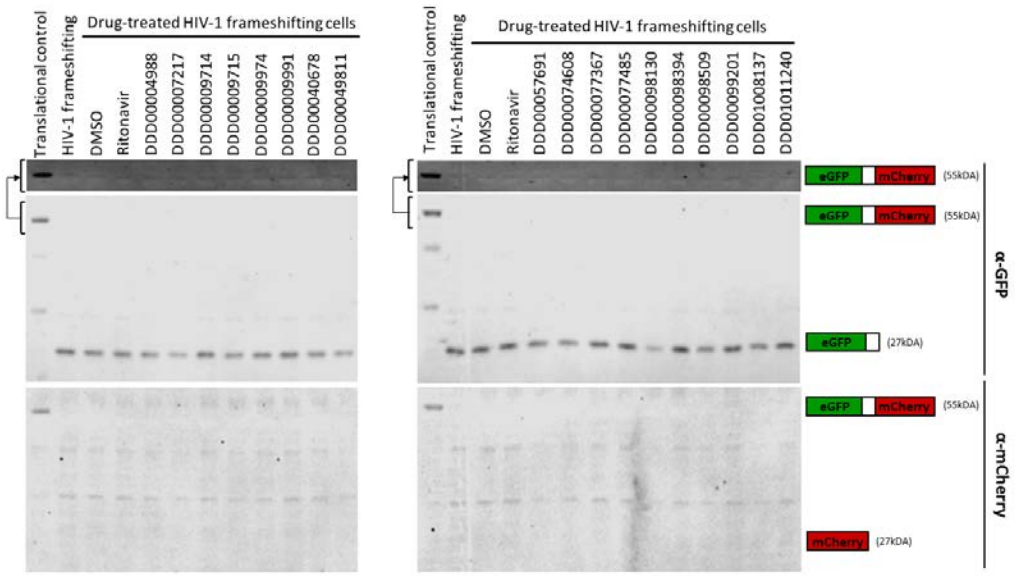

Figure 52 Effect of hit compounds on eGFP-mCherry fusion protein production via HIV-1 frameshifting in cell-based assay

Clonally-derived HIV-1 frameshifting HeLa cells were treated with 0.5% DMSO (v/v), ritonavir (5μM) and hit compounds (50μM) for 48 hours. Cell lysates were prepared and used in western blotting with anti-eGFP and anti-mCherry antibodies to determine the abundance of eGFP-mCherry fusion protein (55kDa) relative to eGFP (27kDa) as an indication of frameshifting. Clonally-derived translational control cells were used as a reference for detecting eGFP-mCherry fusion protein.

4.5.1 Limit of detection

To determine whether activated frameshifting can be identified in the fluorescent cell-based model of HIV-1 frameshifting, I examined the limit of detection of eGFP-and mCherry-probed proteins in western blots using Li-Cor technology. Cell lysate from clonally-derived translational control HeLa cells was serially diluted (1:2), and run on various lanes within a western blot. This was probed with anti-eGFP and anti-mCherry antibodies to detect eGFP and mCherry protein expression, respectively. Upon densitometry analysis of eGFP expression in translational control cells, 7% of the eGFP-mCherry fusion protein observed was detectable in our hands by western blot using an anti-eGFP antibody (Figure 53). Since the production of eGFP-mCherry fusion protein in HIV-1 frameshifting cells is reflective of the frameshifting efficiency, a frameshifting frequency or efficiency of ~7% should theoretically be detectable using an anti-eGFP antibody. This was hypothesized based on the intensity of the faintest band in lane 5 at maximum exposure (Figure 53).

Similarly, since 6.6% of the eGFP-mCherry fusion protein from the most concentrated sample was detected by an anti-mCherry antibody (lane 4), a frameshifting efficiency of ~7% was hypothetically the minimum detectable frequency (Figure 54). This ~7% frequency of frameshifting correlated with the level of eGFP-mCherry fusion protein (7%) observed in clonally-derived HIV-1 frameshifting cells (Figure 55A). This indicated that frameshifting occurs at a frequency of about 7% in clonally-derived HIV-1 frameshifting cells adjudged by using fusion protein detection using western blotting. Therefore, compounds that truly activate HIV-1 frameshifting (>7%) should produce eGFP-mCherry fusion protein within a range detectable by western blotting. The lack of increased eGFP-mCherry fusion protein production in HIV-1 frameshifting cells treated with hit compounds potentially suggests that none of these compounds activate HIV-1 frameshifting.

Alternatively, these hit compounds were identified as frameshifting activators based on increased mCherry fluorescence in clonally-derived HIV-

1 frameshifting HeLa cells, detected by the PherastarFS fluorometer. Fluorescence-based detection revealed that the frameshifting frequency in clonally-derived HIV-1 frameshifting HeLa cells was 15% (Figure 55B), which was 2.3-fold higher than the frequency of frameshifting detected by eGFP-Cherry fusion protein production in western blots (Figure 55A). Therefore, it also raised the possibility that the level of activation detected by a fluorometer may not reflect an increased production of eGFP-mCherry fusion protein corresponding to activated frameshifting. This was probably due to differences in sensitivity between the modes of detecting frameshifting.

A)

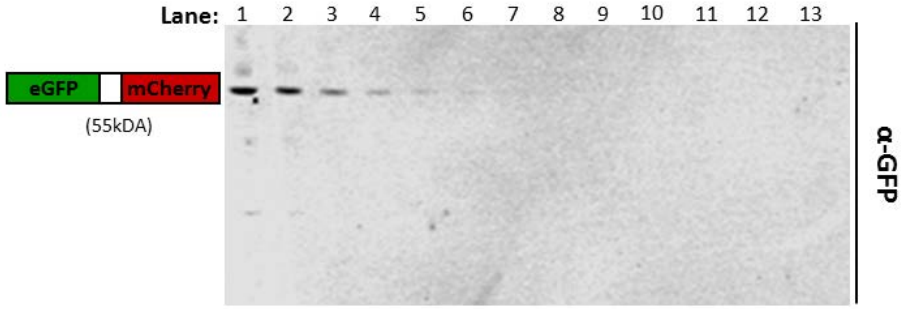

B)

Lane	eGFP signal	% of Lane 1
1	24000	100
2	15500	65
3	7890	33
4	3240	13
5	1700	7
6	393	2
7	402	2
8	306	1
9	-483	-2

Figure 53 Limit of detection of eGFP-probed eGFP-mCherry fusion protein in clonally-derived translational control HeLa cells

A) Cell lysate of clonally-derived translational HeLa cells (Lane 1:15µl) was serially diluted 1:2 and probed with anti-eGFP antibody to detect the eGFP-mCherry fusion protein (55kDa).

B) Densitometry analysis was conducted to quantify the abundance of eGFP-mCherry fusion protein in each lane.

A)

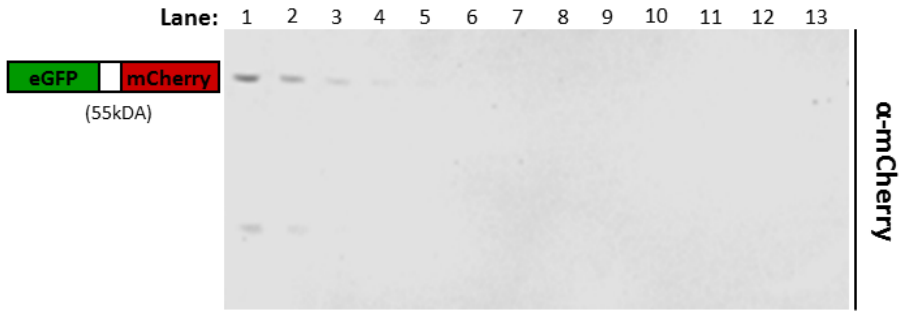

B)

Lane	mCherry signal	% of Lane 1
1	43000	100
2	20900	49
3	11000	25
4	2850	7
5	2960	7
6	422	1
7	-758	-2
8	632	1
9	776	2

Figure 54 Limit of detection of mCherry-probed eGFP-mCherry fusion protein in clonally-derived translational control HeLa cells

A) Cell lysate of clonally-derived translational HeLa cells (Lane 1:15µl) was serially diluted 1:2 and probed with anti-mCherry antibody to detect the eGFP-mCherry fusion protein (55kDa).

B) Densitometry analysis was conducted to quantify the abundance of eGFP-mCherry fusion protein in each lane.

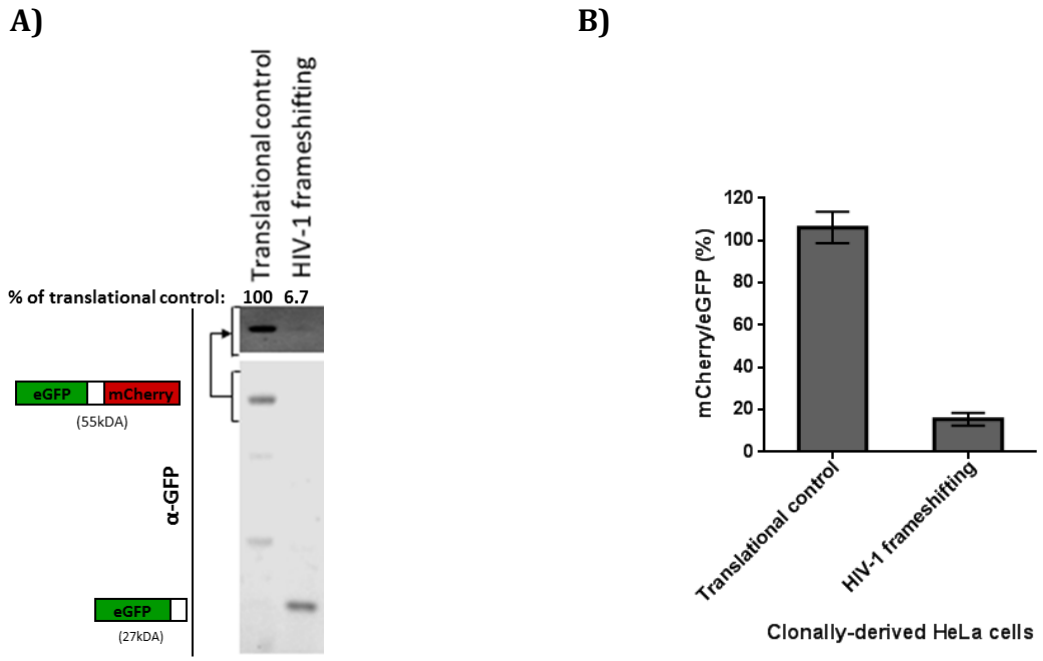

Figure 55 Comparison of methods used to detect HIV-1 frameshifting activity

A) Frequency of HIV-1 frameshifting (6.7%) was determined based on western blot and densitometry analysis of the abundance of eGFP-mCherry fusion protein in clonally-derived HIV-1 frameshifting cells.

B) Frequency of HIV-1 frameshifting (15%) was determined based on the proportion of mCherry fluorescence relative to eGFP fluorescence detected by fluorometer following excitation/emission at 580nm/610nm and 485nm/520nm, respectively.

4.6 Effect of hit compounds on HIV-1 Gag:Gag-Pol ratios in HIV-1 infected cells

To determine whether hit compounds are targeting frameshifting of HIV-1 *gag* and *pol* genes, I examined the effect of hit compounds on the production of Gag and Gag-Pol polyprotein levels in HIV-1 infected cells. HEK293T cells were transfected with protease-deficient proviral HIV-1 DNA and treated with hit compounds at a fixed concentration (50μM) that was not toxic in HeLa cells, but found to exhibit a response in screening of dose-response curves. 48 hours later, protein lysates of transfected cells and virions from purified supernatant were analysed by western blotting to examine the drug-dependent effect on Gag and Gag-Pol polyprotein expression as a result of HIV-1 frameshifting.

During HIV-1 replication, Gag polyprotein is proteolytically cleaved into mature structural proteins: matrix (p17), capsid (p24), nucleocapsid (p7) and p6 protein (Göttlinger, Sodroski, & Haseltine, 1989) and the Gag-Pol polyprotein (produced only upon HIV-1 frameshifting) produces structural proteins in addition to enzymatic proteins such as protease (p10), reverse transcriptase (p66) and integrase (p32) (Jacks, Power, et al., 1988). Therefore, in order to examine the expression levels of Gag and Gag-Pol polyproteins, the viral protease responsible for cleaving these polyproteins into mature structural and enzymatic proteins was inactivated. This in turn, permitted the detection of Gag and Gag-Pol polyproteins produced by HIV-1 frameshifting prior to protease-mediated maturation. Using an anti-capsid antibody, Gag (55kDa) and Gag-Pol (160kDa) polyprotein levels were examined in both HIV-1 transfected cell lysate and released virions (Figure 56). Ritonavir, a HIV-1 protease inhibitor, did not affect levels of Gag-Pol/Gag in this single-cycle of protease-deficient HIV-1 assembly.

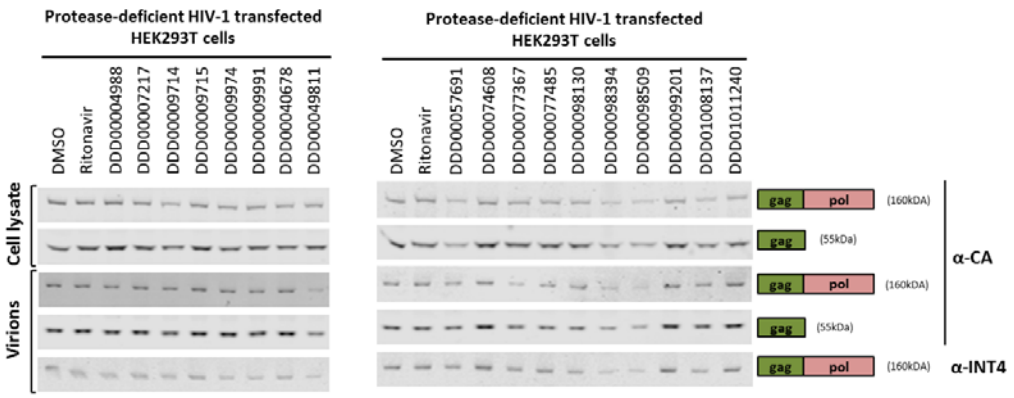

Figure 56 Effect of hit compounds on HIV-1 Gag-Pol polyprotein production through HIV-1 frameshifting

HEK293T cells were transfected with protease-deficient proviral HIV-1 DNA followed by treatment with 0.5% DMSO (v/v), ritonavir (5μM) and hit compounds (50μM) for 48 hours. Cell lysates were prepared and used in western blotting with anti-capsid and anti-integrase antibodies to determine the abundance of Gag (55kDa) and Gag-Pol polyproteins (160kDa) as an indication of HIV-1 frameshifting.

Similarly, none of the 17 initial hit compounds had a stimulatory effect or a significant inhibitory effect on the production of Gag and Gag-Pol polyproteins in whole cell lysates. However, in virions from purified supernatant, DDD00049811 and DDD00098509 treatment reduced the proportion of Gag-Pol to Gag by approximately 2-fold and 1.6 fold, respectively (Figure 56). Reduced Gag-Pol:Gag levels in DDD00098509-treated cells was likely to due to decreased cell viability examined from previously reduced cellular β-actin levels (Figure 52) and reduced cell viability in HeLa cells (Figure 66 in Appendix 4.8.9). Alternatively, reduced virion-associated Gag-Pol:Gag levels were observed in DDD00049811-treated HIV-1 transfected cells. To determine whether the effects of DDD00049811 on Gag and Gag-Pol levels are anti-viral or cellular, the effect of hit compounds was tested on HIV-1 replication kinetics.

4.7 Summary

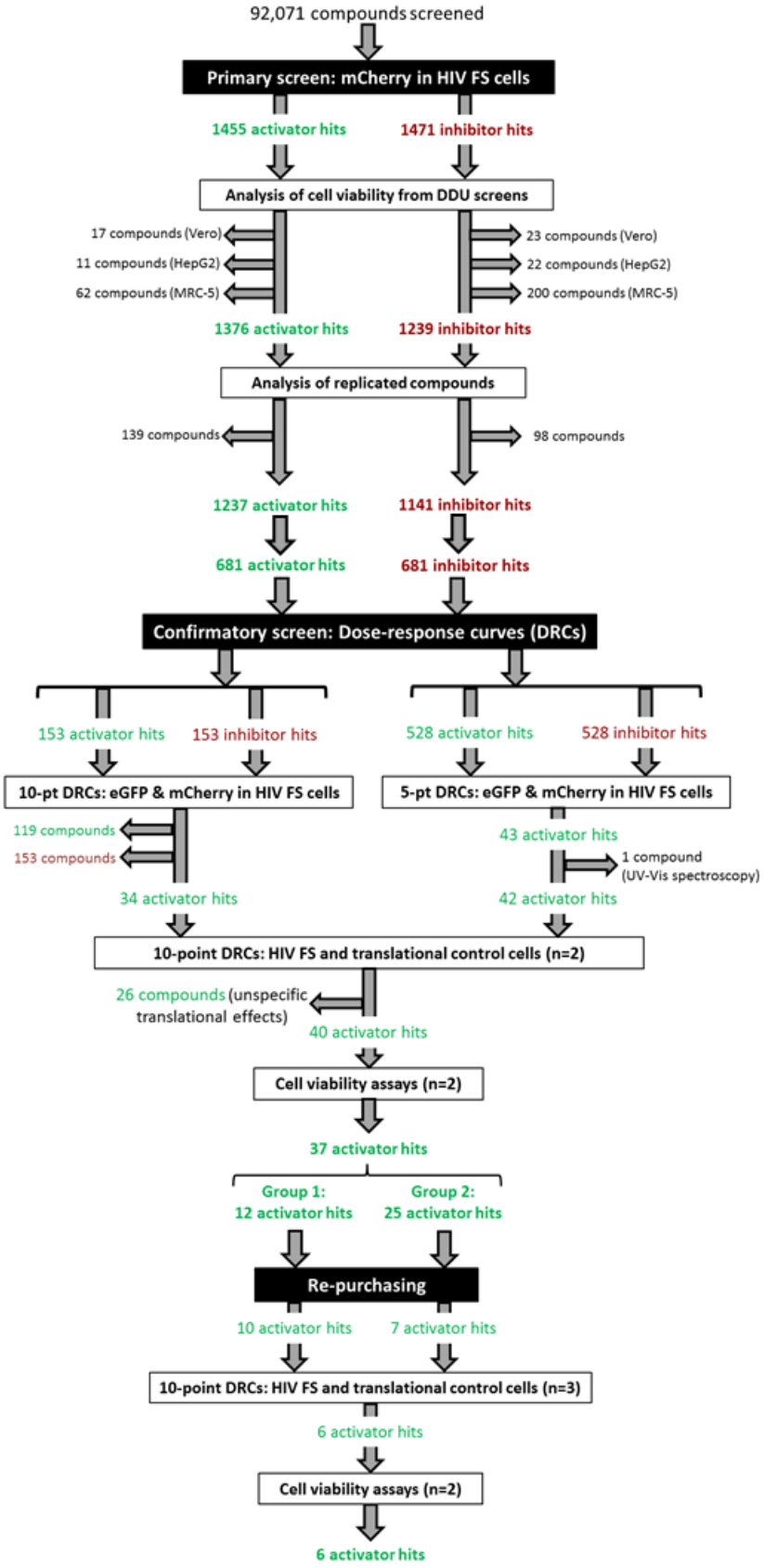

Figure 57 Workflow of entire screening cascade conducted to identify hits targeting HIV-1 frameshifting

In summary, this chapter outlined the results obtained from the series of screens conducted to identify modulators of HIV-1 frameshifting. The screening cascade consisted of a primary diversity screen, confirmatory screening using dose-response curves and re-confirmation of active hit compounds following re-purchasing of hit compounds (Figure 57).

Using a cell culture model of HIV-1 frameshifting whereby mCherry expression is indicative of frameshifting efficiency, a primary screen of 92,071 diverse compounds led to the identification of 1455 activators of mCherry (activator hits) and 1471 inhibitors of mCherry (inhibitor hits). By analysing the DDU database with other screening information associated with these hit compounds, ~15% of activator hits and 22.4% of inhibitor hits were eliminated based on low cell viability and irreproducible effects among replicated compounds belonging to different batches.

From the resulting 1237 activator hits and 1141 inhibitor hits, 681 activators and 681 inhibitors were selected for confirmatory screening using dose-response curves (DRCs) to identify potent activators and inhibitors of HIV-1 frameshifting. This was done by examining the dose-dependent effect of compounds in clonally-derived HIV-1 frameshifting HeLa cells. Furthermore, to identify HIV-1 frameshift-specific and selective hits, compounds active in clonally-derived translational control HeLa cells were eliminated based on off-target cellular translational effects. These clonally-derived translational control HeLa cells were also used to eliminate compounds with unspecific effects on eGFP and mCherry fluorescence, hence disregarding false positive hits associated with auto-fluorescence or fluorophore quenching. Auto-fluorescent compounds were also eliminated by conducting UV-Visible spectroscopy on a large subset of hit compounds. By examining the dose-dependent effects of hit compounds on cell viability, toxic compounds were also eliminated. Consequently, 37 active, non-toxic hit compounds were ultimately identified to activate HIV-1 frameshifting.

Interestingly, inhibitors of HIV-frameshifting were not identified in this screen for diverse small molecules. Compounds capable of inhibiting HIV-1 frameshifting demonstrated inhibitory cellular translational effects, an adverse effect that was also observed in other studies. It is also likely that several compounds impacted cell viability due to general toxic effects. This signified the challenge of specifically reducing frameshifting efficiency without affecting global translation.

To confirm HIV-1 frameshifting-specific activity, a new batch of hit compounds was re-purchased from commercial vendors. This was done to eliminate compounds whereby potential organic or inorganic impurities conferred activity. 17 commercially available re-purchased compounds were re-tested for their effect on HIV-1 frameshifting, cellular translation and cell viability using dose-response curves. Of the 17 tested compounds, 6 compounds, DDD00004988, DDD00009714, DDD00009715, DDD00009974, DDD00009991 and DDD00077485, were true active hits with HIV-1 frameshift-stimulating effects and no adverse cellular translational effects.

Liquid chromatography and mass spectrometry (LC-MS) analysis revealed that many samples from the original screening batch did not contain the compound of interest and was most likely contaminated with impurities. These impurities could have potentially conferred activity during the screening cascade prior to re-purchasing, and therefore contributed to the re-tested inactivity in re-purchased batch. Nevertheless the screening cascade conducted thus far successfully generated 6 hit compounds, DDD00004988, DDD00009714, DDD00009715, DDD00009974, DDD00009991 and DDD00077485, which activated HIV-1 frameshifting using mCherry fluorescence-based detection.

Examination of polyprotein production (eGFP-mCherry) regulated by HIV-1 frameshifting confirmed the inactive effect on frameshifting that was also recapitulated in HIV-1 Gag and Gag-Pol polyprotein production. This also revealed dissimilarity in the degree of frameshifting detected between

fluorescence-based and polyprotein-based assays of HIV-1 frameshifting. The 17 re-purchased batch of compounds did not activate HIV-1 frameshifting, as evident by the steady levels of eGFP-mCherry and Gag-Pol polyprotein, but were initially identified as frameshifting activators due to potentially increased sensitivity of fluorescence-based detection. However, reduced virion-associated HIV-1 Gag and Gag-Pol protein levels indicate potential off-target effects of DDD00049811 that will be investigated further. These small molecules were therefore further characterized using secondary *in vitro* assays.

4.8 Appendix

4.8.1 Frequency distribution of hits in the pilot screen

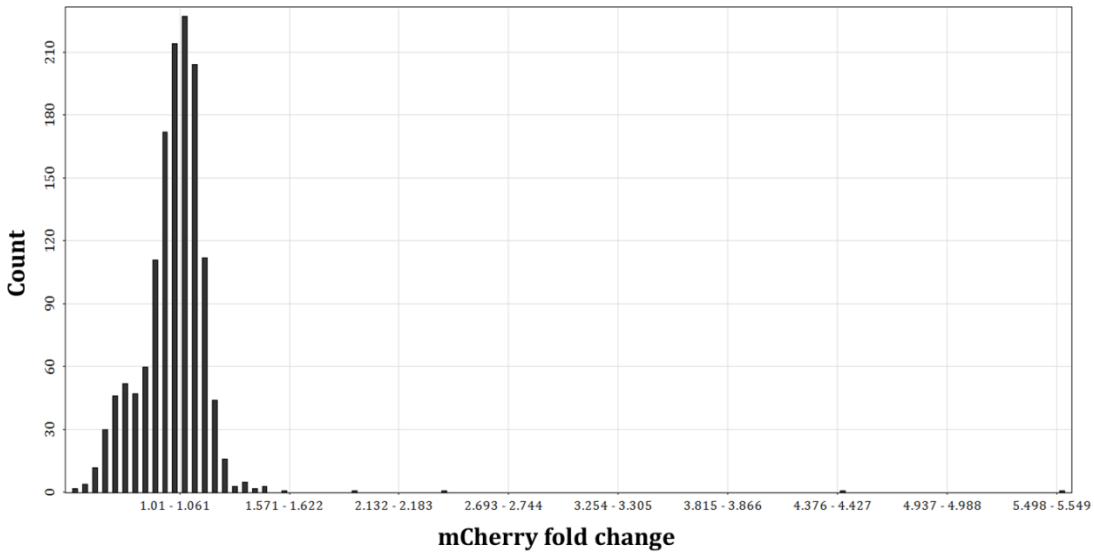

Figure 58 Frequency distribution of 1,167 compounds tested in the pilot screen for modulators of HIV-1 frameshifting.

4.8.2 Frequency distribution of hits in the primary screen

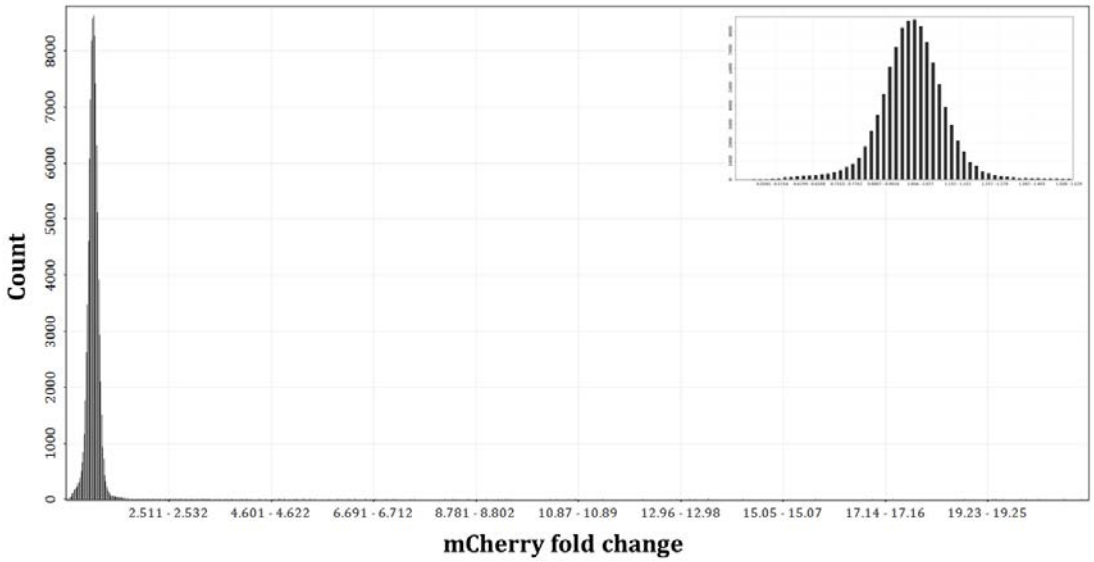

Figure 59 Frequency distribution of 92,071 compounds run in the primary diversity screen

4.8.3 Example of eliminated hit compounds with less than 0.29 fold activation or inhibition

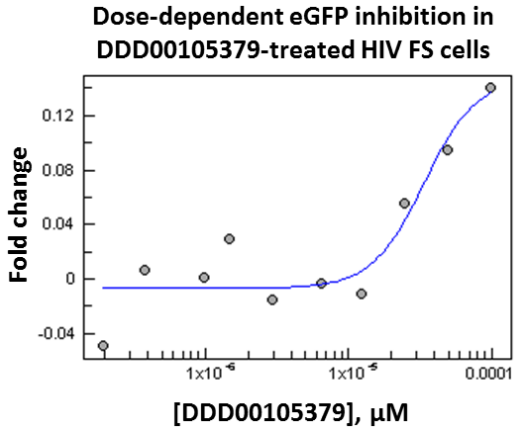

Figure 60 Representative 10-point dose-response curve (DRC) of inactive compound that was initially algorithmically fit to an active DRC. Using Activitybase XC and XE Runner (IDBS, Guilford, Surrey, UK) software, some compounds with dose-dependent effects (pXC_{50}>4) on either eGFP or mCherry expression were fitted to a four-parameter logistic curve and deemed active despite the insignificant effect. These compounds (such as DDD00105379) were manually invalidated if difference between minimal and maximal fold change was lower than 0.29 fold change.

4.8.4 Scatter plot of compounds run in 5-point DRCs

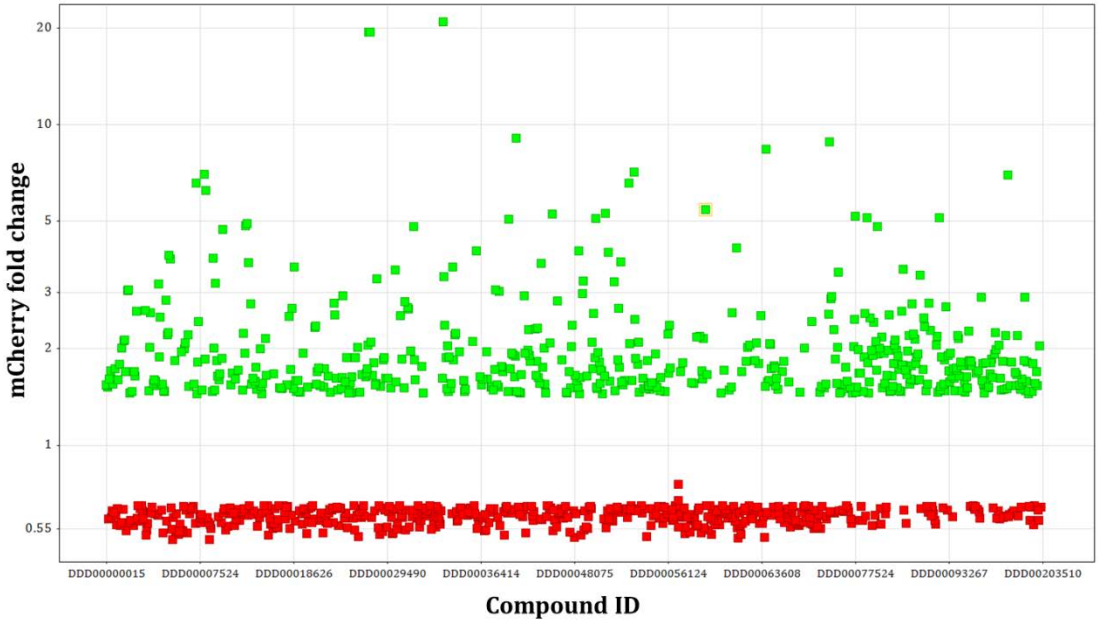

Figure 61 Scatter plot of mCherry fold change from 528 activator hits (green) and 528 inhibitor hits (red) chosen for 5-point dose-response curves.

4.8.5 Library composition of compounds run in 5-point DRCs

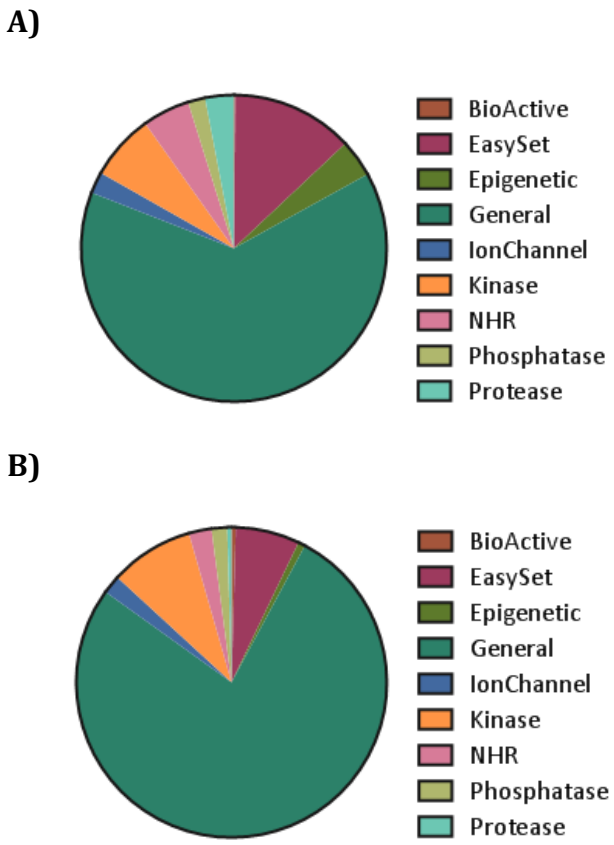

Figure 62. Library composition of compounds screened in confirmatory screens with 10-point and 5-point dose-response curves.

A) Library composition of 681 mCherry activator hits used in confirmatory screens

B) Library composition of 681 mCherry inhibitor hits used in confirmatory screens

4.8.6 Library composition of 76 compounds obtained from confirmatory screening cascade

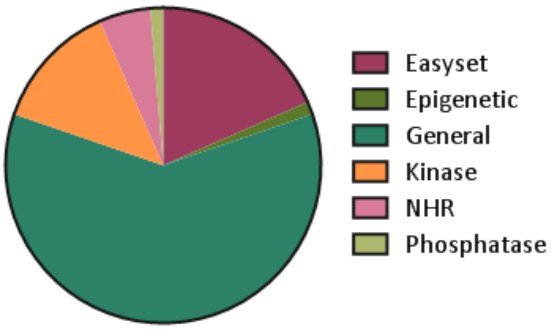

Figure 63 Library composition of 76 hits identified from screening cascade so far

4.8.7 DDD00049811 was rejected as a hit compound due to inactivity in re-purchased batch

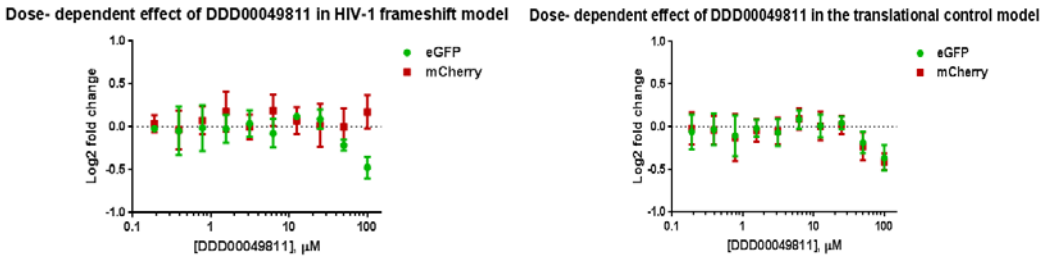

Figure 64 The re-purchased batch of DDD00049811 was inactive against HIV-1 frameshifting

Clonally-derived HIV-1 frameshifting HeLa cells (left) and translational control HeLa cells (right) were used to determine the dose-dependent effect of the new purchased batch of DDD00049811 on HIV-1 frameshifting efficiency and cellular translation, respectively. Graphs were generated using GraphPad Prism and error bars represent the standard deviation of the mean fold (n=3).

4.8.8 Eliminated hit compounds due to adverse effects on cellular translation

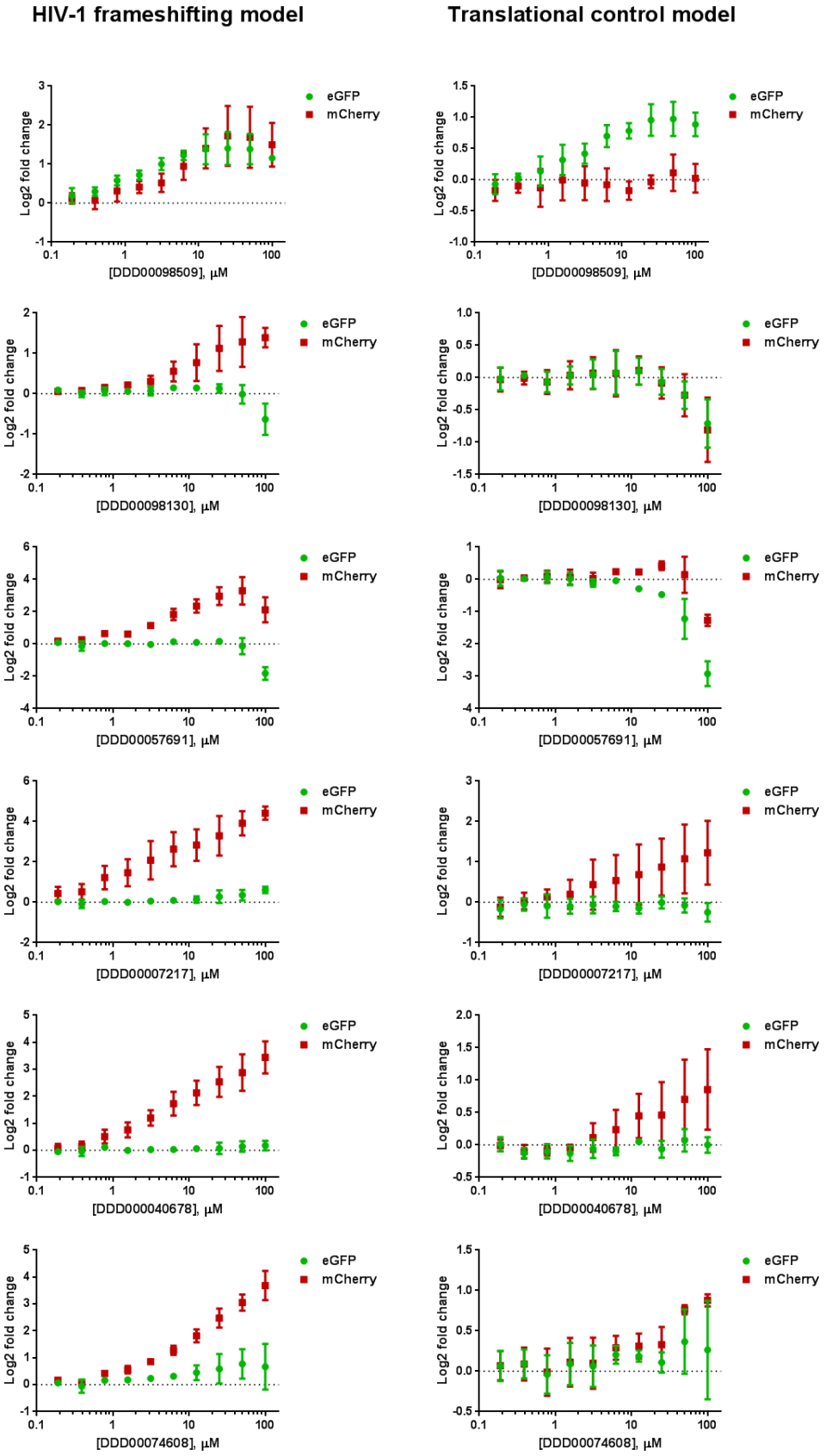

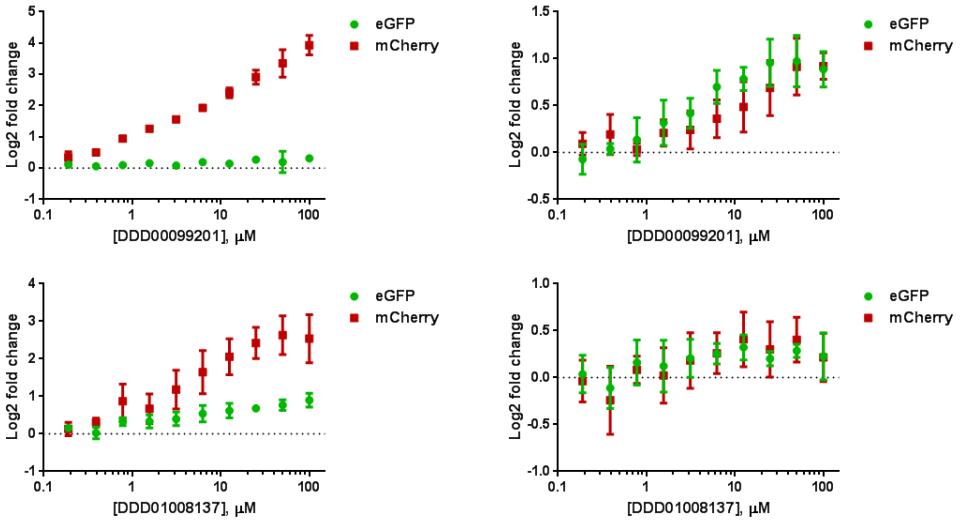

Figure 65 Hit compounds rejected from re-testing of re-purchased batches based on unspecific effects on cellular translation.

Clonally-derived HIV-1 frameshifting HeLa cells (left) and translational control HeLa cells (right) were used to determine the dose-dependent effect of the new purchased batch of 8 compounds on HIV-1 frameshifting efficiency and cellular translation, respectively. Graphs were generated using GraphPad Prism and error bars represent the standard deviation of the mean fold (n=3).

4.8.9 Hit compounds eliminated due to inhibitory effect on viability of HeLa cells

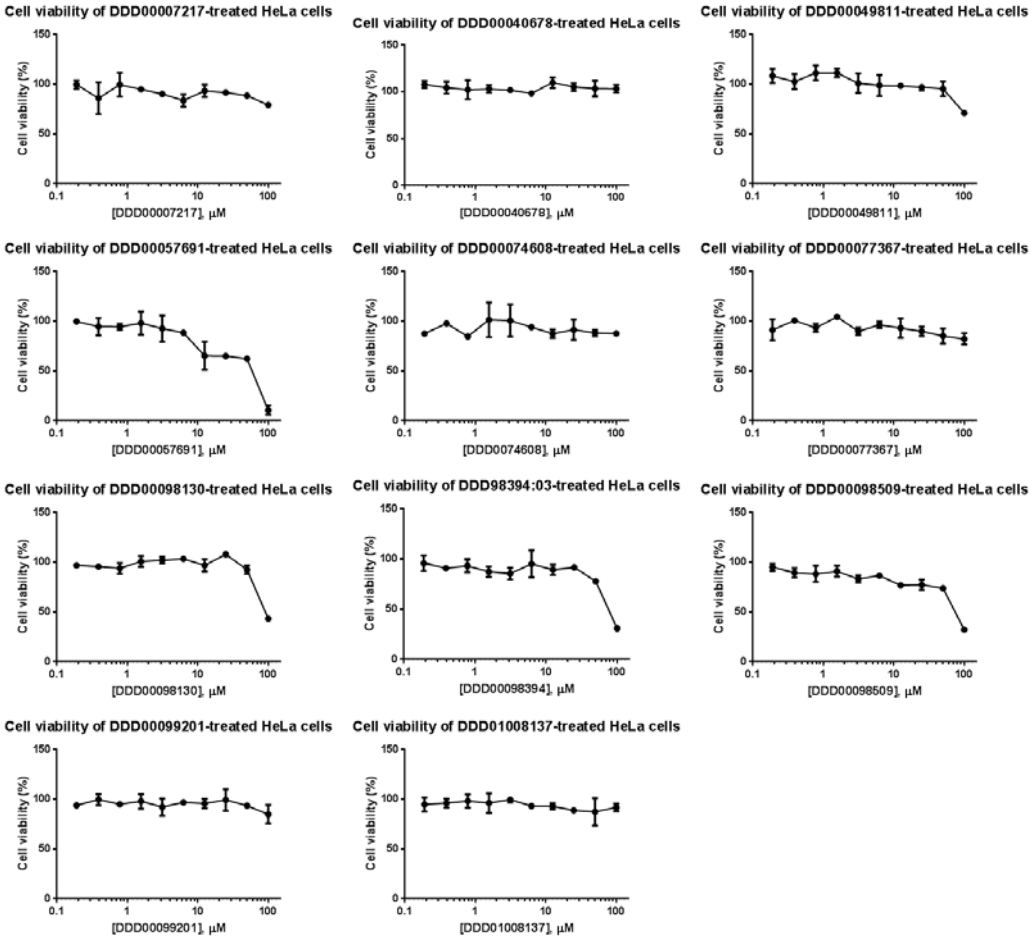

Figure 66 Cell viability of inactive compounds from re-purchased batch
HeLa cells were treated with 10 different doses of compounds. After 48 hours, compound-treated HeLa cells were treated with resazurin (45µM) for four hours. Cell viability was quantified by measuring the fluorescence (excitation 550nm/emission 590nm) using a PheraStar FS plate reader. Points indicate the percentage of cell viability determined by the RFUs (relative fluorescent units) of compound-treated HeLa cells relative to DMSO-treated HeLa cells. Error bars represent the standard deviation of the mean (n=3).

Chapter 5

Results: Effect of hit compounds on *in vitro* HIV-1 replication kinetics

This chapter outlines the *in vitro* secondary assays conducted to examine the effect of hit compounds on HIV-1 replication kinetics. Of the 17 hit compounds proposed to activate HIV-1 frameshifting based on diversity and confirmatory screens (described in Chapter 4), 6 of these re-tested as active in a new re-purchased batch using fluorescence-based detection (Table 6). However, while these compounds did not stimulate production of eGFP-mCherry and Gag-Pol polyprotein production as expected, DDD00049811 potentially exhibited off-target effects based on reduced virion-associated Gag and Gag-Pol levels. Nevertheless, all 17 compounds were tested for a complete analysis of the effect on HIV-1 replication kinetics.

Table 6 Basic properties of hit compounds identified from the screening cascade for HIV-1 frameshifting modulators

Hit compounds	Structure	MW	TPSA	logD	logP	HBA	HBD
DDD00004988*	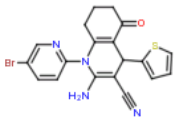	427.16	83.01	3.53	3.53	5	1
DDD00007217	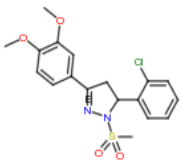	394.69	68.2	2.25	2.25	6	0
DDD00009714*	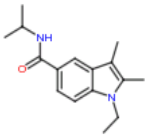	258.16	34.03	3.68	3.68	3	1
DDD00009715*	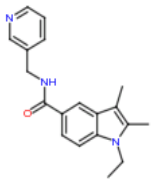	307.19	46.92	3.39	3.39	4	1
DDD00009974*	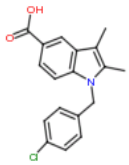	313.63	42.23	1.65	5.12	3	1
DDD00009991*	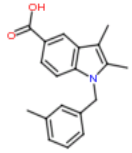	293.19	42.23	1.30	4.87	3	1

DDD00040678	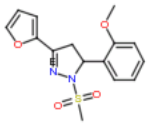	320.21	72.11	1.85	1.85	6	0
DDD00049811	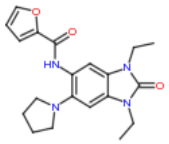	368.2	72.41	1.84	2.39	7	1
DDD00057691	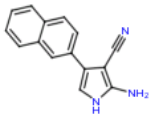	233.15	65.6	2.06	3.14	3	2
DDD00074608	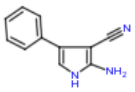	183.11	65.6	1.00	1.96	3	2
DDD00077367	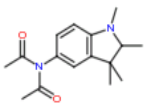	274.16	40.62	0.79	1.85	4	0
DDD00077485*	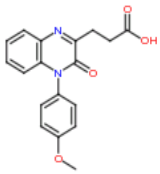	324.18	81.42	0.00	2.16	6	1
DDD00098130	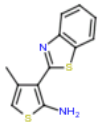	246.24	38.91	2.32	3.49	2	1

DDD00098394	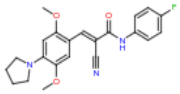	395.22	74.59	2.40	3.54	6	1
DDD00098509	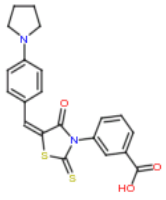	410.33	60.85	0.04	3.58	5	1
DDD00099201	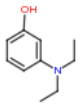	165.1	23.47	1.22	2.54	2	1
DDD01008137	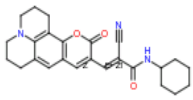	417.25	86.34	2.63	3.70	6	1

MW=molecular weight; TPSA= topological polar surface area; logD= Distribution coefficient of lipophilicity; logP= Partition coefficient of lipophilicity; HBA= Number of hydrogen bond acceptors; HBD= Number of hydrogen bond donors.

*Compounds that re-tested as active in re-purchased batch as HIV-1 frameshifting activators based on fluorescence-based detection.

5.1 Effect of previously identified HIV-1 frameshifting activator, RG501 (DDD01011240) on HIV-1 replication kinetics

Prior to testing the effect of 17 hit compounds, I tested the effect of RG501 {1,4-bis-[N-(3-N,N-dimethylpropyl)amidino] benzene tetrahydrochloride}, a small molecule (Figure 67) that has been reported to bind to the HIV-1 frameshift region and activate frameshifting by about 2-fold (Hung et al., 1998). This in turn inhibited the spread of HIV-1 replication by approximately 50%, and affected cellular replication, but to a lesser degree. Furthermore, this compound inhibited mature capsid (p24) expression and increased Gag-Pol polyprotein production in HIV-1 infected cells. I therefore obtained this compound (re-named DDD01011240) to use as a positive control.

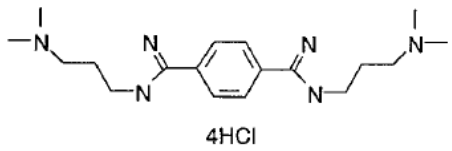

Figure 67 Chemical structure of compound RG501 (DDD01011240)
Chemical structure of DDD01011240 (referred to as RG501 (Hung et al., 1998)), a previously identified HIV-1 frameshifting activator that inhibited HIV-1 replication

However, varying doses of DDD01011240 did not reduce infectious particle production (Figure 68A). Furthermore, the lack of an effect in a single-cycle of HIV-1 replication also correlated with normal levels of Gag and Gag-Pol polyprotein in HIV-1 transfected cells (Figure 68B).

A)

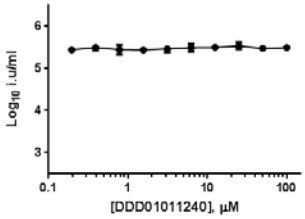

B)

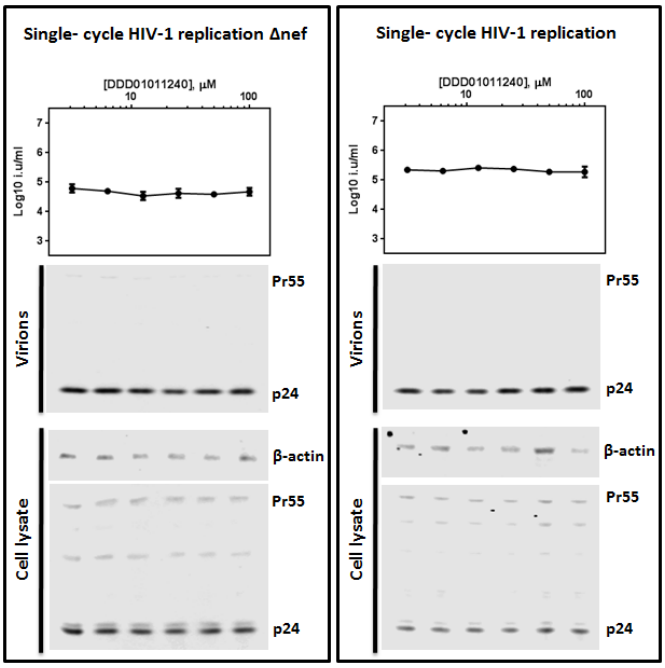

Figure 68 DDD01011240 did not effect a single-cycle of HIV-1 replication

A) Four hours after transfection of HEK293T cells with NHG DNA (HIV-1 with GFP in place of *nef*), DDD01011240 was added at 10 different doses. Replication-competent virions harvested 48 hours post-transfection were used to infect target MT-4 cells. The number of GFP-positive MT-4 cells quantified by flow cytometry was indicative of the effect compounds on a single cycle of HIV-1 replication. Data represented mean ± standard deviation (n=3).

B) HEK293T cells were transfected with either the pNHG or pNL4-3 HIV-1 proviral plasmids followed by treatment with DDD01011240 at 6 different doses. 48 hours later, cell lysate was prepared from transfected HEK293T cells and supernatant was purified to prepare lysate of release HIV-1 virions. Western blotting was used to detect precursor Gag (Pr55) and capsid (p24) protein levels in pelleted virions from purified supernatant and transfected cells to examine Gag processing. Moreover, target MT-4 cells and MT-4 R5 cells were infected with NHG and NL4-3 infectious virions, respectively. 48 hours post-infection, flow cytometry was used to quantify the number of GFP-positive cells, indicative of HIV-1 infection. Infectivity data represented mean ± standard deviation (n=3).

To determine whether this drug had an effect on the spread of HIV-1 infection, infected MT-4 cells were treated with DDD01011240 (50μM) for 10 days. As Figure 69 demonstrates, this drug did not perturb the spread of HIV-1 infection. Furthermore, DDD01011240 did not impact the levels of frameshifting in the cell-based assay of frameshifting (Figure 52) or in Gag-Pol/Gag production in HIV-1 infected cells (Figure 56). All secondary viral experiments with hit compounds, and DDD01011240, were conducted using a maximum compound concentration of 100μM. The discrepancy between the effect of DDD01011240 in our assays and those performed by Hung et al (1998) lies in the concentration used. Hung and colleagues concluded that this compound activated HIV-1 frameshifting, but was observed using 2090μM of the drug which was within the concentration range that conferred cell toxicity. They also concluded that RG501/DDD01011240 increases HIV-1 Gag-Pol polyprotein production by 2.8-fold through increased HIV-1 frameshifting and reduces mature capsid (p24) levels (Hung et al., 1998). However, these conclusions were also based on drug concentrations (1045μM) within the toxic range. Meanwhile, I did not observe any HIV-1 inhibitory effects below 100μM, which was at the threshold of toxic levels.

While Hung and colleagues (2008) used different cell lines and conditions, these results indicate that RG501 is likely not an HIV-1 frameshifting activator and the results obtained by Hung *et al.* (1998) might be due to very high compound concentrations that were toxic and therefore the observed anti-HIV-1 activity was potentially a result of off-target adverse effects.

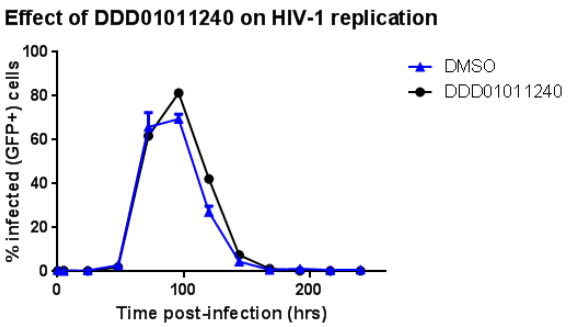

Figure 69 DDD01011240 did not impact the spread of HIV-1 infection
MT-4 cells were infected with replication-competent HIV-1 virions (from NHG transfected of HEK293T cells) at MOI of 0.001. DDD01011240 (50μM) was added four hours post-infection and HIV-1 infection was monitored every 24 hours over 10 days by quantifying the percentage of GFP-positive MT-4 cells using flow cytometry. Data was representative of two independent experiments.

5.2 Effect of hit compounds on single-cycle of HIV-1 replication

As described previously (section 1.5.4), altering the levels of Gag and Gag-Pol polyprotein levels regulated by -1 frameshifting inhibits the late stages of HIV-1 replication. Increased Gag-Pol levels corresponding to stimulated HIV-1 frameshifting perturbs viral assembly and consequently inhibits the production of infectious particles. Thus, since hit compounds identified in the screening cascade were proposed to stimulate HIV-1 frameshifting, I examined their dose-dependent effects on infectious particle production. This was done using a medium-throughput HIV-1 replication assay optimized for a 96-well plate format (detailed in section 2.9).

5.2.1 Effect of hit compounds on infectious virion yield

To determine the dose-dependent effect of hit compounds on the yield of infectious virus-like particles (VLPs), I used a GFP-expressing replication-incompetent HIV-1 reporter system to produce VSV-G pseudotyped HIV-1 particles. This was done by co-transfecting HEK293T cells with plasmids encoding a GFP-expressing HIV-1 based vector, VSV-G pseudotyped envelope and HIV-1 *gag*, *pol* and *rev* genes in the presence of compounds at 10 concentrations (maximum of 100μM); these concentrations corresponded to doses used in the screening cascade. Viral supernatant (from multiple viral doses within a linear range) was added to target MT-4 cells and flow cytometry was used to quantify GFP expression to determine the dose-dependent effect of hit compounds on VLP infectious yield. Hit compounds DDD00004988, DDD00009714, DDD00009715, DDD00009974, DDD00009991 and DDD00077485 had no impact on VLP infectivity (Figure 70A). While 6 compounds inactive against frameshifting in the re-purchased batch did not affect VLP infectivity (Figure 82 in Appendix 5.7.1), DDD00049811, DDD00057691, DDD00098130, DDD00098394 and DDD0098509 reduced the infectivity of VSV-G-pseudotyped particles in a dose-dependent manner (Figure 70B). This reduction however, was minimal and occurred at high concentrations (≥25μM) compared to the effective dose-dependent effect of ritonavir, a currently approved HIV-1 protease inhibitor.

Nevertheless, these effects were not due to the drug solvent as no inhibition of HIV-1 was observed in the presence of DMSO.

A)

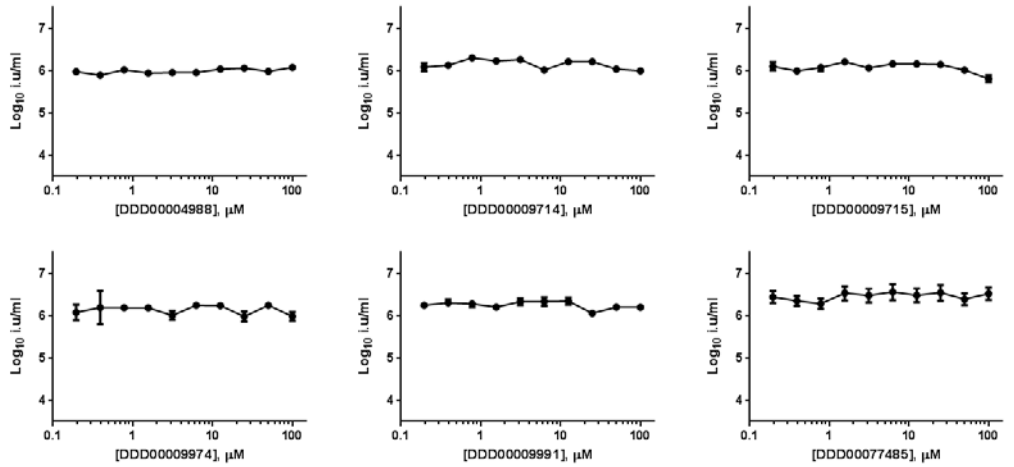

B)

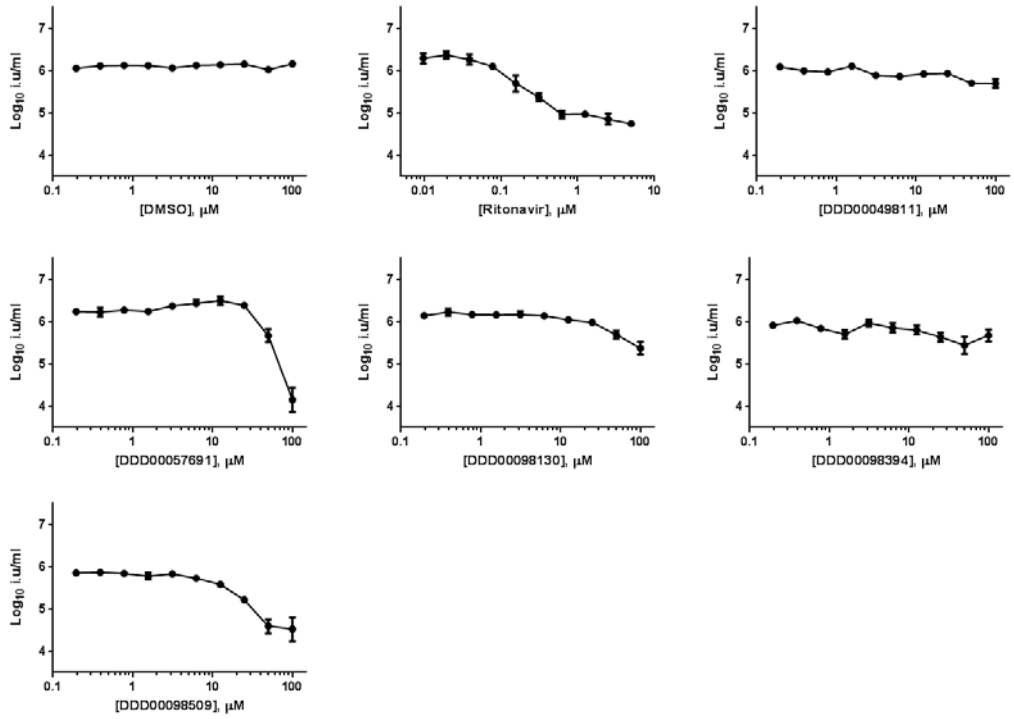

Figure 70 Dose-dependent effect of compounds on HIV-1 infectious particle production using replication-incompetent system

Four hours after transfection of HEK293T cells with plasmids required to produce VSV-G-pseudotyped HIV-1 particles, compounds were added at 10 different doses. Harvested VLPs were titrated onto target MT-4 cells. The number of GFP-positive (infected) MT-4 cells quantified by flow cytometry was used to determine the infectious yield. Data represented mean ± standard deviation (n=3).

A) Hit compounds proposed to activate HIV-1 frameshifting had no effect on infectivity of VSV-G-pseudotyped HIV-1 particles.

B) Inactive re-purchased compounds led to a slight dose-dependent decrease in VLP infectivity.

To confirm the effect of these compounds on infectious virion yield, HEK293T cells transfected with a replication competent HIV-1 proviral plasmid (containing GFP in place of the *nef* accessory gene), were treated with varying doses of hit compounds. MT-4 cells were then infected with serially diluted viral supernatant and infectious units per ml were calculated using multiple viral doses within a linear range. This confirmed that DDD00004988, DDD00009714, DDD00009715, DDD00009974, DDD00009991 and DDD00077485 which activated frameshifting in the cell-based assay of HIV-1 frameshifting, did not impact infectious virion yield (Figure 71A). This suggested that mCherry activation in the cell-based assay did not faithfully recapitulate HIV-1 frameshifting, or that the level of activated frameshifting was insufficient to inhibit the HIV-1 infectious yield. Similar to previous results using VSV-G pseudotyped HIV-1 VLPs, DDD00049811, DDD00057691, DDD00098130, DDD00098394 and DDD00098509, led to a dose-dependent reduction in HIV-1 infectivity (Figure 71B). Furthermore, while DDD01008137 did not impact VLP infectivity (Figure 84 in Appendix 5.7.1), it did slightly inhibit infectious virion yield (NHG) at high concentrations (Figure 71B). Interestingly, the re-purchased batch of compounds DDD00049811, DDD00057691, DDD00098130, DDD00098394, DDD00098509 and DDD01008137 did not activate frameshifting in the fluorescent cell-based assay of HIV-1 frameshifting (Chapter 4) yet seemed to reduce infectious virion yield at high concentrations. This suggests that these compounds might have an off-target inhibitory effect that potentially affects another stage of HIV-1 replication.

Alternatively, these compounds with slight inhibitory effects on HIV-1 infectivity could be due to nonspecific cellular effects including viability or metabolic state. Previous investigation of the effect of 17 re-purchased batch of compounds on the viability of HeLa cells (Figure 51 & Figure 66) revealed that DDD00057691 exhibited a dose-dependent inhibition, while DDD00049811, DDD00098130, DDD00098394 and DDD00098509 reduced HeLa cell viability at the highest concentration (100μM). While cell viability was assessed in a different cell type (HeLa compared to MT-4 cells), it is

possible that the minor reduction in infectivity at very high concentrations, could be due to reduced cell viability. To confirm whether these compounds are targeting HIV-1 assembly, I examined their role on infectious particle production and processing of the viral Gag polyprotein and infectious yield of HIV-1 particles.

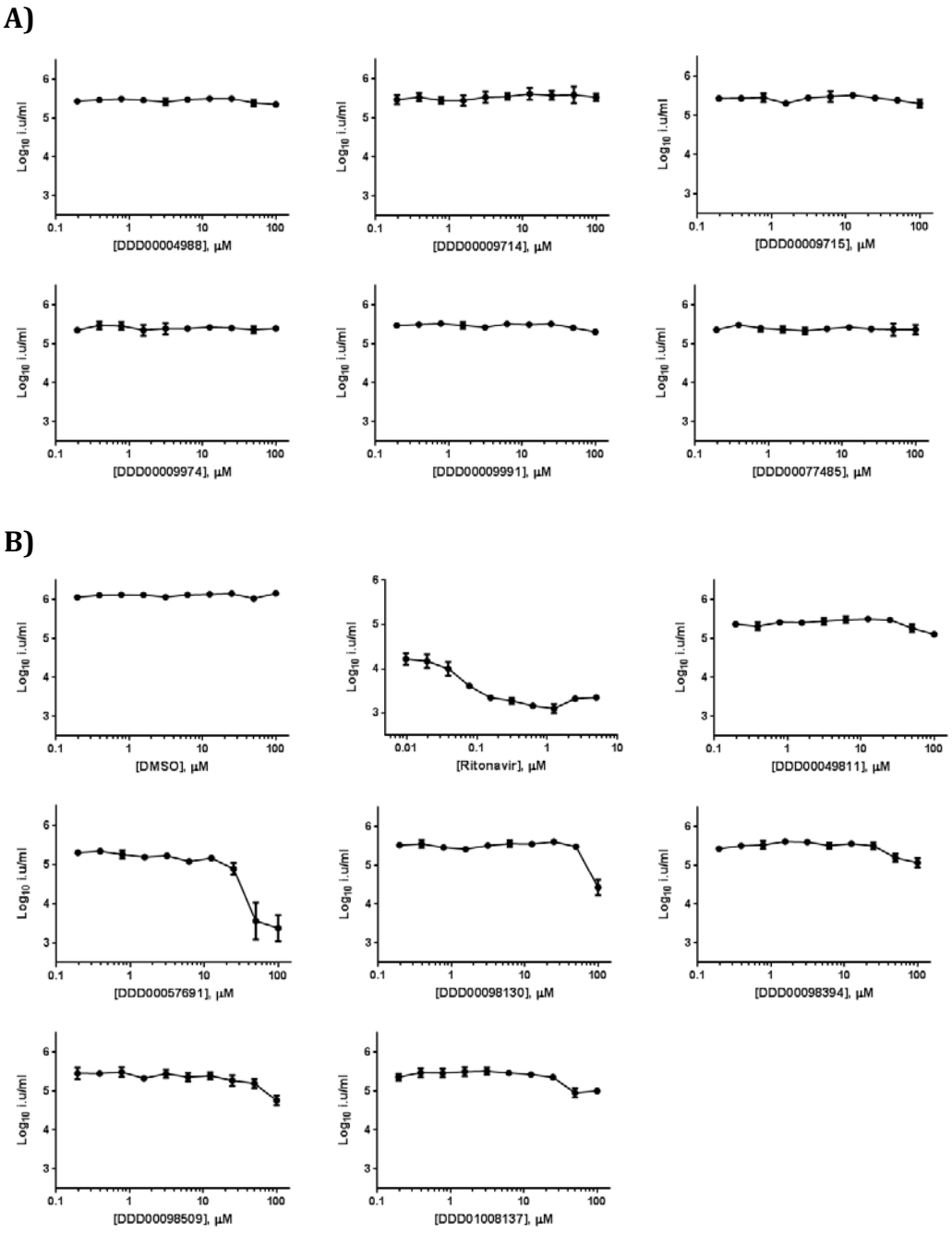

Figure 71 Dose-dependent effect of compounds on the yield of replication-competent HIV-1 virions

Four hours after transfection of HEK293T cells with NHG DNA (HIV-1 with GFP in place of *nef*), compounds were added at 10 different doses. Harvested HIV-1 virions were titrated onto target MT-4 cells. The number of GFP-positive (infected) MT-4 cells quantified by flow cytometry was used to determine the infectious yield. Data represented mean ± standard deviation (n=3).

A) Hit compounds proposed to activate HIV-1 frameshifting had no effect on infectious virion yield

B) Inactive re-purchased compounds led to a slight dose-dependent decrease in HIV-1 infectivity.

5.3 Effect of hit compounds on HIV-1 virion production, Gag processing and HIV-1 infectivity

Reduced infectious virion yield following treatment with DDD00049811, DDD00057691, DDD00098130, DDD00098394, DDD00098509 and DDD01008137 was suggestive of defective HIV-1 assembly or the production of defective (non-infectious) viral particles. Since virion-associated Gag polyprotein processing is a hallmark of viral maturation, this was examined in released virions from compound-treated HIV-1 transfected cells. Furthermore, Gag expression was also examined in transfected cells to determine the effect of compounds on viral gene expression.

HEK293T cells were transfected with HIV-1 proviral DNA (NHG or pNL4-3) following drug treatment at six doses. Western blots probing for capsid (p24) protein were used to detect Gag polyprotein and processing of viral proteins in both transfected cells and released virions from purified supernatant (Figure 72A). Furthermore, infectivity of released HIV-1 virions was determined by quantifying GFP-positive (infected) MT-4 and MT-4 R5 cells infected with NHG and NL4-3 HIV-1 virions, respectively.

Ritonavir, an approved HIV-1 protease inhibitor, exhibited a cell-associated and virion-associated dose-dependent defect in Gag processing (Figure 72B), indicative of non-infectious particle production. This was evident by the accumulation of Gag precursor ($Pr55^{Gag}$) levels corresponding to reduced mature capsid protein (p24) levels. Ritonavir also decreased HIV-1 infectivity, thereby confirming the efficacious inhibitory role of this drug on viral maturation through abrogated protease-mediated cleavage of viral polyproteins. In comparison, DDD00049811, DDD00057691, DDD00098130, DDD00098394, DDD00098509 and DDD01008137, which slightly reduced HIV-1 infectious yield, did not exhibit such a defect in Gag processing, demonstrating no significant defect in protease-mediated viral maturation (Figure 72B).

Replication competent HIV-1 transfected cells treated with DDD00057691 (≥25μM) led to a severe decrease in the production of mature capsid (p24) levels in both cells and released virions (Figure 72C). However, reduced β-actin levels indicated that this inhibitory effect was likely due to cell toxicity. This was further corroborated by the inhibitory dose-dependent effect of DDD00057691 on viability of HeLa cells at concentrations ≥12.5μM (Figure 66 in section 4.8.9).

Similarly, but to a lesser extent, DDD00098130, DDD00098394 and DDD00098509 decreased mature capsid (p24) levels and Gag precursor (Pr55) levels at concentrations ≥ 50μM (Figure 72D). However, decreased β-actin expression in HIV-1 transfected cells and reduced viability of HeLa cells (Figure 66 in section 4.8.9) following 100μM treatment with these drugs suggested a cellular impact, rather than a HIV-1 specific inhibition. DDD01008137 did not significantly inhibit viability of HeLa cells (Figure 66 in section 4.8.9) or β-actin levels in HIV-1 transfected cells, however, did reduce cell-associated and virion-associated capsid (p24) levels following treatment with 100μM of compound (Figure 72D). Since this was not recapitulated in NL4-3-transfected cells, future efforts will attempt to validate the effect of DDD01008137.

Finally, DDD00049811 treatment led to a noticeable dose-dependent reduction in virion-associated capsid (p24) levels and a slight reduction of HIV-1 infectivity at concentrations ≥50μM (Figure 72E). While this effect may be due to cell toxicity, relatively comparable β-actin levels and Gag polyprotein expression in HIV-1 transfected cells suggested otherwise. The virion-specific impact of DDD00049811 indicated the possible production of non-infectious particles or fewer infectious viral particles.

Consequently, the subtle dose-dependent decrease in HIV-1 infectious yield and capsid (p24) levels in response to DDD00057691, DDD00098130, DDD00098394 and DDD00098509 was likely a cellular impact rather than an anti-HIV-1 effect. Conversely, while the seemingly inhibitory effect of

DDD00049811 on the late stages of HIV-1 replication was potentially due to minor inhibitory effects on infectious particle production, a cellular or metabolic defect is also plausible. However, conclusions cannot be made based on these effects since they are minor, occur at very high concentrations, have not been quantified over three replicates and are likely due to toxicity.

A)

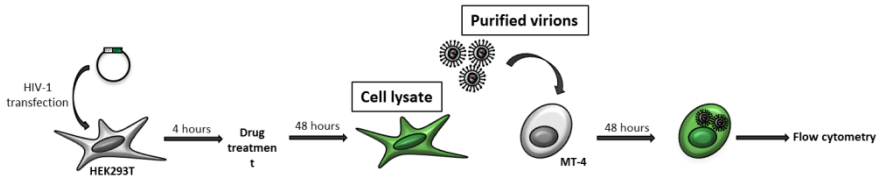
HIV-1
transfection
HEK293T
4 hours
Drug
treatmen
t
48 hours
Cell lysate
Purified virions
MT-4
48 hours
Flow cytometry

B)

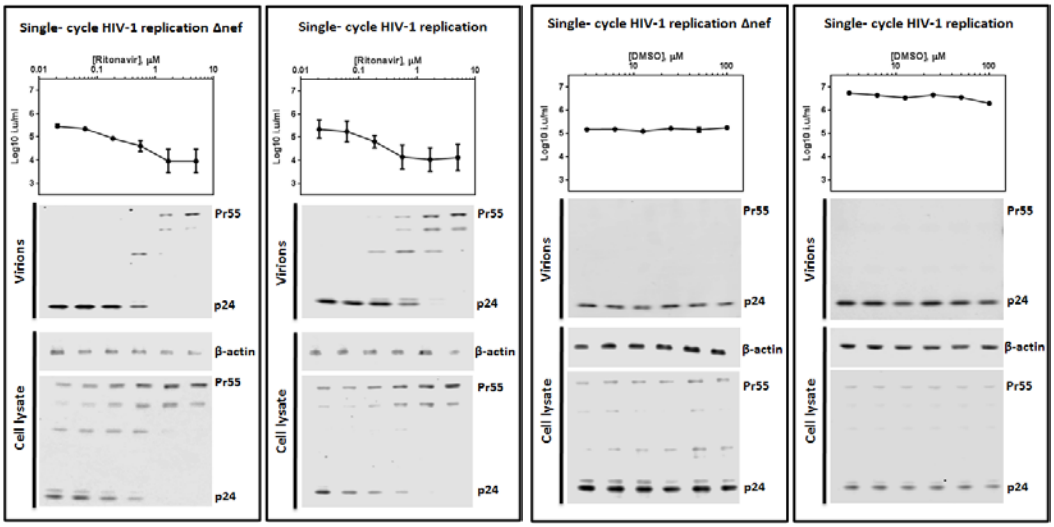
Single- cycle HIV-1 replication Δnef
Single- cycle HIV-1 replication
Single- cycle HIV-1 replication Δnef
Single- cycle HIV-1 replication
[Ritonavir], µM
[DMSO], µM
Log10 (Lu/ml)
Virions
Cell lysate
Pr55
p24
β-actin

C)

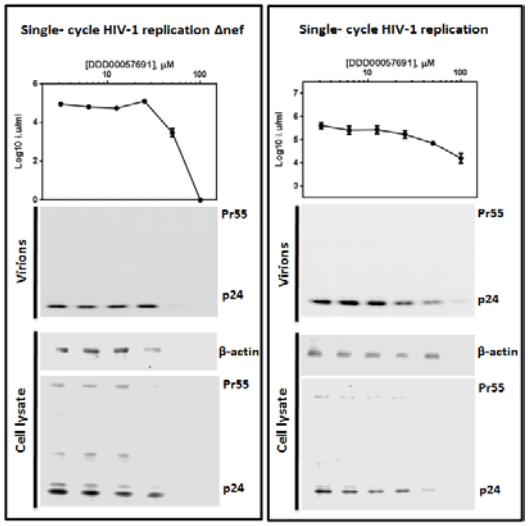
Single- cycle HIV-1 replication Δnef
Single- cycle HIV-1 replication
[DDD00057691], µM
Log10 (Lu/ml)
Virions
Cell lysate
Pr55
p24
β-actin

D)

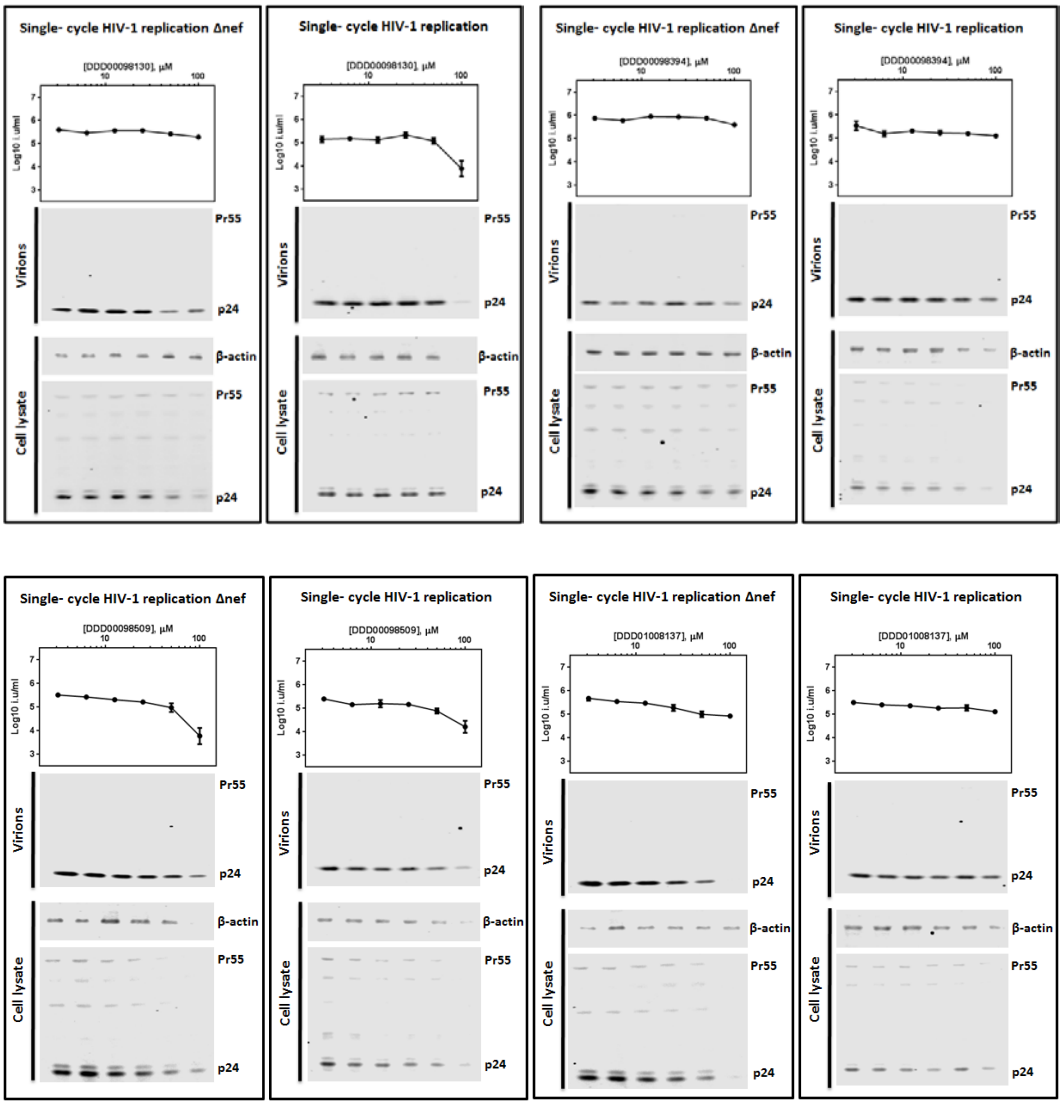
Single- cycle HIV-1 replication Δnef
[DDD00098130], µM
Log10 f.u/ml
Virions
Pr55
p24
Cell lysate
β-actin
Pr55
p24
Single- cycle HIV-1 replication
[DDD00098130], µM
Log10 f.u/ml
Virions
Pr55
p24
Cell lysate
β-actin
Pr55
p24
Single- cycle HIV-1 replication Δnef
[DDD00098394], µM
Log10 f.u/ml
Virions
Pr55
p24
Cell lysate
β-actin
Pr55
p24
Single- cycle HIV-1 replication
[DDD00098394], µM
Log10 f.u/ml
Virions
Pr55
p24
Cell lysate
β-actin
Pr55
p24
Single- cycle HIV-1 replication Δnef
[DDD00098509], µM
Log10 f.u/ml
Virions
Pr55
p24
Cell lysate
β-actin
Pr55
p24
Single- cycle HIV-1 replication
[DDD00098509], µM
Log10 f.u/ml
Virions
Pr55
p24
Cell lysate
β-actin
Pr55
p24
Single- cycle HIV-1 replication Δnef
[DDD01008137], µM
Log10 f.u/ml
Virions
Pr55
p24
Cell lysate
β-actin
Pr55
p24
Single- cycle HIV-1 replication
[DDD01008137], µM
Log10 f.u/ml
Virions
Pr55
p24
Cell lysate
β-actin
Pr55
p24

E)

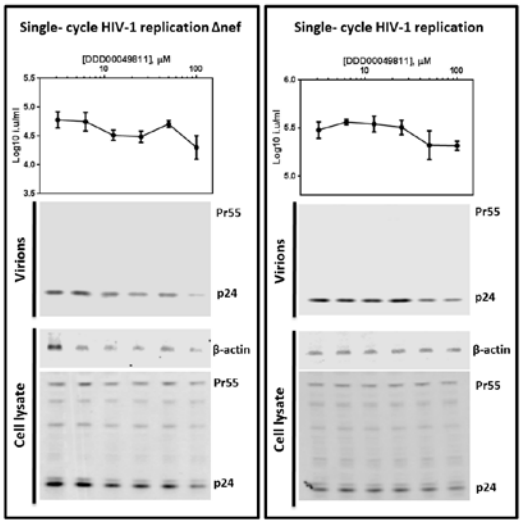

Figure 72 Effect of compounds on HIV-1 virion production, Gag processing and HIV-1 infectivity

A) HEK293T cells were transfected with either the pNHG or pNL4-3 HIV-1 proviral plasmids followed by treatment with compounds at 6 different doses. 48 hours later, cell lysate was prepared from transfected HEK293T cells and supernatant was purified to prepare lysate of release HIV-1 virions. Western blotting was used to detect precursor Gag (Pr55) and capsid (p24) protein levels in pelleted virions from purified supernatant and transfected cells to examine Gag processing. Moreover, target MT-4 cells and MT-4 R5 cells were infected with NHG and NL4-3 infectious virions, respectively. 48 hours post-infection, flow cytometry was used to quantify the number of GFP-positive cells, indicative of HIV-1 infection. Infectivity data represented mean ± standard deviation (n=3). **B)** Ritonavir (positive control), an established HIV-1 protease inhibitor led to dose-dependent defect in Gag processing and reduced infectivity while DMSO (negative control) did not exhibit any effect. **C)** ≥50µM of DDD00057691 decreased cell-associated and virion-associated Gag (Pr55), capsid (p24) and β-actin levels, indicating a potentially toxic effect. Infectivity was also decreased in a dose-dependent manner. **D)** DDD00098130, DDD00098394, DDD00098509 (100µM) led to slight decrease in capsid (p24) levels and infectivity potentially due to cell toxicity. DDD01008137 decreased Gag (Pr55) and capsid (p24) protein levels of NHG-transfected cells and infectious virions in a dose-dependent manner. **E)** DDD00049811 treatment decreased virion-associated capsid (p24) and infectivity in a dose-dependent manner, while having negligible effects on cell-associated Gag (Pr55), capsid (p24) and β-actin protein levels, indicating a potentially anti-viral effect.

5.4 HIV-1 spreading replication assay

Due to the very subtle inhibitory effects of hit compounds on infectious virion yield following a single-cycle of HIV-1 replication, I examined the effect of compounds on the spread of HIV-1 infection which mimicked cell-to-cell transmission and HIV-1 pathogenesis observed *in vivo*. This was done by infecting MT-4 cells at low multiplicities with GFP-expressing HIV-1 replication competent virus containing GFP in place of *nef* (NHG). Infected cells were treated with DMSO (negative control), ritonavir (positive control; 5μM) or hit compounds (50μM). A concentration of 50μM was used because this concentration corresponded to pronounced HIV-1 inhibitory effects and no overt toxic cellular effects in HeLa cells. For 10 days, GFP-positive cells (indicative of infected cells) were enumerated by flow cytometry every 24 hours to examine the spread of HIV-1 infection. DMSO-treated infected cells reached the maximum level of HIV-1 infection 3-4 days post-infection, after which, a decrease in infection correlated with decreased cell viability (Figure 73).

HIV-1 spreading of infected MT-4 cells treated with hit compounds DDD00004988, DDD00009714, DDD00009974, DDD00009991, and DDD00077485 was comparable to DMSO-treated cells, and therefore had no impact on HIV-1 replication (Figure 73). DDD00009715 did slightly attenuate HIV-1 spreading 3-4 days post-infection, but was modest and likely due to the minor reduction of viability observed in HeLa cells (Figure 51). These compounds proposed to activate HIV-1 frameshifting therefore did not substantially impact HIV-1 replication, following both single and multiple cycles of HIV-1 infection.

A)

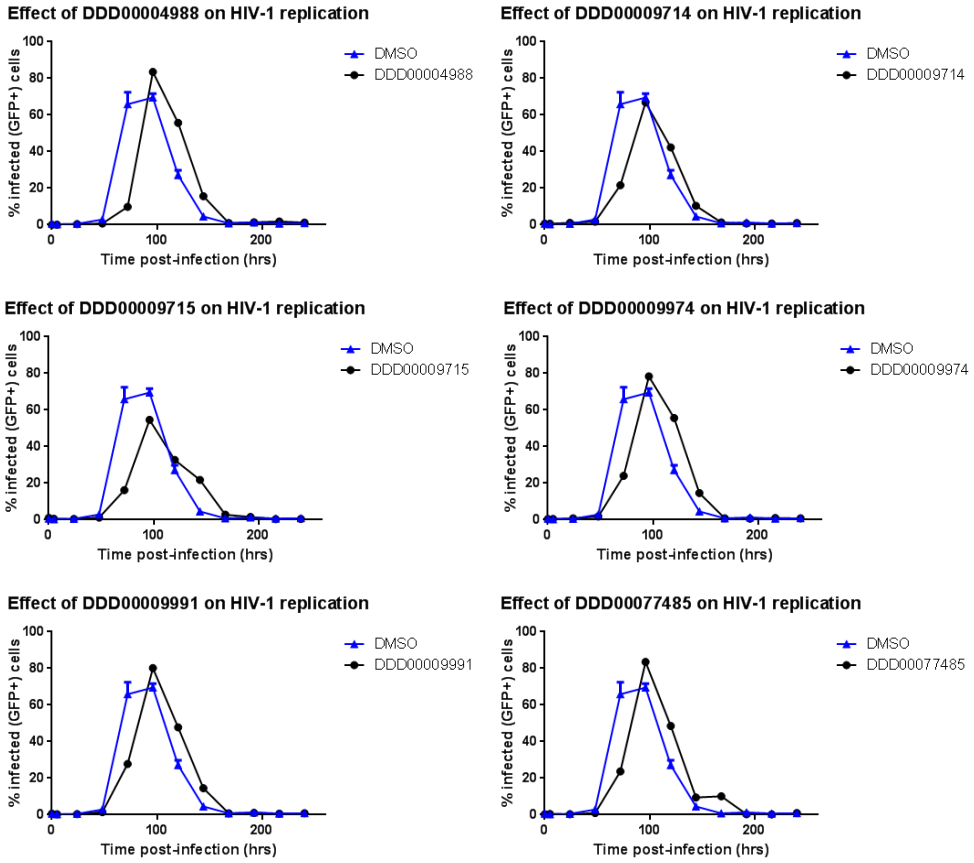

B)

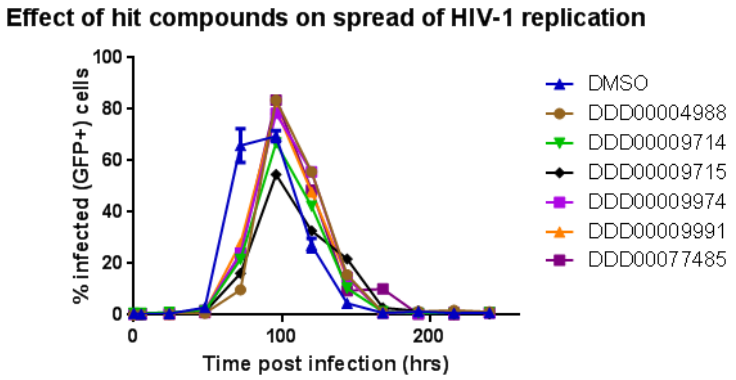

Figure 73 Hit compounds had no significant effect on HIV-1 replication
MT-4 cells infected with replication-competent HIV-1 virions (from NHG transfected of HEK293T cells) at MOI of 0.001 were treated with 0.5% DMSO (v/v) and 50µM of hit compounds four hours post-infection. HIV-1 infection was monitored every 24 hours over 10 days by quantifying the percentage of GFP-positive MT-4 cells using flow cytometry.

A) The effect of DDD00004988, DDD00009714, DDD00009974, DDD00009991 and DDD00077485 on HIV-1 spreading was comparable to DMSO-treated infected cells. HIV-1 spreading was slightly attenuated following DDD00009715 treatment.

B) Overlap of the effect of hit compounds on HIV-1 spreading. Data is representative of two independent experiments.

While hit compounds did not have any impact on the spread of HIV-1 infection, some compounds inactive against frameshifting in the re-purchased batch, had minor effects. DDD00040678 and DDD00074608 led to nominal attenuation of HIV-1 infection relative to DMSO-treated cells 4 days post-infection (Figure 74), similar to the effect of DDD00009715. The lack of an effect of these compounds on infectivity of VSV-G pseudotyped HIV-1 particles and replication-competent HIV-1 virions confirmed the insignificance of this minor attenuation in HIV-1 infection.

A)

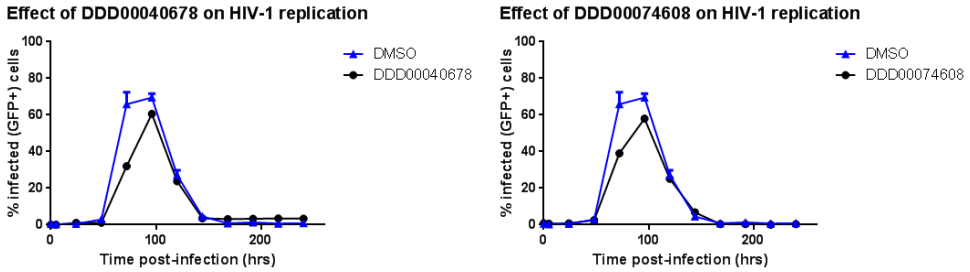

B)

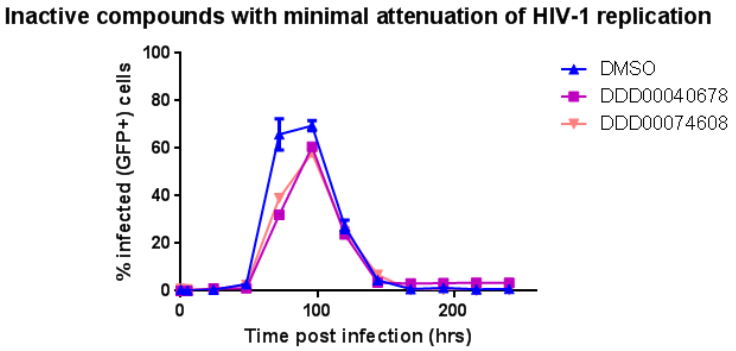

Figure 74 Inactive re-purchased compounds DDD00040678 and DDD00074608 minimally attenuate the spread of HIV-1 infection

MT-4 cells were infected with replication-competent HIV-1 virions (from NHG transfected of HEK293T cells) at MOI of 0.001. 0.5% DMSO (v/v) and 50µM of compounds were added four hours post-infection. HIV-1 infection was monitored every 24 hours over 10 days by quantifying the percentage of GFP-positive MT-4 cells using flow cytometry.

A) The effect of DDD00040678 and DDD00074608 on HIV-1 spreading was slightly decreased compared to DMSO-treated infected cells.

B) Overlap of the effect of hit compounds on HIV-1 spreading. Data is representative of two independent experiments.

Interestingly, DDD00098130-treated infected MT-4 cells delayed HIV-1 replication by three days compared to DMSO-treated infected cells (Figure 75). This effect along with the minor dose-dependent reduction of infectious virion yield (Figure 70 & Figure 71) and reduced cell-associated and virion-associate capsid (p24) levels in NHG HIV-1 transfected cells signify a possible anti-viral effect by DDD00098130. However, dose-dependent reduction of cell viability in HeLa cells (Figure 66 in Appendix 4.8.9) and reduced cell-associated β-actin levels in HIV-1 transfected cells (Figure 72) implied this compound exerts a global or toxic cellular impact.

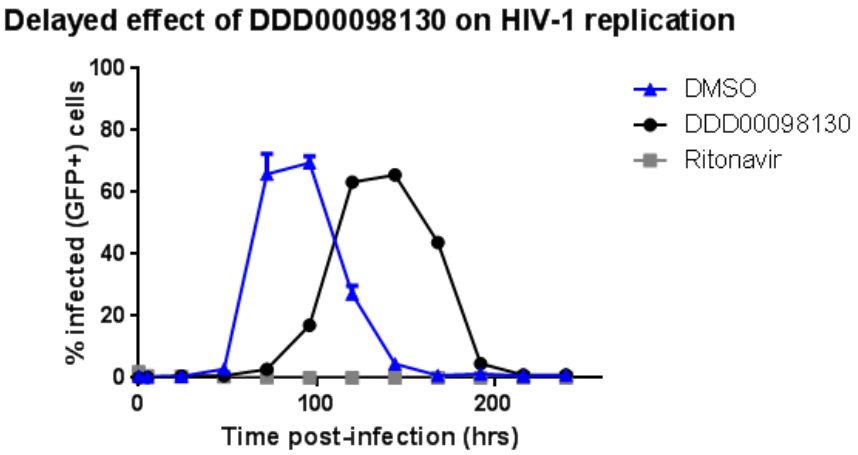

Figure 75 Effect of DDD00098130 in HIV-1 replication spreading assay
MT-4 cells were infected with replication-competent HIV-1 virions (from NHG transfected of HEK293T cells) at MOI of 0.001. 0.5% DMSO (v/v) and 50µM of hit compounds were added four hours post-infection. HIV-1 infection was monitored every 24 hours over 10 days by quantifying the percentage of GFP-positive MT-4 cells using flow cytometry. The effect of DDD00098130 on HIV-1 spreading was delayed in comparison to DMSO-treated infected cells. Data is representative of two independent experiments.

Four inactive re-purchased compounds (DDD00007217, DDD00098394, DDD00098509 and DDD01008137) could not be assessed for their impact on the spread of HIV-1 infection due to unspecific GFP-fluorescence induced by the compound itself. In the HIV-1 spreading assay, GFP-positive cells (quantified by flow cytometry) were indicative of the number of HIV-1 infected cells. Infection was monitored every 24 hours including at the time of infection (t=0hrs) and immediately after drug treatment (t=4hrs), four hours post-infection. Since a single-cycle of HIV-1 replication takes about 24 hours (Daelemans, Pauwels, De Clercq, & Pannecouque, 2011), infected cells, and thus GFP-positive cells, should not be detected four hours-post infection. Unfortunately, saturated levels of GFP were observed in cells following treatment with DDD00007217, DDD00098394, DDD00098509 and DDD01008137 (Figure 76). Since this occurred four hours-post infection, the GFP-positive expression in these cells was not indicative of HIV-1 infection, but likely due to drug-induced GFP auto-fluorescence. Alternative ways of determining the effect of these compounds on HIV-1 replication kinetics include RT activity and p24 levels detected by enzyme-linked immunosorbent assay (ELISA).

Previously conducted assays to test the effect of these drugs on VLP infectivity and infectious virion yield (Section 5.2) also used GFP expression as a measure of HIV-1 infectivity. It is therefore possible that maintained infectivity, determined by maintained GFP levels in DDD00007217, DDD00098394, DDD00098509 and DDD01008137-treated transfected cells were due to auto-fluorescent properties of the drug rather than the lack of an anti- viral effect.

A)

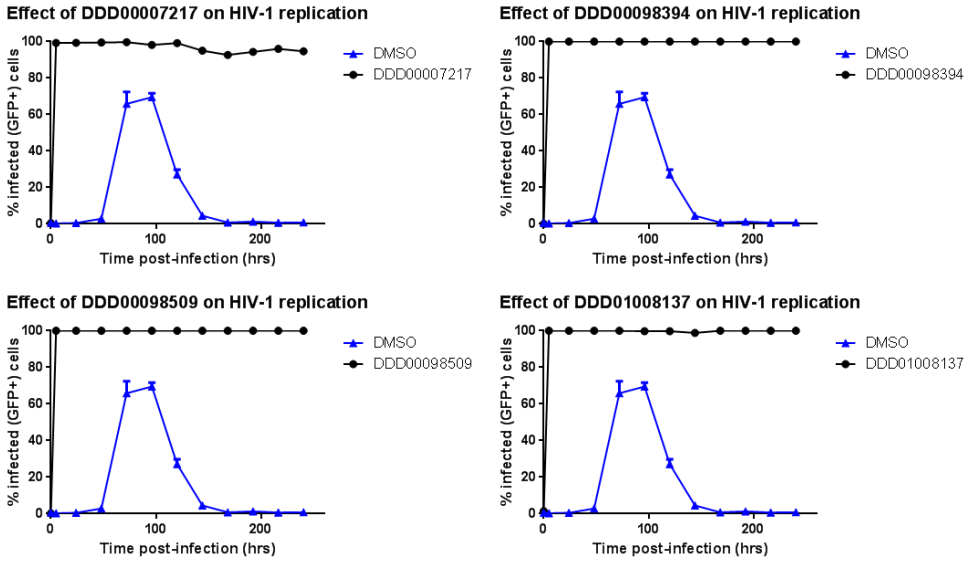

B)

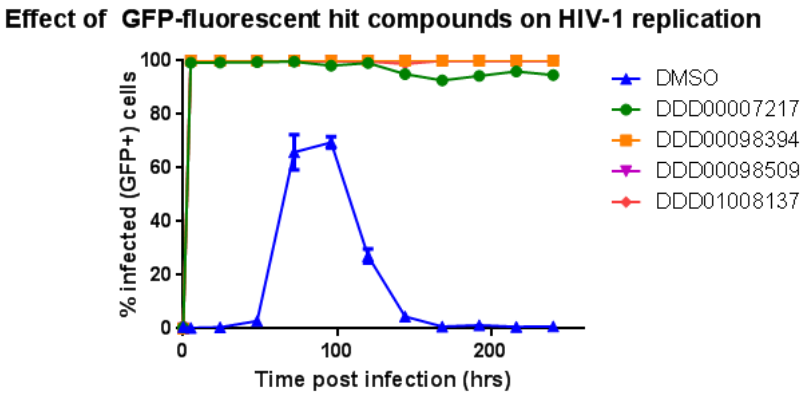

Figure 76 Four hit compounds with GFP-fluorescent activity in HIV-1 replication spreading assay

MT-4 cells were infected with replication-competent HIV-1 virions (from NHG transfected of HEK293T cells) at MOI of 0.001. 0.5% DMSO (v/v) and 50µM of hit compounds were added four hours post-infection. HIV-1 infection was monitored every 24 hours over 10 days by quantifying the percentage of GFP-positive MT-4 cells using flow cytometry.

A) The effect of DDD00007217, DDD00098394, DDD00098509 and DDD01008137 on HIV-1 spreading couldn't be determined due to compound-inducing GFP fluorescence.

B) Data of individual hit compounds are representative of two independent experiments.

Interestingly, DDD00049811 not only delayed the onset of HIV-1 replication, but reduced the spread of HIV-1 infection by 12-fold compared to DMSO-treatment 4 days post-infection (Figure 77). To determine whether this significant reduction was attributed to cellular defects, I examined the effect of DDD00049811 on cell viability of target MT-4 cells using a resazurin assay. DDD00049811 treatment led to a slight decrease in cell viability relative to DMSO-treated infected cells following 48 hours post-drug treatment (Figure 78). However, the 12-fold reduction in HIV-1 infection only corresponded to a 15% reduction in cell viability, four days post-infection (Figure 78). While nonspecific cellular or metabolic defects could account for reduced HIV-1 spreading, DDD00049811 could also possess antiretroviral activity. I previously found that DDD00049811 treatment of HIV-1-transfected cells led to reduced capsid (p24) levels in released virions and a slight decrease in infectivity. This inferred potentially compromised infectious particle production. Therefore, the dramatic inhibition of HIV-1 spreading in DDD00049811-treated cells could potentially result from perturbed infectious particle production that led to minimal inhibition of infectivity in a single-cycle of replication, but an amplified inhibitory effect over multiple cycles of HIV-1 replication. To confirm whether DDD00049811 is specifically targeting HIV-1, the mechanism and mode of action of this drug was further examined.

A)

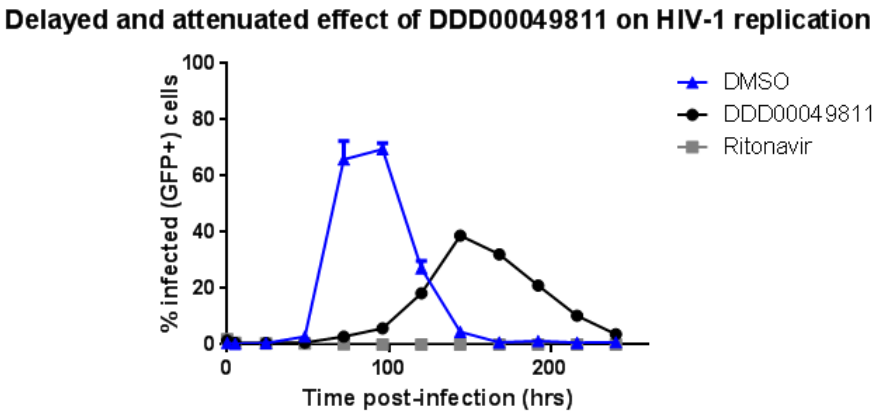

B)

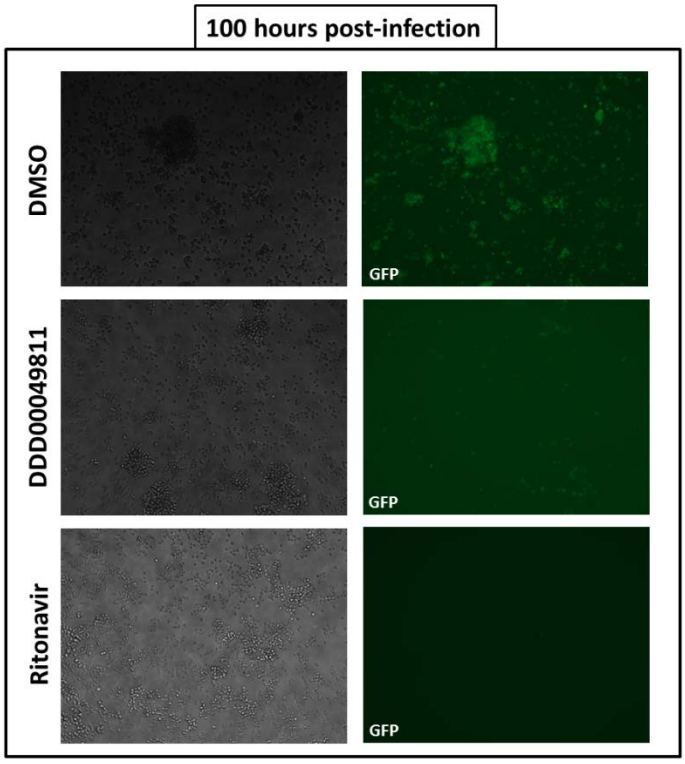

Figure 77 Effect of DDD00049811 in HIV-1 spreading replication assay
MT-4 cells were infected with replication-competent HIV-1 virions (from NHG transfected of HEK293T cells) at MOI of 0.001. 0.5% DMSO (v/v), ritonavir (5µM) and DDD00049811 (50µM) were added four hours post-infection.

A) HIV-1 infection was monitored every 24 hours over 10 days by quantifying the percentage of GFP-positive MT-4 cells using flow cytometry. DDD00049811 delayed the onset and decreased the replicative capacity of HIV-1.

B) Microscopy analysis of infected and drug-treated MT4 cells four days post-infection. Data is representative of two independent experiments.

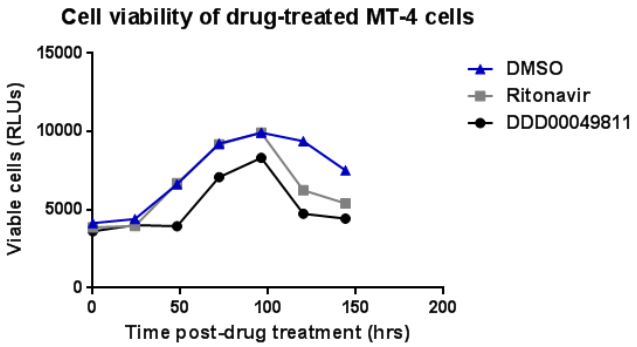

Figure 78 Effect of DDD00049811 on cell viability in MT-4 cells

MT-4 cells were treated with 0.5% DMSO (v/v), ritonavir (5µM) and DDD00049811 (50µM). Every 24 hours, viable cells were quantified. Cell viability was determined by treating cells with resazurin (45µM) for four hours and measuring fluorescence emitted at 590nm following excitation at 550nm. Data is representative of two independent experiments.

5.5 Investigation of the potentially anti-viral mechanism of DDD00049811

To determine the mechanism through which DDD00049811 inhibited the spread of HIV-1 replication, I investigated the effect of this compound on HIV-1 entry using two replication-competent HIV-1 systems.

Replication competent HIV-1 virions were generated by transfecting HEK293T cells with GFP-expressing proviral HIV-1 (NHG) DNA or the complete HIV-1 proviral (NL4-3) DNA. To assess the infectivity of GFP-expressing HIV-1 virions (NHG) in a single-cycle of replication on host MT-4 cells, dextran sulfate was added 6 hours post-infection to prevent subsequent rounds of replication. While this was required for NHG virus, NL4-3 virus which was used to infect MT-4 R5 cells (GFP under HIV-1 promoter) did not require dextran sulfate 6 hours post-infection as the kinetics of replication are slowed in this system (the underlying cause of the delayed replication kinetics in this MT-4 cell clone is unclear). Thus, cells fixed 48 hours post-infection contained negligible levels of infection resulting from a second round of infection (Figure 87 in Appendix 5.7.4). Therefore, the HIV-1 entry inhibitor, dextran sulfate, wasn't added to experiments conducted with pNL4-3 HIV-1 virus.

5.5.1 Effect of DDD00049811 on HIV-1 entry

Since DDD00049811 had a minor inhibitory effect on infectious particle production and infectivity of released virions from HIV-1 transfected cells, but dramatically decreased the spread of HIV-1 infection, I hypothesized that this compound may be acting at an early stage of HIV-1 replication. I therefore examined the effect of DDD00049811 on entry and subsequent replication of infectious HIV-1 particles (Figure 79). Ritonavir, a HIV-1 protease inhibitor, acts on the late stages of HIV-1 replication and therefore did not affect HIV-1 entry, as expected. Alternatively, dextran sulfate, a HIV-1 entry inhibitor, significantly inhibited HIV-1 entry. AZT, which acts on an early stage of HIV-1 replication by targeting reverse transcription, inhibited HIV-1 entry by approximately 12.5-fold. On the other hand, DDD00049811 inhibited the entry of replication-competent HIV-1 (NHG and NL4-3) into

host cells by approximately 2-2.5 fold. The degree of inhibition in response to DDD00049811 was in-between the effects of the reverse transcriptase inhibitor and protease inhibitor, potentially indicative of the targeted stage of HIV-1 replication. Thus, it is possible that DDD00049811 weakly inhibits the early stages of HIV-1 replication, including entry and viral transcription.

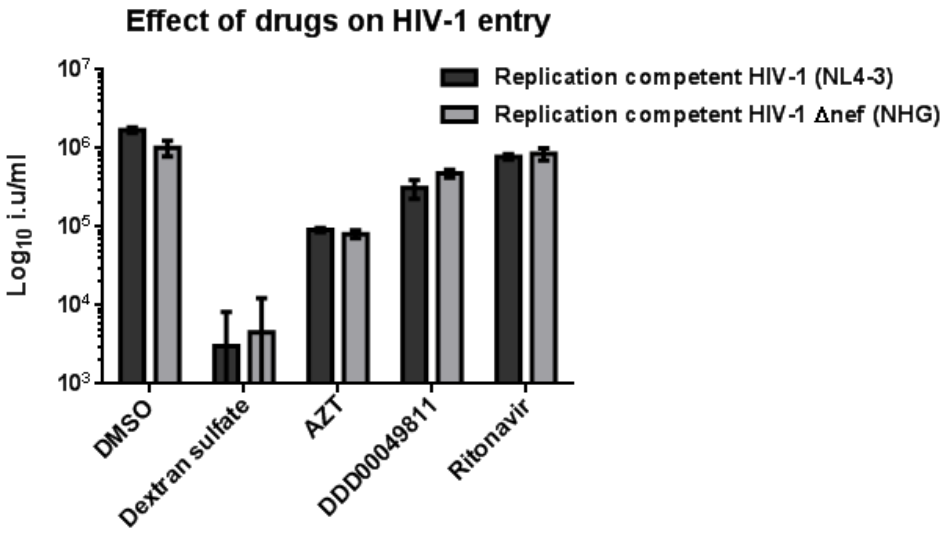

Figure 79 Effect of compounds on entry of replication-competent HIV-1 particles

Target MT-4 and MT-4 R5 cells were infected with infectious NHG (light bars) and NL4-3 (dark bars) HIV-1 virions, respectively, along with 0.5% DMSO (v/v), dextran sulfate (100µM), AZT (3µM), DDD00049811 (50µM) and ritonavir (5µM). 48 hours post-infection, flow cytometry was used to determine HIV-1 infection by quantifying GFP-positive MT-4 and MT-4 R5 cells. Data represents the mean ± standard deviation (n=3).

5.5.2 Bunyavirus replication

To determine whether the inhibitory effect of DDD00049811 is HIV-1 specific, or a general viral inhibitor, (as might be expected if inhibition was due to global nonspecific effects such as toxicity), I examined the effect of this compound on bunyamwera replication. Bunyamwera virus belongs to *Bunyaviridae* family and *Orthobunyavirus* genus of arthropod-borne viruses that can be detrimental to humans through encephalitis and hemorrhagic fever (Elliott, 1997). Bunyamwera, a prototype virus, contains a negative-sense, tripartite RNA genome that encodes six proteins with non-structural, structural and enzymatic activity (Bouloy, Krams-Ozden, Horodniceanu, & Hannoun, 1973). These direct cytoplasmic viral transcription, translation and replication which result in viral assembly and budding at the Golgi apparatus, followed by vesicular transport to the plasma membrane where mature viral particles are released.

To determine the effect of hit compound DDD00049811 on bunyamwera virus replication in comparison to DMSO and currently approved anti-HIV-1 drugs, a monolayer of Vero cells was infected with serial dilutions of bunyamwera virus (generated by Junjie Feng, University of Glasgow) following drug treatment and overlaid with avicel media to prevent unsystematic viral spread. Three days post-infection, I examined the formation of plaques which indicated an infected area of cells, and therefore representative of the replicative capacity of bunyamwera virus in response to drugs. DMSO (0.5%, v/v), DDD00049811 (50μM), ritonavir (5μM) and AZT (3μM) had no impact on bunyamvera viral replication, therefore indicating that the inhibitory effect of DDD00049811 on the spread of HIV-1 infection was not solely due to cytotoxicity or at least not cytotoxicity at levels sufficient to inhibit bunyamwera replication in Vero cells. It remains possible that this inhibitory effect is HIV-specific (Figure 80).

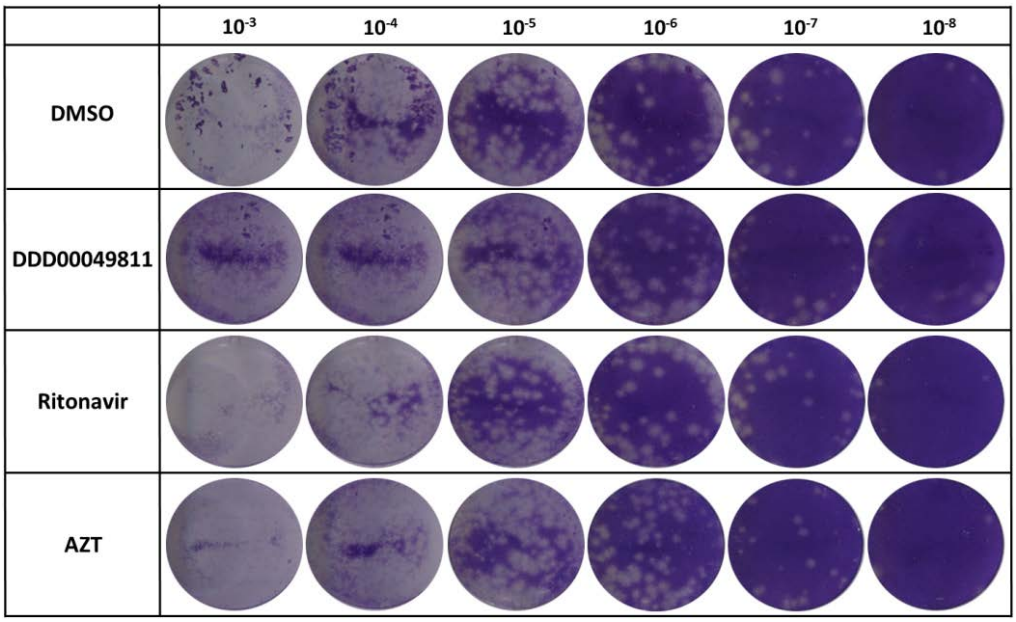

Figure 80 Effect of drugs on bunyamwera viral replication
Serially titrated bunyamwera virus was used to infect Vero cells pre-treated with 0.5% DMSO (v/v), DDD00049811 (50µM), ritonavir (5µM) and AZT (3µM). 3 days post-infection, plaque formation of DDD00049811-treated infected Vero cells was comparable to treatment with DMSO, ritonavir and AZT.

5.5.3 Determination of HIV-1 resistance to DDD00049811

To examine the potential antiretroviral mechanism of DDD00049811, I examined the replication kinetics of HIV-1 in response to prolonged treatment with DDD00049811. Following optimization of parameters (described in section 2.14), HIV-1-(NHG) infected MT-4 cells were treated with DMSO (negative control), DDD00049811 or AZT (positive control) and infection was monitored every 24 hours using flow cytometry to enumerate infected (GFP-positive) cells. Upon maximum infection, virions from DDD00049811-treated infected cells were harvested and used to infect fresh DMSO-, DDD00049811- and AZT- treated cells in the next cell passage. Virus from DDD00049811-treated infected cells was repeatedly harvested and used to infect a fresh passage of cells while monitoring HIV-1 replication kinetics to determine whether DDD00049811 treatment led to the selection of HIV-1 variants resistant to DDD00049811.

As Figure 81 shows, the replication kinetics of DDD00049811-treated MT-4 cells was reduced and delayed over time, compared to DMSO-treated cells. HIV-1 virus continually passaged in the presence of DDD00049811 did not develop resistance to the drug over five cell passages conducted to date. From the results obtained thus far, I cannot conclude whether the effects of DDD00049811 are viral or cellular since it may take more cell passages for drug resistance to emerge.

As a positive control for the development of HIV-1 resistance, HIV-1 virions were continually passaged in the presence of AZT. This is a currently used reverse transcriptase inhibitor that HIV-1 developed resistance to following prolonged therapy in patients (Land et al., 1990; Larder, Darby, & Richman, 1989; Rooke et al., 1989). As Figure 81B shows, HIV-1 did not develop resistance to AZT over 5 passages of MT-4 cells, which are highly permissible to infection. This also supports the theory that perhaps more passages are required for the potential of drug resistance to arise.

A)

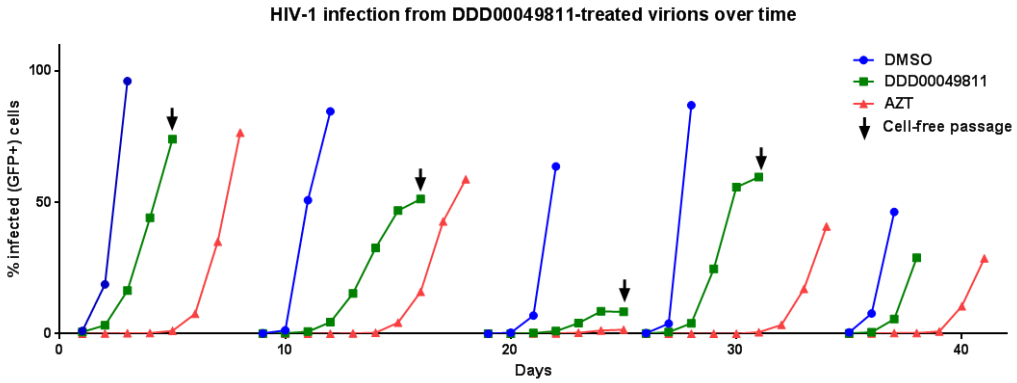

B)

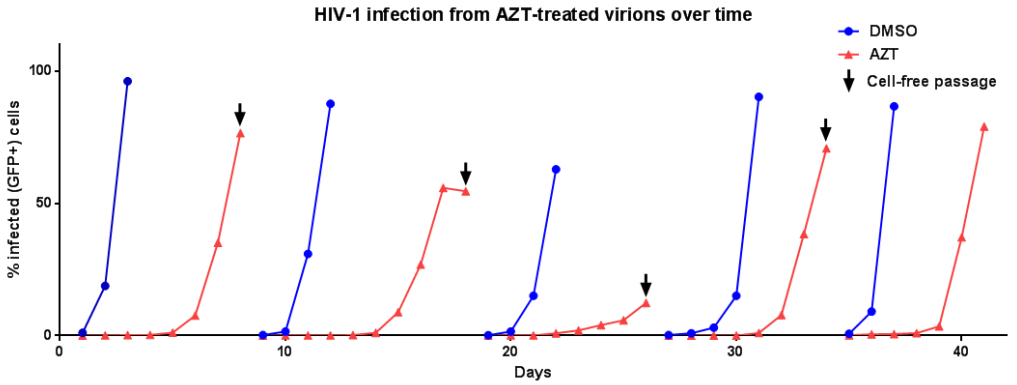

Figure 81 The spread of HIV-1 infection over time does not indicate the development of resistance to DDD00049811 and AZT

A) HIV-1 (NHG)-infected MT-4 cells were treated with either 0.5% DMSO (v/v), DDD00049811 (50µM) or AZT (1.87µM). Upon maximum HIV-1 infection, DDD00049811-treated virions were harvested (arrows) and used to infect fresh passage of drug-treated cells. The level of HIV-1 infection monitored over five cell passages does not reveal the emergence of resistance to DDD00049811.

B) HIV-1 (NHG)-infected MT-4 cells were treated with either 0.5% DMSO (v/v) or AZT (1.87µM). Upon maximum HIV-1 infection, AZT-treated virions were harvested (arrows) and used to infect fresh passage of drug-treated cells. The level of HIV-1 infection monitored over five cell passages does not reveal the emergence of resistance to AZT.

5.6 Summary

This chapter describes the results obtained from examining the effect of the 17 initial hit compounds on the kinetics of HIV-1 replication. A re-purchased batch of six hit compounds DDD00004988, DDD00009714, DDD00009715, DDD00009974, DDD00009991 and DDD00077485 that stimulated frameshifting in my fluorescent cell-based model of HIV-1 frameshifting (Chapter 4), did not impact infectious virion yield in a single-cycle of HIV-1 production. Furthermore, none of these six hit compounds had significant inhibitory effects on HIV-1 replication kinetics, thereby confirming that they do not have antiretroviral effects on HIV-1.

Of the 11 compounds that did not activate HIV-1 frameshifting in the re-purchased batch of compounds, six compounds DDD00057691, DDD00098130, DDD00098394, DDD00098509, DDD00049811 and DDD01008137 slightly decreased infectious virion yield in a dose-dependent manner. Reduced cell-associated and virion-associated Gag precursor polyprotein and capsid (p24) levels in DDD00057691-treated HIV-1 transfected cells were due to low cell viability.

Reduced Gag and mature capsid levels, albeit to a lesser degree, were also observed in HIV-1 transfected cells and virions in response to DDD00098394 and DDD00098509 treatment following a single-cycle of replication. This however, was likely a cellular translational inhibition due to reduced β-actin expression levels. DDD00098130 led to reduced Gag precursor and mature capsid (p24) levels at high concentrations in a single-cycle of HIV-1 replication and a notable delay in the spread of HIV-1 infection. While this could potentially be an antiviral effect, it was more likely a cellular translational defect, due to decreased eGFP production in clonally-derived HIV-1 frameshifting HeLa cells, representative of cap-dependent cellular translation.

DDD01008137 treatment of HIV-1 (NHG)-transfected cells led to a dose-dependent reduction in cell-associated and virion-associated capsid (p24)

protein levels. Maintained β-actin protein expression and sustained viability in HeLa cells indicated that reduced capsid (p24) was likely not a cellular effect. However, the impact of this drug on HIV-1 spreading could not be determined due to unspecific drug-induced GFP fluorescence. Future efforts should use alternative non-fluorescent based assays to determine the effect of auto-fluorescent drugs on HIV-1 replication kinetics. Examples include ELISA-based quantification of capsid (p24) antigen in viral supernatant from infected cells and examination of virion-associated reverse-transcriptase activity.

Finally, DDD00049811 treatment in HIV-1 transfected cells led to virions with decreased capsid (p24) levels, reduced Gag-Pol polyprotein production and diminished infectivity. Furthermore, DDD00049811 reduced entry of HIV-1 virions by ~2-fold. These subtle inhibitory effects from a single-cycle of replication suggest that DDD00049811 potentially targets infectious particle production and/or the early stages of HIV-1 replication. Interestingly, DDD00049811 treatment led to a significant 12-fold reduction in the spread of HIV-1 infection, possibly due to an amplified defect in infectious particle production over multiple rounds of infection and/or the additive effects of a modest attenuation of infection as well as a reduction in infectious particle production.. Furthermore, DDD00049811 did not affect bunyamwera replication, indicating that DDD00049811-treated cells could support robust viral replication. This could be due to different cell types used in these experiments responding differently to this compound or these vastly different viruses could have differing sensitivities to target cell ‘state’. We are unable to rule out whether DDD00049811 targets HIV-1 directly. However, a slight decrease in the viability of MT-4 cells following 48 hours post-infection suggested that the observed HIV-1 inhibitory effects could be due to cellular defects.

So far, resistant HIV-1 variants have rapidly emerged when currently available therapeutics are administered alone. Following this, I hypothesized that HIV-1 would develop resistance to DDD00049811 if inhibitory effects were HIV-1 specific and not due to cellular defects. I therefore tested the

prolonged effect of both DDD00049811 and AZT (current RT inhibitor) on HIV-1 infection and found no evidence of DDD00049811-resistant HIV-1 variants over 5 cell passages. I also did not observe AZT-resistant HIV-1 infection, which has been previously established following prolonged therapy *in vitro* and in HIV-positive patients. These results indicated that further cell passages may be required to develop drug resistance. I therefore cannot conclusively distinguish between a viral and cellular impact on HIV-1 replication kinetics in response to DDD00049811 treatment.

5.7 Appendix

5.7.1 Inactive hit compounds had no effect on infectivity of virus-like particles (VLPs)

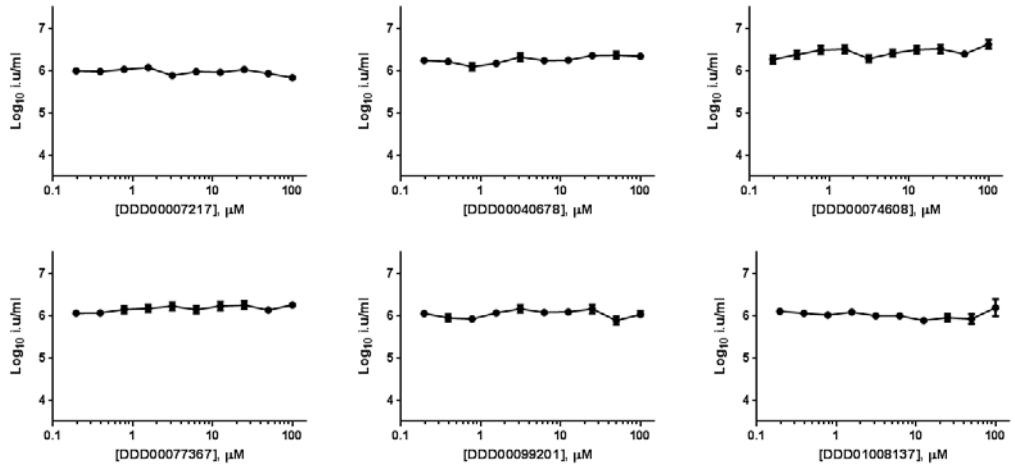

Figure 82 Inactive re-purchased hit compounds had no dose-dependent effect on VLP infectivity

Four hours after transfection of HEK293T cells with plasmids required to produce VSV-G-pseudotyped HIV-1 particles, compounds were added at 10 different doses. Harvested VLPs were titrated onto target MT-4 cells. The number of GFP-positive MT-4 cells quantified by flow cytometry was indicative of the effect of each compound on infectivity of VSV-G-pseudotyped HIV-1 particles. Data represented mean ± standard deviation (n=3).

5.7.2 Inactive hit compounds had no effect on infectious virion yield

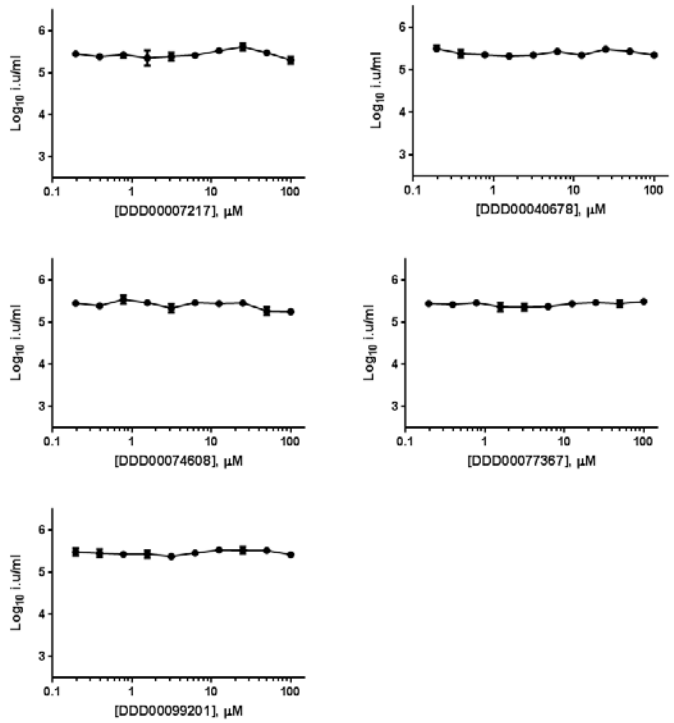

Figure 83 Dose-dependent effect of inactive re-purchased compounds on infectivity of replication-competent HIV-1 virions
Four hours after transfection of HEK293T cells with NHG DNA (HIV-1 with GFP in place of *nef*), compounds were added at 10 different doses. Harvested HIV-1 virions were titrated onto target MT-4 cells. The number of GFP-positive (infected) MT-4 cells quantified by flow cytometry was used to determine the infectious yield. Data represented mean ± standard deviation (n=3).

5.7.3 Inactive hit compounds had no effect on spread of HIV-1 replication

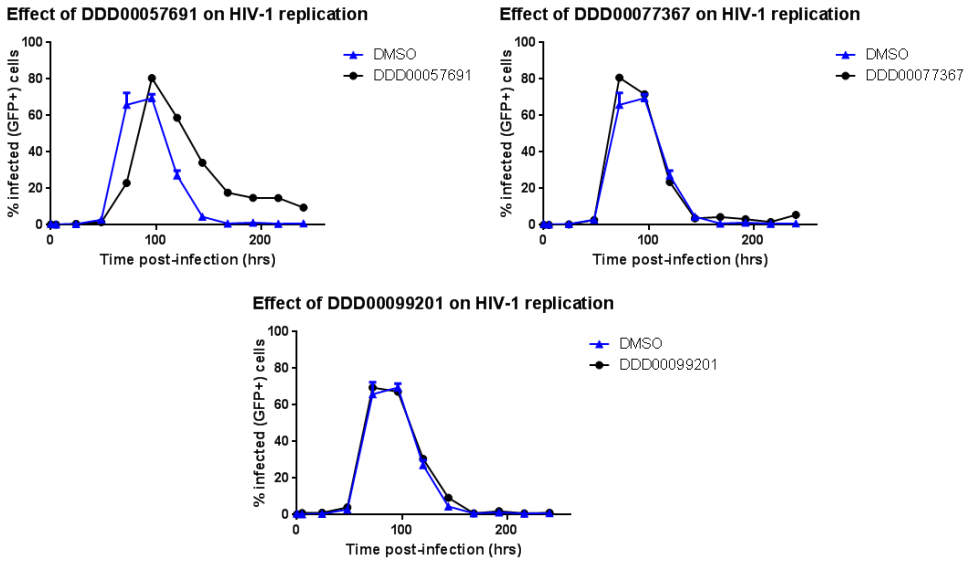

Figure 84 Inactive re-purchased compounds had no significant effect on the spread of HIV-1 infection

MT-4 cells infected with replication-competent HIV-1 virions (from NHG transfected of HEK293T cells) at MOI of 0.001 were treated with compounds (50μM) four hours post-infection. HIV-1 infection was monitored every 24 hours over 10 days by quantifying the percentage of GFP-positive MT-4 cells using flow cytometry.

5.7.4 Verifying the effect of dextran sulfate of infectivity of HIV-1 virions

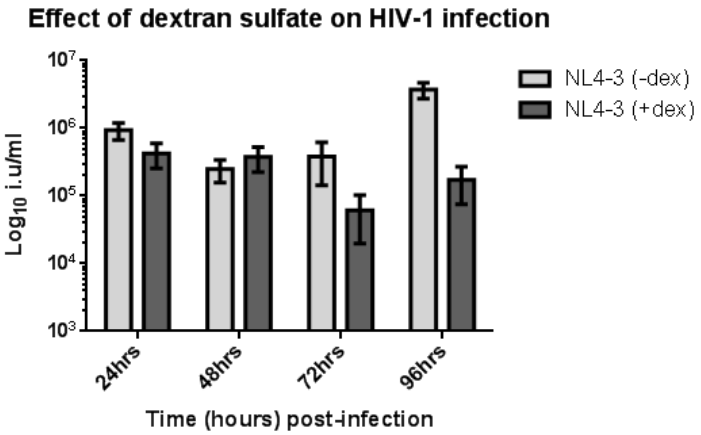

Figure 85 Time-dependent effect of dextran sulfate on HIV-1 replication
Target MT-4 R5 cells were infected with infectious NL4-3 HIV-1 virions harvested 48 hours post-transfection of HEK293T cells. Dextran sulfate (100μM) (+dex; dark bars) or media (-dex; light bars) was added to infected cells 6 hours post-infection. Using flow cytometry, HIV-1 infection was monitored every 24 hours over 4 days by quantifying GFP-positive MT-4 R5 cells.

Chapter 6

Results: Second screening cascade for HIV-1 frameshifting activators using alternate strategy

The screening campaign for HIV-1 frameshifting modulators (detailed in Chapter 4) used a readout of mCherry fluorescence in clonally-derived HIV-1 frameshifting cells as a determinant of frameshifting efficiency. However, none of the hit compounds (DDD00004988, DDD00009714, DDD00009715, DDD00009974, DDD00009991 and DDD000077485) increased eGFP-mCherry polyprotein expression or HIV-1 Gag-Pol production as a result of activated frameshifting efficiency. This chapter outlines the second screening cascade undertaken to identify specific activators of HIV-1 frameshifting. In contrast to previously used clonally-derived HIV-1 frameshifting cells, this cascade involved a primary counter-screen with parental HeLa cells due to the identification of auto-fluorescent false positive hits in the first screening cascade.

6.1 Hit compounds were intrinsically auto-fluorescent

I previously outlined the discrepancy in the degree of frameshifting detected by fluorescence and polyprotein production in clonally-derived frameshifting HeLa cells (section 5). DDD00004988, DDD00009714, DDD00009715, DDD00009974, DDD00009991 and DDD000077485 activated mCherry fluorescence in HIV-1 frameshifting cells in a dose-dependent manner, implying a stimulated effect on HIV-1 frameshifting. However, the unaffected levels of eGFP-mCherry fusion protein and HIV-1 Gag-Pol polyprotein, raised the possibility of unspecific mCherry fluorescence. I therefore investigated the effect of these six hit compounds on eGFP and mCherry fluorescence in parental HeLa cells.

HeLa cells were treated with 50μM of each hit compound DDD00004988, DDD00009714, DDD00009715, DDD00009974, DDD00009991 and DDD000077485 for 48 hours. Subsequent microscopy analysis of eGFP and mCherry fluorescence revealed that all compound-treated HeLa cells expressed varying levels of mCherry, while DDD00004988 and

DDD00009714-treated HeLa cells slightly expressed eGFP as well (Figure 86). This unspecific compound-induced mCherry fluorescence in HeLa cells correlated with increased mCherry fold change detected by the fluorescence during the screening cascade. It is therefore likely that increased mCherry fluorescence in clonally-derived HIV-1 frameshifting cells following treatment of hit compounds was due to auto-fluorescent properties of these compounds rather than activated frameshifting. Furthermore, this potentially explains why DDD00004988, DDD00009714, DDD00009715, DDD00009974, DDD00009991 and DDD000077485 did not inhibit HIV-1 replication or cause an increase in the production of eGFP-mCherry and HIV-1 Gag-Pol polyproteins expected upon stimulated frameshifting.

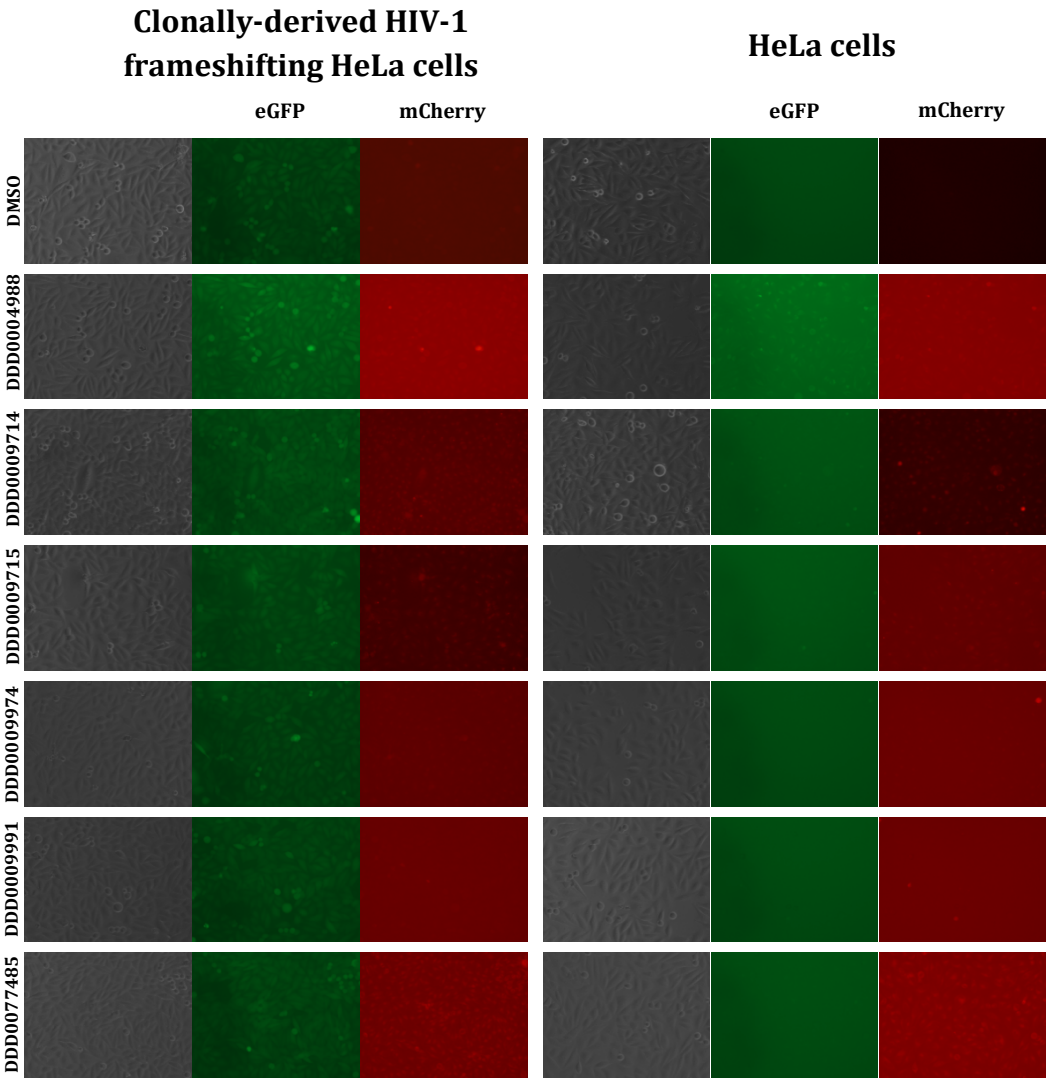

Figure 86 Effect of hit compounds on eGFP and mCherry expression in clonally-derived HIV-1 frameshifting cells and HeLa cells

Clonally-derived HIV-1 frameshifting HeLa cells and HeLa cells were treated with 0.5% DMSO (v/v) and 50μM of each hit compound DDD00004988, DDD00009714, DDD00009715, DDD00009974, DDD00009991 and DDD00077485. 48 hours post-treatment, an EVOS cell imaging system was used to detect eGFP and mCherry fluorescence. Results indicate that all hit compounds were fluorescent in the red channel in parental HeLa cells. Furthermore, DDD00004988 and DDD00009714 were slightly fluorescent in the green channel.

Moreover, I examined the effect of the other 11 compounds (inactive in the re-purchased batch) in parental HeLa cells and found that the relative levels of eGFP and mCherry fluorescence observed by microscopy correlated with levels detected by the fluorometer (PherastarFS) in confirmatory screens with HIV-1 frameshifting cells (Figure 93). Compound-treated HeLa cells led to localization of fluorescence in either the nucleus or cytoplasm. One such example is DDD00077367, which caused cytoplasmic localization of mCherry fluorescence. This raised the possibility that some compounds could be staining specific proteins or cellular components. Alternatively, the insoluble particles of DDD00098394 and DDD01008137 added to HeLa cells were highly fluorescent and also account for the increased fluorescence observed in the HIV-1 frameshifting model.

In the initial screening cascade (Chapter 4), efforts to eliminate auto-fluorescent compounds used ultraviolet-visible (UV-Vis) spectroscopy and clonally-derived translational control HeLa cells. UV-Vis spectroscopy was conducted on a subset of compounds over 350nm-650nm wavelengths to identify and eliminate auto-fluorescent compounds with absorbance spectra corresponding to the excitation profile of eGFP and mCherry. However, of the 17 compounds, only DDD00004988 and DDD00009714 were tested, and did not exhibit unspecific absorbance at any wavelengths. Since UV-Vis spectroscopy was done with the original batch of compounds in PBS alone, auto-fluorescence observed in parental HeLa cells could be batch specific or due to staining of cellular components. Furthermore, the lack of activated fluorescence in clonally-derived HeLa cells could be due to already saturated levels of mCherry as a result of cellular translation. Nevertheless, this signified the importance eliminating false positive hits early in the screening cascade.

6.2 Hit identification from primary screen in HeLa cells

In the initial primary screen for HIV-1 frameshifting modulators with 92,071 compounds, 1455 compounds were identified as activator hits of HIV-1 frameshifting. This was based on increased mCherry fluorescence in clonally-derived HIV-1 frameshifting HeLa cells. From these 1455 hits, 681 compounds were selected for confirmatory screening involving dose-response curves. This chapter details the alternate screening strategy employed to identify true HIV-1 frameshift activators from the remaining 774 hits (Figure 87).

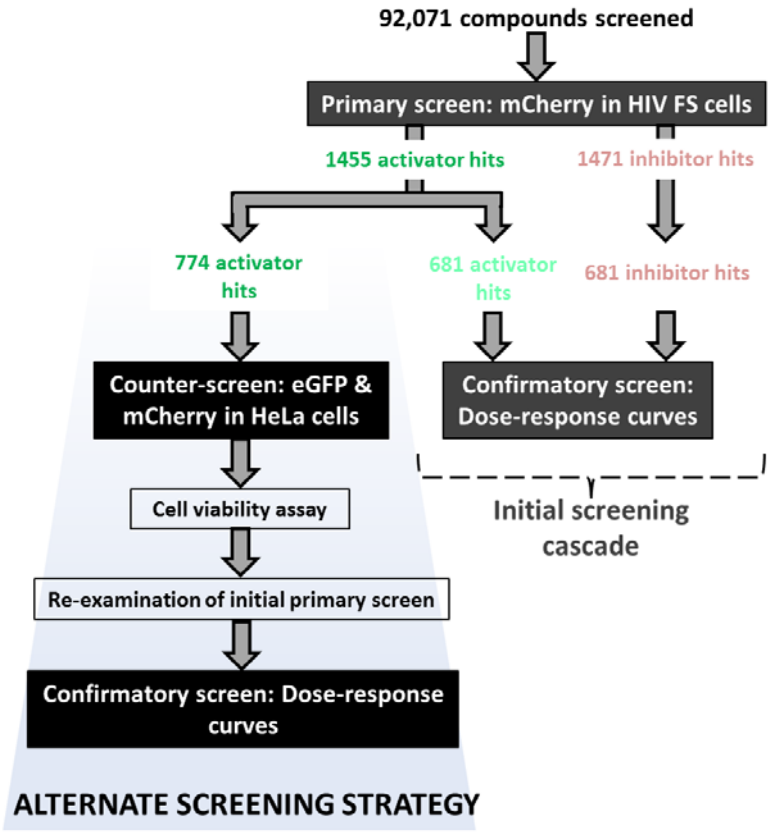

Figure 87 Workflow of alternate screening strategy to eliminate false positive hits and identify HIV-1 frameshifting modulators (detailed in sections 6.2-6.6)

Due to intrinsic fluorescent properties of final hit compounds in parental HeLa cells (Figure 86), I employed a different strategy of screening with the remaining 774 primary hit compounds that were not previously selected for confirmatory screening. This was done by treating parental HeLa cells with 774 compounds at a fixed concentration (30μM) for 48 hours, after which, fold change of eGFP and mCherry fluorescence was quantified relative to DMSO-treated HeLa cells. The purpose of this strategy was to eliminate false positive compounds characterized by intrinsic fluorescence and to thereby identify compounds that truly stimulate HIV-1 frameshifting. By arbitrarily setting 1.2 fold change in fluorescence as a cut-off to identify fluorescent compounds, 302 compounds that exhibited greater than 1.2 fold increase of mCherry and eGFP fluorescence in HeLa cells were eliminated. This threshold was comparable to the 1.27 fold change cut-off set in the initial primary screen for mCherry activators in clonally-derived HIV-1 frameshifting HeLa cells. Therefore the remaining 472 compounds, which did not exhibit fluorescent activity in HeLa cells, but activated mCherry in HIV-1 frameshifting cells in the initial primary screen, were selected through into the next screening stage to eliminate toxic compounds.

6.3 Cell viability in HeLa cells

To eliminate toxic compounds, I tested the effect of 472 hit compounds on cell viability. Resazurin assays were conducted in HeLa cells treated with 472 compounds at a single concentration (30μM) for 48 hours. The percentage of cell viability in compound-treated cells was determined relative to DMSO-treated cells. Compounds that reduced viability in HeLa cells by more than 20% were eliminated. This threshold was arbitrarily set to eliminate compounds with global translational defects early in the screening campaign. From the 472 compounds that did not exhibit unspecific eGFP and mCherry fluorescence, 61 were eliminated due to low cell viability. Therefore, the 411 non-toxic hit compounds identified so far increased mCherry expression in clonally-derived HIV-1 frameshifting cells in the initial primary screen and were not auto-fluorescent.

6.4 Hit identification: comparison to primary screen results

From the 774 compounds screened in HeLa cells thus far, 411 compounds were identified as hits. Due to the impracticality of conducting dose-response curves with all 411 compounds, I re-examined the effect of these compounds on mCherry expression in clonally-derived HIV-1 frameshifting cells from the primary screen conducted earlier (Chapter 4). In the initial primary screen for HIV-1 frameshifting modulators, hits that activated frameshifting were identified by compounds causing more than 1.27 fold increase in mCherry fluorescence (whereby three times the median's standard deviation was set as the threshold). As a result, this included compounds that stimulated mCherry expression near this threshold. From our understanding of the highly sensitive fluorescence-based detection of mCherry, a new and more rigorous cut-off of 1.5 fold change was set. As a result, from the 411 hits, 37 compounds were prioritized (Figure 88). This was a feasible number of hits that were used to conduct confirmatory screens.

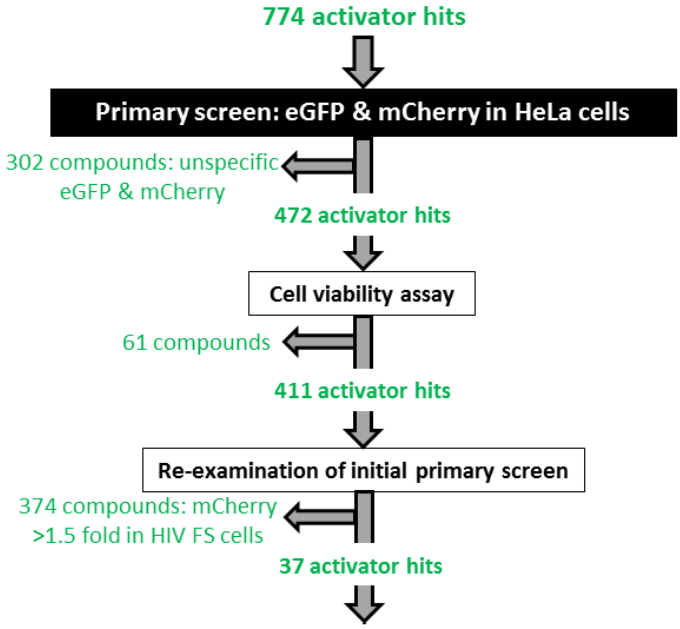

Figure 88 Workflow of hit identification and selection following second primary screen.
The mCherry activator hits (green) identified from the initial primary diversity screen were narrowed down by eliminating auto-fluorescent compounds, compounds with low cell viability those with minimal effect on mCherry expression in the initial primary screen.

6.5 Dose-dependent effect of 37 hit compounds in HIV-1 frameshifting model and HeLa cells

To delineate the activity profile of the 37 hits identified from the second screen for HIV-1 frameshifting activators, I conducted confirmatory screens using dose-response curves (DRCs). To identify compounds that specifically activate mCherry expression by stimulating frameshifting, I examined the dose-dependent effect of 37 hit compounds in clonally-derived HIV-1 frameshifting HeLa cells compared to parental HeLa cells. 34 compounds were eliminated as hits due to the lack of an effect on mCherry expression in the cell culture model of HIV-1 frameshifting.

Of the 37 compounds, DDD00092738, DDD00043315 and DDD00031749 increased mCherry expression in the HIV-1 frameshifting model to varying degrees, while leaving eGFP mainly unaffected. However DDD00092738 and DDD00043315 treatment also led to a dose-dependent increase of mCherry expression in HeLa cells indicating that these compounds possess fluorescent characteristics, particularly in excitation/emission wavelengths of 580nm/610nm, corresponding to mCherry fluorescence (Figure 90A).

On the other hand, DDD00031749 maintained cell viability (Figure 89) while increasing mCherry expression in the HIV-1 frameshifting model at high doses (≥50μM) (Figure 90B). However, increased eGFP expression in DDD00031749-treated HeLa cells (≥50μM) was indicative of potentially unspecific eGFP-fluorescent properties or stimulated cellular translation. Nevertheless, due to maintained mCherry fluorescence in HeLa cells, I was interested to determine whether DDD00031749 was capable of activating HIV-1 frameshifting.

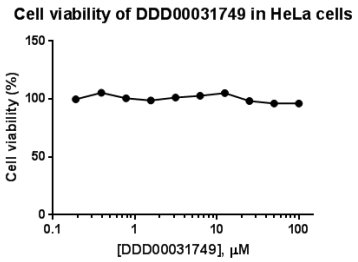

Figure 89 Effect of DDD00031749 on cell viability of HeLa cells
HeLa cells were treated with 10 different doses of DDD00031749. 48 hours post-treatment, cells were treated with resazurin (45µM) for four hours. Cell viability was quantified by measuring the fluorescence (excitation 550nm/emission 590nm) using a PheraStar FS plate reader. Points indicate the percentage of cell viability determined by the RFUs (relative fluorescent units) of compound-treated HeLa cells relative to DMSO-treated HeLa cells.

A)

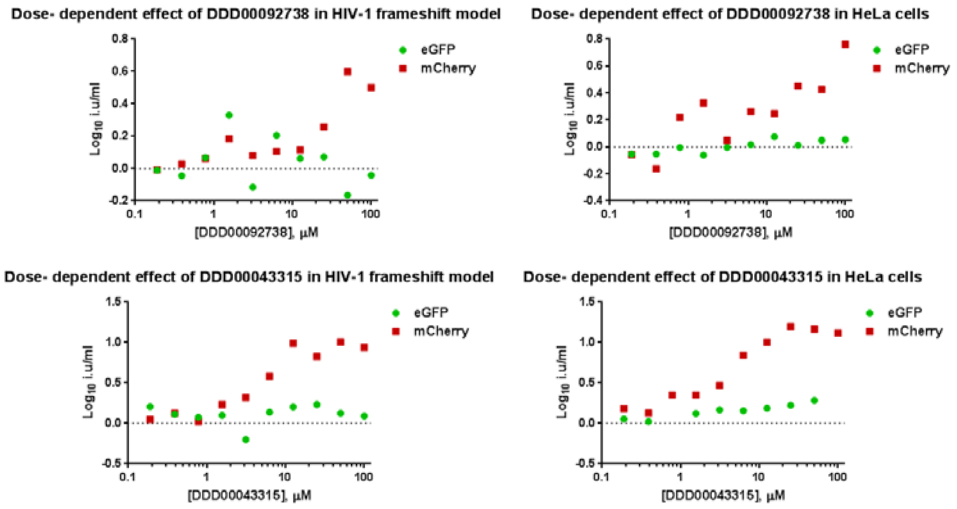

B)

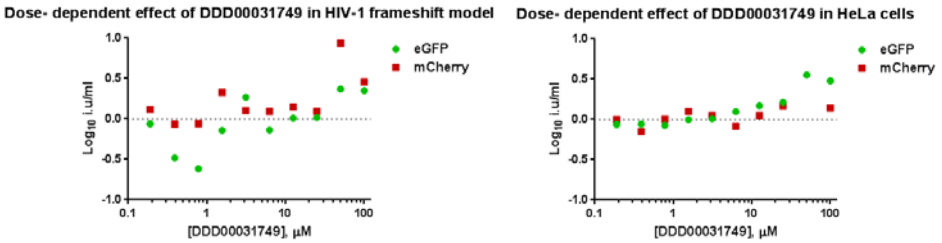

Figure 90 Dose-dependent effect of compounds in HIV-1 frameshifting and HeLa cells

The dose-dependent effect of hit compounds **A)** DDD00092738, DDD00043314 and **B)** DDD00031749 was determined on eGFP (green) and mCherry (red) fluorescence in clonally-derived HIV-1 frameshifting HeLa cells (left) and parental HeLa cells (right). Graphs were generated using GraphPad Prism (n=1).

6.6 Effect of hit compound on frameshifting

To test whether DDD00031749 truly activated HIV-1 frameshifting, I re-purchased a new batch of this compound and examined the production of eGFP-mCherry polyprotein expected upon frameshifting in the cell culture model of HIV-1 frameshifting. This was done by treating clonally-derived HIV-1 frameshifting HeLa cells with 50μM of DDD00031749. 48 hours post-treatment, cell lysates were prepared and western blotting was used to detect the abundance of eGFP-mCherry polyprotein using antibodies targeting eGFP and mCherry. Unfortunately, there were no detectable levels of the eGFP-mCherry polyprotein in HIV-1 frameshifting cells treated with DMSO, ritonavir, or DDD00031749 (Figure 91). As mentioned previously, this was potentially due to low assay sensitivity thereby impeding detection of low protein levels. Nevertheless, since DDD00031749 did not activate frameshifting enough to produce detectable levels of eGFP-Cherry polyprotein, it is most likely not an activator of HIV-1 frameshifting.

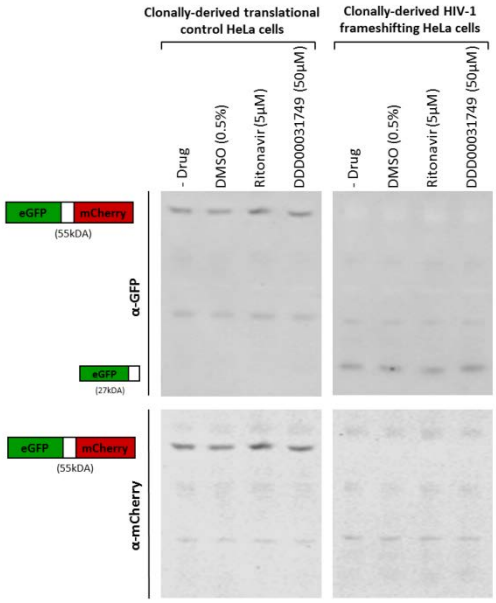

Figure 91 Effect of DDD00031749 on eGFP-mCherry polyprotein production via HIV-1 frameshifting in cell-based assay

Clonally-derived translational control and HIV-1 frameshifting HeLa cells were treated with 0.5% DMSO (v/v), ritonavir (5μM) and DDD00031749 (50μM) for 48 hours. Cell lysates were prepared and used in western blotting with anti-eGFP and anti-mCherry antibodies to determine the abundance of eGFP-mCherry polyprotein (55kDa) relative to eGFP (27kDa) as an indication of frameshifting. Clonally-derived translational control cells were used as a reference for detecting eGFP-mCherry polyprotein.

6.7 Summary

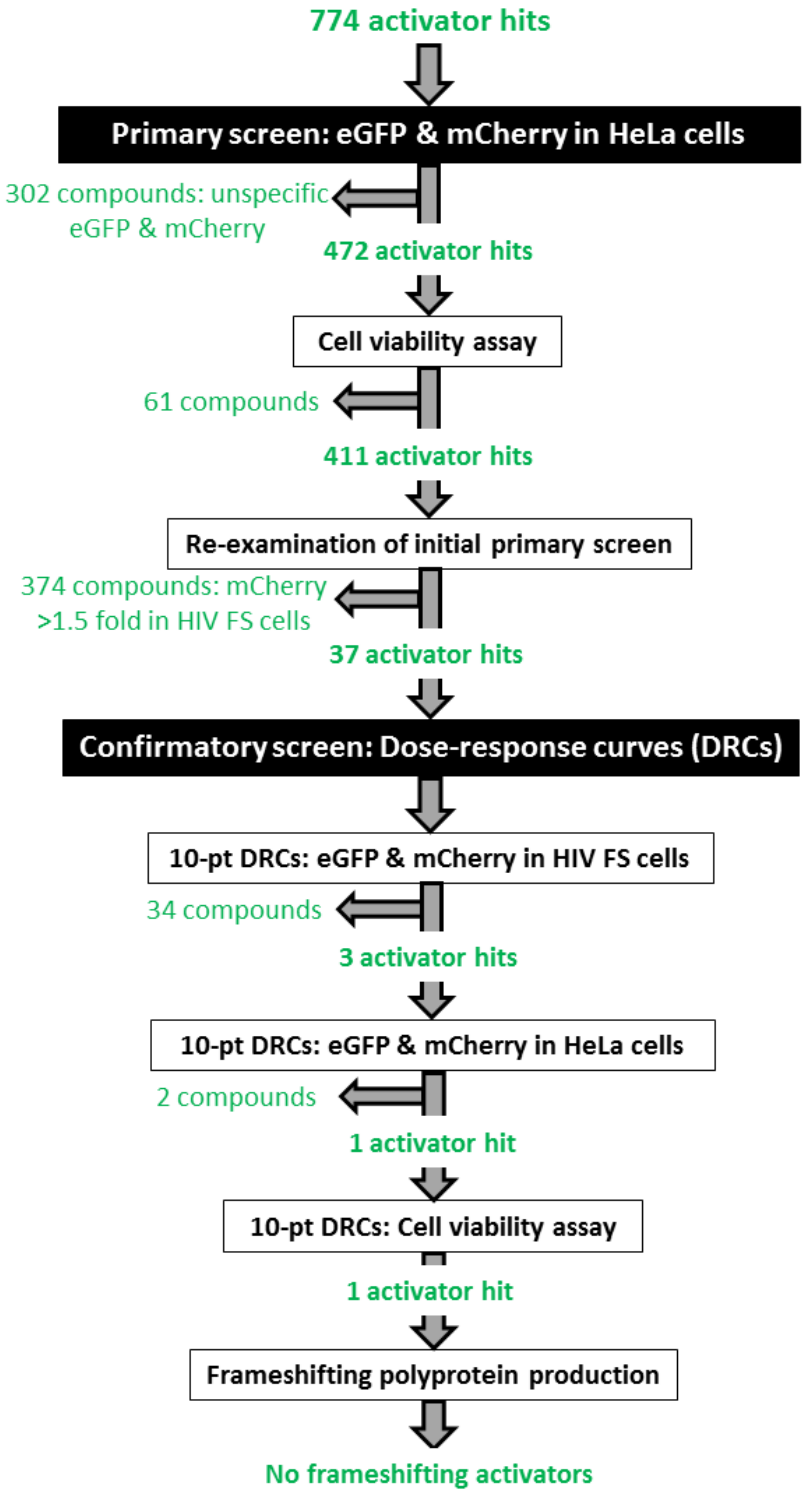

Figure 92 Workflow of hit identification and selection from confirmatory screening of 37 hit compounds identified from second primary screen

In the initial screening cascade, compounds that activated HIV-1 frameshifting were identified based on increased fold change of mCherry expression in clonally-derived HIV-1 frameshifting HeLa cells. To eliminate fluorescent compounds, eGFP and mCherry fluorescence in clonally-derived translational control cells (represent conventional translation) were used as a measure of unspecific effects on fluorescence and cellular translation. However, auto-fluorescent properties (Figure 86) explained why hit compounds did not increase eGFP-mCherry and HIV-1 Gag-Pol polyprotein production expected as a result of stimulated frameshifting.

I therefore used parental HeLa cells to conduct a counter-screen for HIV-1 frameshifting activators with 774 hit compounds that were not tested further in the first screening cascade (Figure 92). This counter-screen was effective at eliminating auto-fluorescent compounds and toxic compounds at an early stage of the screening cascade. In contrast to the previous cut-off of 1.2 fold change, I applied a more stringent statistical cut-off for HIV-1 frameshifting modulators by disregarding compounds with <1.5 mCherry fold change. This eliminated 91% of compounds, revealing that the activity of most hit compounds was close to the baseline and hence, likely false positives. It was also unlikely that these eliminated compounds were capable of inhibiting HIV-1 replication, since previous studies found that greater than 2-fold activation of HIV-1 frameshifting may be required to inhibit HIV-1 replication (Telenti et al., 2002). Dose-response curve analysis of the remaining 37 compounds in both HIV-1 frameshifting cells and HeLa cells, along with examination of frameshifting-induced polyprotein production revealed that none of the compounds in the DDU library were capable of activating HIV-1 frameshifting.

Nevertheless, this chapter revealed that clonally-derived translational control HeLa cells were not an effective control to eliminate false positive hits due to auto-fluorescence. This was potentially due to saturated levels of eGFP and mCherry in translational control cells, thereby making it challenging to detect small increases in fluorescence. While HeLa cells were deemed the

best control to eliminate auto-fluorescent compounds, translational control cells would be best suited to eliminating compounds that quench fluorescence. As a result, future efforts to identify activators of HIV-1 frameshifting should use the counter-screen with parental HeLa cells to eliminate false positive hits early in the screening cascade. According, the modified standard operating procedure (SOP) to identify activators of HIV-1 frameshifting is outlined in Appendix 6.8.2.

6.8 Appendix

6.8.1 Auto-fluorescent properties of compounds that were inactive in re-purchased batch

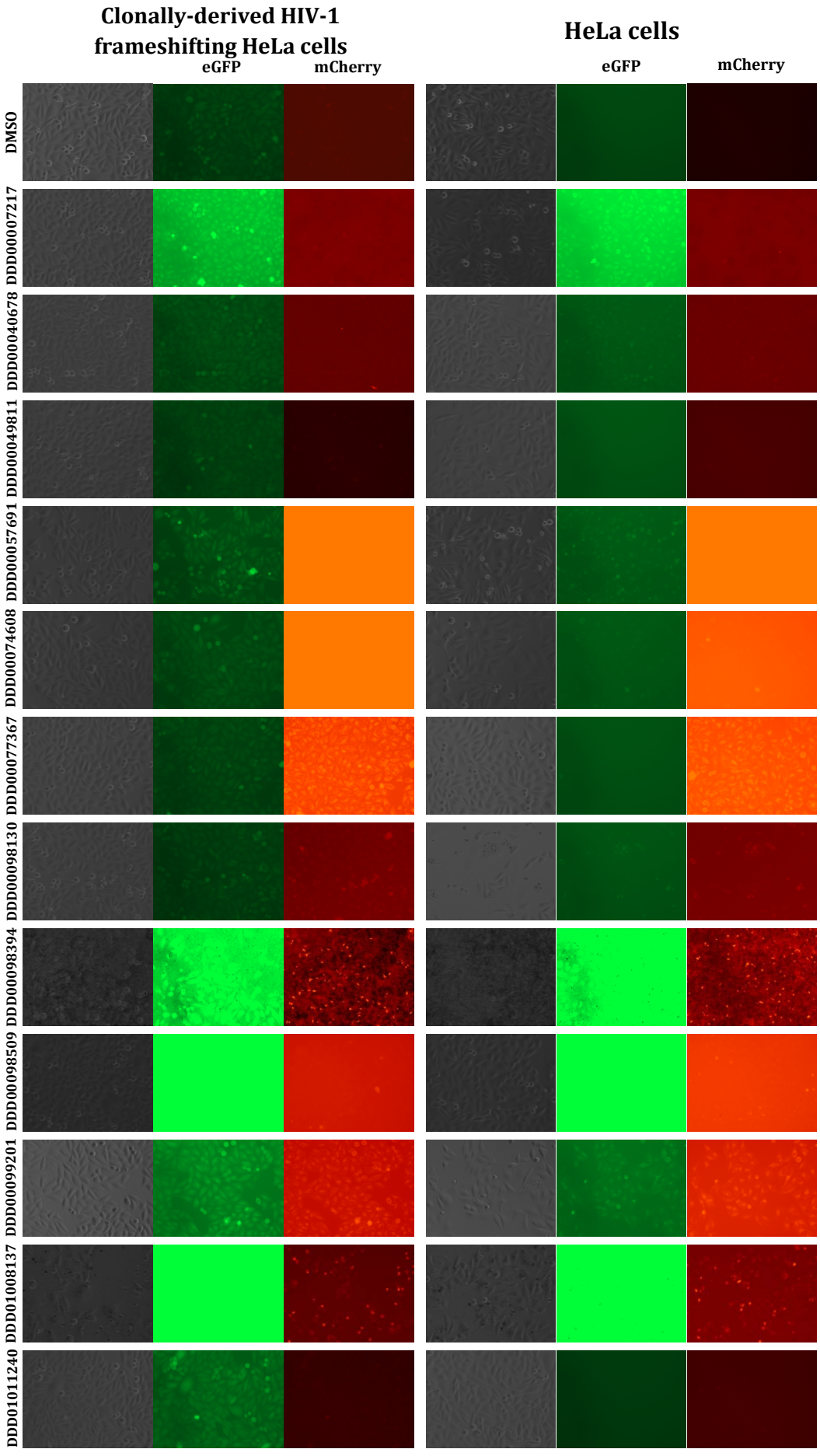
Clonally-derived HIV-1 frameshifting HeLa cells
eGFP
mCherry
HeLa cells
eGFP
mCherry
DMSO
DDD00007217
DDD00040678
DDD00049811
DDD00057691
DDD00074608
DDD00077367
DDD00098130
DDD00098394
DDD00098509
DDD00099201
DDD01008137
DDD01011240

Figure 93 Effect of inactive re-tested compounds on eGFP and mCherry fluorescence in clonally-derived HIV-1 frameshifting HeLa cells and parental HeLa cells

Clonally-derived HIV-1 frameshifting HeLa cells and HeLa cells were treated with 0.5% DMSO (v/v) and 50μM of each compound found inactive in re-purchased batch. 48 hours post-treatment, an EVOS cell imaging system was used to detect eGFP and mCherry fluorescence.

6.8.2 Standard Operating Procedure (SOP) to identify activators of HIV-1 frameshifting

HIV-TFS eGFP and mCherry Assay
Screen to identify HIV-1 frameshifting activators

Table 1: Reagents

Reagent Number	Reagent Name	Reagent Concentration	Reagent Source	Catalogue Number
1	0.05% Trypsin EDTA	0.05%	Life technologies	25300
2	Phosphate Buffered Saline (PBS)	1x	Life technologies	14190
3	DMEM cell culture media		Life technologies	41966
4	Fetal bovine serum (FBS)		Life technologies	10082
5	Cell freezing medium-DMSO 1X		Sigma	C6164
6	Geneticin (G-418)	50mg/ml	Roche	04727878001

Table 2: Equipment and consumables

	Tool Name	Tool Source	Catalogue Number
1	Echo 550	Labcyte	
2	Pherastar FS	BMG Labtech	
3	Matrix Wellmate microplate dispenser Xrd-384	Fluid X	
4	384- well black plate	Greiner	781091
5	Matrix WellMate disposable tubing assembly	ThermoScientific	

Table 3: Preparation of cell culture media

Stock cell culture media	
DMEM	500mls
FBS	50mls

Supplements added to cell culture media immediately prior to use	
Supplement concentration	**Dilution factor and final concentration**
Geneticin (50mg/ml)	Dilute 125x Final concentration 0.4mg/ml

Table 4: Primary screen to identify HIV-1 frameshift activators

Step	*Step Description*
1	48 hours prior to reading mCherry and eGFP expression, compounds are acoustically transferred to 384- well assay plates (in duplicates) by Echo 550 (plate map 1)
2	Clonally-derived HIV-1 frameshift HeLa cells (HIV-TFS) and parental HeLa cells are washed in PBS, trypsinized, counted and re-suspended in cell culture media at $8x10^4$ cells/ml. 50µL of each cell suspension was added to each duplicated 384-well plate using the wellmate resulting in 4000 cells being seeded per well, such that the final concentration of test compound is 30µM. Cells are incubated at 37°C in 5% CO_2 for 48 hours (Table 6).
3	On day of assay, HIV-TFS and HeLa cells incubated with compounds are washed twice with 50µL of PBS using the wellmate and then incubated with 50µL of PBS for assay.
4	Using the Pherastar FS, plates are read at 580nm/610nm for mCherry expression and 485nm/520nm for eGFP expression.
5	Data analysis will select for mCherry-specific increase or decrease in clonally-derived HIV-1 frameshifting HeLa cells

Table 5: Dose-response curves to identify HIV-1 frameshift-specific activators

Step	*Step Description*
1	48 hrs prior to reading mCherry expression, compounds ('activator' hits from primary screen) are acoustically transferred to 384- well assay plates (in duplicates) by Echo 550 for 10- point dose- response curves (DRC) (plate map 2).
2	Clonally-derived HIV-1 frameshift HeLa cells (HIV-TFS) and parental HeLa cells are washed in PBS, trypsinized, counted and re-suspended in cell culture media at $8x10^4$ cells/ml. 50µL of each cell suspension was added to each duplicated 384-well plate using the wellmate resulting in 4000 cells being seeded per well. The final concentration of test compound in the first point of the DRC is 100µM, followed by 1:2 serial dilutions. Cells are incubated at 37°C in 5% CO_2 for 48hours.
3	On day of assay, HIV- TFS cells incubated with compounds are washed twice with 50µL of PBS using the wellmate and then incubated with 50µL of PBS for assay.
4	Using the Pherastar FS, plates are read at 580nm/610nm for mCherry expression and 485nm/520nm for eGFP expression.
5	Data analysis will select for a dose-dependent increase in mCherry expression in clonally-derived translational control HeLa cells

Plate Maps

Plate map 1

	1	2	3	4	5	6	7	8	9	10	11	12	13	14	15	16	17	18	19	20	21	22	23	24
A	Compounds from diversity set at final concentration of 30µM (Single- point)										DMSO	DMSO	Compounds from diversity set at final concentration of 30µM (Single- point)										DMSO	DMSO
B											DMSO	DMSO											DMSO	DMSO
C											DMSO	DMSO											DMSO	DMSO
D											DMSO	DMSO											DMSO	DMSO
E											DMSO	DMSO											DMSO	DMSO
F											DMSO	DMSO											DMSO	DMSO
G											DMSO	DMSO											DMSO	DMSO
H											DMSO	DMSO											DMSO	DMSO
I											DMSO	DMSO											DMSO	DMSO
J											DMSO	DMSO											DMSO	DMSO
K											DMSO	DMSO											DMSO	DMSO
L											DMSO	DMSO											DMSO	DMSO
M											DMSO	DMSO											DMSO	DMSO
N											DMSO	DMSO											DMSO	DMSO
O											DMSO	DMSO											DMSO	DMSO
P											DMSO	DMSO											DMSO	DMSO

Plate map 2

	1	2	3	4	5	6	7	8	9	10	11	12	13	14	15	16	17	18	19	20	21	22	23	24
A	Dose- response curve 1										DMSO	DMSO	Dose- response curve 17										DMSO	DMSO
B	Dose- response curve 2										DMSO	DMSO	Dose- response curve 18										DMSO	DMSO
C	Dose- response curve 3										DMSO	DMSO	Dose- response curve 19										DMSO	DMSO
D	Dose- response curve 4										DMSO	DMSO	Dose- response curve 20										DMSO	DMSO
E	Dose- response curve 5										DMSO	DMSO	Dose- response curve 21										DMSO	DMSO
F	Dose- response curve 6										DMSO	DMSO	Dose- response curve 22										DMSO	DMSO
G	Dose- response curve 7										DMSO	DMSO	Dose- response curve 23										DMSO	DMSO
H	Dose- response curve 8										DMSO	DMSO	Dose- response curve 24										DMSO	DMSO
I	Dose- response curve 9										DMSO	DMSO	Dose- response curve 25										DMSO	DMSO
J	Dose- response curve 10										DMSO	DMSO	Dose- response curve 26										DMSO	DMSO
K	Dose- response curve 11										DMSO	DMSO	Dose- response curve 27										DMSO	DMSO
L	Dose- response curve 12										DMSO	DMSO	Dose- response curve 28										DMSO	DMSO
M	Dose- response curve 13										DMSO	DMSO	Dose- response curve 29										DMSO	DMSO
N	Dose- response curve 14										DMSO	DMSO	Dose- response curve 30										DMSO	DMSO
O	Dose- response curve 15										DMSO	DMSO	Dose- response curve 31										DMSO	DMSO
P	Dose- response curve 16										DMSO	DMSO	Dose- response curve 32										DMSO	DMSO

	1	2	3	4	5	6	7	8	9	10	11	12	13	14	15	16	17	18	19	20	21	22	23	24
A	Curve starting at 100uM (A1); 2- fold dilution steps										DMSO	DMSO	Curve starting at 100uM (A13); 2- fold dilution steps										DMSO	DMSO
B											DMSO	DMSO											DMSO	DMSO
C											DMSO	DMSO											DMSO	DMSO
D											DMSO	DMSO											DMSO	DMSO
E											DMSO	DMSO											DMSO	DMSO
F											DMSO	DMSO											DMSO	DMSO
G											DMSO	DMSO											DMSO	DMSO
H											DMSO	DMSO											DMSO	DMSO
I											DMSO	DMSO											DMSO	DMSO
J											DMSO	DMSO											DMSO	DMSO
K											DMSO	DMSO											DMSO	DMSO
L											DMSO	DMSO											DMSO	DMSO
M											DMSO	DMSO											DMSO	DMSO
N											DMSO	DMSO											DMSO	DMSO
O											DMSO	DMSO											DMSO	DMSO
P											DMSO	DMSO											DMSO	DMSO

Table 6: Summary of screening conditions for primary screen

Component	[Final assay]
HIV –TFS cells	4000cells / 50µl
HeLa cells	4000cells / 50µl
Test Compound	30µM

Table 7: Summary of screening conditions for primary screen

Component	[Final assay]
HIV –TFS cells	4000cells / 50µl
HeLa cells	4000cells / 50µl
Test Compound	100µM (+2- fold dil^{n}) 10-pt DRC

Chapter 7
Discussion and future directions

7.1 Significance of this study

Following the discovery of HIV-1 32 years ago, it still remains a global health issue affecting approximately 35 million people worldwide (World Health Organization, 2014). Despite the development of several drugs over the past 28 years, there is still no available cure. These drugs target various stages of the HIV-1 life cycle, and have to be administered as a combination (known as HAART) to not only suppress viral replication as long-term therapy, but also prevent rapid drug resistance observed with mono-therapy (Thomson et al., 2002). However, the high degree of genetic heterogeneity and rapid rates of HIV-1 replication with an error-prone viral polymerase, still leads to drug resistance with multi-drug therapy (CF et al., 2008; Chen et al., 2007; Núñez & Soriano, 2000; Simon et al., 2006; Temesgen et al., 2006). This raises the need for effective therapeutics with novel targets to avoid cross-resistance in the same class of drugs. One such target that has not yet been successfully exploited is the HIV-1 frameshifting mechanism that is vital for the late stages of HIV-1 replication (Ian Brierley & Dos Ramos, 2006; Dulude et al., 2006; Maia et al., 1996). This thesis outlines the first diversity screen conducted with a bicistronic fluorescent-based assay to discover HIV-1 frameshift-targeted small molecules in mammalian cells.

Previous efforts to identify compounds that targeted HIV-1 frameshifting used enzymatic reporter assays with mono-cistronic luciferase constructs, and more recently, dual luciferase constructs. However, these assays revealed that several compounds have a high affinity for the active site of Firefly luciferase while others have a tendency to inhibit Renilla luciferase (Berry et al., 2011). This posed several issues, particularly the selection of false positive hits. To avoid this, fluorescent-based screens were employed to recapitulate HIV-1 frameshifting in bacteria, yeast (Rakauskait et al., 2011), bacteria (Dulude et al., 2008) and mammalian cells (Cardno et al., 2009). This thesis subsequently used a bicistronic fluorescent-based assay whereby

Cherry and eGFP fluorescence in clonally-derived HIV-1 frameshifting cells was indicative of the effect on HIV-1 frameshifting and cellular translation, respectively. Unlike luciferase genes, fluorophores such as eGFP do not have active binding sites that enhance assay interference. Fluorescent assays do however pose the risk of assay interference through auto-fluorescence and quenching; particularly for heterocyclic compounds that may prove to be problematic due to spectroscopic interference. In the first screening cascade (Chapter 4), I intended to eliminate such false positives using clonally-derived translational control HeLa cells which placed mCherry in frame with eGFP under conventional cellular translation. The translational control cell line used in this study is very similar to controls used in other studies and have primarily been used to eliminate compounds with global translational effects. Unfortunately, this screening strategy identified hit compounds that were later identified as auto-fluorescent false positive hits. It is possible that the saturated levels of mCherry fluorescence as a result of cellular translation in these cells, thus could not detect any further increased fluorescence as a result of auto-fluorescent properties. This also explains the 3.2% hit rate in the primary diversity screen, which was slightly higher than other high-throughput screens which range from 0.1-1%. While the hit rate can be influenced by many factors such as arbitrary thresholds and compound concentration, the high hit rate observed in this study was likely representative of false positive auto-fluorescent hits.

Consequently, I employed an alternate screening strategy (Chapter 6) using parental HeLa cells. While no hits were obtained, data signified the importance of conducting a counter-screen early in the screening cascade to eliminate false positives associated with auto-fluorescence. Concomitant decrease of mCherry and eGFP expression in both clonally-derived HIV-1 frameshifting and translational control cells suggested that inhibitors of HIV-1 frameshifting also inhibited cellular translation. This was consistent with previous findings, and emphasized the difficulty of inhibiting a translational phenomenon such as frameshifting, that is not only vital for HIV-1 but also uses cellular machinery. Conversely, while results obtained in this thesis

indicate that the fluorescent bi-cistronic translational control cell line is effective at identifying translational inhibitors and fluorescent quenchers, it does not detect translational enhancers and auto-fluorescent compounds, most likely due to saturated levels of eGFP and mCherry fluorescence. This emphasizes the need to establish effective controls early in the screening process.

The primary aim of this dissertation was to identify small molecules that effectively targeted the HIV-1 frameshifting mechanism by either increasing or decreasing frameshifting efficiency. This was done using a bicistronic cell-based assay that not only recapitulated HIV-1 frameshifting, but was a simple, robust and cost-effective way of screening for HIV-1 frameshifting modulators. The use of automated liquid handling, few processing steps and a rapid readout made it ideal for high-throughput screening. Moreover, the mode of detection was highly sensitive to small changes in reporter expression indicative of effects on cellular translation and HIV-1 frameshifting. Due to the scarcity of established HIV-1 frameshift-targeted drugs, the library of diverse low complexity small molecules used in this screen contained a variety of core fragments, thereby strengthening the prospect of identifying hit compounds. Furthermore, compounds that occupy a wide chemical space potentially have the capacity to affect a target in many ways, such as through conformational changes, molecular interactions and binding to structural elements. However, while HIV-1 frameshift activators hits were identified based on enhanced mCherry fluorescence, increased polyprotein production expected upon stimulated frameshifting was not investigated till the late stages of the screening process. This was another contributing factor that delayed the identification of false positive hits. This also signified the importance of validating select hit compounds early in the screening process to determine that activity is specific and selective. That is, following the primary screen, a manageable selection of hit compounds identified as frameshifting activators should have been used to determine the abundance of eGFP-mCherry fusion protein to verify frameshifting activity.

These issues should be addressed in future screens for HIV-1 frameshifting modulators or other viral translational elements.

7.2 Off-target effects of compound DDD00049811

While this study did not successfully identify HIV-1 frameshift-targeting compounds, one compound, DDD00049811, was inactive against HIV-1 frameshifting and exhibited potential off-target activity towards HIV-1 replication. HIV-1 transfected cells treated with DDD00049811 reduced infectious virion yield and virion-associated capsid (p24) levels. Furthermore, DDD00049811 reduced the entry of HIV-1 replication-competent virions by approximately 2-fold. While these effects were minimal following a single-cycle of HIV-1 replication, DDD00049811 significantly reduced the spread of HIV-1 infection by 12-fold. This reduction could possibly reflect an amplified defect in infectious particle production and/or an early stage of HIV-1 replication, following multiple rounds of infection. The mechanism through which this occurs is unclear, but could potentially be due to reduced virion-associated HIV-1 Gag-Pol levels, which as described previously, leads to the production of non-infectious viral particles. Alternatively, it is also possible that the binding capability of released virions is compromised in response to DDD00049811. While the unaffected replication of bunyamwera virus implied an HIV-1 specific inhibitory effect by DDD00049811, different experimental conditions and cellular defects could potentially account for the antiviral effects observed. This was evident by the slight decrease in the viability of MT-4 cells following 48 hours post-infection. To confirm whether DDD00049811 was specifically targeting HIV-1 replication, I examined the effect of this drug on the emergence of drug-resistant HIV-1 infection. Due to the highly replicative capacity of HIV-1, current anti-HIV-1 therapeutics developed resistance to drugs when administered alone. Thus, prolonged treatment with DDD00049811 alone should hypothetically lead to drug resistance if specifically targeting HIV-1 replication and not cellular translation or metabolism. Results to date indicated that HIV-1 did not develop resistance to DDD00049811 treatment over 5 cell passages spanning 41 days. However, this is inconclusive since

more cell passages may be required for HIV-1 to develop drug resistance. This is also supported by the lack of AZT-resistant HIV-1 replication observed in this study, which has previously been found resistant following long-term therapy in HIV-1 positive patients.

It is important to note that the antiviral effects of DDD00049811 (Chapter 5) were conducted using 50μM of compound. This is a very high concentration and indicates the extremely low potency of DDD00049811, especially compared to currently available anti-HIV therapeutics. For example, the inhibitory drug concentrations (IC_{50}) of AZT and ritonavir are <0.08μM and 0.006μM, respectively, in MT-4 R5 cells (Krowicka et al., 2008). Due to the high concentration required to elicit an antiviral response, the minimal effect in a single-cycle of HIV-1 replication and the slight cellular viability defect in uninfected MT-4 cells, DDD00049811 is not a good anti-HIV-1 candidate drug. The antiviral effects observed are likely due to cellular toxicity. Currently available ant-HIV-1 drugs have been developed and optimized by modifying molecular chemical groups to improve potency. For example, an initial integrase inhibitor, L-708906, inhibited HIV-1 replication with an EC_{50} value of 0.2μM and was further modified to improve potency (X. Li & Vince, 2006). This approach however, is likely futile with DDD00049811 since the initial potency is already poor and the effect in a single-cycle of HIV-1 replication is negligible.

7.3 Is HIV-1 frameshifting a good drug target?

The tightly regulated synthesis of HIV-1 Gag and Gag-Pol by ribosomal frameshifting makes it an attractive drug target, but a challenging one. A previous study by Hung et al. (1998) screened 56,000 chemical agents and found a hit compound, RG501 (also referred to as DDD01011240 in Chapter 5). RG501 increased HIV-1 frameshifting by 2-fold and reduced multiple cycles of HIV-1 replication. Marcheschi et al. (2011) confirmed that RG501 bound to the HIV-1 frameshift signal, but also to other RNA helices, indicating unspecificity and potential toxicity as an issue. To date, this is the only reported compound that modulated HIV-1 frameshifting and inhibited HIV-1

replication kinetics. I therefore obtained this compound to use as a positive control, but found conflicting results. The discrepancy was due to the concentrations used. In this study, up to 100μM of RG501/DDD01011240 had no effect on HIV-1 frameshifting and HIV-1 replications kinetics. Conversely, Hung et al. (1998) found that 2090μM was required to activate frameshifting and HIV-1 replication kinetics was inhibited following treatment with 1045μM of RG501. While different cell types could attribute to the difference in activity, concentrations used by Hung et al. (1998) were within the toxic range. Several other studies attempting to identify HIV-1 frameshifting modulators (detailed in section 1.6) were unsuccessful as hit compounds had global translational effects.

Currently available anti-HIV-1 drugs target various stages of the viral life cycle including entry, reverse transcription, integration and protease-mediated viral particle maturation. While these stages are regulated by virally-encoded proteins, HIV-1 frameshifting occurs through the translational activity of the cellular ribosome. It is therefore challenging to identify frameshift-specific drugs without adversely affecting cellular translation, a problem that has been manifested in several studies (Brakier-Gingras et al., 2012). The potential involvement of cellular factors and pathways further contribute to the complexity of the HIV-1 frameshift element as a drug target. In the clonally-derived HIV-1 frameshifting model used in this study, there was a constant accumulation of HeLa cells not expressing either eGFP or mCherry, indicative of reduced bicistronic DNA expression (eGFP-HIV FS-mCherry). This could be due to protein degradation, low translational efficiency, reduced RNA stability or the reduced rate of transcription. Alternatively, another possible factor is nonsense-mediated decay (NMD) which is a surveillance mechanism that degrades mRNA transcripts containing premature termination codons (PTC) (Losson & Lacroute, 1979). Clonally- derived HIV-1 frameshifting HeLa cells express mRNA transcripts (eGFP-HIV FS-mCherry) with a PTC following the HIV-1 frameshift region. This primarily produces a ‘truncated’ polyprotein with eGFP fused to the HIV-1 frameshift element. Frameshifting, which occurs in a small proportion (~5%) of these mRNA transcripts, causes the

ribosome to bypass the PTC and produce the full-length eGFP-HIV FS-mCherry polyprotein. While untested, these PTC-containing mRNA transcripts may be subjected to NMD, thereby resulting in reduced overall eGFP expression in clonally-derived HIV-1 frameshifting HeLa cells, compared to clonally-derived translational control HeLa cells which lack PTC-containing mRNA transcripts. It is possible that the cell culture model of HIV-1 frameshifting used in many studies such as this one may simulate other pathways, such as NMD, that could interfere with drug discovery. Furthermore, it has been proposed that other cellular factors, such as eukaryotic release factor (eRF1), are involved in HIV-1 frameshifting and HIV-1 replication (Kobayashi et al., 2010). This not only increases the risk of undesirable side effects, but challenges the one-target, one-drug paradigm used to discover drugs against HIV-1 frameshifting. For these various reasons, frameshifting of HIV-1 Gag and Gag-Pol is a challenging target

7.4 Future directions

The approach used in this study comprised a random screen with 92,071 diverse small molecules. An approach such as this has been successful and widely used when not much information (regarding structure) is known about the target. Since the structure of the HIV-1 frameshift element was resolved (Dulude et al., 2002; Gaudin et al., 2005; Staple & Butcher, 2005), I hypothesize that it would be more effective to employ a focused (also known as rational) approach to identify HIV-1 frameshift modulators.

This rational approach was successful in discovering and developing HIV-1 protease inhibitors following the published 3D crystal structures of HIV-1 protease (Kubinyi, 1998; Navia et al., 1989; Vacca & Condra, 1997; Vondrasek et al., 1997; Weber, 1990). The structure-based drug design (SBDD) of HIV-1 protease inhibitors led to the creation of peptides with structural similarity to protease substrates. Following a search for analogs in a 3D database, and modification of chemical groups, potency of these inhibitors was improved with the purpose of developing a desirable compound (Kubinyi, 1998). A targeted approach was also successful with severe acute respiratory

syndrome coronavirus (SARS-CoV), where an antisense peptide nucleic acid was created to target a specific region of the SARS frameshift element (and not any other human mRNA). This not only led to 94% inhibition of frameshifting efficiency in a dual luciferase system, but subsequently reduced replication of the SARS-CoV replicon by 50% (Ahn et al., 2011). While the use of antisense oligonucleotides as a therapy raised the issue of immune stimulation through toll-like receptors (Agrawal & Kandimalla, 2004), future efforts should use a focused approach to design anti-virals that are non-toxic, but highly specific and selective for HIV-1 frameshifting.

Since the upper stem of the HIV-1 frameshift region is vital for frameshifting (Gaudin et al., 2005; Mazauric et al., 2009; Staple & Butcher, 2005), the ideal compound would be designed to alter the stability of this upper stem and subsequently perturb the ratio of Gag and Gag-Pol polyproteins (Brakier-Gingras et al., 2012). Theoretically, increased stability of the upper stem could prevent ribosomes from translating and therefore reduce frameshifting efficiency. This in turn is expected to abrogate the production of Gag-Pol polyprotein which is vital for the maturation of immature viral particles (detailed in section 1.5.4). Conversely, decreased stability of the HIV-1 frameshift structure could deter ribosomal pausing that takes place during frameshifting, hence theoretically enhancing frameshifting to increase production of Gag-Pol and subsequently decrease Gag production (detailed in section 1.5.4). Since Gag is vital for the production of infectious virions, this is expected to perturb HIV-1 replication. Therefore, molecules capable of binding to the upper stem of the HIV-1 frameshift element and subsequently alter the frameshifting efficiency, serve as good drug candidates.

Due to the necessary function of the cellular ribosome in mediating HIV-1 frameshifting, and the presence of human genes that undergo frameshifting, it is vital that efforts should focus on targeting structures or regions that are unique to the HIV-1 frameshift element. Furthermore, as a control, the expression of human frameshifting genes PEG10, paraneoplastic antigen M3 and APC should be monitored to ensure no adverse and unspecific effects by

candidate drugs. Furthermore, since compounds previously found to modulate frameshifting by binding to the frameshift region also unspecifically bound to other similar structures (Marcheschi et al., 2011), one would need to confirm that a novel frameshift modulator does not have unspecific binding partners, such as the ribosome.

The SBDD approach to identify HIV-1 frameshift-specific compounds would use several established techniques including in situ click chemistry (Whiting et al., 2006) and ligand-protein docking to predict the configuration and energy of the ligand docking with the target protein (Cosconati et al., 2010). A focused approach using computational and chemical approaches would also involve investigating various parameters related to the interaction between compound and target. This includes the flexibility of the HIV-1 frameshift region and potential compound, the role of various side chains, the binding energy, electrostatic and hydrophobic interactions as well as charged and hydrogen bonding between functional groups (Bohm & Klebe, 1996; Kubinyi, 1998). Furthermore, it is vital to understand the structure-activity relationship of lead molecules. This facilitates lead expansion and the synthesis of analogues with the aim of not only improving potency, but also improving pharmacological parameters such as absorption, distribution, metabolism and excretion (ADME). A highly potent compound would administer the desired affect at a low concentration with no off-target effects and hence no side effects. Some potential off-targets that should be monitored include cytochrome P450 enzyme family members as they are involved in drug metabolism, and may therefore alter the levels of other simultaneously administered drugs. Furthermore, absorption and distribution of the lead compound from the site of administration to the rest of the body should also be optimal. This can be quantified by determining the solubility, distribution coefficient and partition coefficient (described in section 1.7.4). The examination of drug metabolites following excretion is also important to ensure no adverse effects from potentially volatile metabolites. Furthermore, it would be vital to fully elucidate the lead compound's mechanism of action and confirm no adverse cellular effects,

including the frameshifting of human genes, PEG10 and Ma3, as mentioned previously. To examine the breadth of antiviral activity, the lead candidate should be tested in various HIV-1 positive laboratory strains and patient isolates. Of particular importance is determining the effect of lead compounds on replication of drug resistant HIV-1 strains, in addition to the effect of a lead compound in combination with other established HIV-1 inhibitors. The effect of this lead compound should be significant in a single-cycle of HIV-1 replication in primary T- cells. With the increased knowledge underlying the mechanism of HIV-1 replication, it is important to investigate unexplored stages as drug targets. The desirable compound would alter the ratio of Gag and Gag-Pol polyproteins to inhibit HIV-1 replication at very low concentrations, while leaving cellular processes unaffected.

While new anti-HIV-1 drugs are required, other aspects of treatment can also be improved. This includes the access of drugs to third world countries and promoting adherence to drug regimens. While 35 million people are affected by AIDS worldwide, only 12.9 million have access to treatment in the form of drugs (World Health Organization, 2014). Adherence is a vital part of the drug regimen since studies have found that less than 95% adherence can lower rate of success by 20% (Knobel et al., 1999; Paterson et al., 2000). Moreover, a patient with a past of non-adherent drug treatment has a significantly higher chance of regimen failure regardless of the new drug combination (Struble et al., 2005). Adherence has been problematic due to the complexity of the treatment regimens. In the early 1990s, 2-4 doses of drug combinations with a boost of protease inhibitors were required daily (For example, Epzicom and Truvada in 2004). However, improvements were made by creating a single pill at a fixed highly potent dose in 2006 (ex. Atripla) (Flexner, 2007). Therefore, efforts should also be focused on ensuring adherence to prevent the emergence of resistance to novel drugs. There is a continued need to identify novel drugs that suppress HIV-1 replication and reconstitute the immune system, prevent AIDS-related diseases, reduce morbidity and mortality and prevent HIV transmission until a cure is discovered.

References

Agostini, I., Popov, S., Hao, T., Li, J. H., Dubrovsky, L., Chaika, O., … Bukrinsky, M. (2002). Phosphorylation of Vpr regulates HIV type 1 nuclear import and macrophage infection. *AIDS Research and Human Retroviruses*, *18*, 283–288.

Agrawal, S., & Kandimalla, E. R. (2004). Antisense and siRNA as agonists of Toll-like receptors. *Nature Biotechnology*. doi:10.1038/nbt1042

Ahn, D. G., Lee, W., Choi, J. K., Kim, S. J., Plant, E. P., Almazán, F., … Oh, J. W. (2011). Interference of ribosomal frameshifting by antisense peptide nucleic acids suppresses SARS coronavirus replication. *Antiviral Research*, *91*, 1–10.

Alkhatib, G., & Berger, E. A. (2007). HIV coreceptors: from discovery and designation to new paradigms and promise. *European Journal of Medical Research*, *12*, 375–384.

Alkhatib, G., Combadiere, C., Broder, C. C., Feng, Y., Kennedy, P. E., Murphy, P. M., & Berger, E. A. (1996). CC CKR5: a RANTES, MIP-1alpha, MIP-1beta receptor as a fusion cofactor for macrophage-tropic HIV-1. *Science (New York, N.Y.)*, *272*(5270), 1955–8.

Allan, J. S., Coligan, J. E., Barin, F., McLane, M. F., Sodroski, J. G., Rosen, C. A., … Essex, M. (1985). Major glycoprotein antigens that induce antibodies in AIDS patients are encoded by HTLV-III. *Science (New York, N.Y.)*, *228*, 1091–1094.

Arenas-Pinto, A., Grant, A., Edwards, S., & Weller, I. (2003). Lactic acidosis in HIV infected patients: a systematic review of published cases. *Sexually Transmitted Infections*, *79*, 340–343.

Arion, D., Kaushik, N., McCormick, S., Borkow, G., & Parniak, M. A. (1998). Phenotypic mechanism of HIV-1 resistance to 3’-azido-3'-deoxythymidine (AZT): Increased polymerization processivity and enhanced sensitivity to pyrophosphate of the mutant viral reverse transcriptase. *Biochemistry*, *37*, 15908–15917.

Arnaudo, E., Dalakas, M., Shanske, S., Moraes, C. T., DiMauro, S., & Schon, E. A. (1991). *Depletion of muscle mitochondrial DNA in AIDS patients with zidovudine-induced myopathy. Lancet* (Vol. 337, pp. 508–510).

Arts, E. J., & Hazuda, D. J. (2012). HIV-1 antiretroviral drug therapy. *Cold Spring Harbor Perspectives in Medicine*, *2*. doi:10.1101/cshperspect.a007161

Ashton, M. J., Jaye, M. C., & Mason, J. S. (1996). New perspectives in lead generation II: Evaluating molecular diversity. *Drug Discovery Today*. doi:10.1016/1359-6446(96)89091-X

Baranov, P. V, Wills, N. M., Barriscale, K. A., Firth, A. E., Jud, M. C., Letsou, A., … Atkins, J. F. (n.d.). Programmed ribosomal frameshifting in the expression of the regulator of intestinal stem cell proliferation, adenomatous polyposis coli (APC). *RNA Biology*, *8*(4), 637–47.

Baril, M., Dulude, D., Steinberg, S. V, & Brakier-Gingras, L. (2003). The frameshift stimulatory signal of human immunodeficiency virus type 1 group O is a pseudoknot. *J Mol Biol*, *331*, 571–583.

Barre-Sinoussi, F., Chermann, J. C., Rey, F., Nugeyre, M. T., Chamaret, S., Gruest, J., … Montagnier, L. (1983). Isolation of a T-lymphotropic retrovirus from a patient at risk for acquired immune deficiency syndrome (AIDS). *Science*, *220*, 868–871.

Baumgärtel, V., Ivanchenko, S., Dupont, A., Sergeev, M., Wiseman, P. W., Kräusslich, H.-G., … Lamb, D. C. (2011). Live-cell visualization of dynamics of HIV budding site interactions with an ESCRT component. *Nature Cell Biology*, *13*, 469–474.

Belew, A. T., Advani, V. M., & Dinman, J. D. (2011). Endogenous ribosomal frameshift signals operate as mRNA destabilizing elements through at least two molecular pathways in yeast. *Nucleic Acids Research*, *39*, 2799–2808.

Berry, K. E., Peng, B., Koditek, D., Beeman, D., Pagratis, N., Perry, J. K., … Shih, I. (2011). Optimized high-throughput screen for hepatitis C virus translation inhibitors. *Journal of Biomolecular Screening : The Official Journal of the Society for Biomolecular Screening*, *16*, 211–220.

Bieniasz, P. D., Grdina, T. A., Bogerd, H. P., & Cullen, B. R. (1998). Recruitment of a protein complex containing Tat and cyclin T1 to TAR governs the species specificity of HIV-1 Tat. *The EMBO Journal*, *17*, 7056–7065.

Biswas, P., Jiang, X., Pacchia, A. L., Dougherty, J. P., & Peltz, S. W. (2004). The human immunodeficiency virus type 1 ribosomal frameshifting site is an invariant sequence determinant and an important target for antiviral therapy. *Journal of Virology*, *78*, 2082–2087.

Blanco, J.-L., Varghese, V., Rhee, S.-Y., Gatell, J. M., & Shafer, R. W. (2011). HIV-1 integrase inhibitor resistance and its clinical implications. *The Journal of Infectious Diseases*, *203*, 1204–1214.

Bohm, H. J., & Klebe, G. (1996). What can we learn from molecular recognition in protein-ligand complexes for the design of new drugs? *ANGEWANDTE CHEMIE-INTERNATIONAL EDITION IN ENGLISH*, *35*, 2589–2614.

Bor, J., Herbst, A. J., Newell, M.-L., & Bärnighausen, T. (2013). Increases in adult life expectancy in rural South Africa: valuing the scale-up of HIV treatment. *Science (New York, N.Y.)*, *339*, 961–5.

Boubaker, K., Flepp, M., Sudre, P., Furrer, H., Haensel, A., Hirschel, B., … Telenti, A. (2001). Hyperlactatemia and antiretroviral therapy: the Swiss HIV Cohort Study. *Clinical Infectious Diseases : An Official Publication of the Infectious Diseases Society of America*, *33*, 1931–1937.

Bouloy, M., Krams-Ozden, S., Horodniceanu, F., & Hannoun, C. (1973). Three-segment RNA genome of Lumbo virus (Bunyavirus). *Intervirology*, *2*(3), 173–80.

Bouyac-Bertoia, M., Dvorin, J. D., Fouchier, R. A. M., Jenkins, Y., Meyer, B. E., Wu, L. I., … Malim, M. H. (2001). HIV-1 Infection Requires a Functional Integrase NLS. *Molecular Cell*, *7*, 1025–1035.

Bozzette, S. A., Ake, C. F., Tam, H. K., Chang, S. W., & Louis, T. A. (2003). Cardiovascular and cerebrovascular events in patients treated for human immunodeficiency virus infection. *The New England Journal of Medicine*, *348*, 702–710.

Brakier-Gingras, L., Charbonneau, J., & Butcher, S. E. (2012). Targeting frameshifting in the human immunodeficiency virus. *Expert Opinion on Therapeutic Targets*.

Brenk, R., Schipani, A., James, D., Krasowski, A., Gilbert, I. H., Frearson, J., & Wyatt, P. G. (2008). Lessons learnt from assembling screening libraries for drug discovery for neglected diseases. *ChemMedChem*, *3*, 435–444.

Brierley, I. (1995). Ribosomal frameshifting on viral RNAs. *Journal of General Virology*. doi:10.1099/0022-1317-76-8-1885

Brierley, I., Digard, P., & Inglis, S. C. (1989). Characterization of an efficient coronavirus ribosomal frameshifting signal: requirement for an RNA pseudoknot. *Cell*, *57*, 537–547.

Brierley, I., & Dos Ramos, F. J. (2006). Programmed ribosomal frameshifting in HIV-1 and the SARS-CoV. *Virus Research*, *119*, 29–42.

Brierley, I., Jenner, A. J., & Inglis, S. C. (1992). Mutational analysis of the "slippery-sequence" component of a coronavirus ribosomal frameshifting signal. *Journal of Molecular Biology*, *227*, 463–479.

Brierley, I., Meredith, M. R., Bloys, A. J., & Hagervall, T. G. (1997). Expression of a coronavirus ribosomal frameshift signal in Escherichia coli: influence of tRNA anticodon modification on frameshifting. *Journal of Molecular Biology*, *270*, 360–373.

Brierley, I., & Pennell, S. (2001). Structure and function of the stimulatory RNAs involved in programmed eukaryotic-1 ribosomal frameshifting. *Cold Spring Harbor Symposia on Quantitative Biology*, *66*, 233–48.

Briggs, J. A. G., Grünewald, K., Glass, B., Förster, F., Kräusslich, H.-G., & Fuller, S. D. (2006). The mechanism of HIV-1 core assembly: insights from three-dimensional reconstructions of authentic virions. *Structure (London, England : 1993)*, *14*(1), 15–20.

Briggs, J. A. G., & Kräusslich, H. G. (2011). The molecular architecture of HIV. *Journal of Molecular Biology*. doi:10.1016/j.jmb.2011.04.021

Briggs, J. A. G., Riches, J. D., Glass, B., Bartonova, V., Zanetti, G., & Kräusslich, H.-G. (2009). Structure and assembly of immature HIV. *Proceedings of the National Academy of Sciences of the United States of America*, *106*, 11090–11095.

Bukrinsky, M. I., Sharova, N., McDonald, T. L., Pushkarskaya, T., Tarpley, W. G., & Stevenson, M. (1993). Association of integrase, matrix, and reverse transcriptase antigens of human immunodeficiency virus type 1 with viral nucleic acids following acute infection. *Proceedings of the National Academy of Sciences of the United States of America*, *90*, 6125–6129.

Bushman, F. D., Fujiwara, T., & Craigie, R. (1990). Retroviral DNA integration directed by HIV integration protein in vitro. *Science (New York, N.Y.)*, *249*, 1555–1558.

Cadigan, K. M., & Nusse, R. (1997). Wnt signaling: A common theme in animal development. *Genes and Development*. doi:10.1101/gad.11.24.3286

Cardno, T. S., Poole, E. S., Mathew, S. F., Graves, R., & Tate, W. P. (2009). A homogeneous cell-based bicistronic fluorescence assay for high-throughput identification of drugs that perturb viral gene recoding and read-through of nonsense stop codons. *RNA (New York, N.Y.)*, *15*, 1614–1621.

Carlson, T. L., Green, K. A., & Green, W. R. (2010). Alternative translational reading frames as a novel source of epitopes for an expanded CD8 T-cell repertoire: use of a retroviral system to assess the translational requirements for CTL recognition and lysis. *Viral Immunology*, *23*(6), 577–83.

Caron, M., Auclair, M., Vigouroux, C., Glorian, M., Forest, C., & Capeau, J. (2001). The HIV protease inhibitor indinavir impairs sterol regulatory element-binding protein-1 intranuclear localization, inhibits preadipocyte differentiation, and induces insulin resistance. *Diabetes*, *50*, 1378–1388.

Carr, A., Samaras, K., Burton, S., Law, M., Freund, J., Chisholm, D. J., & Cooper, D. A. (1998). A syndrome of peripheral lipodystrophy, hyperlipidaemia and insulin resistance in patients receiving HIV protease inhibitors. *AIDS (London, England)*, *12*, F51–F58.

CF, P., Moyle, G., Tsoukas, C., Ratanasuwan, W., Gatell, J., & Schechter, M. (2008). Overcoming resistance to existing therapies in HIV-infected patients: the role of new antiretroviral drugs. *Journal of Medical Virology*, *80*, 565–576.

Chandler, M., & Fayet, O. (1993). Translational frameshifting in the control of transposition in bacteria. *Molecular Microbiology*. doi:10.1111/j.1365-2958.1993.tb01140.x

Charbonneau, J., Gendron, K., Ferbeyre, G., & Brakier-Gingras, L. (2012). The 5' UTR of HIV-1 full-length mRNA and the Tat viral protein modulate the programmed -1 ribosomal frameshift that generates HIV-1 enzymes. *RNA*.

Checkley, M. A., Luttge, B. G., & Freed, E. O. (2011). HIV-1 envelope glycoprotein biosynthesis, trafficking, and incorporation. *Journal of Molecular Biology*. doi:10.1016/j.jmb.2011.04.042

Chen, L. F., Hoy, J., & Lewin, S. R. (2007). Ten years of highly active antiretroviral therapy for HIV infection. *The Medical Journal of Australia*, *186*, 146–151.

Chiu, T. K., & Davies, D. R. (2004). Structure and function of HIV-1 integrase. *Current Topics in Medicinal Chemistry*, *4*, 965–977.

Chunsong, H., Yuling, H., Li, W., Jie, X., Gang, Z., Qiuping, Z., … Jinquan, T. (2006). CXC chemokine ligand 13 and CC chemokine ligand 19 cooperatively render resistance to apoptosis in B cell lineage acute and chronic lymphocytic leukemia CD23+CD5+ B cells. *Journal of Immunology (Baltimore, Md. : 1950)*, *177*, 6713–6722.

Clark, M. B., Jänicke, M., Gottesbühren, U., Kleffmann, T., Legge, M., Poole, E. S., & Tate, W. P. (2007). Mammalian gene PEG10 expresses two reading frames by high efficiency - 1 Frameshifting in embryonic-associated tissues. *Journal of Biological Chemistry*, *282*, 37359–37369.

Clavel, F., Race, E., & Mammano, F. (2000). HIV drug resistance and viral fitness. *Advances in Pharmacology (San Diego, Calif.)*, *49*, 41–66.

Coakley, E., Petropoulos, C. J., & Whitcomb, J. M. (2005). Assessing chemokine co-receptor usage in HIV. *Current Opinion in Infectious Diseases*, *18*, 9–15.

Cochrane, A. W., Chen, C. H., & Rosen, C. A. (1990). Specific interaction of the human immunodeficiency virus Rev protein with a structured region in

the env mRNA. *Proceedings of the National Academy of Sciences of the United States of America*, *87*(3), 1198–202.

Coffin, J. M. (1995). HIV population dynamics in vivo: implications for genetic variation, pathogenesis, and therapy. *Science (New York, N.Y.)*, *267*, 483–489.

Coghlan, M. E., Sommadossi, J. P., Jhala, N. C., Many, W. J., Saag, M. S., & Johnson, V. A. Symptomatic lactic acidosis in hospitalized antiretroviral-treated patients with human immunodeficiency virus infection: a report of 12 cases., 33 Clinical infectious diseases : an official publication of the Infectious Diseases Society of America 1914–1921 (2001).

Cohen, J. (2002). Therapies. Confronting the limits of success. *Science (New York, N.Y.)*, *296*(5577), 2320–4.

Concentrations, P. I., & Kim, R. B. (2003). Drug transporters in HIV Therapy. *Top HIV Med*, *11*, 136–139.

Connor, E. M., Sperling, R. S., Gelber, R., Kiselev, P., Scott, G., O'Sullivan, M. J., … Balsley, J. (1995). Reduction of Maternal-Infant Transmission of Human Immunodeficiency Virus 1 with Zidovudine Treatment. *Obstetrical & Gynecological Survey*.

Cosconati, S., Forli, S., Perryman, A. L., Harris, R., Goodsell, D. S., & Olson, A. J. (2010). Virtual screening with AutoDock: theory and practice. *Expert Opinion on Drug Discovery*.

Cullen, B. R. (2003). Nuclear mRNA export: Insights from virology. *Trends in Biochemical Sciences*. doi:10.1016/S0968-0004(03)00142-7

Daelemans, D., Pauwels, R., De Clercq, E., & Pannecouque, C. (2011). A time-of-drug addition approach to target identification of antiviral compounds. *Nature Protocols*, *6*, 925–933.

Daniel, R., Greger, J. G., Katz, R. A., Taganov, K. D., Wu, X., Kappes, J. C., & Skalka, A. M. (2004). Evidence that stable retroviral transduction and cell survival following DNA integration depend on components of the nonhomologous end joining repair pathway. *Journal of Virology*, *78*, 8573–8581.

Datta, S. A. K., Temeselew, L. G., Crist, R. M., Soheilian, F., Kamata, A., Mirro, J., … Rein, A. (2011). On the role of the SP1 domain in HIV-1 particle assembly: a molecular switch? *Journal of Virology*, *85*(9), 4111–21.

Dayton, A. I., Sodroski, J. G., Rosen, C. A., Goh, W. C., & Haseltine, W. A. (1986). The trans-activator gene of the human T cell lymphotropic virus type III is required for replication. *Cell*, *44*(6), 941–7.

Demaison, C., Parsley, K., Brouns, G., Scherr, M., Battmer, K., Kinnon, C., … Thrasher, A. J. (2002). High-level transduction and gene expression in hematopoietic repopulating cells using a human immunodeficiency [correction of imunodeficiency] virus type 1-based lentiviral vector containing an internal spleen focus forming virus promoter. *Human Gene Therapy*, *13*(7), 803–13.

Demirov, D. G., Ono, A., Orenstein, J. M., & Freed, E. O. (2002). Overexpression of the N-terminal domain of TSG101 inhibits HIV-1 budding by blocking late domain function. *Proceedings of the National Academy of Sciences of the United States of America*, *99*, 955–960.

Di Marzio, P., Choe, S., Ebright, M., Knoblauch, R., & Landau, N. R. (1995). Mutational analysis of cell cycle arrest, nuclear localization and virion packaging of human immunodeficiency virus type 1 Vpr. *Journal of Virology*, *69*, 7909–7916.

Dillon, P. J., Nelbock, P., Perkins, A., & Rosen, C. A. (1990). Function of the human immunodeficiency virus types 1 and 2 Rev proteins is dependent on their ability to interact with a structured region present in env gene mRNA. *Journal of Virology*, *64*, 4428–4437.

Dinman, J. D., Icho, T., & Wickner, R. B. (1991). A -1 ribosomal frameshift in a double-stranded RNA virus of yeast forms a gag-pol fusion protein. *Proceedings of the National Academy of Sciences of the United States of America*, *88*(1), 174–8.

Dinman, J. D., Ruiz-Echevarria, M. J., Czaplinski, K., & Peltz, S. W. (1997). Peptidyl-transferase inhibitors have antiviral properties by altering programmed -1 ribosomal frameshifting efficiencies: development of model systems. *Proceedings of the National Academy of Sciences of the United States of America*, *94*(13), 6606–11.

Dinman, J. D., & Wickner, R. B. (1992). Ribosomal frameshifting efficiency and gag/gag-pol ratio are critical for yeast M1 double-stranded RNA virus propagation. *Journal of Virology*, *66*, 3669–3676.

Doms, R. W., & Trono, D. (2000). The plasma membrane as a combat zone in the HIV battlefield. *Genes & Development*, *14*(21), 2677–88.

Doyon, L., Payant, C., Brakier-Gingras, L., & Lamarre, D. (1998). Novel Gag-Pol frameshift site in human immunodeficiency virus type 1 variants resistant to protease inhibitors. *Journal of Virology*, *72*, 6146–6150.

Dreher, T. W., & Miller, W. A. (2006). Translational control in positive strand RNA plant viruses. *Virology*. doi:10.1016/j.virol.2005.09.031

Dressman, J., Kincer, J., Matveev, S. V., Guo, L., Greenberg, R. N., Guerin, T., … Smart, E. J. (2003). HIV protease inhibitors promote atherosclerotic

lesion formation independent of dyslipidemia by increasing CD36-dependent cholesteryl ester accumulation in macrophages. *Journal of Clinical Investigation*, *111*, 389–397.

Dulude, D., Baril, M., & Brakier-Gingras, L. (2002). Characterization of the frameshift stimulatory signal controlling a programmed -1 ribosomal frameshift in the human immunodeficiency virus type 1. *Nucleic Acids Research*, *30*(23), 5094–102.

Dulude, D., Berchiche, Y. A., Gendron, K., Brakier-Gingras, L., & Heveker, N. (2006). Decreasing the frameshift efficiency translates into an equivalent reduction of the replication of the human immunodeficiency virus type 1. *Virology*, *345*, 127–136.

Dulude, D., Théberge-Julien, G., Brakier-Gingras, L., & Heveker, N. (2008). Selection of peptides interfering with a ribosomal frameshift in the human immunodeficiency virus type 1. *RNA (New York, N.Y.)*, *14*, 981–991.

Ehrlich, L. S., & Carter, C. a. (2012). HIV Assembly and Budding: Ca(2+) Signaling and Non-ESCRT Proteins Set the Stage. *Molecular Biology International*, *2012*, 851670.

Elia, N., Sougrat, R., Spurlin, T. A., Hurley, J. H., & Lippincott-Schwartz, J. (2011). Dynamics of endosomal sorting complex required for transport (ESCRT) machinery during cytokinesis and its role in abscission. *Proceedings of the National Academy of Sciences of the United States of America*, *108*, 4846–4851.

Elliott, R. M. (1997). Emerging viruses: the Bunyaviridae. *Molecular Medicine (Cambridge, Mass.)*, *3*(9), 572–7.

Entzeroth, M., Flotow, H., & Condron, P. (2009). Overview of high-throughput screening. *Current Protocols in Pharmacology*. doi:10.1002/0471141755.ph0904s44

Ertl, P., Rohde, B., & Selzer, P. (2000). Fast calculation of molecular polar surface area as a sum of fragment-based contributions and its application to the prediction of drug transport properties. *Journal of Medicinal Chemistry*, *43*, 3714–3717.

Fanales-Belasio, E., Raimondo, M., SuligoI., B., & Buttò, S. (2010). HIV virology and pathogenetic mechanisms of infection: A brief overview. *Annali dell'Istituto Superiore Di Sanita*, *46*(1), 5–14.

Farabaugh, P. J. (1996). Programmed translational frameshifting. *Annual Review of Genetics*, *30*, 507–528.

Farabaugh, P. J. (2000). Translational frameshifting: implications for the mechanism of translational frame maintenance. *Progress in Nucleic Acid Research and Molecular Biology*, *64*, 131–170.

Fassati, A. (2006). HIV infection of non-dividing cells: a divisive problem. *Retrovirology*, *3*, 74.

Fätkenheuer, G., Nelson, M., Lazzarin, A., Konourina, I., Hoepelman, A. I. M., Lampiris, H., … van der Ryst, E. (2008). Subgroup analyses of maraviroc in previously treated R5 HIV-1 infection. *The New England Journal of Medicine*, *359*, 1442–1455.

Fellay, J., Marzolini, C., Meaden, E. R., Back, D. J., Buclin, T., Chave, J. P., … Telenti, A. (2002). Response to antiretroviral treatment in HIV-1-infected individuals with allelic variants of the multidrug resistance transporter 1: A pharmacogenetics study. *Lancet*, *359*, 30–36.

Feng, J. Y., Johnson, A. A., Johnson, K. A., & Anderson, K. S. (2001). Insights into the Molecular Mechanism of Mitochondrial Toxicity by AIDS Drugs. *Journal of Biological Chemistry*, *276*, 23832–23837.

Flexner, C. (2007). HIV drug development: the next 25 years. *Nature Reviews. Drug Discovery*, *6*, 959–966.

Frank, J., & Gonzalez, R. L. (2010). Structure and dynamics of a processive Brownian motor: the translating ribosome. *Annual Review of Biochemistry*, *79*, 381–412.

Freed, E. O., & Martin, M. A. (1995). Virion incorporation of envelope glycoproteins with long but not short cytoplasmic tails is blocked by specific, single amino acid substitutions in the human immunodeficiency virus type 1 matrix. *Journal of Virology*, *69*, 1984–1989.

Friis-Møller, N., Reiss, P., Sabin, C. A., Weber, R., Monforte, A. d'Arminio, El-Sadr, W., … Lundgren, J. D. (2007). Class of antiretroviral drugs and the risk of myocardial infarction. *The New England Journal of Medicine*, *356*, 1723–1735.

Fu, J., Munro, J. B., Blanchard, S. C., & Frank, J. (2011). Cryoelectron microscopy structures of the ribosome complex in intermediate states during tRNA translocation. *Proceedings of the National Academy of Sciences of the United States of America*, *108*, 4817–4821.

Fujii, K., Munshi, U. M., Ablan, S. D., Demirov, D. G., Soheilian, F., Nagashima, K., … Freed, E. O. (2009). Functional role of Alix in HIV-1 replication. *Virology*, *391*, 284–292.

Fujinaga, K., Cujec, T. P., Peng, J., Garriga, J., Price, D. H., Graña, X., & Peterlin, B. M. (1998). The ability of positive transcription elongation factor B to

transactivate human immunodeficiency virus transcription depends on a functional kinase domain, cyclin T1, and Tat. *Journal of Virology*, *72*, 7154–7159.

Fujiwara, T., & Mizuuchi, K. (1988). Retroviral DNA integration: structure of an integration intermediate. *Cell*, *54*, 497–504.

Fuller, S. D., Wilk, T., Gowen, B. E., Kräusslich, H. G., & Vogt, V. M. (1997). Cryo-electron microscopy reveals ordered domains in the immature HIV-1 particle. *Current Biology : CB*, *7*, 729–738.

Gallay, P., Hope, T., Chin, D., & Trono, D. (1997). HIV-1 infection of nondividing cells through the recognition of integrase by the importin/karyopherin pathway. *Proceedings of the National Academy of Sciences of the United States of America*, *94*(18), 9825–30.

Gallay, P., Swingler, S., Song, J., Bushman, F., & Trono, D. (1995). HIV nuclear import is governed by the phosphotyrosine-mediated binding of matrix to the core domain of integrase. *Cell*, *83*(4), 569–76.

Gallo, R. C., Sarin, P. S., Gelmann, E. P., Robert-Guroff, M., Richardson, E., Kalyanaraman, V. S., … Popovic, M. (1983). Isolation of human T-cell leukemia virus in acquired immune deficiency syndrome (AIDS). *Science (New York, N.Y.)*, *220*, 865–867.

Gallo, S. A., Finnegan, C. M., Viard, M., Raviv, Y., Dimitrov, A., Rawat, S. S., … Blumenthal, R. (2003). The HIV Env-mediated fusion reaction. *Biochimica et Biophysica Acta - Biomembranes*.

Garrus, J. E., Von Schwedler, U. K., Pornillos, O. W., Morham, S. G., Zavitz, K. H., Wang, H. E., … Sundquist, W. I. (2001). Tsg101 and the vacuolar protein sorting pathway are essential for HIV-1 budding. *Cell*, *107*, 55–65.

Gaudin, C., Mazauric, M. H., Traïkia, M., Guittet, E., Yoshizawa, S., & Fourmy, D. (2005). Structure of the RNA signal essential for translational frameshifting in HIV-1. *Journal of Molecular Biology*, *349*, 1024–1035.

Gendron, K., Charbonneau, J., Dulude, D., Heveker, N., Ferbeyre, G., & Brakier-Gingras, L. (2008). The presence of the TAR RNA structure alters the programmed -1 ribosomal frameshift efficiency of the human immunodeficiency virus type 1 (HIV-1) by modifying the rate of translation initiation. *Nucleic Acids Research*, *36*(1), 30–40.

Gheysen, D., Jacobs, E., de Foresta, F., Thiriart, C., Francotte, M., Thines, D., & De Wilde, M. (1989). Assembly and release of HIV-1 precursor Pr55gag virus-like particles from recombinant baculovirus-infected insect cells. *Cell*, *59*, 103–112.

Gilbert, W. V. (2011). Functional specialization of ribosomes? *Trends in Biochemical Sciences*.

Gillet, V. J. (2008). New directions in library design and analysis. *Current Opinion in Chemical Biology*.

Gleeson, M. P. (2008). Generation of a set of simple, interpretable ADMET rules of thumb. *Journal of Medicinal Chemistry*, *51*(4), 817–34.

Goldman, M. E., Nunberg, J. H., O'Brien, J. A., Quintero, J. C., Schleif, W. A., Freund, K. F., … Hoffman, J. M. (1991). Pyridinone derivatives: specific human immunodeficiency virus type 1 reverse transcriptase inhibitors with antiviral activity. *Proceedings of the National Academy of Sciences of the United States of America*, *88*, 6863–6867.

Göttlinger, H. G., Dorfman, T., Sodroski, J. G., & Haseltine, W. A. (1991). Effect of mutations affecting the p6 gag protein on human immunodeficiency virus particle release. *Proceedings of the National Academy of Sciences of the United States of America*, *88*, 3195–3199.

Göttlinger, H. G., Sodroski, J. G., & Haseltine, W. A. (1989). Role of capsid precursor processing and myristoylation in morphogenesis and infectivity of human immunodeficiency virus type 1. *Proceedings of the National Academy of Sciences of the United States of America*, *86*, 5781–5785.

Grentzmann, G., Ingram, J. A., Kelly, P. J., Gesteland, R. F., & Atkins, J. F. (1998). A dual-luciferase reporter system for studying recoding signals. *RNA (New York, N.Y.)*, *4*, 479–486.

Gulick, R. M., Lalezari, J., Goodrich, J., Clumeck, N., DeJesus, E., Horban, A., … Mayer, H. (2008). Maraviroc for previously treated patients with R5 HIV-1 infection. *The New England Journal of Medicine*, *359*(14), 1429–41.

Gupta, K. K. (1993). Acute immunosuppression with HIV seroconversion. *The New England Journal of Medicine*, *328*(4), 288–9.

Hadzopoulou-Cladaras, M., Felber, B. K., Cladaras, C., Athanassopoulos, A., Tse, A., & Pavlakis, G. N. (1989). The rev (trs/art) protein of human immunodeficiency virus type 1 affects viral mRNA and protein expression via a cis-acting sequence in the env region. *Journal of Virology*, *63*, 1265–1274.

Haffar, O. K., Popov, S., Dubrovsky, L., Agostini, I., Tang, H., Pushkarsky, T., … Bukrinsky, M. (2000). Two nuclear localization signals in the HIV-1 matrix protein regulate nuclear import of the HIV-1 pre-integration complex. *Journal of Molecular Biology*, *299*(2), 359–68.

Hammer, S. M., Squires, K. E., Hughes, M. D., Grimes, J. M., Demeter, L. M., Currier, J. S., … Fischl, M. A. (1997). A controlled trial of two nucleoside analogues plus indinavir in persons with human immunodeficiency virus infection and CD4 cell counts of 200 per cubic millimeter or less. AIDS Clinical Trials Group 320 Study Team. *The New England Journal of Medicine*, *337*(11), 725–33.

Hansen, T. M., Reihani, S. N. S., Oddershede, L. B., & Sørensen, M. A. (2007). Correlation between mechanical strength of messenger RNA pseudoknots and ribosomal frameshifting. *Proceedings of the National Academy of Sciences of the United States of America*, *104*, 5830–5835.

Hanson, P. I., Roth, R., Lin, Y., & Heuser, J. E. (2008). Plasma membrane deformation by circular arrays of ESCRT-III protein filaments. *Journal of Cell Biology*, *180*, 389–402.

Harger, J. W., & Dinman, J. D. (2003). An in vivo dual-luciferase assay system for studying translational recoding in the yeast Saccharomyces cerevisiae. *RNA (New York, N.Y.)*, *9*, 1019–1024.

Hazuda, D. J., Anthony, N. J., Gomez, R. P., Jolly, S. M., Wai, J. S., Zhuang, L., … Young, S. D. (2004). A naphthyridine carboxamide provides evidence for discordant resistance between mechanistically identical inhibitors of HIV-1 integrase. *Proceedings of the National Academy of Sciences of the United States of America*, *101*, 11233–11238.

Hazuda, D. J., Felock, P., Witmer, M., Wolfe, A., Stillmock, K., Grobler, J. A., … Miller, M. D. (2000). Inhibitors of strand transfer that prevent integration and inhibit HIV-1 replication in cells. *Science (New York, N.Y.)*, *287*, 646–650.

Hazuda, D. J., Young, S. D., Guare, J. P., Anthony, N. J., Gomez, R. P., Wai, J. S., … Shiver, J. W. (2004). Integrase inhibitors and cellular immunity suppress retroviral replication in rhesus macaques. *Science (New York, N.Y.)*, *305*, 528–532.

He, J., Choe, S., Walker, R., Di Marzio, P., Morgan, D. O., & Landau, N. R. (1995). Human immunodeficiency virus type 1 viral protein R (Vpr) arrests cells in the G2 phase of the cell cycle by inhibiting p34cdc2 activity. *Journal of Virology*, *69*, 6705–6711.

Heinzinger, N. K., Bukinsky, M. I., Haggerty, S. A., Ragland, A. M., Kewalramani, V., Lee, M. A., … Emerman, M. (1994). The Vpr protein of human immunodeficiency virus type 1 influences nuclear localization of viral nucleic acids in nondividing host cells. *Proceedings of the National Academy of Sciences of the United States of America*, *91*, 7311–7315.

Hermann, J. C., Chen, Y., Wartchow, C., Menke, J., Gao, L., Gleason, S. K., … Gan, Q. F. (2013). Metal impurities cause false positives in high-throughput screening campaigns. *ACS Medicinal Chemistry Letters*, *4*, 197–200.

Hertogs, K., Bloor, S., Kemp, S. D., Van den Eynde, C., Alcorn, T. M., Pauwels, R., … Larder, B. A. (2000). Phenotypic and genotypic analysis of clinical HIV-1 isolates reveals extensive protease inhibitor cross-resistance: a survey of over 6000 samples. *AIDS (London, England)*, *14*, 1203–1210.

Hibbert, C. S., & Rein, A. (2005). Preliminary physical mapping of RNA-RNA linkages in the genomic RNA of Moloney murine leukemia virus. *Journal of Virology*, *79*, 8142–8148.

Hilditch, L., & Towers, G. J. (2014). A model for cofactor use during HIV-1 reverse transcription and nuclear entry. *Current Opinion in Virology*, *4*, 32–36.

Ho, D. D., Neumann, A. U., Perelson, A. S., Chen, W., Leonard, J. M., & Markowitz, M. (1995). Rapid turnover of plasma virions and CD4 lymphocytes in HIV-1 infection. *Nature*, *373*, 123–126.

Hoshikawa, N., Kojima, A., Yasuda, A., Takayashiki, E., Masuko, S., Chiba, J., … Kurata, T. (1991). Role of the gag and pol genes of human immunodeficiency virus in the morphogenesis and maturation of retrovirus-like particles expressed by recombinant vaccinia virus: an ultrastructural study. *The Journal of General Virology*, *72 (Pt 10*, 2509–17.

Howard, M. T., Gesteland, R. F., & Atkins, J. F. (2004). Efficient stimulation of site-specific ribosome frameshifting by antisense oligonucleotides. *RNA (New York, N.Y.)*, *10*, 1653–1661.

Huang, H., Chopra, R., Verdine, G. L., & Harrison, S. C. (1998). Structure of a covalently trapped catalytic complex of HIV-1 reverse transcriptase: implications for drug resistance. *Science (New York, N.Y.)*, *282*, 1669–1675.

Huang, M., Orenstein, J. M., Martin, M. A., & Freed, E. O. (1995). p6Gag is required for particle production from full-length human immunodeficiency virus type 1 molecular clones expressing protease. *Journal of Virology*, *69*, 6810–6818.

Hung, M., Patel, P., Davis, S., & Green, S. R. (1998). Importance of ribosomal frameshifting for human immunodeficiency virus type 1 particle assembly and replication. *Journal of Virology*, *72*, 4819–4824.

Inglese, J., Auld, D. S., Jadhav, A., Johnson, R. L., Simeonov, A., Yasgar, A., … Austin, C. P. (2006). Quantitative high-throughput screening: a titration-based approach that efficiently identifies biological activities in large

chemical libraries. *Proceedings of the National Academy of Sciences of the United States of America*, *103*, 11473–11478.

Jablonski, J. A., Amelio, A. L., Giacca, M., & Caputi, M. (2009). The transcriptional transactivator Tat selectively regulates viral splicing. *Nucleic Acids Research*, *38*, 1249–1260.

Jacks, T., Madhani, H. D., Masiarz, F. R., & Varmus, H. E. (1988). Signals for ribosomal frameshifting in the Rous sarcoma virus gag-pol region. *Cell*, *55*, 447–458.

Jacks, T., Power, M. D., Masiarz, F. R., Luciw, P. A., Barr, P. J., & Varmus, H. E. (1988). Characterization of ribosomal frameshifting in HIV-1 gag-pol expression. *Nature*, *331*, 280–283.

Jacks, T., & Varmus, H. E. (1985). Expression of the Rous sarcoma virus pol gene by ribosomal frameshifting. *Science (New York, N.Y.)*, *230*, 1237–1242.

Jacobo-Molina, A., Ding, J., Nanni, R. G., Clark, A. D., Lu, X., Tantillo, C., … Clark, P. (1993). Crystal structure of human immunodeficiency virus type 1 reverse transcriptase complexed with double-stranded DNA at 3.0 A resolution shows bent DNA. *Proceedings of the National Academy of Sciences of the United States of America*, *90*, 6320–6324.

Jacquot, G., Le Rouzic, E., David, A., Mazzolini, J., Bouchet, J., Bouaziz, S., … Benichou, S. (2007). Localization of HIV-1 Vpr to the nuclear envelope: impact on Vpr functions and virus replication in macrophages. *Retrovirology*, *4*, 84.

Jalalirad, M., & Laughrea, M. (2010). Formation of immature and mature genomic RNA dimers in wild-type and protease-inactive HIV-1: differential roles of the Gag polyprotein, nucleocapsid proteins NCp15, NCp9, NCp7, and the dimerization initiation site. *Virology*, *407*(2), 225–36.

Johnson, J. A., & Sax, P. E. (2014). Beginning antiretroviral therapy for patients with HIV. *Infectious Disease Clinics of North America*, *28*(3), 421–38.

Johnson, M. C. (2011). Mechanisms for Env glycoprotein acquisition by retroviruses. *AIDS Research and Human Retroviruses*, *27*, 239–247.

Jouvenet, N., Zhadina, M., Bieniasz, P. D., & Simon, S. M. (2011). Dynamics of ESCRT protein recruitment during retroviral assembly. *Nature Cell Biology*, *13*, 394–401.

Kang, H. (1998). Direct structural evidence for formation of a stem-loop structure involved in ribosomal frameshifting in human

immunodeficiency virus type 1. *Biochimica et Biophysica Acta*, *1397*(1), 73–8.

Karacostas, V., Wolffe, E. J., Nagashima, K., Gonda, M. A., & Moss, B. (1993). Overexpression of the HIV-1 gag-pol polyprotein results in intracellular activation of HIV-1 protease and inhibition of assembly and budding of virus-like particles. *Virology*, *193*(2), 661–71.

Katzman, M., Katz, R. A., Skalka, A. M., & Leis, J. (1989). The avian retroviral integration protein cleaves the terminal sequences of linear viral DNA at the in vivo sites of integration. *Journal of Virology*, *63*, 5319–5327.

Katzmann, D. J., Babst, M., & Emr, S. D. (2001). Ubiquitin-dependent sorting into the multivesicular body pathway requires the function of a conserved endosomal protein sorting complex, ESCRT-I. *Cell*, *106*, 145–155.

Kaye, J. F., & Lever, A. M. (1996). trans-acting proteins involved in RNA encapsidation and viral assembly in human immunodeficiency virus type 1. *Journal of Virology*, *70*, 880–886.

Kestler, H. W., Ringler, D. J., Mori, K., Panicali, D. L., Sehgal, P. K., Daniel, M. D., & Desrosiers, R. C. (1991). Importance of the nef gene for maintenance of high virus loads and for development of AIDS. *Cell*, *65*(4), 651–62.

Klatzmann, D., Champagne, E., Chamaret, S., Gruest, J., Guetard, D., Hercend, T., … Montagnier, L. (n.d.). T-lymphocyte T4 molecule behaves as the receptor for human retrovirus LAV. *Nature*, *312*(5996), 767–8.

Kleiman, L., Jones, C. P., & Musier-Forsyth, K. (2010). Formation of the tRNALys packaging complex in HIV-1. *FEBS Letters*.

Knobel, H., Carmona, A., López, J. L., Gimeno, J. L., Saballs, P., González, A., … Díez, A. (1999). *Adherence to very active antiretroviral treatment: impact of individualized assessment*. *Enfermedades infecciosas y microbiologia clinica* (Vol. 17, pp. 78–81).

Kobayashi, Y., Zhuang, J., Peltz, S., & Dougherty, J. (2010). Identification of a cellular factor that modulates HIV-1 programmed ribosomal frameshifting. *Journal of Biological Chemistry*, *285*, 19776–19784.

Kohlstaedt, L. A., Wang, J., Friedman, J. M., Rice, P. A., & Steitz, T. A. (1992). Crystal structure at 3.5 A resolution of HIV-1 reverse transcriptase complexed with an inhibitor. *Science (New York, N.Y.)*, *256*, 1783–1790.

Kollmus, H., Honigman, A., Panet, A., & Hauser, H. (1994). The sequences of and distance between two cis-acting signals determine the efficiency of ribosomal frameshifting in human immunodeficiency virus type 1 and

human T-cell leukemia virus type II in vivo. *Journal of Virology*, *68*(9), 6087–91.

Kontos, H., Napthine, S., & Brierley, I. (2001). Ribosomal pausing at a frameshifter RNA pseudoknot is sensitive to reading phase but shows little correlation with frameshift efficiency. *Molecular and Cellular Biology*, *21*, 8657–8670.

Krowicka, H., Robinson, J. E., Clark, R., Hager, S., Broyles, S., & Pincus, S. H. (2008). Use of tissue culture cell lines to evaluate HIV antiviral resistance. *AIDS Research and Human Retroviruses*, *24*, 957–967.

Kubinyi, H. (1998). Structure-based design of enzyme inhibitors and receptor ligands. *Current Opinion in Drug Discovery & Development*, *1*, 4–15.

Kümmel, A., & Parker, C. N. (2011). The Interweaving of Cheminformatics and HTS. *Methods in Molecular Biology (Clifton, N.J.)*, *672*, 435–457.

Kutluay, S. B., & Bieniasz, P. D. (2010). Analysis of the initiating events in HIV-1 particle assembly and genome packaging. *PLoS Pathogens*, *6*.

Kutluay, S. B., Zang, T., Blanco-Melo, D., Powell, C., Jannain, D., Errando, M., & Bieniasz, P. D. (2014). Global Changes in the RNA Binding Specificity of HIV-1 Gag Regulate Virion Genesis. *Cell*, *159*(5), 1096–109.

Laguette, N., Brégnard, C., Benichou, S., & Basmaciogullari, S. (2010). Human immunodeficiency virus (HIV) type-1, HIV-2 and simian immunodeficiency virus Nef proteins. *Molecular Aspects of Medicine*.

Land, S., Terloar, G., McPhee, D., Birch, C., Doherty, R., Cooper, D., & Gust, I. (1990). Decreased in vitro susceptibility to zidovudine of HIV isolates obtained from patients with AIDS. *The Journal of Infectious Diseases*, *161*, 326–329.

Larder, B. A., Darby, G., & Richman, D. D. (1989). HIV with reduced sensitivity to zidovudine (AZT) isolated during prolonged therapy. *Science (New York, N.Y.)*, *243*, 1731–1734.

Léger, M., Dulude, D., Steinberg, S. V., & Brakier-Gingras, L. (2007). The three transfer RNAs occupying the A, P and E sites on the ribosome are involved in viral programmed -1 ribosomal frameshift. *Nucleic Acids Research*, *35*, 5581–5592.

Lenhard, J. M., Furfine, E. S., Jain, R. G., Ittoop, O., Orband-Miller, L. A., Blanchard, S. G., … Weiel, J. E. (2000). HIV protease inhibitors block adipogenesis and increase lipolysis in vitro. *Antiviral Research*, *47*, 121–129.

Levin, J. G., Guo, J., Rouzina, I., & Musier-Forsyth, K. (2005). Nucleic Acid Chaperone Activity of HIV-1 Nucleocapsid Protein: Critical Role in Reverse Transcription and Molecular Mechanism. *Progress in Nucleic Acid Research and Molecular Biology*.

Li, C. M., Margolin, A. A., Salas, M., Memeo, L., Mansukhani, M., Hibshoosh, H., … Tycko, B. (2006). PEG10 is a c-MYC target gene in cancer cells. *Cancer Research*, *66*, 665–672.

Li, S., Hill, C. P., Sundquist, W. I., & Finch, J. T. (2000). Image reconstructions of helical assemblies of the HIV-1 CA protein. *Nature*, *407*, 409–413.

Li, X., & Vince, R. (2006). Conformationally restrained carbazolone-containing ??,??-diketo acids as inhibitors of HIV integrase. *Bioorganic and Medicinal Chemistry*, *14*, 2942–2955.

Liao, P. Y., Choi, Y. S., Dinman, J. D., & Lee, K. H. (2011). The many paths to frameshifting: Kinetic modelling and analysis of the effects of different elongation steps on programmed -1 ribosomal frameshifting. *Nucleic Acids Research*, *39*, 300–312.

Lipinski, C. A., Lombardo, F., Dominy, B. W., & Feeney, P. J. (2012). Experimental and computational approaches to estimate solubility and permeability in drug discovery and development settings. *Advanced Drug Delivery Reviews*.

Llibre, J. M., Imaz, A., & Clotet, B. (2013). From TMC114 to darunavir: Five years of data on efficacy. *AIDS Reviews*.

Lopinski, J. D., Dinman, J. D., & Bruenn, J. A. (2000). Kinetics of ribosomal pausing during programmed -1 translational frameshifting. *Molecular and Cellular Biology*, *20*, 1095–1103.

Losson, R., & Lacroute, F. (1979). Interference of nonsense mutations with eukaryotic messenger RNA stability. *Proceedings of the National Academy of Sciences of the United States of America*, *76*, 5134–5137.

Lux, H., Flammann, H., Hafner, M., & Lux, A. (2010). Genetic and molecular analyses of PEG10 reveal new aspects of genomic organization, transcription and translation. *PLoS ONE*, *5*.

Maia, I. G., Séron, K., Haenni, A. L., & Bernardi, F. (1996). Gene expression from viral RNA genomes. *Plant Molecular Biology*, *32*, 367–391.

Malim, M. H., & Emerman, M. (2008). HIV-1 Accessory Proteins-Ensuring Viral Survival in a Hostile Environment. *Cell Host and Microbe*.

Manktelow, E., Shigemoto, K., & Brierley, I. (2005). Characterization of the frameshift signal of Edr, a mammalian example of programmed -1 ribosomal frameshifting. *Nucleic Acids Research*, *33*, 1553–1563.

Marchand, C., Johnson, A. A., Karki, R. G., Pais, G. C. G., Zhang, X., Cowansage, K., … Pommier, Y. (2003). Metal-dependent inhibition of HIV-1 integrase by beta-diketo acids and resistance of the soluble double-mutant (F185K/C280S). *Molecular Pharmacology*, *64*, 600–609.

Marcheschi, R. J., Tonelli, M., Kumar, A., & Butcher, S. E. (2011). Structure of the HIV-1 frameshift site RNA bound to a small molecule inhibitor of viral replication. *ACS Chemical Biology*, *6*, 857–864.

Margottin, F., Bour, S. P., Durand, H., Selig, L., Benichou, S., Richard, V., … Benarous, R. (1998). A novel human WD protein, h-beta TrCp, that interacts with HIV-1 Vpu connects CD4 to the ER degradation pathway through an F-box motif. *Molecular Cell*, *1*, 565–574.

Marriott, D. P., Dougall, I. G., Meghani, P., Liu, Y. J., & Flower, D. R. (1999). Lead generation using pharmacophore mapping and three-dimensional database searching: Application to muscarinic M3 receptor antagonists. *Journal of Medicinal Chemistry*, *42*, 3210–3216.

Martin-Serrano, J., Zang, T., & Bieniasz, P. D. (2001). HIV-1 and Ebola virus encode small peptide motifs that recruit Tsg101 to sites of particle assembly to facilitate egress. *Nature Medicine*, *7*, 1313–1319.

Matreyek, K. A., & Engelman, A. (2013). Viral and cellular requirements for the nuclear entry of retroviral preintegration nucleoprotein complexes. *Viruses*. doi:10.3390/v5102483

Mazauric, M.-H., Seol, Y., Yoshizawa, S., Visscher, K., & Fourmy, D. (2009). Interaction of the HIV-1 frameshift signal with the ribosome. *Nucleic Acids Research*, *37*(22), 7654–64.

McDougal, J. S., Kennedy, M. S., Sligh, J. M., Cort, S. P., Mawle, A., & Nicholson, J. K. (1986). Binding of HTLV-III/LAV to T4+ T cells by a complex of the 110K viral protein and the T4 molecule. *Science (New York, N.Y.)*, *231*(4736), 382–5.

McNaughton, B. R., Gareiss, P. C., & Miller, B. L. (2007). Identification of a selective small-molecule ligand for HIV-1 frameshift-inducing stem-loop RNA from an 11,325 member resin bound dynamic combinatorial library. *Journal of the American Chemical Society*, *129*(37), 11306–7.

Meyer, P. R., Matsuura, S. E., Mohsin Mian, A., So, A. G., & Scott, W. A. (1999). A mechanism of AZT resistance: An increase in nucleotide-dependent primer unblocking by mutant HIV-1 reverse transcriptase. *Molecular Cell*, *4*, 35–43.

Miller, V. (2001). International perspectives on antiretroviral resistance. Resistance to protease inhibitors. *Journal of Acquired Immune Deficiency Syndromes (1999)*, *26 Suppl 1*, S34–S50.

Mitsuya, H., Weinhold, K. J., Furman, P. A., St Clair, M. H., Lehrman, S. N., Gallo, R. C., … Broder, S. (1985). 3'-Azido-3'-deoxythymidine (BW A509U): an antiviral agent that inhibits the infectivity and cytopathic effect of human T-lymphotropic virus type III/lymphadenopathy-associated virus in vitro. *Proceedings of the National Academy of Sciences of the United States of America*, *82*, 7096–7100.

Miyauchi, K., Komano, J., Myint, L., Futahashi, Y., Urano, E., Matsuda, Z., … Yamamoto, N. (2006). Rapid propagation of low-fitness drug-resistant mutants of human immunodeficiency virus type 1 by a streptococcal metabolite sparsomycin. *Antiviral Chemistry and Chemotherapy*, *17*, 167–174.

Montal, M. (2003). Structure-function correlates of Vpu, a membrane protein of HIV-1. In *FEBS Letters* (Vol. 552, pp. 47–53).

Morgan, D., Mahe, C., Mayanja, B., Okongo, J. M., Lubega, R., & Whitworth, J. A. G. (2002). HIV-1 infection in rural Africa: is there a difference in median time to AIDS and survival compared with that in industrialized countries? *AIDS (London, England)*, *16*, 597–603.

Mouzakis, K. D., Lang, A. L., Vander Meulen, K. A., Easterday, P. D., & Butcher, S. E. (2013). HIV-1 frameshift efficiency is primarily determined by the stability of base pairs positioned at the mRNA entrance channel of the ribosome. *Nucleic Acids Research*, *41*, 1901–1913.

Muesing, M. A., Smith, D. H., & Capon, D. J. (1987). Regulation of mRNA accumulation by a human immunodeficiency virus trans-activator protein. *Cell*, *48*, 691–701.

Muriaux, D., & Darlix, J.-L. (2010). Properties and functions of the nucleocapsid protein in virus assembly. *RNA Biology*.

Navia, M. A., Fitzgerald, P. M., McKeever, B. M., Leu, C. T., Heimbach, J. C., Herber, W. K., … Springer, J. P. (1989). Three-dimensional structure of aspartyl protease from human immunodeficiency virus HIV-1. *Nature*, *337*, 615–620.

Neil, S. J. D., Zang, T., & Bieniasz, P. D. (2008). Tetherin inhibits retrovirus release and is antagonized by HIV-1 Vpu. *Nature*, *451*, 425–430.

Nekrutenko, A., Makova, K. D., & Li, W. H. (2002). The KA/KS ratio test for assessing the protein-coding potential of genomic regions: An empirical and simulation study. *Genome Research*, *12*, 198–202.

Nijhuis, M., Deeks, S., & Boucher, C. (2001). Implications of antiretroviral resistance on viral fitness. *Current Opinion in Infectious Diseases*, *14*, 23–28.

Núñez, M., & Soriano, V. (2000). Salvage therapy for HIV infection: when and how. *AIDS Patient Care and STDs*, *14*(9), 465–76.

Okabe, H., Satoh, S., Furukawa, Y., Kato, T., Hasegawa, S., Nakajima, Y., … Nakamura, Y. (2003). Involvement of PEG10 in human hepatocellular carcinogenesis through interaction with SIAH1. *Cancer Research*, *63*, 3043–3048.

Olsthoorn, R. C. L., Laurs, M., Sohet, F., Hilbers, C. W., Heus, H. A., & Pleij, C. W. A. (2004). Novel application of sRNA: stimulation of ribosomal frameshifting. *RNA (New York, N.Y.)*, *10*, 1702–1703.

Ono, A., Ablan, S. D., Lockett, S. J., Nagashima, K., & Freed, E. O. (2004). Phosphatidylinositol (4,5) bisphosphate regulates HIV-1 Gag targeting to the plasma membrane. *Proceedings of the National Academy of Sciences of the United States of America*, *101*, 14889–14894.

Paillart, J. C., Skripkin, E., Ehresmann, B., Ehresmann, C., & Marquet, R. (2002). In Vitro evidence for a long range pseudoknot in the 5???-untranslated and matrix coding regions of HIV-1 genomic RNA. *Journal of Biological Chemistry*, *277*, 5995–6004.

Paillart, J.-C., Shehu-Xhilaga, M., Marquet, R., & Mak, J. (2004). Dimerization of retroviral RNA genomes: an inseparable pair. *Nature Reviews. Microbiology*, *2*, 461–472.

Palde, P. B., Ofori, L. O., Gareiss, P. C., Lerea, J., & Miller, B. L. (2010). Strategies for recognition of stem-loop RNA structures by synthetic ligands: Application to the HIV-1 frameshift stimulatory sequence. *Journal of Medicinal Chemistry*, *53*, 6018–6027.

Palella, F. J., Delaney, K. M., Moorman, A. C., Loveless, M. O., Fuhrer, J., Satten, G. A., … Holmberg, S. D. (1998). Declining morbidity and mortality among patients with advanced human immunodeficiency virus infection. HIV Outpatient Study Investigators. *The New England Journal of Medicine*, *338*, 853–860.

Park, J., & Morrow, C. D. (1991). Overexpression of the gag-pol precursor from human immunodeficiency virus type 1 proviral genomes results in efficient proteolytic processing in the absence of virion production. *Journal of Virology*, *65*, 5111–5117.

Park, J., & Morrow, C. D. (1992). The nonmyristylated Pr160gag-pol polyprotein of human immunodeficiency virus type 1 interacts with

Pr55gag and is incorporated into viruslike particles. *Journal of Virology*, *66*, 6304–6313.

Paterson, D. L., Swindells, S., Mohr, J., Brester, M., Vergis, E. N., Squier, C., … Singh, N. (2000). Adherence to protease inhibitor therapy and outcomes in patients with HIV infection. *Annals of Internal Medicine*, *133*, 21–30.

Paxton, W., Connor, R. I., & Landau, N. R. (1993). Incorporation of Vpr into human immunodeficiency virus type 1 virions: requirement for the p6 region of gag and mutational analysis. *Journal of Virology*, *67*(12), 7229–37.

Pettit, S. C., Moody, M. D., Wehbie, R. S., Kaplan, A. H., Nantermet, P. V, Klein, C. A., & Swanstrom, R. (1994). The p2 domain of human immunodeficiency virus type 1 Gag regulates sequential proteolytic processing and is required to produce fully infectious virions. *Journal of Virology*, *68*, 8017–8027.

Plant, E. P., & Dinman, J. D. (2006). Comparative study of the effects of heptameric slippery site composition on -1 frameshifting among different eukaryotic systems. *RNA (New York, N.Y.)*, *12*(4), 666–73.

Plant, E. P., & Dinman, J. D. (2008). The role of programmed-1 ribosomal frameshifting in coronavirus propagation. *Frontiers in Bioscience : A Journal and Virtual Library*, *13*, 4873–4881.

Quiñones-Mateu, M. E., & Arts, E. J. (2002). Fitness of drug resistant HIV-1: Methodology and clinical implications. *Drug Resistance Updates*.

Quiñones-Mateu, M. E., Moore-Dudley, D. M., Jegede, O., Weber, J., & J Arts, E. (2008). Viral drug resistance and fitness. *Advances in Pharmacology (San Diego, Calif.)*, *56*, 257–96.

Rakauskait, R., Liao, P. Y., Rhodin, M. H. J., Lee, K., & Dinman, J. D. (2011). A rapid, inexpensive yeast-based dual-fluorescence assay of programmed-1 ribosomal frameshifting for high-throughput screening. *Nucleic Acids Research*, *39*.

Rein, A., Henderson, L. E., & Levin, J. G. (1998). Nucleic-acid-chaperone activity of retroviral nucleocapsid proteins: Significance for viral replication. *Trends in Biochemical Sciences*.

Richman, D. D. (2000). Principles of HIV resistance testing and overview of assay performance characteristics. In *Antiviral Therapy* (Vol. 5, pp. 27–31).

Rodgers, D. W., Gamblin, S. J., Harris, B. A., Ray, S., Culp, J. S., Hellmig, B., … Harrison, S. C. (1995). The structure of unliganded reverse transcriptase from the human immunodeficiency virus type 1. *Proceedings of the*

National Academy of Sciences of the United States of America, *92*, 1222–1226.

Rogel, M. E., Wu, L. I., & Emerman, M. (1995). The human immunodeficiency virus type 1 vpr gene prevents cell proliferation during chronic infection. *Journal of Virology*, *69*, 882–888.

Rooke, R., Tremblay, M., Soudeyns, H., DeStephano, L., Yao, X. J., Fanning, M., … Tsoukas, C. (1989). Isolation of drug-resistant variants of HIV-1 from patients on long-term zidovudine therapy. Canadian Zidovudine Multi-Centre Study Group. *AIDS (London, England)*, *3*, 411–415.

Rosen, C. A., Terwilliger, E., Dayton, A., Sodroski, J. G., & Haseltine, W. A. (1988). Intragenic cis-acting art gene-responsive sequences of the human immunodeficiency virus. *Proceedings of the National Academy of Sciences of the United States of America*, *85*, 2071–2075.

Ryan, A. J., Gray, N. M., Lowe, P. N., & Chung, C. W. (2003). Effect of detergent on "promiscuous" inhibitors. *Journal of Medicinal Chemistry*, *46*, 3448–3451.

Saad, J. S., Miller, J., Tai, J., Kim, A., Ghanam, R. H., & Summers, M. F. (2006). Structural basis for targeting HIV-1 Gag proteins to the plasma membrane for virus assembly. *Proceedings of the National Academy of Sciences of the United States of America*, *103*, 11364–11369.

Sarafianos, S. G., Das, K., Clark, A. D., Ding, J., Boyer, P. L., Hughes, S. H., & Arnold, E. (1999). Lamivudine (3TC) resistance in HIV-1 reverse transcriptase involves steric hindrance with beta-branched amino acids. *Proceedings of the National Academy of Sciences of the United States of America*, *96*, 10027–10032.

Schröder, A. R. W., Shinn, P., Chen, H., Berry, C., Ecker, J. R., & Bushman, F. (2002). HIV-1 integration in the human genome favors active genes and local hotspots. *Cell*, *110*, 521–529.

Seligmann, H. (2012). An overlapping genetic code for frameshifted overlapping genes in Drosophila mitochondria: Antisense antitermination tRNAs UAR insert serine. *Journal of Theoretical Biology*, *298*, 51–76.

Shaner, N. C., Campbell, R. E., Steinbach, P. A., Giepmans, B. N. G., Palmer, A. E., & Tsien, R. Y. (2004). Improved monomeric red, orange and yellow fluorescent proteins derived from Discosoma sp. red fluorescent protein. *Nature Biotechnology*.

Sheehy, A. M., Gaddis, N. C., Choi, J. D., & Malim, M. H. (2002). Isolation of a human gene that inhibits HIV-1 infection and is suppressed by the viral Vif protein. *Nature*, *418*, 646–650.

Shehu-Xhilaga, M., Crowe, S. M., & Mak, J. (2001). Maintenance of the Gag/Gag-Pol ratio is important for human immunodeficiency virus type 1 RNA dimerization and viral infectivity. *Journal of Virology*, *75*(4), 1834–41.

Shen, Q.-T., Schuh, A. L., Zheng, Y., Quinney, K., Wang, L., Hanna, M., … Audhya, A. (2014). Structural analysis and modeling reveals new mechanisms governing ESCRT-III spiral filament assembly. *The Journal of Cell Biology*, *206*(6), 763–777.

Shigemoto, K., Brennan, J., Walls, E., Watson, C. J., Stott, D., Rigby, P. W., & Reith, A. D. (2001). Identification and characterisation of a developmentally regulated mammalian gene that utilises -1 programmed ribosomal frameshifting. *Nucleic Acids Research*, *29*, 4079–4088.

Shkriabai, N., Datta, S. A. K., Zhao, Z., Hess, S., Rein, A., & Kvaratskhelia, M. (2006). Interactions of HIV-1 Gag with assembly cofactors. *Biochemistry*, *45*, 4077–4083.

Silverman, R. B., & Holladay, M. W. (2014). *The Organic Chemistry of Drug Design and Drug Action*. *The Organic Chemistry of Drug Design and Drug Action* (pp. 19–122).

Simon, V., Ho, D., & Karim, Q. A. (2006). HIV/AIDS epidemiology, pathogenesis, prevention, and treatment. *The Lancet*, *368*, 489–504.

Smith, A. J., Srinivasakumar, N., Hammarskjöld, M. L., & Rekosh, D. (1993). Requirements for incorporation of Pr160gag-pol from human immunodeficiency virus type 1 into virus-like particles. *Journal of Virology*, *67*, 2266–2275.

Somogyi, P., Jenner, A. J., Brierley, I., & Inglis, S. C. (1993). Ribosomal pausing during translation of an RNA pseudoknot. *Molecular and Cellular Biology*, *13*, 6931–6940.

Stahl, G., Bidou, L., Rousset, J. P., & Cassan, M. (1995). Versatile vectors to study recoding: conservation of rules between yeast and mammalian cells. *Nucleic Acids Research*, *23*, 1557–1560.

Staple, D. W., & Butcher, S. E. (2005). Solution structure and thermodynamic investigation of the HIV-1 frameshift inducing element. *Journal of Molecular Biology*, *349*, 1011–1023.

Strebel, K. (2003). Virus-host interactions: role of HIV proteins Vif, Tat, and Rev. *AIDS (London, England)*, *17 Suppl 4*, S25–34.

Struble, K., Murray, J., Cheng, B., Gegeny, T., Miller, V., & Gulick, R. (2005). Antiretroviral therapies for treatment-experienced patients: current status and research challenges. *AIDS (London, England)*, *19*(8), 747–56.

Sundquist, W. I., & Kräusslich, H. G. (2012). HIV-1 assembly, budding, and maturation. *Cold Spring Harbor Perspectives in Medicine*.

Swanson, C. M., & Malim, M. H. (2008). SnapShot: HIV-1 proteins. *Cell*, *133*(4), 742, 742.e1.

Swanstrom, R., & Coffin, J. (2012). HIV-1 pathogenesis: The virus. *Cold Spring Harbor Perspectives in Medicine*, *2*.

Takyar, S., Hickerson, R. P., & Noller, H. F. (2005). mRNA helicase activity of the ribosome. *Cell*, *120*, 49–58.

Tang, M. W., & Shafer, R. W. (2012). HIV-1 antiretroviral resistance: Scientific principles and clinical applications. *Drugs*.

Telenti, A., Martinez, R., Munoz, M., Bleiber, G., Greub, G., Sanglard, D., & Peters, S. (2002). Analysis of Natural Variants of the Human Immunodeficiency Virus Type 1 gag-pol Frameshift Stem-Loop Structure. *Journal of Virology*.

Temesgen, Z., Cainelli, F., Poeschla, E. M., Vlahakis, S. A., & Vento, S. (2006). Approach to salvage antiretroviral therapy in heavily antiretroviral-experienced HIV-positive adults. *Lancet Infectious Diseases*. doi:10.1016/S1473-3099(06)70550-3

Thomson, M. M., Pérez-Álvarez, L., & Nájera, R. (2002). Molecular epidemiology of HIV-1 genetic forms and its significance for vaccine development and therapy. *Lancet Infectious Diseases*. doi:10.1016/S1473-3099(02)00343-2

Thorne, N., Auld, D. S., & Inglese, J. (2010). Apparent activity in high-throughput screening: origins of compound-dependent assay interference. *Current Opinion in Chemical Biology*. doi:10.1016/j.cbpa.2010.03.020

Tsuchihashi, Z. (1991). Translational frameshifting in the Escherichia coli dnaX gene in vitro. *Nucleic Acids Research*, *19*(9), 2457–62.

Tu, C., Tzeng, T. H., & Bruenn, J. A. (1992). Ribosomal movement impeded at a pseudoknot required for frameshifting. *Proceedings of the National Academy of Sciences of the United States of America*, *89*, 8636–8640.

Vacca, J. P., & Condra, J. H. (1997). Clinically effective HIV-1 protease inhibitors. *Drug Discovery Today*. doi:10.1016/S1359-6446(97)01053-2

Valler, M. J., & Green, D. (2000). Diversity screening versus focussed screening in drug discovery. *Drug Discovery Today*. doi:10.1016/S1359-6446(00)01517-8

Van de Waterbeemd, H., Camenisch, G., Folkers, G., Chretien, J. R., & Raevsky, O. A. (1998). Estimation of blood-brain barrier crossing of drugs using molecular size and shape, and H-bonding descriptors. *Journal of Drug Targeting*, *6*(2), 151–65.

Van Engelenburg, S. B., Shtengel, G., Sengupta, P., Waki, K., Jarnik, M., Ablan, S. D., … Lippincott-Schwartz, J. (2014). Distribution of ESCRT machinery at HIV assembly sites reveals virus scaffolding of ESCRT subunits. *Science (New York, N.Y.)*, *343*, 653–6.

Veronese, F. D., DeVico, A. L., Copeland, T. D., Oroszlan, S., Gallo, R. C., & Sarngadharan, M. G. (1985). Characterization of gp41 as the transmembrane protein coded by the HTLV-III/LAV envelope gene. *Science (New York, N.Y.)*, *229*, 1402–1405.

VerPlank, L., Bouamr, F., LaGrassa, T. J., Agresta, B., Kikonyogo, A., Leis, J., & Carter, C. A. (2001). Tsg101, a homologue of ubiquitin-conjugating (E2) enzymes, binds the L domain in HIV type 1 Pr55(Gag). *Proceedings of the National Academy of Sciences of the United States of America*, *98*, 7724–7729.

Vink, C., van Gent, D. C., & Plasterk, R. H. (1990). Integration of human immunodeficiency virus types 1 and 2 DNA in vitro by cytoplasmic extracts of Moloney murine leukemia virus-infected mouse NIH 3T3 cells. *Journal of Virology*, *64*, 5219–5222.

Vondrasek, J., van Buskirk, C. P., & Wlodawer, A. (1997). Database of three-dimensional structures of HIV proteinases. *Nature Structural Biology*, *4*(1), 8.

Votteler, J., & Sundquist, W. I. (2013). Virus budding and the ESCRT pathway. *Cell Host and Microbe*.

Weber, I. T. (1990). Evaluation of homology modeling of HIV protease. *Proteins*, *7*, 172–184.

Wensing, A. M., Calvez, V., Günthard, H. F., Johnson, V. a, Paredes, R., Pillay, D., … Richman, D. D. (2014). 2014 update of the drug resistance mutations in HIV-1. *Topics in Antiviral Medicine*, *22*, 642–50.

Whiting, M., Muldoon, J., Lin, Y.-C., Silverman, S. M., Lindstrom, W., Olson, A. J., … Fokin, V. V. (2006). Inhibitors of HIV-1 protease by using in situ click chemistry. *Angew. Chem., Int. Ed.*, *45*, 1435–1439.

Wills, N. M., Gesteland, R. F., & Atkins, J. F. (1991). Evidence that a downstream pseudoknot is required for translational read-through of the Moloney murine leukemia virus gag stop codon. *Proceedings of the National Academy of Sciences of the United States of America*, *88*(16), 6991–5.

Wills, N. M., Moore, B., Hammer, A., Gesteland, R. F., & Atkins, J. F. (2006). A functional -1 ribosomal frameshift signal in the human paraneoplastic Ma3 gene. *Journal of Biological Chemistry*, *281*, 7082–7088.

Wilson, W., Braddock, M., Adams, S. E., Rathjen, P. D., Kingsman, S. M., & Kingsman, A. J. (1988). HIV expression strategies: ribosomal frameshifting is directed by a short sequence in both mammalian and yeast systems. *Cell*, *55*, 1159–1169. doi:10.1016/0092-8674(88)90260-7

Wlodawer, A., & Erickson, J. W. (1993). Structure-based inhibitors of HIV-1 protease. *Annual Review of Biochemistry*, *62*, 543–85.

Wright, E. R., Schooler, J. B., Ding, H. J., Kieffer, C., Fillmore, C., Sundquist, W. I., & Jensen, G. J. (2007). Electron cryotomography of immature HIV-1 virions reveals the structure of the CA and SP1 Gag shells. *The EMBO Journal*, *26*, 2218–2226.

Wu, Z., Liu, D., & Sui, Y. (2008). Quantitative assessment of hit detection and confirmation in single and duplicate high-throughput screenings. *Journal of Biomolecular Screening : The Official Journal of the Society for Biomolecular Screening*, *13*, 159–167.

Yamashita, M., & Emerman, M. (2004). Capsid is a dominant determinant of retrovirus infectivity in nondividing cells. *Journal of Virology*, *78*, 5670–5678.

Yarchoan, R., & Broder, S. (1987). Development of antiretroviral therapy for the acquired immunodeficiency syndrome and related disorders. A progress report. *The New England Journal of Medicine*, *316*, 557–564.

Yoder, K. E., & Bushman, F. D. (2000). Repair of gaps in retroviral DNA integration intermediates. *Journal of Virology*, *74*, 11191–11200.

Yu, C. H., Noteborn, M. H. M., & Olsthoorn, R. C. L. (2010). Stimulation of ribosomal frameshifting by antisense LNA. *Nucleic Acids Research*, *38*, 8277–8283.

Yusupova, G. Z., Yusupov, M. M., Cate, J. H., & Noller, H. F. (2001). The path of messenger RNA through the ribosome. *Cell*, *106*(2), 233–41.

Zapp, M. L., & Green, M. R. (1989). Sequence-specific RNA binding by the HIV-1 Rev protein. *Nature*, *342*, 714–716.

Zhang, Y. M., Imamichi, H., Imamichi, T., Lane, H. C., Falloon, J., Vasudevachari, M. B., & Salzman, N. P. (1997). Drug resistance during indinavir therapy is caused by mutations in the protease gene and in its Gag substrate cleavage sites. *Journal of Virology*, *71*(9), 6662–70.

Zhuang, L., Wai, J. S., Embrey, M. W., Fisher, T. E., Egbertson, M. S., Payne, L. S., … Young, S. D. (2003). Design and synthesis of 8-hydroxy-[1,6]naphthyridines as novel inhibitors of HIV-1 integrase in vitro and in infected cells. *Journal of Medicinal Chemistry*, *46*, 453–456.